

Tonic GABA_A Current in Absence Epilepsy

A thesis submitted to Cardiff University for the degree of
Philosophiae Doctor

by
Sarah J. Fyson BSc (Hons)

Cardiff School of Biosciences,
Cardiff University
August 2010

UMI Number: U585423

All rights reserved

INFORMATION TO ALL USERS

The quality of this reproduction is dependent upon the quality of the copy submitted.

In the unlikely event that the author did not send a complete manuscript and there are missing pages, these will be noted. Also, if material had to be removed, a note will indicate the deletion.



UMI U585423

Published by ProQuest LLC 2013. Copyright in the Dissertation held by the Author.
Microform Edition © ProQuest LLC.

All rights reserved. This work is protected against
unauthorized copying under Title 17, United States Code.



ProQuest LLC
789 East Eisenhower Parkway
P.O. Box 1346
Ann Arbor, MI 48106-1346

Declaration and Statements

Declaration:

This work has not previously been accepted in substance for any degree and is not concurrently submitted in candidature for any degree.

Signed Sarah Fyson (candidate) Date 19/8/10

Signed (supervisor) Date

Statement 1

This thesis is being submitted in partial fulfilment of the requirements for the degree of PhD

Signed Sarah Fyson (candidate) Date 19/8/10

Signed (supervisor) Date

Statement 2

This thesis is the result of my own independent work/investigation, except where otherwise stated (see page 4). Other sources are acknowledged by explicit references.

Signed Sarah Fyson (candidate) Date 19/8/10

Signed (supervisor) Date

Statement 3

I hereby give consent for my thesis, if accepted, to be available for photocopying and for inter-library loan, and for the title and summary to be made available to outside organisations.

Signed Sarah Fyson (candidate) Date 19/8/10

Signed (supervisor) Date

Summary

Typical absence seizures are characteristic of many idiopathic generalised epilepsies and the only seizure-type in childhood absence epilepsy. We know that absence seizures arise in thalamocortical networks and that GABAergic agents exacerbate or induce absences. Furthermore, raised levels of GABA have been identified in the ventrobasal thalamus in an established genetic animal model (genetic absence epilepsy rats from Strasbourg; GAERS), which was later suggested as a result of aberrant GABA uptake.

I have shown that enhanced tonic GABA_A current in TC neurons of the VB is a common phenomenon across genetic and pharmacological models of absence seizures. Furthermore, my data show that increased extrasynaptic GABA_AR (eGABA_AR) function in the VB is both sufficient and necessary to induce SWDs. This is supported by the fact that focal intrathalamic application of a selective agonist for eGABA_ARs, THIP, was sufficient to elicit SWDs in normal animals and that mice lacking eGABA_ARs were resistant to absence seizure induction by γ -butyrolactone.

Moreover, I have presented data that directly implicate aberrant type-1 GABA transporters (GAT-1) in SWD generation *in vivo*, with GAT-1 knockout mice exhibiting spontaneous SWDs and focal thalamic administration of the GAT-1 blocker, NO711, inducing SWDs in normal rats; a potential new model of absence epilepsy.

In addition, my data indicate that activation of postsynaptic GABA_BRs enhances tonic GABA_A current, presumably via the G_{i/o} protein coupled adenylyl cyclase pathway, which was present under control conditions and occurred in several brain areas. This postsynaptic GABA_B-eGABA_AR link is further supported by the fact that GBL failed to induce SWDs in δ -subunit knockout mice.

Thus, one of the cellular thalamic pathologies that characterises absence seizures is an astrocyte-specific aberrant GAT-1 with the resulting elevated extracellular GABA level enhancing tonic GABA_A current through two mechanisms: direct activation of high affinity eGABA_ARs and indirect increase in eGABA_AR function due to activation of postsynaptic GABA_BRs.

Collaborations

Sections of this thesis were formed in collaboration with other members of Professor Vincenzo Crunelli's laboratory:

- Data for Chapter 3.3.1, Figure 3.1 and 3.2 and Table 3.1 were recorded by Dr. David Cope.
- Professor Giuseppe DiGiovanni and Gergely Orban were involved in recording data for Chapter 4.

Acknowledgements

I would like to thank a number of people who have helped me throughout this PhD:

Firstly, Professor Vincenzo Crunelli for giving me the opportunity to do this PhD, for his support when things were tough, for encouraging me when things were good and for always having his door open.

Dr. David Cope for teaching me patch-clamp technique, for patiently listening to my stupid questions and from whom I have learnt that you don't have to be loud to be heard.

Thanks to Dr. Adam Errington for his friendship, willingness to help and to his mind that never switches-off.

Dr. Magor Lorincz and Dr. Gergely Orban for teaching me *in vivo* techniques. In particular, thanks to Gergely for the Hungarian snacks and to Magor for getting the H₂O₂ off my face so quickly!

Thanks to Professor Giuseppe DiGiovanni for his friendship and ability to bring the best out in everyone. For making me belly-laugh when we were “breaking our balls” together at our rigs and for creating a memory that will make me laugh forever.

To Tim Gould for being human. For our laughs, our rants, his kindness, thoughtfulness and for always having chocolate.

To the ladies that have given me sanity when the testosterone became too much: Jill Watson, Dr. Katja Burk, Anne Kirtly, Dr. Saj Jaffer and in particular, Sam Austen. For lunches, for understanding, for their strength and resilience. Sam – for just “getting it”.

I would like to thank my family for making me who I am today, their support and belief. There isn't enough room to list them all, but I appreciate every single one of them, very much. Thanks to Pauline, Des and G'ma for providing the best escape in the world; to the Banwen Witches for wine-soaked moments in the kitchen; to Dad (Ron) for his sound and practical advice, genuine interest and support; to Nanny B for trying her hardest to understand, her energy and pride; to Dad (Craig) for telling me that I didn't have to do it, his support and for suggestions of what to do when everything felt FUBAR, and my Mum a.k.a “Warrior Woman”, who has felt everything that I have felt everyday, both as a Mum and as a best friend... thanks for our 6th sense and infallible or “inflammable” force. In particular, thanks to my Mum and Dad for “seeing the light” and for knowing me so well.

Last but by no means least, I would like to say thank you to Dom. For his unrelenting positivity, tireless understanding and unquestioning support. For making me smile when I really didn't want to or even think that I could. For cooking. For letting me be right when I really needed to be. For procrastinating with me to make me work sooner. For making me sleep. For putting up with the long hours, many tears and “Scary Sarah”. For always knowing what to say and seeing the other side of every argument. For his unconditional love and friendship. Thank you.

Table of Contents

<u>Chapter 1: General introduction</u>	15
1.0 Epilepsy	16
1.1 Childhood absence epilepsy	17
1.1.1 Absence seizures	17
1.1.2 Incidence and genetic aetiology of childhood absence epilepsy	18
1.1.3 Clinical ictal symptoms of childhood absence epilepsy	20
1.1.4 EEG appearance of absence seizures	21
1.1.5 Treatment of childhood absence epilepsy	21
1.1.5.1 Working mechanisms of drugs used to treat CAE	23
1.1.6 Prognosis of childhood absence epilepsy	24
1.2 Animal models of childhood absence epilepsy	24
1.2.1 Genetic models of absence epilepsy	25
1.2.1.1 Rats	26
1.2.1.2 Mice	27
1.2.2 Pharmacological models of absence epilepsy	29
1.2.2.1 GHB model	29
1.2.2.1.1 Introduction to GHB	29
1.2.2.1.2 GHB-induced absence seizures	31
1.2.2.2 Penicillin model	33
1.2.2.3 THIP model	33
1.3 The thalamus	35
1.3.1 Gross anatomy of the thalamus	35
1.3.2 Thalamic relay nuclei and their connectivity	37
1.3.2.1 TC neurons of the ventrobasal thalamus	38
1.3.2.2 Neurons of the NRT	39
1.3.2.3 Neurons of the somatosensory cortex	40
1.3.2.4 Diffusely projecting inputs to the thalamus	41
1.3.3 Membrane currents of thalamic neurons	41
1.3.3.1 Na ⁺ currents	42
1.3.3.2 Ca ²⁺ currents	42
1.3.3.3 Mixed cation current	43
1.3.3.4 K ⁺ currents	44
1.3.4 Electrophysiology of TC neurons	44
1.3.4.1 Tonic firing	45
1.3.4.2 Burst firing	45
1.3.5 Synaptic physiology of thalamic circuitry	46
1.4 SWD mechanism	46
1.4.1 Thalamocortical loop involvement in absence seizures	46
1.4.2 Cellular activity during an absence seizure	51
1.4.2.1 Cortex	51
1.4.2.2 NRT	52
1.4.2.3 Ventrobasal thalamus	54
1.5 GABA	57
1.5.1 GABA _A receptors	58
1.5.1.1 Synaptic GABA _A receptors	59
1.5.1.2 Extrasynaptic GABA _A receptors	59
1.5.2 GABA _B receptors	65

1.5.2.1 G-protein coupled metabotropic receptors	65
1.5.2.2 G-proteins	68
1.5.2.3 Cellular localisation of GABA _B receptors	69
1.5.2.4 Function of GABA _B receptors	71
1.5.3 GABA and absence seizures	74
1.5.3.1 Human genetics	74
1.5.3.2 Interplay of GABA with absence seizures	74
1.6 Aims	76
<u>Chapter 2: Methods</u>	78
2.1 <i>In vitro</i> experiments: whole-cell patch clamp recordings	79
2.1.1 Animals	79
2.1.2 Slice preparation	79
2.1.3 Whole-cell patch clamp recordings	80
2.1.3.1 Cell identification	81
2.1.3.2 Pipettes	82
2.1.3.3 Obtaining whole-cell patch	82
2.1.4 Isolation of GABA _A currents	84
2.1.5 Experimental protocol	85
2.1.5.1 Short protocol	85
2.1.5.2 Long protocol	85
2.1.6 Data acquisition	87
2.1.7 Data analysis	87
2.1.7.1 Tonic GABA _A current	87
2.1.7.1.1 Analysis of tonic current amplitude in the short protocol	88
2.1.7.1.2 Analysis of tonic current amplitude in the long protocol	89
2.1.7.1.3 Normalised tonic GABA _A current	89
2.1.7.2 IPSC analysis	90
2.2 <i>In vivo</i> experiments: Reverse microdialysis and EEG recordings	90
2.2.1 Animals	91
2.2.1.1 Rats	91
2.2.1.2 Mice	91
2.2.1.3 Genotyping mutant mice	91
2.2.2 Anaesthesia and analgesia	92
2.2.3 Surgical procedures	93
2.2.3.1 Surgical procedures: Implanting EEG electrodes in rat	93
2.2.3.2 Surgical procedures: Implanting microdialysis probes in rat	94
2.2.3.3 Surgical procedures: Implanting EEG electrodes in mice	94
2.2.4 Experimental protocols	94
2.2.4.1 EEG recording	95
2.2.4.1.1 EEG recording: GAERS and NEC	95
2.2.4.1.2 EEG recording: GAT-1 knockout mice	96
2.2.4.1.3 EEG recording: δ -subunit knockout mice	96
2.2.4.2 Reverse microdialysis and EEG recording	96
2.2.4.2.1 Microdialysis probes	96
2.2.4.2.2 Recording protocol	96
2.2.4.2.3 Behavioural observations	98
2.2.5 Data analysis	99

2.2.5.1 SWD identification	99
2.2.5.2 SWD frequency analysis	99
2.2.5.3 Quantification of SWDs	99
2.3 Drugs	100
2.3.1 Sources of drugs	100
2.3.2 Drugs into solution	100
<u>Chapter 3: Tonic GABA_A current in models of typical absence epilepsy</u>	102
3.1 Introduction	103
3.2 Methods	104
3.3 Results	104
3.3.1 Enhanced tonic GABA _A current in GAERS	104
3.3.2 SWD-inducing agents enhance tonic GABA _A current in VB TC neurons	108
3.3.2.1 GHB enhances tonic GABA _A current	108
3.3.2.2 GHB enhances tonic GABA _A current via GABA _B Rs	111
3.3.2.3 The δ -subunit specific agonist THIP enhances tonic GABA _A current	115
3.3.3 A specific GABA _B antagonist reduces tonic GABA _A current in GAERS	119
3.3.4 Penicillin has no effect on tonic GABA _A current	122
3.4 Discussion	125
3.4.1 Enhanced tonic current in GAERS	125
3.4.2 Processes underlying augmented tonic GABA _A current in the VB of GAERS	127
3.4.3 GHB-induced increase of eGABA _A R-mediated inhibition	130
3.4.3.1 Simultaneous GHB effects at the presynaptic terminals	132
3.4.3.2 GHB action and possible receptor heterogeneity	133
3.4.4 THIP-induced increase of tonic GABA _A inhibition	134
3.4.5 GABA _B antagonist reduction of tonic GABA _A current in GAERS	135
3.4.6 Penicillin failed to enhance tonic GABA _A current	136
3.5 Conclusion	139
<u>Chapter 4: Extrasynaptic GABA_AR gain-of-function in the ventrobasal thalamus is crucial for SWD generation <i>in vivo</i></u>	140
4.1 Introduction	141
4.2 Methods	141
4.2.1 Principles and methodological considerations of reverse microdialysis	142
4.3 Results	145
4.3.1 Enhanced eGABA _A R function is sufficient for absence seizures	145
4.3.2 δ -subunit containing eGABA _A Rs are essential for SWD generation	152
4.3.3 Blocking GABA uptake via GAT-1 in the VB provokes absence seizures	158
4.3.4 GAT-1 knockout mice exhibit spontaneous absence seizures	164
4.4 Discussion	168
4.4.1 eGABA _A R gain-of-function induces SWDs	168
4.4.2 eGABA _A Rs are required for the appearance of absence seizures	172
4.4.3 Block of GABA uptake in the VB results with SWDs	173
4.4.4 Spontaneous absence seizures observed in GAT-1 knockout mice	177
4.4.5 Parameters of SWDs vary across strains and pharmacological induction	178
4.5 Conclusion	178

<u>Chapter 5: Postsynaptic GABA_B receptors facilitate eGABA_A receptor function</u>	180
5.1 Introduction	181
5.2 Methods	181
5.3 Results	182
5.3.1 Baclofen dose-dependently enhances tonic GABA _A current	182
5.3.2 Postsynaptic GABA _B Rs modulate eGABA _A Rs under control conditions	187
5.3.3 Baclofen increases tonic GABA _A current independently of K ⁺ channels	190
5.3.4 GABA _B receptors modulate tonic GABA _A current in several brain regions	194
5.4 Discussion	197
5.4.1 Baclofen effects on mIPSCs and tonic GABA _A current	197
5.4.2 Baclofen augments tonic GABA _A current at the postsynaptic membrane and independently from K ⁺ conductance through GIRK channels	198
5.4.3 Postsynaptic GABA _B Rs tonically modulate eGABA _A Rs	201
5.4.4 Postsynaptic GABA _B R facilitation of eGABA _A function is ubiquitous	201
5.4.5 Potential intracellular pathways of GABA _B -eGABA _A R interaction	202
5.5 Conclusion	205
<u>Chapter 6: General discussion</u>	206
6.1 Summary of findings	207
6.2 Role of enhanced tonic GABA _A current in the pathophysiological mechanisms of absence seizures	208
6.3 GABA transporters and absence seizures	209
6.4 Sensitivity of absence seizures to GABA _B antagonists	211
6.5 Physiological role of the postsynaptic GABA _B -eGABA _A R link	213
6.6 The future direction of investigations	215
<u>References</u>	217
<u>List of publications</u>	246
<u>DVD</u>	Back Cover

Figures

Chapter 1: Introduction

1.1 A simplified illustration of the major divisions between seizure types	17
1.2 Appearance of a SWD	22
1.3 Gross organisation of the thalamus	36
1.4 Schematic representation of the principle circuitry and connections of thalamic relay nuclei	38
1.5 Intrinsic electrophysiological properties of TC neurons	43
1.6 Intracellular activities during a SWD	48
1.7 SWDs are initiated in the facial somatosensory cortex	50
1.8 Hyperactivity of layer V/VI cortical focus neurons	52
1.9 Intracellular activity of NRT neurons during a SWD	54
1.10 TC neurons of the VB are inhibited during a SWD	56
1.11 GABA synthesis and metabolism	57
1.12 Schematic illustration of an ionotropic GABA _A receptor	60
1.13 Phasic and tonic GABA _A inhibition	63
1.14 Metabotropic GPCR activation	67
1.15 Amplification in signal transduction pathways	69
1.16 Schematic representation of the GABA _B receptor	72

Chapter 2: Methods

2.1 Schematic illustration of typical recordings under short (A) and long (B) protocols	86
2.2 Microdialysis probe and guide cannula	95
2.3 Microdialysis probe coordinates	98

Chapter 3: Tonic GABA_A current in models of typical absence epilepsy

3.1 Increased tonic GABA _A current in GAERS	105
3.2 Developmental profile of tonic GABA current in NEC and GAERS	106
3.3 GHB enhances tonic GABA _A current in Wistar TC neurons	109
3.4 GHB dose-dependently enhances tonic GABA _A inhibition	112
3.5 Comparison of tonic GABA _A current amplitudes with varying concentrations of GHB, CGP55845 and NCS382	113
3.6 The δ -subunit GABA _A agonist THIP enhances tonic GABA _A current	116
3.7 Comparison of tonic with varying concentrations of THIP	117
3.8 A specific GABA _B receptor antagonist reduces tonic GABA _A current in GAERS	120
3.9 Tonic GABA _A current in the presence of penicillin	123

Chapter 4: Extrasynaptic GABA_AR gain-of-function in the ventrobasal thalamus is crucial for SWD generation *in vivo*

4.1 Selective activation of thalamic extrasynaptic GABA _A receptors initiates absence seizures	146
4.2 THIP elicits ETX-sensitive SWDs	149

4.3 Properties of THIP-induced SWDs	151
4.4 δ -containing extrasynaptic GABA _A Rs are essential for SWD generation	153
4.5 GBL does not elicit SWDs in GABA _A R δ -subunit knockout mice	156
4.6 Selective block of GAT-1 in the VB elicits absence seizures	159
4.7 Block of GAT-1 in the VB induces ETX-sensitive SWDs	162
4.8 GAT-1 knockout mice exhibit spontaneous absence seizures	165
4.9 Spontaneous SWDs in GAT-1 knockout mice are sensitive to ETX	166
4.10 GAERS and NEC EEG	167
4.11 Tonic current amplitudes in TC neurons of the VB in GAERS and NEC in the presence of GAT blockers	174

Chapter 5: Postsynaptic GABA_B receptors facilitate eGABA_A receptor function

5.1 Baclofen enhances tonic GABA _A current in Wistar TC neurons of the VB	183
5.2 Baclofen dose-dependently increases tonic GABA _A current	185
5.3 Baclofen increases tonic GABA _A current through GABA _B Rs	188
5.4 Facilitation of eGABA _A Rs by baclofen occurs independently of K ⁺ channel activity	191
5.5 GABA _B R modulation of tonic GABA _A occurs in several brain areas	195
5.6 Schematic illustration of the potential signalling cascade leading to activation of eGABA _A Rs by GABA _B Rs	204

Tables

Chapter 1: Introduction

1.1 Generalised seizure types	19
1.2 Mutations associated with childhood absence epilepsy	20
1.3 Features of seizures in rat genetic models of absence epilepsy	28
1.4 Features of seizures in mouse genetic models of absence epilepsy	30
1.5 Features of seizures in pharmacological models of absence epilepsy	34

Chapter 2: Methods

2.1 Table showing the concentration of compounds in aCSF solutions	81
--	----

Chapter 3: Tonic GABA_A current in models of typical absence epilepsy

3.1 Comparison of sIPSC parameters in TC neurons of NEC and GAERS	107
3.2 Comparison of mIPSC parameters in TC neurons of Wistar rats in the presence of GHB (3mM) under long protocol	110
3.3 Comparison of mIPSC parameters in TC neurons from Wistar rats in the presence of various drugs under short protocol	114
3.4 Comparison of mIPSC parameters in TC neurons from Wistar rats in the presence of different concentrations of THIP	118
3.5 Comparison of mIPSC parameters in TC neurons from GAERS and NEC under control conditions and in the presence of CGP55845	121
3.6 Comparison of mIPSC parameters in TC neurons from Wistar rats in the presence of varying concentrations of penicillin	124

Chapter 5: Postsynaptic GABA_B receptors facilitate eGABA_A receptor function

5.1 Comparison of mIPSC parameters in TC neurons of Wistar rats in the presence of baclofen (10 μ M) using long protocol	184
5.2 Comparison of mIPSC parameters in TC neurons of Wistar rats in the presence of varying concentrations of baclofen	186
5.3 Comparison of mIPSC parameters in TC neurons of Wistar rats in the presence of various GABA _B receptor antagonists	189
5.4 Comparison of mIPSC parameters in TC neurons of Wistar rats with K ⁺ channels blocked	193
5.5 Comparison of mIPSC parameters in CGC and DGGC neurons of Wistar rats in the presence of baclofen and CGP55845	196

Abbreviations

AC	Adenylate cyclase
aCSF	Artificial cerebral spinal fluid
AMPA	α -amino-3-hydroxy-5-methyl-isoxazolepropionic acid
CAE	Childhood absence epilepsy
cAMP	Cyclic adenosine monophosphate
CBZ	Carbamazepine
CGC	Cerebellar granule cell
CNS	Central nervous system
dLGN	Dorsal lateral geniculate nucleus
DGGC	Dentate gyrus granule cell
EPSC	Excitatory postsynaptic current
EPSP	Excitatory postsynaptic potential
EEG	Electroencephalogram
eGABA _A R	Extrasynaptic GABA _A receptor
ETX	Ethosuximide
fMRI	Functional magnetic resonance imaging
FS	Febrile seizures
FS+	Febrile seizures plus
GABA	γ -aminobutyric acid
GABA _A R	γ -aminobutyric acid receptor type A
GABA _B R	γ -aminobutyric acid receptor type B
GAERS	Genetic absence epilepsy rats from Strasbourg
GAD	Glutamate acid decarboxylase
GAT	GABA transporter
GAT-1	GABA transporter type 1
GAT-3	GABA transporter type 3
GBL	γ -butyrolactone
GBZ	Gabazine (SR95311)
GEFS	Generalised epilepsy with febrile seizures
GDP	Guanosine diphosphate
GHB	γ -hydroxybutyrate
GHBR	γ -hydroxybutyrate receptor
G _i _o	Inhibitory G-protein
GIRK	G protein-coupled inward rectifying potassium channel
GPCR	G protein-coupled receptor
GTP	Guanosine triphosphate
I _T	T-type Ca ²⁺ current
IPSC	Inhibitory postsynaptic current
IPSP	Inhibitory postsynaptic potential
IGE	Idiopathic generalised epilepsy
ILAE	International league against epilepsy
i.p.	Intra-peritoneum
IM	Intra- muscular
JAE	Juvenile absence epilepsy
JME	Juvenile myoclonic epilepsy
KCl	Potassium chloride
KO	Knock-out

LTCP	Low-threshold Ca ²⁺ potential
<i>lh</i>	Lethargic mutant mouse
LGN	Lateral geniculate nucleus
LFP	Local field potential
mIPSC	Miniature inhibitory postsynaptic current
MoCtx	Motor cortex
mGluR	Metabotropic glutamate receptor
NEC	Non-epileptic control
NMDA	N-methyl-D-aspartate
NRT	Nucleus reticularis thalami
PTx	Pertussis toxin
PET	Positron emission tomography
PKA	Protein kinase A
PKC	Protein kinase C
PTZ	Pentylentetrazol
PMDD	Premenstrual dysphoric disorder
S1	Somatosensory cortex area 1
S2	Somatosensory cortex area 2
SoCtx	Somatosensory cortex
SSADH	Succinic semialdehyde dehydrogenase
<i>stg</i>	Stargazer
SWC	Spike-and-wave complex
SWD	Spike-and-wave discharge
<i>tg</i>	Tottering mutant mouse
TC	Thalamocortical
TTX	Tetrodotoxin
TM	Transmembrane
WAG/Rij	Wistar albino Glaxo laboratory rats from Rijswijk
WT	Wild-type
VB	Ventrobasal complex
VPL	Ventroposterolateral
VPM	Ventroposteromedial
5-HT	5-Hydroxytryptamine (serotonin)

Chapter 1

General Introduction

1.0 Epilepsy

Excessive and hypersynchronous electrical activity among neurons underlie recurrent and unprovoked epileptic seizures, which are characteristic of the chronic neurological disorder known as epilepsy (Blume et al., 2001; Engel, 2006a & b; Fisher et al., 2005). Since these transient electrical discharges interrupt normal brain function, an epileptic seizure manifests in a patient through a temporary change of movement, awareness and behaviour. Identifying a seizure-type involves examination of epileptic seizures or “ictal” and inter-ictal electrical discharges in the electroencephalogram (EEG), alongside the expression of clinical ictal behaviour. Precise identification of ictal events reveals aetiology of the seizure, thus implicate diagnosis and treatment of an epilepsy disorder (Engel, 2001). The involvement of more than one seizure type defines an epilepsy “syndrome” (Engel, 2001); whereas the definition of epilepsy requires the occurrence of one epileptic seizure and/or one epileptic seizure type (Fisher et al. 2005). Overall, epilepsy is not one condition, but is a diverse family of disorders that all cause transient interruption of ordinary brain activity.

Many factors such as age, presence of brain damage or disease, behavioural and cognitive manifestations, electrographic pattern of a seizure and incidence of one or more seizure type, impact on the final diagnosis of an epilepsy. To overcome such complexities, the International League Against Epilepsy (ILAE) established standardised characterisations and terminology for epileptic seizures (ILAE Commission: classification of epileptic seizures, 1981) and syndromes (ILAE Commission: classification of epileptic syndromes, 1989). These classifications took significant steps to simplify identification and treatment of epilepsies and provided a universal vocabulary that not only facilitated communication among clinicians, but also established a foundation for performing quantitative clinical and basic research (Engel, 2001). Terminologies have since been reviewed and revised (Engel, 2001 & 2006), and these up-to-date characterisations have been used throughout this thesis.

The ILAE primarily classifies epilepsies by segregating seizures along 2 divisions: focal onset versus generalised onset and idiopathic aetiology versus symptomatic aetiology (Engel, 2001 & 2006a, b) (Fig. 1.1). A study investigating a transition between focal and generalised seizures using video EEG of patients that had idiopathic generalised

epilepsy found that some focal brain abnormalities existed in patients with “generalised” epilepsies (Leutmezer et al., 2002). This study as well as many others, emphasises the use of caution in diagnosing patients who suffer with epilepsy and highlights that seizures do not always fit into the stringent dichotomy between focal and generalised seizures (Leutmezer et al., 2002). Overlap across the two divisions has been addressed by the ILAE characterisation of epilepsy (ILAE Commission: classification of epileptic seizures and syndromes, 1981 & 1989; Blume et al., 2001; Engel, 2001). For instance, Lennox-Gastaut Syndrome consists of generalised seizures that can have a symptomatic aetiology (ILAE Commission: classification of epileptic syndromes, 1989).

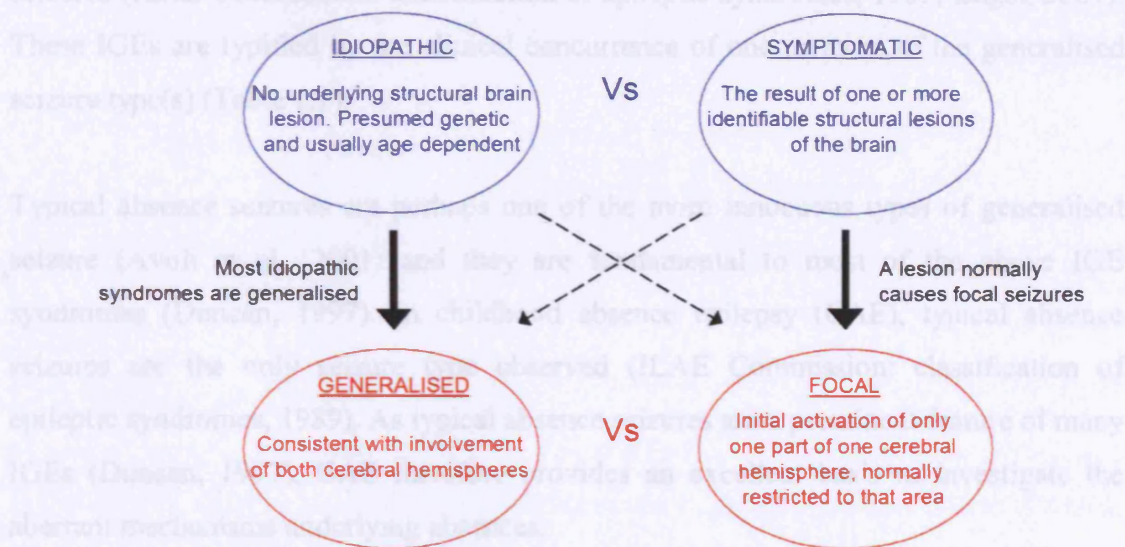


Figure 1.1

Simplified illustration of the major divisions between seizures types

Blue circles correspond to seizure aetiology and red circles correspond to seizure onset. Dotted lines represent those seizure types that overlap these divisions. Modified from Blume et al., 2001; Engel., 2001 and ILAE Commission: classification of epileptic seizures and syndromes, 1981 & 1989.

1.1 Childhood Absence Epilepsy

1.1.1 Absence seizures

Generalised epileptic disorders are characterised by seizures where synchronous abnormal activity is recorded in both hemispheres at seizure onset and are often the

expression of a hereditary predisposition i.e. idiopathic (ILAE Commission: classification of epileptic syndromes, 1989) (Fig. 1.1). Idiopathic epilepsies are categorised according to the age of onset, clinical and EEG characteristics and genetic aetiology (Commission on Classification and Terminology: classification of epileptic syndromes, 1989). According to the ILAE definition, idiopathic generalised epilepsies (IGEs) consist of the following syndromes: benign myoclonic epilepsy in infancy; epilepsy with myoclonic astatic seizures; childhood absence epilepsy; idiopathic generalised epilepsies with variable phenotypes, including juvenile absence epilepsy (JAE), juvenile myoclonic epilepsy (JME), and epilepsy with generalised tonic-clonic seizures only; epilepsy with myoclonic absences and generalised epilepsies with febrile seizures (ILAE Commission: classification of epileptic syndromes, 1989; Engel, 2001). These IGEs are typified by the clinical concurrence of one or more of the generalised seizure type(s) (Table 1.1).

Typical absence seizures are perhaps one of the more innocuous types of generalised seizure (Avoli et al., 2001) and they are fundamental to most of the above IGE syndromes (Duncan, 1997). In childhood absence epilepsy (CAE), typical absence seizures are the only seizure type observed (ILAE Commission: classification of epileptic syndromes, 1989). As typical absence seizures are a prominent feature of many IGEs (Duncan, 1997), CAE therefore provides an excellent basis to investigate the aberrant mechanisms underlying absences.

1.1.2 Incidence and genetic aetiology of childhood absence epilepsy

In childhood absence epilepsy (CAE), absences begin between the ages of 2 and 8 years and peak at ~5 years (ILAE Commission: classification of epileptic syndromes, 1989). The annual incidence is low and may vary from 1.8 to 8 per 100,000 children below the age of 16 years (Loiseau et al., 1990; Panayiotopolous, 1997) and the prevalence is in the range of 2–10% of children with epileptic disorders (Panayiotopolous, 1997). Girls are believed to be at twice the risk of developing CAE than boys (Panayiotopolous, 1997); however some studies have suggested that boys and girls are equally affected (Rocca et al., 1987). Genetic concordance for absences is high, with around 70-85% of monozygotic twins (Berkovic et al., 1994) and 33.3% of close relatives (Bianchi et al., 1995) exhibiting seizures. Additionally, the impact of exogenous factors on CAE induction is believed to be minimal (Panayiotopolous, 1997).

Generalised seizure type	Clinical features of ictal activity	EEG
Typical absence seizures	Loss of consciousness for 4-30 seconds, no aura, no postictal state, only a few automatisms	Spike and slow wave discharges (SWDs)
Tonic seizures	Sudden onset, tonic extension (rigidity) of head and trunk that lasts several seconds; also related to drowsiness	Beta "Buzz"
Myoclonic seizures	Brief (<1 sec) arrhythmic jerks that cluster within a few minutes; may evolve into rhythmic jerking movements (clonic seizures).	Fast polyspike and slow wave complexes
Atonic seizures	Brief loss of postural tone which causes patient to fall	Similar to tonic Seizures
Generalised tonic-clonic seizures (GTCS)	"Grand mal" epilepsy; several motor behaviours – tonic then clonic seizures; prolonged postictal confusion	Bilateral complexes of spikes, polyspikes and slow waves

Table 1.1

Generalised seizure types

Modified from ILAE Commission: classification of epileptic syndromes (1989) and Engel (2001). Additional generalised seizure types include: atypical absence seizures, clonic seizures, eyelid myoclonia, and atonic seizures.

This incomplete penetrance suggests a multifactoral genetic disposition and that CAE has a complex polygenic genotypic aetiology (Crunelli & Leresche, 2002a). A population-based case-control meta-analysis study of risk factors for absence seizures found that a history of febrile seizures was significantly linked to absences (Rocca et al., 1987). It was suggested that these febrile seizures may be the first expression of a seizure diathesis (Rocca et al., 1987) and therefore any genetic aetiology revealed for febrile seizures could aid further identification of a genetic mutation linked to absence seizures. So far, a GABA_AR γ 2 subunit mutation at chromosome 5 has been identified in patients with CAE (Table 1.2), however the families sampled had CAE in combination with febrile seizures (FS) and generalised epilepsy with febrile seizures plus (GEFS+) (Wallace et al., 2001). In addition, a different GABA_AR γ 2 subunit

mutation in chromosome 5 has been detected in another family which express FS/GEFS+ only (Baulac et al., 2001), thus these mutations may have a stronger link with FS/GEFS+, than CAE (Crunelli & Leresche, 2002a).

Receptor or channel (gene)	Chromosomal locus	Effect of mutant protein	Pedigree	Phenotype
GABA _A receptor $\gamma 2$ subunit (GABRG2)	5q31.1-33.1 (R43Q)	Loss of BDZ-mediated potentiation of GABA _A receptor No effect on GABA action	1 family	7 CAE (6 with previous FS), 12 FS, 3 FS+, 7 with more severe IGE/other epilepsies
GABA _A receptor $\gamma 2$ subunit (GABRG2)	5q31.1-33.1 (K289M)	Loss of GABA action No effect on BDZ-mediated potentiation of GABA _A receptor	1 family	13 FS, 7 GEFS+

Table 1.2

Mutations associated with childhood absence epilepsy

Taken from Crunelli & Leresche (2002a). BDZ, benzodiazepine; FS, febrile seizures; FS+, febrile seizures plus and GEFS+, generalised epilepsy with febrile seizures plus. References: top row, Wallace et al (2001); bottom row, Baulac et al (2001).

1.1.3 Clinical ictal symptoms of childhood absence epilepsy

1. Absences can occur between tens to ~200 times a day (ILAE Commission: classification of epileptic syndromes, 1989);
2. Episodes consist of an abrupt loss of and regained consciousness, through which there is a blank stare, brief loss of awareness, unresponsiveness and cessation of activity with no, or minimal, motor manifestation, lasting from anywhere between 4 and 30 seconds (ILAE Commission: classification of epileptic syndromes, 1989; Panayiotopoulos et al., 1989; Sadleir et al., 2006);
3. When consciousness returns, after a momentary lapse, the child will return to the task at hand i.e. no aura or post-ictal state (Panayiotopoulos et al., 1989);
4. Shortly after onset of spike-wave activity, upward deviation of the eyes, temporary and rhythmic blinking of the eyelids (3Hz) and automatism that include mild jerks of facial muscles around the mouth, can occur (Panayiotopoulos et al., 1989; Sadleir et al., 2006). The eyes may stare, but they will also move during an episode, particularly if they are called loudly by name (Panayiotopoulos et al., 1989; Sadleir et al., 2006). These ictal behaviours are not considered stereotypical of CAE because they are only present in two thirds of cases (Panayiotopoulos et al., 1989);

5. Absences are easily precipitated by hyperventilation in 90% of cases, a tool sometimes used during clinical examination (Panayiotopoulos, 1997). Such over-breathing stops within 3 seconds from seizure onset (Panayiotopoulos et al., 1989);
6. Absence seizures occur regularly in states of decreased or fluctuating vigilance i.e. during quiet wakefulness, inattention and in the transition between sleep and awakening (Shouse et al., 1996; Shouse & Silva, 1997; Laufs et al., 2006; Nobili et al., 2001), and
7. Sufferers of CAE lack any abnormal development or neurological state (ILAE Commission: classification of epileptic syndromes, 1989).

1.1.4 EEG appearance of absence seizures

The EEG of CAE has a normal background with ictal discharges consisting of bilateral, synchronous and high-amplitude spike or double spike and slow-wave complexes (SWCs) (Panayiotopoulos et al., 1989). These spike-and-wave discharges (SWDs) have an abrupt onset and cessation (Fig. 1.2). They are rhythmic and have a frequency around 3Hz (2.7–4 Hz), with a gradual and smooth decline in frequency (0.5–1 Hz) towards the end of the discharge (Sadleir et al., 2006). The opening phase of the seizure is normally fast and often difficult to determine, however the remaining discharge is regular, with well formed spikes that retain a constant oscillatory relationship with slow waves (Panayiotopoulos et al., 1989). The duration is usually around 10-12 seconds (average 9.4 seconds), but no less than 4 seconds (Sadleir et al., 2006).

1.1.5 Treatment of childhood absence epilepsy

Ethosuximide and sodium valproate (the sodium salt of valproic acid) are equally successful at treating absence seizures, achieving suppression in 70-80% of patients (Richens, 1995; Schachter, 1997). Sodium valproate is often preferred by clinicians as it also controls GTCs, however for CAE this is not a concern (Panayiotopoulos, 1997). If one of these drugs does not control the absences, it is common to change to the other and if this is not successful then a combination of both ethosuximide and sodium valproate can be used (Duncan, 1997; Schachter, 1997). Another drug identified to successfully treat absence seizures is lamotrigine. If typical absence seizures remain intractable, then a combination drug therapy of lamotrigine and sodium valproate can be administered (Panayiotopoulos et al., 1993; Schachter, 1997; Schlumberger et al., 1994). It should be noted that ethosuximide and sodium valproate are more effective

than lamotrigine in the treatment of childhood absence epilepsy (Glauser et al., 2010). After two years free of absence seizures, medication can gradually be withdrawn over a 3 to 6 month period (Panayiotopoulos, 1997).

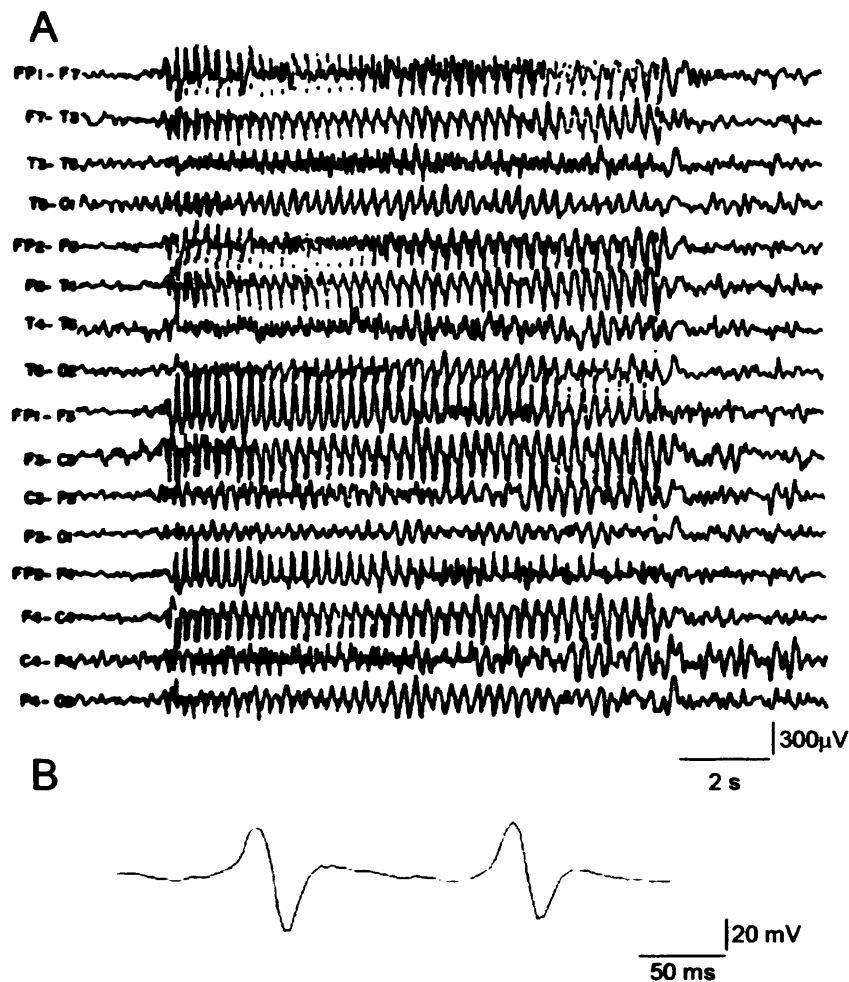


Figure 1.2

Appearance of a SWD

A) EEG recording of a typical absence seizure from an 8 year-old girl with childhood absence epilepsy. The seizure was induced by hyperventilation. The EEG discharge is rhythmic with gradual slowing from the opening to the terminal phase. Taken and modified from Panayiotopolous et al (1989). B) Two spike-and-wave complexes in the EEG of an animal that spontaneously expresses absence seizures. Taken and modified from Charpier at al (1999).

Phenytoin, barbiturates, carbamazepine (CBZ), vigabatrin and tiagabine all exacerbate absence seizures (Perucca et al., 1998; Schachter, 1997) and in some cases, these agents can induce clinical absence seizures. For instance, Ettinger et al (1999) found that patients receiving treatment for partial convulsive seizures using tiagabine, developed absence seizures when they had no prior history of SWDs.

1.1.5.1 Working mechanisms of drugs used to treat CAE

Ethosuximide: Studies have shown that ethosuximide reduces the amplitude of the T-type Ca^{2+} channel current (I_T) that underlies the low-threshold Ca^{2+} potential (LTCP) in ventrobasal (VB) and NRT neurons (see Section 1.3.3.2 for full description), with no changes to its kinetics or steady-state properties (Coulter et al., 1989a, b & 1990; Huguenard and Prince, 1994). Discrepancies on the action of ETX have however been highlighted by alternate studies failing to identify such action and whilst this may be explained through different Ca^{2+} channel subunit expression in some brain areas (Leresche et al., 1998), ETX has failed to act on I_T in thalamic neurons in other experiments (Pfrieger et al., 1992). Indeed, direct thalamic (VB and NRT) application of ETX in GAERS *in vivo* required concentrations above the therapeutic range to reduce SWDs, and did so after a significant delay (Richards et al., 2003). In the same study however, systemic application of ETX produced an immediate and substantial reduction of SWDs in GAERS, therefore concomitant or exclusive action at cortical neurons may be necessary for therapeutic reduction of absence seizures (Richards et al., 2003).

ETX has been observed to decrease the persistent Na^+ and sustained K^+ currents in TC and cortical neurones (Leresche et al., 1998; Crunelli and Leresche, 2002b). Furthermore, ETX has been shown to convert hyperactive cortical neurons at the cortical focus site (peri-oral S1; see Section 1.4.3.1) in GAERS into normal firing patterns (Polack et al., 2009). Specifically, ETX caused membrane hyperpolarisation and a decreased firing rate, also suggesting a reduction of a persistent Na^+ current (Polack et al., 2009). Therefore, a reduction of persistent Na^+ current at cortical focus neurons alongside a reduction of I_T amplitude in NRT neurons, as TC cells of the VB are largely silent throughout a SWD (see Section 1.4.3.3), are likely mechanisms through which ETX mediates its anti-absence effects.

Sodium valproate: Sodium valproate is effective against a wide spectrum of epileptic seizures including GTCS and absence seizures (White et al., 1997). *In vitro* studies with sodium valproate demonstrate blockade of sustained repetitive firing in mouse neurons in culture (Mclean & Macdonald, 1986) and reduction of Na⁺ current in neocortical neurons (Zona & Avoli, 1990). In addition, VPA has been shown to reduce T-type Ca²⁺ currents in primary afferent neurons (Kelly et al., 1990). However, this effect was modest and was observed only at high VPA concentrations (White et al., 1997).

Lamotrigine: Like sodium valproate, lamotrigine is a broad-spectrum anticonvulsant in addition to efficacy in treating generalised absence seizures (Pellock, 1994; Stefani et al., 1997). The prominent mechanism of lamotrigine action appears to be mediated through inhibition of voltage-activated Na⁺ channels (Lees & Leach, 1993), inhibiting sustained repetitive action potential firing in mouse cultured spinal cord neurons, in a dose-dependent manner (Cheung et al., 1992) and at presynaptic terminals to reduce glutamate release (Waldmeier et al., 1995). Furthermore, lamotrigine blocks high-voltage activated Ca²⁺ channel currents (Stefani et al., 1996) and weakly blocks I_T in HEK cells containing α 1G and α 1I Ca²⁺ channel subunit (Hainsworth et al., 2003).

1.1.6 Prognosis of childhood absence epilepsy

Overall, prognosis of CAE is good. About 80% of patients become seizure free with medication (Richens, 1995); with a recent study reporting a 93% remission rate (Callenbach et al., 2009). Absence seizures tend to fade spontaneously and progressively during adolescence (Loiseau, 1992). The 20% of sufferers that do not experience full remission go on to develop GTCSs during adolescence and early adulthood (Loiseau, 1992). In fact, there appears to be a direct correlation with the age of CAE onset and remission of seizures (Panayiotopoulos, 1997). Younger patients i.e. onset before 9 years, are more likely to fully remit with only 16% experiencing GTCSs into adolescence, as compared with 44% of patients with absence seizure onset at age 9 or 10 years (Loiseau et al., 1995).

1.2 Animal models of childhood absence epilepsy

As typical absence seizures occur predominantly in children, ethical limitations prevent studying pathophysiological mechanisms in humans (Danober et al., 1998). A number

of animal models of absence seizures have been developed and have advanced our understanding of some of the basic pathophysiologies involved (Snead, 1995). In order for an animal model to be a valid investigative tool, it must exhibit the clinical and pharmacological characteristics that accurately reflect human absence (Danober et al., 1998; Marescaux et al., 1992b; Snead, 1995). Criteria for experimental absence seizures are:

- Bilaterally synchronous SWD and associated behavioural arrest;
- SWDs that originate from the thalamocortical loop;
- Hippocampus is silent throughout the seizure discharge;
- Similar developmental profile with appropriate ontogeny;
- Consistently reproducible and predictable;
- Quantifiable;
- Similar pharmacological profile to the human condition i.e. absence seizures blocked by ethosuximide, sodium valproate, benzodiazepines and lamotrigine and aggravated by CBZ and phenytoin, and
- Absence seizures are exacerbated by GABAergic drugs including GABA transaminase inhibitors as well as GABA_A and GABA_B receptor agonists,

Models exhibiting these clinical and pharmacological features of absence seizure are either experimentally induced or genetically determined. SWDs can be pharmacologically elicited in normal rodents, cats and primates by injection of γ -hydroxybutyrate (GHB), penicillin or a GABA agonist such as 4,5,6,7-tetrahydroisoxazolo-[5,4-C]pyridine-3-ol (THIP). Spontaneous SWDs can be observed in genetic rodent models that include the Genetic Absence Epilepsy Rats from Strasbourg (GAERS) and the Wistar Albino Glaxo rats from Rijswijk (WAG/Rij). Several genetic mouse models have been recognised however the SWDs are normally associated with other neurological discharges and defects. For a full categorisation of the different models see Tables 1.3, 1.4 and 1.5.

1.2.1 Genetic models of absence epilepsy

Several genetic models express the EEG and behavioural changes associated with a SWD and are invaluable tools for investigating cellular mechanisms involved. These

animals spontaneously express recurring and persistent absence seizures; however seizures persist into adulthood and thus do not accurately reflect the human ontogeny.

1.2.1.1 Rats

From an initial breeding colony of Wistar rats, 31% of 6-12 month old animals were identified as presenting spontaneous, bilateral and synchronous electrical discharges accompanied by behavioural arrest and vibrissal twitching (Marescaux et al., 1984 & 1992b; Vergnes et al., 1982). Selecting and cross-breeding these animals resulted in an increased number and incidence of these paroxysms, now known as Genetic Absence Epilepsy Rats from Strasbourg (GAERS) (Danober et al., 1998; Marescaux et al., 1992b; Vergnes et al., 1990). Similarly, a control strain that is free of any spontaneous SWD was outbred, known as non-epileptic control (NEC) animals (Danober et al., 1998; Marescaux et al., 1992b). The advantage of this inbred animal model is that it results from what was a naturally occurring polygenic mutation in otherwise normal Wistar rats, and whilst the genetic mutation(s) has yet to be fully elucidated, these rats display all of the EEG and behavioural manifestations of absences and abrupt nature of the SWD on the EEG (see Table 1.3 for details and Figure 4.10 for SWD on EEG).

The Wag/Rij is an inbred, polygenic mutant rat that is very similar to GAERS, differing only in developmental profile, thus has equal validity as an absence seizure model (Coenen and Van Luijtelaar, 2003) (Table 1.3). The WAG/Rij strain is a subline of the WAG strain that was created from Wistar stock at the Glaxo Laboratories in 1924 and can be compared to the ACI rat, which is an inbred non-epileptic control animal. Whilst these rats display all of the electroencephalographic and behavioural manifestations of absences (Drinkenburg et al., 1993; van Luijtelaar & Coenen, 1986), a disadvantage of the WAG/Rij model is the presence of two rather than one type of SWD in the EEG (van Luijtelaar & Coenen, 1986). This second type of SWD lasts for a shorter time, has a lower frequency, lower incidence, has no obvious clinical manifestation and remains localised at the parietal region of the brain (Midzianovskaia et al., 2001).

The frequency of SWDs in human absence seizures is 2.5-4 Hz, whereas in both GAERS and WAG/Rij it is higher at 7-11 and 7-10 Hz, respectively (Table 1.3). Only in primates is a 3Hz SWD observed during pharmacologically induced absence seizures

(Snead, 1978a), therefore the frequency of SWDs appears to be species specific and should not detract from the value of these rat models (Danober et al., 1998).

Considering the close correspondence of GAERS and WAG/Rij with human absences in ontogeny, arousal state incidence, pharmacological specificity and behavioural correlates of absence seizures, these two rat models provide an excellent basis for investigation of the underlying mechanisms involved in SWD generation.

1.2.1.2 Mice

In the 1960s and 70s, spontaneous genetic mutations were recognized in inbred strains of mice due to expression of abnormal phenotypes. These animals were crossbred and SWDs were revealed by later studies (Table 1.4). The recent identification of mutant genes responsible for the abnormal phenotypes in these animals has added great investigative value to these models (Burgess et al., 1997; Fletcher et al., 1996; Letts et al., 1998).

Whilst these mutant mice have validity as models of absence seizures (see Table 1.5), neurological manifestations of the mutation include additional phenotypic abnormalities. For instance, the stargazer (*stg*) mouse has a vertical “head toss” phenotype resulting from an inner ear defect (Noebels et al., 1990); the lethargic (*lh*) mouse experiences a critical period between 15 days and 2 months of age in which severe immunological defects occur (Dung & Swigart, 1972; Dung et al., 1977) and tottering (*tg*) mice display a splayed stance and hopping gait, a product of cerebellar defects (Noebels & Sidman, 1979). In addition to SWDs, *tg* express a second discharge in the form of spontaneous motor seizures or “paroxymal dyskinesia”. In *tg* mice, these motor seizures occur 1-3 times a day, between 3-90 days of age and usually last between 20-30 minutes (Noebels & Sidman, 1979). The hind limbs are initially involved in a clonic phase, which progressively involves forelimbs and trunk transforming into a tonic-clonic phase.

These motor seizures have much less stereotyped EEG activity than SWDs, however low voltage, desynchronised activity interspersed with 4-7 Hz waves is common (Noebels & Sidman, 1979). Such phenomena are not present in human CAE which suggests that whilst these mouse models have an underlying absence phenotype, they

Model	EEG	Ontogeny	Genotype	Phenotype	Pharmacological Interactions	References
GAERS	Bursts of bilateral, symmetrical & generalised SWDs at 7-11Hz. Abrupt onset and cessation, 2-6 times background activity ¹ ; Restricted to the cortex and lateral thalamus; Excludes the limbic system ^{2,3}	SWDs begin >30 days; At 40 days 30% of animals express SWDs and 100% at 3 months; 1 st SWDs appear at 1 to 2/Hr, for 1-3 secs and at low frequency (4-5 Hz). Number (1/min) and duration (17±10 seconds) reaches maximum levels at 6 and 18 months, respectively ⁴	Dominant inheritance, variability in ontogeny suggests mutation at >1 gene locus ⁵ ; A homozygous missense single nucleotide mutation of the Ca _v 2.2 T-type Ca ²⁺ channel gene recently identified ⁶	SWDs concomitant with immobility, rhythmic twitching of vibrissae and occasional gradual and slight lowering of the head ¹ ; Responsiveness to mild stimuli is lost during paroxysm ¹ ; Reproductive, feeding and social behaviours are normal ⁷ ; SWDs commonly occur during quiet wakefulness and disappear during active arousal ⁸	SWDs are suppressed by ETX and sodium valproate ² ; Vigabatrin, tiagabine and gabapentin aggravate SWDs ^{2,5} ; GABA _A antagonists picrotoxin and bicuculline have no effect ⁵ ; GABA mimetics induce a dose-dependent increase in duration of SWDs ⁵ ; GABA _B agonist baclofen augments, and GABA _B antagonists block SWDs ⁹	¹ Vergnes et al., 1982 ² Marescaux et al., 1984 ³ Vergnes et al., 1990 ⁴ Vergnes et al., 1986 ⁵ Marescaux et al., 1992c ⁶ Powell et al., 2009 ⁷ Vergnes et al., 1991 ⁸ Lannes et al., 1988 ⁹ Marescaux et al., 1992a & d
WAG/Rij	Bursts of bilateral, symmetrical & generalised SWDs at 7-10Hz ^{2,3} ; Start at 9-11Hz and slow to 7-8Hz ¹ ; Abrupt onset and cessation; Not present in hippocampus ^{1,2,3}	SWDs begin >75 days; At 6 months, 100% of animals exhibit SWDs; Occur 16-20/Hr, with a mean duration of 5 seconds (1-30 secs) ⁴	Mendelian inheritance of one dominant gene, with other modulating genes determining the number of SWDs ⁵ ; Abnormal GABA _A R α3 subunit protein expression found in NRT ⁶	SWDs concomitant with immobility, vibrissal twitching, accelerated breathing, head tilting and blinking ¹ ; Sex differences are minimal ⁴ ; SWDs occur predominantly in passive wakefulness and disappear during active wakefulness ^{7,8}	ETX and sodium valproate suppress SWDs ⁹ ; Carbamazepine increase SWDs ⁹ ; The GABA mimetic tiagabine enhances SWDs ¹⁰ ; SWDs facilitated by GABA agonists ¹¹ and blocked by GABA _B antagonists ¹²	¹ Drinkenburg et al., 1993 ² Meeren et al., 2002 ³ van Luijtelaar & Coenen, 1986 ⁴ Coenen & van Luijtelaar, 1987 ⁵ Peeters et al., 1990 ⁶ Liu et al., 2007 ⁷ Drinkenburg et al., 1991 ⁸ van Luijtelaar & Coenen, 1988 ⁹ Peeters et al., 1988 ¹⁰ Coenen et al., 1995 ¹¹ Kaminski et al., 2001 ¹² Peeters et al., 1989

Table 1.3
Features of seizures in rat genetic models of absence epilepsy

may more accurately be representative as models of ataxia (Crunelli & Leresche, 2002a).

Higher frequency of SWDs in these mice may be due to species specific differences (see Section 1.2.1.1), and the sensitivity of these SWDs to GABA mimetics is still lacking. One advantage of these mutant mouse models however is that the gene mutation have been identified. Thus, if allowances are made for the additional phenotypic abnormalities these mice could provide a genetic link, albeit tentative, to CAE.

1.2.2 Pharmacological models of absence epilepsy

Several pharmacological agents are capable of inducing the EEG and behavioural correlates of SWDs. The use of normal animals in such experiments may prove more financially practicable than mutant strains. These pharmacological models are easy to standardise as brain concentrations of a drug can be determined and the administered dose, controlled. However, the transient nature of pharmacological experimental models compared to the genetic models that express recurring and persistent absence seizures could be considered a considerable drawback. Several pharmacological models of absence seizures have been developed, to varying degrees of characterisation.

1.2.2.1 GHB model

1.2.2.1.1 Introduction to GHB

γ -hydroxybutyric acid (GHB) is a metabolite of GABA (Maitre, 1997) that has been found to occur naturally at micromolar concentrations in various areas of the brain (Bessman & Fishbein., 1963; Maitre, 1997). Radioligand quantitative autoradiography studies have identified GHB binding sites that differ from GABA_B receptors in monkey, human and rat brain (Castelli et al., 2000; Snead, 1994), and are most prominent in the frontal cortex, hippocampus, striatum and substantia nigra. Furthermore, GHB has its own synthesis, degradation and reuptake system (Maitre, 1997) (Fig. 1.11).

The use of GABA_BR antagonists has shown that the effects of exogenously administered GHB e.g. GHB-induced absence seizures (Bearden et al., 1980; Godshalk et al., 1976) are mediated either in part, or fully, by GABA_BRs (Crunelli et al., 2006). Considering that GHB has a signalling system (Maitre, 1997), separate binding sites

Model	EEG	Ontogeny	Genotype	Phenotype	Pharmacological Interactions	References
Stargazer (stg)	Prolonged bursts of bilateral, symmetrical & generalised SWDs at 6-7Hz ¹ .	From 14 days onwards, <i>stg</i> mice display phenotypic consequences of mutation ¹ . At 1 month the mean duration of SWDs is 6 seconds (1-66 seconds) and occur ~125/Hr ¹	Autosomal recessive pattern of inheritance. Mutation of the Ca ²⁺ channel γ_2 subunit gene (<i>Cacng2</i> ^{stg}) on mouse chromosome 15 ² . <i>Cacng2</i> ^{stg} encodes protein stargazin which is an isoform of AMPAR trafficking protein ³ . GABA _A R $\alpha_6\beta\gamma\delta$ expression decreased in cerebellum but ~4 fold compensatory increase of $\alpha_1\beta\gamma\delta$ ⁴	SWDs concomitant with immobility ¹ . Homozygous mutants can be identified at 2 weeks of age by reduced body size and mild ataxic gait ¹ . Due to inner ear defect, exhibit spontaneous "head tossing" when at rest i.e. upward gaze in vertical plane. frequency of head tosses increases with age ¹ . Loss of AMPAR function ⁵ due to loss of trafficking by stargazin in cerebellum ⁶ . Females fertile, males infertile ¹ . Impaired conditioned eyeblink reflex ⁷	ETX attenuates SWDs ⁸ . CGP46381 also blocks SWDs ⁸ . NMDA antagonist (MK801) suppressed SWDs ⁸	¹ Noebels et al., 1990 ² Letts et al., 1998 ³ Letts et al., 1997 ⁴ Payne et al., 2007 ⁵ Hashimoto et al., 1999 ⁶ Chen et al., 2000 ⁷ Qiao et al., 1998 ⁸ Aizawa et al., 1997
Tottering (tg)	Bursts of bilateral, symmetrical & generalised SWDs at 6-7Hz ¹ .	At 3-4 week start to see phenotype ¹ . Fully developed by 4 th week. SWDs last 1-10 seconds, occur 100s of times a day	Autosomal recessive pattern of inheritance. Mutation of the Ca ²⁺ channel α_1 subunit gene (<i>Cacna1d</i> ^{tg}) on mouse chromosome 8 ³ . Enhanced expression of α_2 and β_1 GABA _A subunit mRNA in cortex ³	SWDs concomitant with immobility, fixed staring posture and vibrissal twitching ¹ . Splayed stance and hopping gait most prominent in hind legs ¹ . Weigh less than wildtypes ¹	ETX and diazepam attenuates SWDs ⁴ . Phenytoin had no effect ⁴	¹ Noebels & Sidman, 1979 ² Fletcher et al., 1996 ³ Tehrani et al., 1997 ⁴ Heller et al., 1983
Lethargic (lh)	Bursts of bilateral, symmetrical & generalised SWDs at 5-6Hz ¹	At 15 days ataxia phenotype appears. SWDs appear at 18 days ¹ . Mean duration is 1.5 secs (0.6-55), 127/Hr ¹	Autosomal recessive pattern of inheritance. Mutation of the Ca ²⁺ channel β_4 subunit gene (<i>Cacnb4</i> ^{lh}) on mouse chromosome 8 ²	SWDs concomitant with immobility and decreased responsiveness ¹ . Between 15 days and 2 months: reduction in body weight, immunological problems and increased mortality ³ . Affected mice that survive past 2 months regain weight and immune system, but exhibit decreased fertility ³	ETX ^{1,4} , clonazepam, CGP35348 and trimethadone decrease SWDs ¹ . Baclofen causes dose-dependent increase of seizure frequency ¹ . Tiagabine enhances SWDs ⁵	¹ Hosford et al., 1992 ² Burgess et al., 1997 ³ Dung & Swigart, 1972 ⁴ Aizawa et al., 1997 ⁵ Hosford & Wang, 1997

Table 1.4
Features of seizures in mouse genetic models of absence epilepsy

(Castelli et al., 2000; Snead., 1994) and exists naturally in the brain (Bessman & Fishbein., 1963), findings where exogenous GHB elicits some of its effects via GABA_BRs has generated much controversy over GHB site-of-action. This debate has been fuelled further by uncertainty over the cloning of the GHB receptor (GHBR) (Andriamampandry et al., 2003) and the lack of a selective and potent GHBR antagonist (Castelli et al., 2004). The putative GHBR antagonist, NCS382, did not bind to the cloned GHBR and had a brain distribution different to that described in investigations of normal GHBR expression (Andriamampandry et al., 2003). Whilst there have been reports of NCS382 failing to antagonise GHB (Castelli et al., 2004) it still exists as the only GHB antagonist at present, and is therefore an invaluable tool in studying GHB function (Crunelli et al., 2006). However, many examples of partial agonist actions of NCS-382 have also been described for GHB effects (Crunelli et al., 2006), in particular a potentiation of both the GHB and baclofen-mediated decrease of the EPSP amplitude (Emri et al., 1997b).

More recent work has shown the GHB binding site separate and distinct from GABA_BRs by showing a lack of binding of GHB and NCS382 to recombinant GABA_{B1b}, GABA_{B2} and GABA_{B1+2} receptors in HEK 293 cells (Wu et al., 2004). Conversely, in GABA_{B1}R knockout (KO) mice which lack functional GABA_BRs, the typical pharmacological manifestations of GHB administration were not observed (Kaupmann et al., 2003). NCS382 binding in these GABA_{B1}R KO mice was unchanged (Kaupmann et al., 2003), whereas GHB binding is reduced by 50% in GABA_{B1}R KO mice derived from the C57B16j strain (Wu et al., 2004), but unchanged in BALBc-derived GABA_{B1}R KO mice (Kaupmann et al., 2003). Together, these data indicate that GHBRs and GABA_BRs may be separate molecular entities but highlight several GHB effects that are mediated via GABA_BRs, and indicate the presence of GHBR subtypes (Crunelli et al., 2006). The variation of these data should be considered when studying GHB action.

1.2.2.1.2 GHB-induced absence seizures

The first to identify and characterise GHB-induced absence seizures was Godschalk et al., (1976). 200mg/kg GHB via intraperitoneal (i.p) administration initially induced generalised, intermittent bursts of hypersynchronous spike-and-wave activity on the otherwise normal EEG that had a frequency of 5-6 Hz. This progressed into continuous

hypersynchrony before animals regained normal desynchronised EEG reflective of an awake EEG (Godschalk et al., 1976). These rats behaved before injection and up until the EEG changes. At the onset of bursting activity however, they became immobile with open eyes, alongside some head twitching for the duration of the burst and immediately resumed their previous motor activity on SWD cessation (Godschalk et al., 1976).

The effect of GHB administration has been characterised further and when given to monkeys, cats and rats, GHB reliably produces electrographic and behavioural correlates that closely resemble absence seizures in humans (Bearden et al., 1980; Godshalk et al., 1976 & 1977; Snead, 1976, 1978a, b, c & 1980), and represents the best pharmacologically-induced model of absence epilepsy (Crunelli & Leresche, 2002a).

γ -butyrolactone (GBL), the prodrug of GHB, produces the same EEG and behavioural changes as GHB (Snead, 1980) but with more rapid onset and predictable dose response (Bearden et al., 1980). GBL is therefore more commonly used and represents the standardised GHB model (Table 1.5). GBL is an inactive compound and mediates its effects by being rapidly broken down to GHB by lactonase in the blood (Snead, 1991). By examining regional concentrations of GHB and GBL in relation to SWD expression, Snead (1991) determined the threshold concentration of GHB in the brain as 240 μ M. The standard dose to induce SWDs is 100mg/kg GBL (Snead, 1988, 1990 & 1996) (Table 1.5).

As discussed above, there is controversy over which receptor-type GHB acts. Indeed, there is evidence for GABA_BR-mediated mechanisms in GHB-induced absence seizures. In addition to a GABA_BR agonist prolonging the duration of GBL-induced SWDs and GABA_BR antagonists blocking GBL-mediated seizures (Snead, 1992a & 1996a), a high dose of baclofen administered i.p. (5mg/kg) produced bursts of bilaterally synchronous SWDs associated with behavioural arrest, which appeared to be similar to GBL-induced SWDs (Snead, 1996a). Thus it seems that GBL-induced seizures are a result of GHB action at GHBR and/or GABA_BRs.

Overall, the GHB model of absence seizures meets all of the criteria specified in Section 1.2, with pharmacological specificity and behavioural correlates of absence seizures (Table 1.5). The frequency of SWDs is similar to that observed in the spontaneous

genetic models of GAERS and WAG/Rij, and whilst this is higher than that observed in human absence seizures, it is likely a reflection of species specific differences (Danover et al., 1998) as GHB administered in the cat and monkey induces 3Hz and 2.5Hz SWDs, respectively (Snead, 1976 & 1978a).

1.2.2.2 Penicillin model

Intramuscular injection of high dose of penicillin into the cat consistently produces both the EEG and behavioural correlates of absence seizures (Table 1.5). When administered to rats however, penicillin fails to induce SWDs (Avoli, 1980). Instead, multifocal spikes and occasional bursts are seen on the EEG of rodents treated with peritoneal penicillin and seizure activity is absent from the thalamus (Avoli, 1980). Thus whilst penicillin may prove a useful model in the more expensive cat, it is often carried out under anaesthesia and has not been well characterised in rodents (Snead, 1992b). Furthermore, experimental seizures in the cat lack ontogeny data and have conflicting GABA_{mimetic} data (Fariello, 1979) (Table 1.5), both of which are essential criteria that should be met in order for penicillin-induced SWDs to have full validity as an absence seizure model (Snead, 1992b). An additional limitation to the usefulness of penicillin-induced absence seizures is the suggested development of tolerance to the antibiotic (Bo et al., 1984).

1.2.2.3 THIP model

Considering that investigations of absence seizure properties using the THIP-induced model are limited, it would be wise to state this as a potential, rather than established pharmacological model of absence epilepsy. Whilst i.p. application of the GABA_AR agonist THIP produces bilaterally synchronous SWDs and associated behavioural arrest (Fariello & Golden, 1987), there are limited pharmacological and no ontogeny data to support the electrographic findings (Snead, 1992b). Furthermore, there is a poor thalamic representation of the THIP-induced SWDs that are also prominent in the hippocampus (Fariello & Golden, 1987), a brain area typically not involved in SWD generation.

Model	Dose and target	EEG	Ontogeny	Phenotype	Pharmacological Interactions	References
GHB (GBL)	Threshold brain concentration of GHB-induced SWDs = 240µM ¹ ; GHB _R and/or GABA _B R; Typically 100mg/kg GBL administered i.p. ^{6,10,12,14,15} ; EEG and behavioural changes seen within 4-5 minutes of i.p. injection ^{1,6,14,15} , by ~10 minutes of onset the SWDs become continuous ^{1,6,12,14,15} and return to bursts and subside between 30-40 minutes of initial application ^{1,6,12,14}	Bilaterally synchronous SWDs at 2.5Hz in prepubescent monkey ² , 3Hz in cat ³ , 3-6 Hz in mouse ⁴ and 4-6 Hz in rat ^{12,14,15} develop after administration 200-400µV amplitude ^{12,14,15}	Full array of EEG and associated behavioural effects does not appear until P28 ⁵ ; ETX ineffective until P28 ⁵ ; Concordance of ontogeny of GHB-induced SWDs and developmental appearance of [³ H]GHB binding sites ⁶ ; GABAergic enhancement of GHB-induced seizures has greatest sensitivity during the 4 th week ⁷	SWDs concomitant with immobility, vibrissal twitching, staring and some facial myoclonus (rat, cat, monkey) ^{1,2,3,9} ; Automatism and pupillary dilation (monkey) ²	SWDs antagonised by sodium valproate ^{16,17} and ETX ^{4,8,10,16,17} ; Phenytoin ^{8,16} and carbamazepine ¹⁶ exacerbates SWDs ⁸ ; GABA ⁶ , muscimol ⁶ and THIP ¹⁵ potentiate SWDs; Threshold for GHB-induced SWDs is lowered by penicillin and PTZ ¹⁰ ; SWDs are prolonged by baclofen ^{12,14} , CGP35348 ¹² , saclofen ¹¹ , phaclofen ¹⁴ and NCS 382 ¹⁴ attenuate SWDs; GHB & GBL cause a dose-dependent increase in SWD duration in GAERS ¹¹ , <i>stg</i> ⁴ and <i>ll</i> ⁴	¹ Snead, 1991 ² Snead, 1978a ³ Snead et al., 1976 ⁴ Aizawa et al., 1997 ⁵ Snead, 1984b ⁶ Snead, 1994 ⁷ Snead, 1990 ⁸ Godschalk et al., 1976 ⁹ Godschalk et al., 1977 ¹⁰ Snead, 1988 ¹¹ Depaulis et al., 1988 ¹² Snead, 1992a ¹⁴ Snead, 1996a ¹⁵ Snead, 1998 ¹⁶ Subramanyam et al., 2001 ¹⁷ Kumaresan et al., 2000
Penicillin	Weak GABA _A antagonist; IM injection of 240,000 – 400,000 units (IU) per kg ¹ ; SWDs develop 1 hour ¹ after administration, peak 2-3 hours ¹ and last for 4-6 hours ¹ ; Or diffuse bilateral application of dilute penicillin solution (50–250 IU/hemisphere) ^{2,4}	Bilaterally synchronous SWDs 3-4.5 Hz ^{1,2,3} ; 2-5 second bursts ^{1,2,3} ; 200-400µV amplitude ^{1,3}	Unknown; Adult cats used ^{1,2}	SWDs concomitant with immobility ¹ , twitching of facial muscles ² , reduced vigilance, staring and blinking of the eyes and pupillary dilation ¹	Pretreatment with penicillin prolongs GHB-induced SWDs ⁵ ; ETX ⁶ and sodium valproate ⁷ significantly decrease bursts; Systemic administration of GABA cause brief cessation of epileptic activity ⁸	¹ Quesney et al., 1977 ² Quesney & Gloor, 1978 ³ Fisher & Prince, 1977 ⁴ Gloor et al., 1977 ⁵ Snead, 1988 ⁶ Guberman et al., 1975 ⁷ Pellegrini et al., 1978 ⁸ Fariello, 1979
THIP	GABA _A R δ-subunit agonist; 5-10mg/kg i.p. ¹	Bilaterally synchronous SWDs of 5-6 Hz ¹ , 1-7 seconds long ¹ ; 200-300µV amplitude ¹	Unknown; Adult rats used ¹	SWDs concomitant with immobility ¹ and vibrissal twitching ¹	THIP in GAERS shifted frequency from 6-7 Hz to 4-5 Hz and prolonged GAERS SWDs in a dose-dependent fashion ¹ ; ETX blocked SWDs (preliminary studies) ² ; Diazepam, valproate & ETX suppressed THIP-enhanced SWDs in GAERS ^{3,4}	¹ Fariello & Golden, 1987 ² Fariello & Golden, 1983 ³ Marescaux et al., 1985 ⁴ Vergnes et al., 1985

Table 1.5
Features of seizures in pharmacological models of absence epilepsy

1.3 The Thalamus

The thalamus is seen to have two main roles: relaying and processing sensory and motor signals to the cerebral cortex (Amaral, 2000), and the regulation of consciousness and sleep (Steriade & Llinas, 1988). Apart from olfaction, every sensory system comprises of a thalamic nucleus that receives sensory signals and sends them to the associated primary cortical area (Sherman & Guillery, 1996). For example, inputs from the retina are sent to the lateral geniculate nucleus of the thalamus, which in turn project to the primary visual cortex in the occipital lobe (Amaral, 2000). Similarly the ventral posterior nucleus is a key somatosensory relay, which sends touch and proprioceptive information to the primary somatosensory cortex (Amaral, 2000). Each of the primary sensory relay areas receive strong "back projections" from the cerebral cortex, suggesting that the thalamus is involved in processing these inputs instead of acting as a simple relay for them (Sherman & Guillery, 1996).

There are dense interconnections between the thalamus and cortex (Sherman & Guillery, 1996), forming thalamocortical circuits. Bilaterally synchronous EEG activity observed during sleep is a manifestation of the mutual interconnectivity between the thalamus and cortex, with thalamic neurons possessing specific electrophysiological properties that strongly influence this rhythmic activity e.g. burst and oscillatory firing patterns.

Since an intact and reciprocally connected somatosensory thalamocortical loop is involved in absence seizure expression, particularly in rodents (see Section 1.4), therefore the cellular properties and synaptic connectivity of this loop will be described in this section.

1.3.1 Gross anatomy of the thalamus

The diencephalon or "interbrain" is situated rostrally between the two cerebral hemispheres and above the brainstem, consisting of several main nuclear groups: thalamus, hypothalamus, perithalamus and epithalamus (Groenewegen & Witter, 2004). The dorsally located epithalamus is comprised of the pineal body, connecting the limbic system to the rest of the brain and controlling secretion of melatonin from the pineal gland (Amaral, 2000). The perithalamus, previously known as the "prethalamus" or

“ventral thalamus”, contains the zona incerta (Amaral, 2000). The hypothalamus is located below the thalamus but above the brainstem and contains a number of small nuclei that mediate a number of roles including the control of body temperature, hunger and thirst (Amaral, 2000).

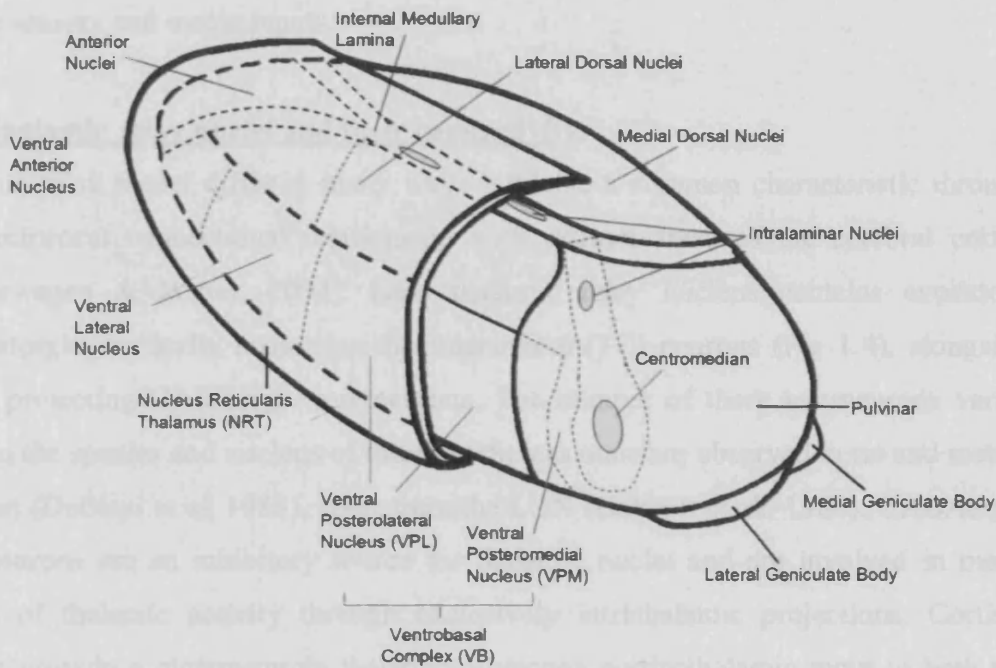


Figure 1.3
Gross organisation of the thalamus

As seen on the left side of the brain, a three dimensional schematic representation of a single thalamus showing anatomical divisions into lateral, medial and anterior portions by the internal medullary lamina. The lateral group is divided into dorsal and ventral tiers. The ventral tier includes the ventral anterior, ventral lateral and ventral posterior nuclei. The dorsal tier is composed of the lateral dorsal, lateral posterior and the pulvinar. Each nucleus in the ventral tier along with the medial and lateral geniculate nucleus receives specific sensory information. The nucleus reticularis thalami cap the lateral aspect of each thalamus. Modified from Amaral, 2000 (*Principles of Neural Science*).

The thalamus is a two-lobed structure that constitutes the largest part of the diencephalon. One lobe or “thalamus” sits on each side of the third ventricle, bordered

laterally by the internal capsule, with the massa intermedia running through the ventricle connecting the two lobes. Each thalamus is comprised of numerous well-defined pairs of nuclei (Amaral, 2000) (Fig 1.3). The internal medullary lamina compartmentalises the thalamus into broad groups: enclosing the anterior group and dividing the medial and lateral groups (Amaral, 2000) (Fig 1.3). The lateral group is further divided into the dorsal and ventral tiers and contains specific relay nuclei that receive sensory and motor inputs.

1.3.2 Thalamic relay nuclei and their connectivity

Thalamic relay nuclei differ in many ways but have a common characteristic through their reciprocal connective relationship with distinct areas of the cerebral cortex (Groenewegen & Witter, 2004). Each thalamic relay nucleus contains excitatory glutamatergic, cortically projecting thalamocortical (TC) neurons (Fig 1.4), alongside locally projecting GABAergic interneurons. The number of these interneurons varies between the species and nucleus of interest whereas none are observed in rat and mouse thalamus (DeBiasi et al, 1988), apart from the LGN (Gabbott et al., 1986). GABAergic NRT neurons are an inhibitory source for thalamic nuclei and are involved in many aspects of thalamic activity through exclusively intrathalamic projections. Cortical neurons provide a glutamatergic thalamic-projecting corticothalamic input to both the thalamus and NRT (Fig 1.4). In addition, thalamic nuclei receive projecting inputs from the brainstem that utilise a number of different neurotransmitters. The following sections will focus on the somatosensory thalamocortical loop as it is involved in absence seizure generation, particularly in rodents (see Section 1.4).

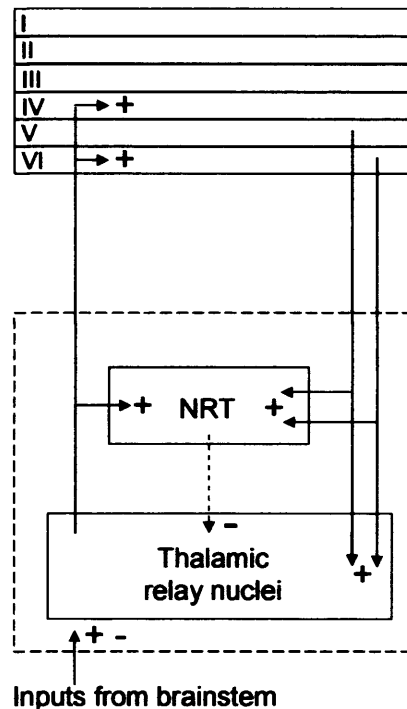


Figure 1.4

Schematic representation of the principal circuitry and connections of thalamic relay nuclei

The principal connections to and from the thalamic relay nuclei are indicated by the black arrows. Excitatory and inhibitory synapses are indicated by + and -, respectively.

1.3.2.1 Thalamocortical neurons of the ventrobasal thalamus

TC neurons are the predominant cell type in all thalamic relay nuclei that have a highly branched dendritic tree. Variation in soma size, orientation and dendritic morphology lead to distinction between different nuclei. The VB is situated in the ventral group of thalamic nuclei and in the rat can be divided into a ventroposteromedial and ventroposterolateral portion (VPM and VPL, respectively) (Fig. 1.3). Most of the neurons in the rat ventrobasal complex (VB) are medium-sized and have dendrites that radiate outwards to give a symmetrical and bushy appearance (Groenewegen & Witter, 2004). VPL neurons are arranged in rostrocaudal and dorsoventral rows that are roughly parallel to the external medullary lamina. In both VPM and VPL a dense plexus of fibres are present. In contrast to other species, the rat VB contains very few GABA-releasing local circuit interneurons, with this cell-type accounting for <1% of the neuronal population (Groenewegen & Witter, 2004; Ohara & Lieberman, 1993).

Thalamic relay nuclei are functionally defined by the sensory modality-specific cortical input. The VPL and VPM are the principal thalamic relays for somatic sensory i.e. nociceptive and kinesthetic, information from the contralateral body and head, respectively (Groenewegen & Witter, 2004). From periphery to the cortex, the somatosensory system is made up of discrete cellular aggregates that replicate the arrangement of the vibrissae on the mastic pad (Jones, 1985; Varga et al., 2002), therefore the VPM portion is unsurprisingly large in rats due to the importance of the vibrissae as sensory organs (Prince, 1995). Analogous to the cortical barrels to which they project i.e. whisker related modules of neurons, the VPM for the most part is divided into barreloids which correspond to single vibrissae (Groenewegen & Witter, 2004; Deschenes et al., 1998; Varga et al., 2002).

The predominant projection site of TC neurons in modality-specific thalamic relay nuclei is to the superficial and deep regions of layer IV, but also to layer VI in the corresponding primary cortical areas (Jones, 1985). In addition, axon collaterals from these cortically projecting neurons terminate in the NRT (Jones, 1985) (Fig. 1.4). TC cells of the VB project glutamatergic output to layer IV and VI of the facial somatosensory (S1) area of the cortex and back to the NRT (Prince, 1995). S1 cortical areas receiving TC axonal projections send reciprocal axonal projections back to the VB from layer VI (Deschenes et al., 1998; Jones, 1985) are glutamatergic (DeBiasi & Rustioni, 1990) and synapse principally on distal dendrites of TC neurons (Liu et al., 1995). Inhibitory GABAergic terminals from the NRT form a substantial part of the synaptic input to TC cells of the VB (Groenewegen & Witter, 2004), in addition to inputs from basal forebrain and brainstem.

1.3.2.2 Neurons of the NRT

The NRT is a thin sheet of GABAergic cells that encapsulates and surrounds the rostral and lateral thalamus, bordering the internal capsule (Groenewegen & Witter, 2004). It contains a homogenous cell-type that is largely ovoid, with a maximum diameter of 25-50µm. The cells have elongated dendritic processes at either end which extend the disc shape appearance and give a bipolar form, with dendrites running parallel to the orientation of the nucleus itself (Groenewegen & Witter, 2004). Dendritic bundles of these GABAergic neurons are embedded in dense neuropil of presynaptic boutons that

mostly arise from the corticothalamic and thalamocortical axons (Scheibel & Scheibel, 1966 & 1972). Rat NRT cells communicate with one another through frequent dendrodendritic junctions, providing an intrinsic GABAergic circuit (Pinault et al., 1997). The organisation of the NRT is not as topographically strict as the somatosensory cortex and sensory thalamus, but does maintain some organisation (Varga et al., 2002).

The NRT is strategically positioned between the dorsal thalamus and the cerebral hemisphere such that all incoming and outgoing fibres of the thalamus pass through it. Considering that very few GABAergic interneurons are present in the rat VB (DeBiasi et al., 1988), GABAergic NRT neurons provide the most important inhibitory input (Prince, 1995). NRT neurons receive synaptic inputs from axon collaterals of corticothalamic glutamatergic neurons of layer VI of the somatosensory cortex and TC cells of dorsal thalamic nuclei, in addition to inputs from basal forebrain and brainstem. Corticothalamic terminals provide the densest inputs to NRT neurons at distal dendritic sites and TC cells predominantly synapse at proximal dendrites (Liu & Jones, 1999). There is evidence indicating that the cortex has more powerful excitatory effect on NRT neurons than TC neurons (Golshani et al., 2001). Unlike the thalamic relay nuclei, the NRT does not project to the cerebral cortex but sends its fibres almost exclusively to the dorsal thalamic nuclei from which it receives its inputs (Groenewegen & Witter, 2004; Prince, 1995).

1.3.2.3 Somatosensory cortical neurons

In the rat there are two main somatosensory areas (S1 and S2) located in the parietal region of the cortex, with S2 located caudally and laterally to S1 (Tracey, 2004). Both S1 and S2 contain a single representation of the body, with S1 exclusively receiving information from the contralateral side of the body and dominated by face and vibrissae inputs. S1 can be subdivided into barrels which correspond to specific whiskers (Tracey, 2004).

The somatosensory cortex of the rat can be divided into 6 layers which contain an array of distinct cell types. Cells in S1 layer IV receive the principal glutamatergic afferent input from the VB and the pyramidal cells in layer VI send glutamatergic corticothalamic fibres to the VB and collaterals to the NRT (Jones, 1985; Tracey, 2004).

Three classes of cells have been identified in rat S1: corticothalamic, corticocortical, and local circuit neurons (Zhang & Deschenes, 1997). Corticothalamic cells make up 46% of the total number of cells in S1. They are small, short pyramidal neurons that project to the VB from layer VI and have apical dendrites terminating and intracortical collaterals ascending to layer IV, creating a narrow column similar in appearance to a barrel (Zhang & Deschenes, 1997). Corticocortical neurons constitute 44% of the cell-type in S1 and are small, short pyramids or bipolar spiny neurons (Zhang & Deschenes, 1997). These cells send collaterals principally to infragranular layers of S1 and branches to S2, the motor cortex, or the corpus callosum. Basket cells make up the remaining 10% and constitute the local circuit neurons, concentrated in upper lamina VI, and have smooth, beaded dendrites and a rich collateral network in layers V and VI (Zhang & Deschenes, 1997).

1.3.2.4 Diffusely projecting inputs to the thalamus

The effect(s) of the numerous inputs to the thalamus from other brain structures are not a topic of investigation for this thesis and thus will not be discussed at length here. However it is important to consider the role of these additional inputs when placing novel findings into the context of a working mechanism.

The thalamus receives 5-hydroxytryptamine (5-HT) containing neurons from the raphe nuclei (Morrison & Foote, 1986), noradrenaline (NA) neurons arising in the locus coeruleus (Morrison & Foote, 1986) and acetylcholine (ACh) containing neurons from the tegmental nuclei of the brainstem (Steriade et al., 1988). These brainstem projections are implicated in cortical arousal and maintaining states of consciousness, acting through the thalamus (Steriade et al., 1993). In particular, a decrease in drive from these fibres, as seen with the progression from wake to deep sleep stages, leads to a steady hyperpolarisation of the TC neuron (McCormick & Prince, 1987).

1.3.3 Membrane currents of thalamocortical neurons

TC neurons have distinctive modes of firing and specific membrane currents underlie these firing sequences.

1.3.3.1 Na⁺ currents

TC neurons can fire TTX-sensitive, Na⁺-dependent action potentials in response to injection of depolarising d.c. current or in response to depolarising steps (Jahnsen & Llinas, 1984a, b) (Fig 1.5) which are due to a fast-activating, fast-inactivating Na⁺ current. In addition, TC neurons have a persistent, small amplitude and non-inactivating Na⁺ current (I_{NaP}) (Parri & Crunelli, 1998).

1.3.3.2 Ca²⁺ currents

Two types of Ca²⁺ current have been identified in TC neurons: high-voltage activated (HVA) channel and low-voltage activated (LVA or “T-type”). Various pharmacological tools separate HVA currents into L, N, P, Q and R-type currents, all activated at more depolarised membrane potentials. Functionally, HVA Ca²⁺ currents are believed to underlie high threshold oscillatory activity at membrane potentials superseding -45mV, predominantly at 25-50Hz (Pedroarena & Llinas, 1997).

The expression of the low-threshold calcium potential (LTCP) is an important characteristic of TC neurons. The LTCP is dependent on the T-type LVA Ca²⁺ current (I_T) (Crunelli et al., 1989). Whereas tonic repetitive Na⁺ action potential firing is observed when the TC neurones are activated from a more positive membrane potential (Jahnsen & Llinas, 1984a), I_T is activated following depolarisation from a hyperpolarised membrane potential (more negative than -60mV) (Jahnsen & Llinas, 1984a) and has fast activation and inactivation properties (Crunelli et al., 1989). If the peak of the LTCP reaches threshold or Na⁺ channel activation threshold, a burst of action potentials may crown the LTCP (Crunelli et al., 1989; Jahnsen & Llinas, 1984a) (Fig 1.5). I_T inactivates at membrane potentials more positive than -55mV (Jahnsen & Llinas, 1984a) and removal of inactivation is necessary prior to activation. Removal of inactivation of I_T is time- and voltage-dependent, being de-inactivated at potentials below -65mV for 500-600ms (Crunelli et al., 1989) (Fig 1.5). These particular kinetics and refractory period of I_T can lead to intrinsic, repetitive burst firing in TC neurons, typically 1-2Hz at fairly hyperpolarised potentials (Leresche et al., 1991).

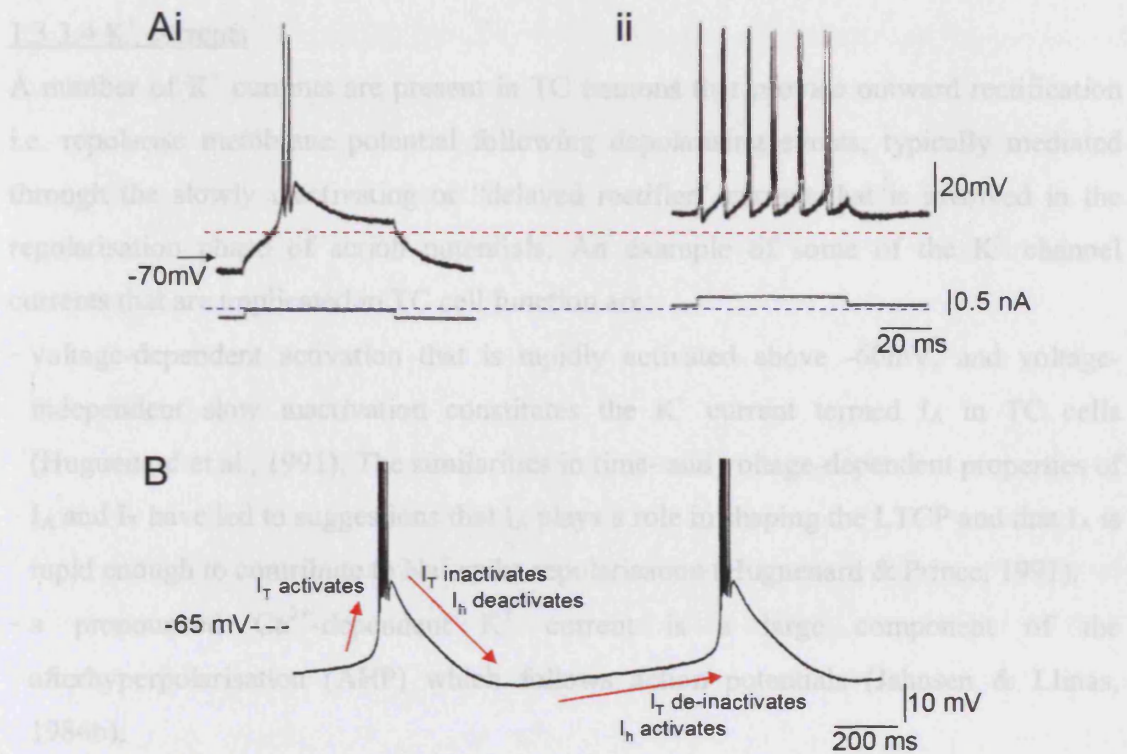


Figure 1.5

Intrinsic electrophysiological properties of TC neurons

TC neurons are commonly quoted as having two main firing modes: burst (Ai) and tonic (Aii). A) Injection of constant amplitude depolarising current pulse administered at 2 different membrane potentials. Ai) while being hyperpolarised by a constant current injection, the stimulation pulse resulted in a LTCP and burst of action potentials. Aii) depolarisation using direct current (d.c) results with a train of action potentials in response to stimulation pulse. Red dotted line indicates same membrane potential, blue dotted line represents level on injected d.c current. Taken and modified from Jahnsen & Llinas, 1984. B) Schematic representation of the interaction between I_T and I_h .

1.3.3.3 Mixed cation current

I_h is a mixed cation (Na^+ and K^+) depolarising current that is activated on hyperpolarisation, between -60 to -90mV (McCormick & Pape, 1990; Soltesz et al., 1991; Williams et al., 1997). The presence of this depolarising potential is regarded as a defining electrophysiological feature of TC neurons and the interplay between I_T and I_h gives rise to rhythmic bursting at delta frequency (see Fig 1.5).

1.3.3.4 K⁺ currents

A number of K⁺ currents are present in TC neurons that provide outward rectification i.e. repolarise membrane potential following depolarising events, typically mediated through the slowly inactivating or “delayed rectifier” current that is involved in the repolarisation phase of action potentials. An example of some of the K⁺ channel currents that are implicated in TC cell function are:

- voltage-dependent activation that is rapidly activated above -60mV, and voltage-independent slow inactivation constitutes the K⁺ current termed I_A in TC cells (Huguenard et al., 1991). The similarities in time- and voltage-dependent properties of I_A and I_T have led to suggestions that I_A plays a role in shaping the LTCP and that I_A is rapid enough to contribute to Na⁺ spike repolarisation (Huguenard & Prince, 1991).
- a pronounced Ca²⁺-dependent K⁺ current is a large component of the afterhyperpolarisation (AHP) which follows action potentials (Jahnsen & Llinas, 1984b);
- in contrast, an inwardly rectifying (hyperpolarising) Ba²⁺-sensitive current termed K_{IR} has been identified in TC cells of the VB. K_{IR} mediates a large inward current with kinetics up to three times slower than those of I_h and the more conventional outward rectifying K⁺ channels (Williams et al., 1997). K_{IR} is activated by membrane potentials more negative than -85 mV and may aid de-inactivation of I_T to promote the occurrence of LTCPs (Williams et al., 1997).

1.3.4 Electrophysiology of TC neurons

Regulation of action potential firing frequency in neurons is an important factor contributing to behaviour (Steriade & Llinas, 1988). Thalamic cells are commonly described as firing with 2 general patterns: one of sustained regular firing or “tonic mode” and the other involving high-frequency bursts of action potentials “burst mode” (Jahnsen & Llinas, 1984a) (Fig 1.5). Thalamic neurons can be switched from “tonic” to “burst” firing mode by intrathalamic, thalamocortical and brainstem aminergic and cholinergic systems; all capable of modulating TC cell membrane and synaptic properties (McCormick, 1992). It is believed that the intrinsic ability of TC neurons to switch firing modes and display self-supporting oscillatory states underlies changes in consciousness related to sleep and awareness (Steriade & McCormick, 1993; Steriade & Contreras, 1995).

An altered membrane potential of a TC neuron subsequently adjusts the firing mode of the cell. Tonic firing of action potentials are observed at depolarised membrane potentials ($\geq -50\text{mV}$), which are typically observed during states of arousal whereas burst firing is typically observed when cell membrane potentials are more hyperpolarised, to allow the de-inactivation of I_T and LTCP induction (Leresch et al., 1991) (see Section 1.3.3.2).

1.3.4.1 Tonic firing

The repetitive tonic firing observed at more depolarised membrane potentials (see above) are classical Na^+/K^+ action potentials, which are followed by AHPs (Jahnsen & Llinas, 1984a,b). In tonic-firing mode, sensory information can be linearly transferred through the sensory thalamus to the associated area of the cerebral cortex (Groenewegen & Witter, 2004).

1.3.4.2 Burst firing

As already mentioned, burst firing is typically observed in TC neurons when cell membrane potentials are hyperpolarised enough to allow the de-inactivation of I_T (Leresch et al., 1991). Activated I_T produces a LTCP that is normally large enough to reach action potential generation and thus elicit a burst of action potentials that crown the LTCP (3-8 action potentials at 100-300 Hz) (Jahnsen & Llinas, 1984a,b).

In this burst-firing mode, transfer of sensory information to the cortex is prevented (Groenewegen & Witter, 2004). The cyclical activation, inactivation and de-activation of I_T , alongside additional membrane currents involved in the oscillation (see Section 1.3.3), effectively “gates” sensory and motor inputs leaving the brain “cut-off” from external stimuli, as it is during sleep. The rhythmic bursts of LTCPs are associated with sleep, occur when the cells are hyperpolarised and appear as synchronised slow-waves on the EEG (Avanzini et al., 2000; Steriade & Llinas, 1988). TC cells receive ascending brainstem projections made of several different neurotransmitters (Steriade et al., 1993), and the membrane potential of sensory TC neurons can be controlled by these brainstem afferents (McCormick & Prince, 1987). A decreased drive from brainstem fibres, as observed with the progression from wake to deep sleep stages, leads to a steady hyperpolarisation of the TC neuron (McCormick & Prince, 1987) and thus switching

from tonic-firing, to slow (<1Hz) oscillatory activity and δ -oscillation (1-4Hz) with further hyperpolarisation (Steriade et al., 1991).

The various different rhythmic firing activities that have been recorded from TC neurons involve LTCPs e.g. slow <1Hz oscillation and δ -oscillation. I_h behaves as a pacemaker current in TC cells exhibiting δ -oscillation (Leresche et al., 1991). As mentioned in Section 1.3.3, I_T and I_h interact such that hyperpolarisation and thus de-inactivation of I_T occurs, resulting in an LTCP and burst of action potentials (Fig 1.5). It is the reactivation of I_h at hyperpolarised membrane potential, alongside the time-dependent de-inactivation of I_T , which causes the cycle to recommence underlying the frequency of 1-4Hz that is characteristic of the δ -oscillation (Leresche et al., 1991).

1.3.5 Synaptic physiology of thalamic circuitry

GABA is the principal inhibitory neurotransmitter and glutamate the principle excitatory neurotransmitter released within the somatosensory thalamocortical loop (Jones, 1985). GABA mediates slow responses by G-protein coupled metabotropic GABA_B receptors (GABA_BRs) at pre- and postsynaptic sites, and fast responses by ionotropic GABA_A receptors (GABA_ARs) at postsynaptic locations, both introduced in Section 1.5 (see below). Similarly, glutamatergic activity arises through metabotropic glutamate receptors (mGluRs), NMDA and AMPA/kainate receptors (Salt & Eaton, 1996). mGluR receptors fall into 3 groups: Group I (mGluR 1 and 5), Group II (mGluR 2 and 3) and Group III (mGluR 3, 6 and 7). Activation of corticothalamic pathways elicits responses through non-NMDA, NMDA and also mGluRs, leading to an initial fast and then a slower, long-lasting response (Salt & Eaton, 1996).

1.4 SWD mechanism

1.4.1 Thalamocortical loop involvement in absence seizures

The strong association of absence seizures with periods of awakening and drowsiness suggests that SWDs arise as aberrations of sleep mechanisms (Shouse et al., 1996; Shouse & Silva, 1997). EEG sleep spindles are the epitome of electrical synchronisation at the onset of sleep. They act as an electrographic landmark for the transition from waking to sleep that is closely linked to the loss of perceptual awareness (Steriade & McCormick, 1993). In cats, penicillin was found to transform sleep spindles into SWDs

(Gloor & Fariello, 1988). An early positron emission tomography (PET) study of children with IGE showed a focal increase in thalamic blood flow at SWD induction via hyperventilation (Prevett et al., 1995). More recent studies clarify thalamic involvement in absence seizures of human IGE sufferers using functional magnetic resonance imaging (fMRI) technique (Labate et al., 2005; Laufs et al., 2006; Salek-Haddadi et al., 2003; Moeller et al., 2008a). In particular, a study on drug-naïve children with newly diagnosed CAE using a combination of EEG recording and fMRI imaging identified increases in the blood oxygen level in the thalamus during SWDs (Moeller et al., 2008b).

Depth electrode recordings in humans (Williams, 1953), cat (Avoli et al., 1983; Fisher & Prince, 1977), rat (Inoue et al., 1993) and mouse models (Hosford et al., 1995), revealed synchronous discharges in the thalamus and cortex that coincided with surface EEG SWDs (Fig. 1.6). In particular, localised EEG recordings showed a predominance of SWD in the frontoparietal cortex and relay nuclei of the thalamus, suggesting that these structures play a principal role in seizure genesis in GAERS (Vergnes et al., 1987). Whilst the largest SWD was observed in the cortex and lateral thalamic nuclei, small amplitude SWD was also recorded from the striatum, hypothalamus, tegmentum and substantia nigra (Vergnes et al., 1990) but was not observed in the hippocampus or limbic structures in the rat brain (Vergnes et al., 1987).

Transecting the corpus callosum of GAERS produced a marked reduction in synchronicity of paroxysms between hemispheres, suggesting that SWDs in thalamus are synchronised with the ipsilateral cortex (Vergnes et al., 1989). Furthermore, lesions to midline thalamus had no effect on bilateral synchrony (Vergnes & Marescaux, 1992), suggesting thalamocortical connections are ipsilateral and interhemispheric fibres that connect the two hemispheres are the principle means by which SWDs are bilaterally synchronised (Danober et al., 1998). Surgical decortication abolished both spindles and SWDs in the feline penicillin model (Avoli & Gloor, 1982a & b). Similarly, decortication of one hemisphere in a transected brain resulted in block of SWD in the ipsilateral thalamus of GAERS (Vergnes & Marescaux et al., 1992).

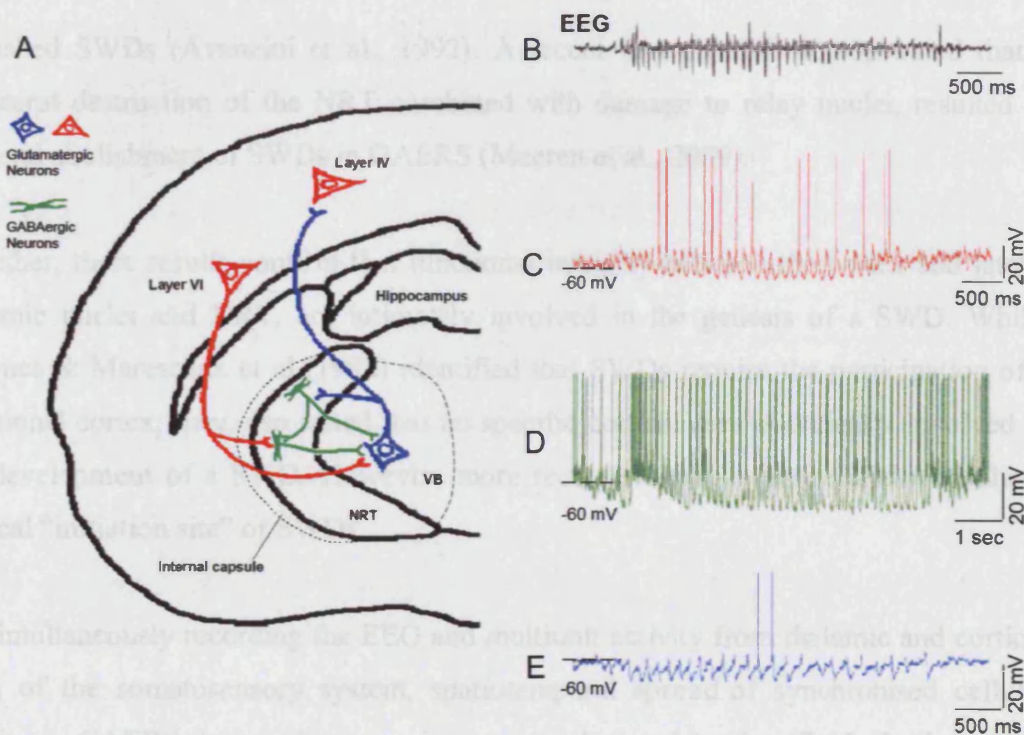


Figure 1.6

Intracellular activities during a SWD

A) Schematic diagram of the thalamocortical loop. The colours of the different neuronal types in A, apply to the intracellular recordings in panels C – E. B) an EEG recording of a SWD. C) layer V cortical neuron showing rhythmic depolarisations superimposed on a long-lasting hyperpolarisation. D) activity starts with a clear hyperpolarisation in NRT cells, followed by rhythmic LTCPs with associated high-frequency bursts of action potentials. E) thalamocortical neuron showing rhythmic sequences of IPSPs superimposed on a long-lasting tonic hyperpolarisation. Taken and modified from Crunelli & Leresche (2002a).

Whilst bilateral lesion of the anterior and ventromedial thalamus did not affect SWD expression in GAERS, lateral thalamic lesions greatly altered seizure activity (Vergnes & Marescaux et al., 1992). In addition, no SWD was recorded from the cortex ipsilateral to the thalamic lesions that included relay nuclei and thalamic nucleus reticulatus (NRT), whereas the unlesioned side expressed normal cortical EEG with many SWD (Vergnes & Marescaux et al., 1992). Thalamic lesions in the feline penicillin model also demonstrated that the anterior and ventromedial thalamus do not play a role in SWD, as only lesion of the lateral nuclear group abolished SWDs (Pellegrini & Gloor, 1979). Isolated lesion of the NRT in GAERS using the excitotoxic agent ibotenic acid also

abolished SWDs (Avanzini et al., 1992). A recent investigation demonstrated that a unilateral destruction of the NRT combined with damage to relay nuclei, resulted in bilateral abolishment of SWDs in GAERS (Meeren et al., 2009).

Together, these results confirm that functional integrity between the cortex and lateral thalamic nuclei and NRT, are intimately involved in the genesis of a SWD. Whilst Vergnes & Marescaux et al (1992) identified that SWDs require the participation of a functional cortex; they also stated that no specific cortical area is critically involved in the development of a SWD. However, more recent studies have revealed a localised cortical “initiation site” of SWDs.

By simultaneously recording the EEG and multiunit activity from thalamic and cortical areas of the somatosensory system, spatiotemporal spread of synchronised cellular activity in GAERS during absence seizures was observed *in vivo* (Seidenbecher et al., 1998). They established that paroxysmal activity in the frontoparietal cortex typically precedes the electrographic manifestation of a SWD (Seidenbecher et al., 1998). Multisite cortical and thalamic field potentials recorded during spontaneous SWDs in WAG/Rij rat and revealed a consistent “cortical focus” within the peri-oral region of the somatosensory cortex (Meeren et al., 2002). SWD activity recorded from other cortical sites consistently lagged the focal site. Furthermore, whilst cortical and thalamic sites could interact bidirectionally during a SWD i.e. the direction of coupling between cortex and thalamus varied for different seizures and within short seizures, the cortical focus consistently led the thalamus during the first 500ms of the seizure (Meeren et al., 2002). *In vivo* intracellular and local field potential (LFP) recordings confirmed this “cortical focus” hypothesis, indicating that epileptic discharges initiated in layer V/VI of the facial somatosensory cortical region in GAERS (Fig. 1.7) (Polack et al., 2007). In addition, topical application of TTX in the facial somatosensory cortex of GAERS prevented the occurrence of SWDs on the EEG and in TC neurons of the thalamus also (Polack et al., 2009).

Overall, it is clear that both cortical and thalamic neurons participate in the SWD firing pattern. Although the steps leading to the generalised SWD take place in the cortex, the thalamus shortly becomes entrained in the SWD rhythm and these mutually interconnected neurons at both levels are critical to full seizure manifestation. The

cellular and synaptic properties of the thalamocortical loop that create this oscillating network that underlies absence seizures are described below.

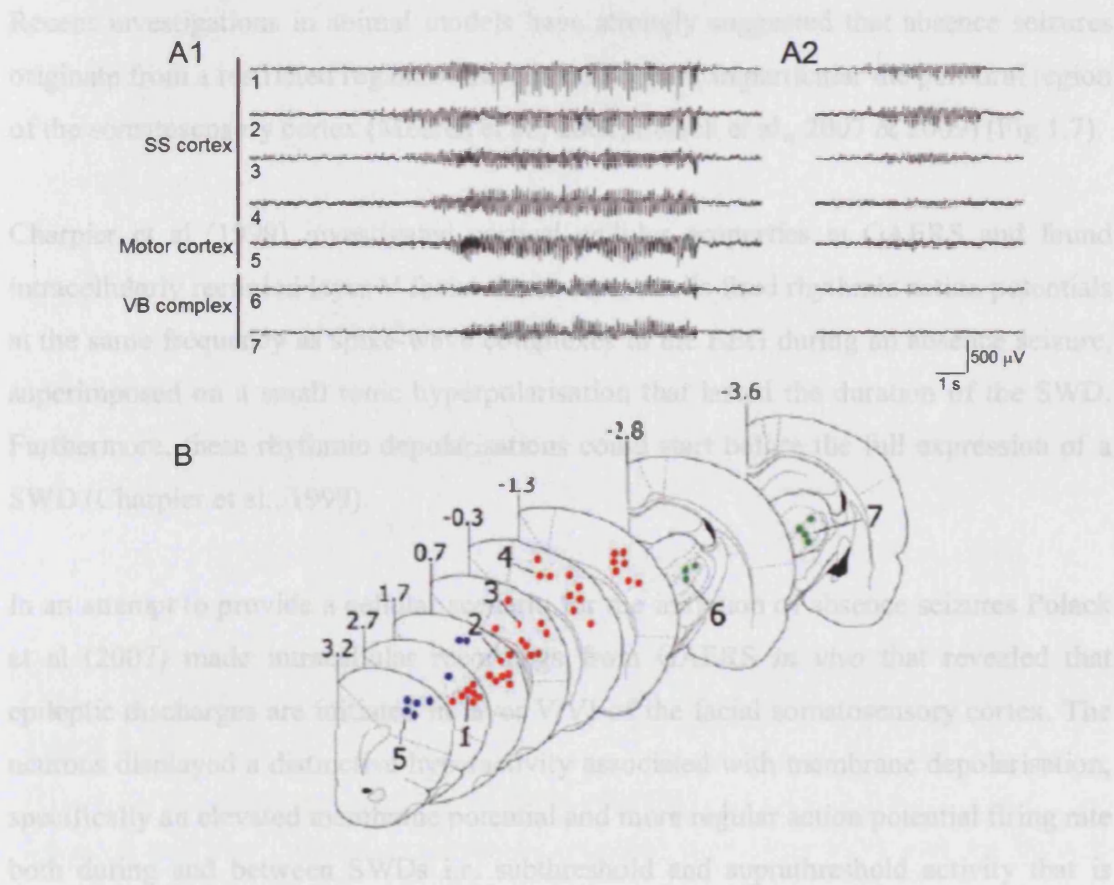


Figure 1.7 SWDs are initiated in the facial somatosensory cortex
A) LFPs recorded from the somatosensory and motor cortices and the VB of GAERS. The location of recording electrodes correspond to numbers in **B**. **B)** Superimposed slice drawings made from the stereotaxic brain atlas of Paxinos & Watson (1986) and distances from bregma are as indicated in mm. Red, blue and green dots represent the recording sites in the somatosensory (SS) cortex, motor cortex and VB thalamus, respectively. Note how short discharges of spike-and-wave complexes were observed at somatosensory cortical sites, without propagation to motor cortex and VB in **A2**, and how the paroxysmal discharge is present in the somatosensory cortex before the neighbouring motor cortex and thalamus (**A1**). Figure taken and modified from Polack et al (2007)

1.4.2 Cellular activity during an absence seizure

1.4.2.1 Cortex

Recent investigations in animal models have strongly suggested that absence seizures originate from a restricted region of the cerebral cortex, in particular the peri-oral region of the somatosensory cortex (Meeren et al., 2002; Polack et al., 2007 & 2009) (Fig 1.7).

Charpier et al (1999) investigated cortical cellular properties in GAERS and found intracellularly recorded layer V facial motor cortex cells fired rhythmic action potentials at the same frequency as spike-wave complexes in the EEG during an absence seizure, superimposed on a small tonic hyperpolarisation that lasted the duration of the SWD. Furthermore, these rhythmic depolarisations could start before the full expression of a SWD (Charpier et al., 1999).

In an attempt to provide a cellular scenario for the initiation of absence seizures Polack et al (2007) made intracellular recordings from GAERS *in vivo* that revealed that epileptic discharges are initiated in layer V/VI of the facial somatosensory cortex. The neurons displayed a distinctive hyperactivity associated with membrane depolarisation, specifically an elevated membrane potential and more regular action potential firing rate both during and between SWDs i.e. subthreshold and suprathreshold activity that is markedly different to cortical neurons in the upper layers of the S1 cortex and other cortex regions in GAERS and the S1 in non-epileptic animals (Fig. 1.8) (Polack et al., 2007). These “leading” neurons displayed short periods of suprathreshold oscillatory activity during interictal periods that initiated an epileptic seizure by systematically guiding the discharge in more superficial cortical cells (Polack et al., 2007) (Fig 1.7).

In agreement with Charpier et al (1999), neurons in all cortical layers at the cortical focus exhibited repetitive depolarisations time-locked with the spike component of the SWD and superimposed on a tonic membrane hyperpolarisation (Polack et al., 2007) (Fig 1.8). The underlying cause of this hyperpolarising shift is unknown; however it was accompanied by increased input resistance and did not reverse in polarity at membrane potentials of -90 mV (Charpier et al., 1999; Polack et al., 2007).

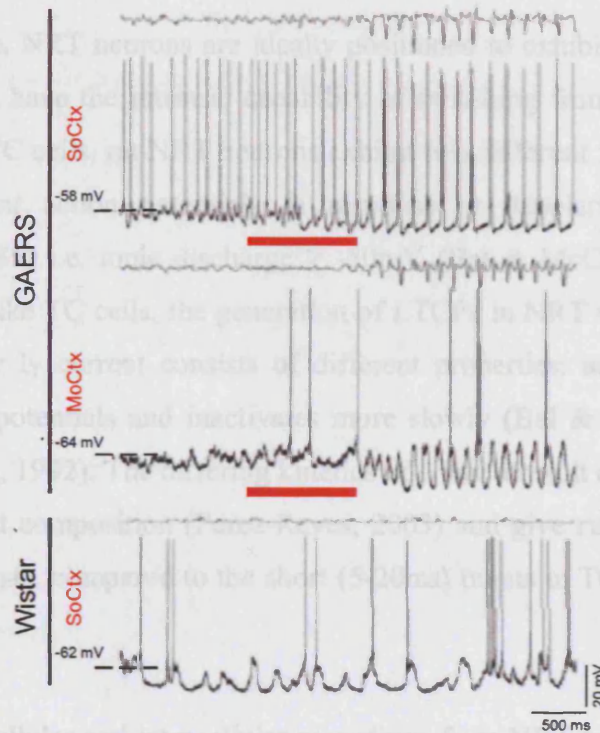


Figure 1.8

Hyperactivity of layer V/VI cortical focus neurons

Interictal and ictal intracellular activities recorded from layer V/VI neurons from the cortical initiation site (SoCtx; top) and motor cortex (MoCtx; middle) of GAERS and SoCtx in normal Wistar rats (bottom), simultaneously with the corresponding EEG (traces above intracellular recordings). Note the more regular firing rate before and during the SWD at the cortical focus neurons of GAERS. Also note the hyperpolarising shift in membrane potential and repetitive, large depolarisations prior to SWD onset in the cortical focus neurons (red bar) which was not present in the motor cortex of GAERS or somatosensory cortex of Wistar rats. Taken and modified from Polack et al (2007).

1.4.2.2 NRT

The action potentials that are associated with the cyclical depolarisations in layer VI of the S1 cortex provide a rhythmic and synchronous input to the thalamus. The GABAergic NRT neurons follow each depolarising shift with cyclical bursts of excitatory postsynaptic potentials (EPSPs) (Crunelli & Leresche, 2002a) (Fig. 1.9).

As mentioned above, NRT neurons are ideally positioned to exhibit some control over dorsal thalamus and have the intrinsic capability of switching from “tonic” to “burst” firing modes. Like TC cells, rat NRT neurons exhibit two different firing modes: single spike, Na⁺-dependent action potentials in response to depolarising current steps (Avanzini et al., 1989) i.e. tonic discharge $\geq -50\text{mV}$ (Bal & McCormick, 1993), and burst-firing mode. Like TC cells, the generation of LTCPs in NRT neurons is mediated through I_T; however I_T current consists of different properties: activated from more positive membrane potentials and inactivates more slowly (Bal & McCormick, 1993; Huguenard & Prince, 1992). The differing kinetics of I_T are a result of differences in the Ca²⁺ channel subunit composition (Perez-Reyes, 2003) and give rise to longer (50ms) non-decelerating bursts, compared to the short (5-20ms) bursts in TC neurons (Domich et al., 1995).

Using *in vivo* extracellular and intracellular recordings from NRT in GAERS, Slaght et al (2002) ascertained the cellular mechanisms underlying NRT neuronal activity during SWDs. When a SWD appeared on the EEG, whatever the background firing, NRT activity changed to large LTCPs crowned by prolonged and high frequency bursts of action potentials tightly linked to the spike-wave complex in the EEG, in agreement with Seidenbecher et al (1998).

The onset and cessation of this burst firing in the NRT varied compared to the corresponding SWDs (Slaght et al., 2002). The first action potential of each burst preceded the peak of the EEG spike component of SWCs and the number of action potentials ranged from 6-15 (Fig. 1.9). In 85% of SWDs, a relatively large hyperpolarisation was observed at the start which was independent of background firing. The first LTCP occurred at the peak of this hyperpolarisation and from this point onwards the LTCPs and associated high frequency action potential bursts became established, with a slowly decaying membrane depolarisation observed toward the end of a SWD (Slaght et al., 2002).

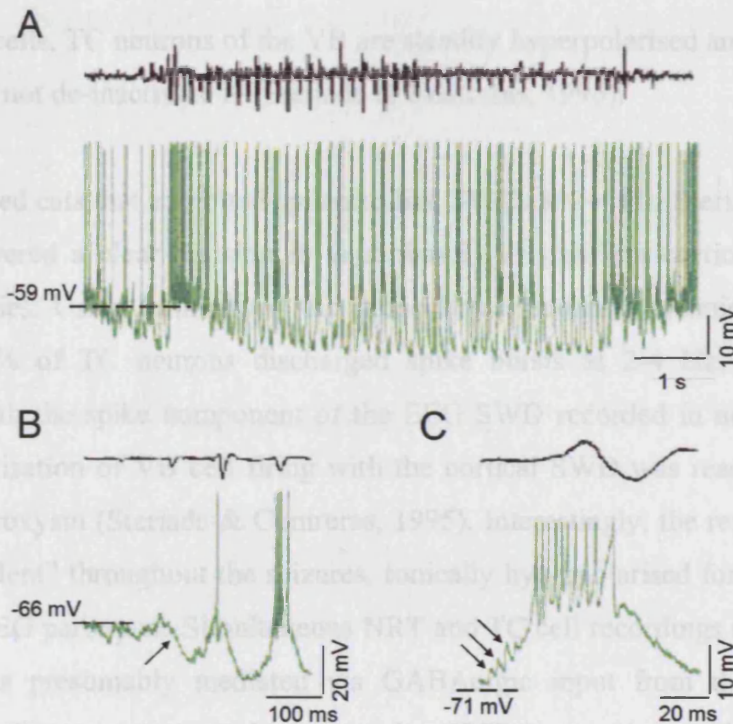


Figure 1.9

Intracellular activity of NRT neurons during a SWD

A) In black, an EEG recording of a SWD and in green, an intracellular recording from an NRT neuron. The background activity of NRT neurons (a mixture of single action potentials and short, low frequency bursts) becomes high-frequency burst activity concomitant with the first and then every SWC of the SWD in the EEG (top trace). B) In a majority of SWDs a large hyperpolarisation (black arrow) could be detected at the start of a SWD. C) All intracellularly recorded cells switched to a firing pattern of prolonged high-frequency bursts of 5-15 action potentials during SWD. Note how the rising phase of the LTCP is shaped by the presence of 3-9 small amplitude (1-8 mV), high frequency depolarising potentials (black arrows) which start during the trough between two successive LTCPs and often sum to the first action potential of a burst. Considering the higher firing strength of cortical compared to thalamocortical neurons, which are largely silent throughout a SWD, these EPSPs are likely to be generated by cortical events. Modified from Slaght et al (2002) and Crunelli & Leresche (2002a).

1.4.2.3 Ventrobasal thalamus

The strong and prolonged inhibitory output of the bursting NRT neurons arrives at the TC cells of the neighbouring VB complex a few milliseconds after the first NRT burst.

Unlike NRT cells, TC neurons of the VB are steadily hyperpolarised and display phasic IPSPs that do not de-inactivate I_T (Steriade & Contreras, 1995).

In anaesthetised cats that exhibited epileptic-like SWCs at 2-4 Hz, Steriade & Contreras (1995) discovered a clear division in ventrobasal (VB) thalamocortical (TC) cellular firing properties. Using both extra- and intracellular recording techniques they found that only 40% of TC neurons discharged spike bursts at 2-4 Hz, which were in synchrony with the spike component of the EEG SWD recorded in neocortical areas. Full synchronisation of VB cell firing with the cortical SWD was reached toward the end of the paroxysm (Steriade & Contreras, 1995). Interestingly, the remaining 60% of cells were “silent” throughout the seizures, tonically hyperpolarised for the duration of the cortical EEG paroxysm. Simultaneous NRT and TC cell recordings showed that this inhibition was presumably mediated via GABAergic input from the NRT, as the repetitive inhibitory postsynaptic potentials (IPSPs) superimposed on the tonic hyperpolarisation was accompanied by concurrent NRT cell excitation which both had close time relation to cortical SWD (Steriade & Contreras, 1995).

A later study by Pinault et al (1998) investigated this phenomenon in GAERS rats. *In vivo* intracellular recordings of TC cells of the VB revealed that a larger proportion of neurons (~93%) exhibited a small tonic hyperpolarisation throughout a SWD, with rhythmic sequences of one EPSP and 2-6 IPSPs occurring concomitantly with SWCs with small membrane depolarisation toward the end of a SWD (Fig. 1.10). The intracellular activity of the remaining 7% of cells consisted of rhythmic LTCPs with a few EPSP/IPSP sequences at SWD onset. It appears that whilst the phasic inhibitory potentials are mediated by activation of $GABA_A$ Rs, presumably by the GABAergic input from the NRT (Charpier et al., 1999; Pinault et al., 1998; Steriade & Contreras, 1995), the tonic hyperpolarisation is not likely to be a result of synaptic $GABA_A$ R activation as the current did not reverse at a membrane potential of -68 mV nor appear as a depolarising event with KCl filled electrodes (Charpier et al., 1999; Pinault et al., 1998), and was thus suggested to represent long-lasting $GABA_B$ IPSPs (Charpier et al., 1999). The absence of LTCPs in TC cells can be explained by the summated, repetitive and long bursts of the neighbouring NRT neurons during the cortical “spike” of a SWD somehow rendering TC neurons in a state that prevents their discharge (Steriade & Contreras, 1995). The massive GABAergic input to the thalamus may increase

membrane conductance of TC cells to a level that prevents generation of LTCPs (Cope et al., 2009).

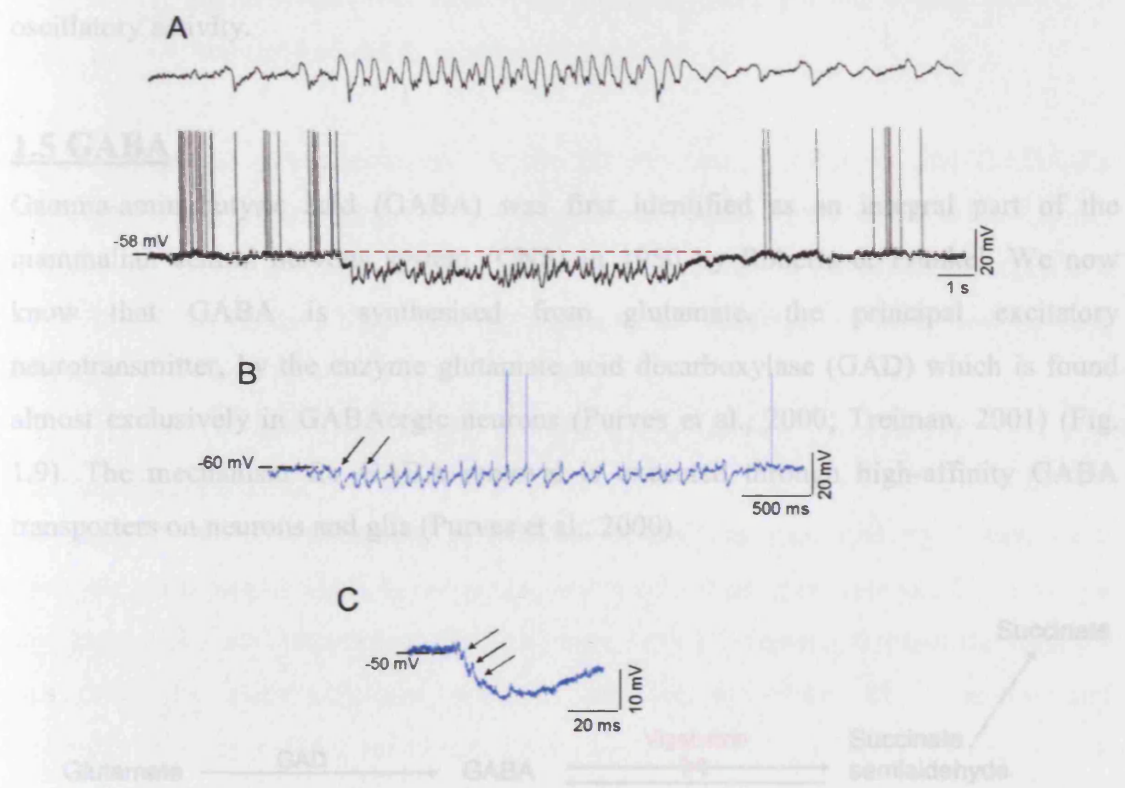


Figure 1.10

TC neurons of the VB are inhibited during a SWD

A) An intracellular recording shows tonic hyperpolarisation (~15 mV) started at the onset of a SWD (highlighted by red dotted line). Resting membrane potential resumed immediately at the end of the depth cortical EEG seizure (top trace) and the end of the SWD in the cerebral cortex was followed by depolarisation and increased firing of VB neurons. **B)** Superimposed on the tonic hyperpolarisation are rhythmic sequences of one excitatory (black arrows) and 4-6 inhibitory postsynaptic potentials (IPSPs). The EPSP/IPSP sequence is enlarged in **C** where IPSPs are this time indicated by arrows. The IPSPs occur concomitantly with the bursts of action potentials observed in NRT cells during a SWD. Taken and modified from Charpier et al (2002); Crunelli & Leresche (2002a); Pinault et al (1998) and Steriade & Contreras (1995).

Such long lasting hyperpolarisation of the overwhelming majority of TC neurons prevent the transfer of action potentials to the cortex, and this obliteration of synaptic transmission through the thalamus may contribute to the loss of the consciousness that

occurs throughout an absence seizure (Steriade & Contreras, 1995). However, the thalamocortical neurons that are not tonically hyperpolarised will still likely converge onto reticular and cortical neurons with sufficient activity to facilitate their rhythmic oscillatory activity.

1.5 GABA

Gamma-aminobutyric acid (GABA) was first identified as an integral part of the mammalian central nervous system (CNS) in 1950 by Roberts & Frankel. We now know that GABA is synthesised from glutamate, the principal excitatory neurotransmitter, by the enzyme glutamate acid decarboxylase (GAD) which is found almost exclusively in GABAergic neurons (Purves et al., 2000; Treiman, 2001) (Fig. 1.9). The mechanism for GABA removal is executed through high-affinity GABA transporters on neurons and glia (Purves et al., 2000).

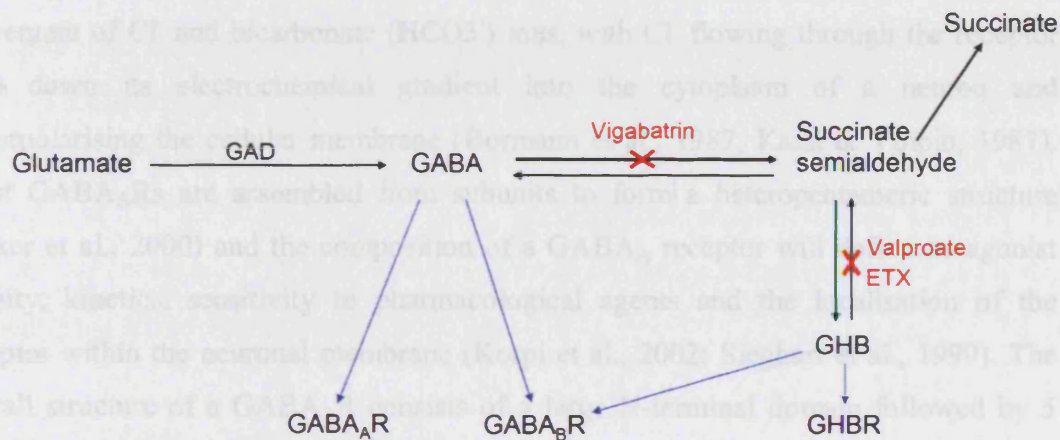


Figure 1.11

GABA synthesis and metabolism

Schematic diagram representing the synthesis and metabolism of GABA. Because GHB can be converted into GABA, some of the GHB-mediated actions of GHB could be elicited by the GHB-derived GABA pool. GABA is eventually converted to succinate in the mitochondria of cells by GABA aminotransferase and succinic semialdehyde dehydrogenase.

Three major types of GABA receptor have been identified so far:

- Ionotropic GABA_A receptor (GABA_AR);
- Metabotropic G-protein coupled GABA_B receptor (GABA_BR), and
- Ionotropic GABA_C receptor (GABA_CR)

GABA_CRs have a pharmacological profile distinct from GABA_ARs and GABA_BRs (Johnston, 1996). Considering that this receptor is largely found in the retina (Boue-Grabot et al., 1998; Johnston, 1996), they are not of interest to this thesis and thus will not be discussed further. The following sections will introduce GABA_A and GABA_B receptors.

1.5.1 GABA_A receptors

The majority of fast inhibitory actions of GABA are mediated by ligand-gated ionotropic postsynaptic GABA_A receptors, where activation gives rise to a bidirectional movement of Cl⁻ and bicarbonate (HCO₃⁻) ions, with Cl⁻ flowing through the receptor pore down its electrochemical gradient into the cytoplasm of a neuron and hyperpolarising the cellular membrane (Bormann et al., 1987; Kaila & Voipio, 1987). Most GABA_ARs are assembled from subunits to form a heteropentameric structure (Pirker et al., 2000) and the composition of a GABA_A receptor will define its agonist affinity, kinetics, sensitivity to pharmacological agents and the localisation of the receptor within the neuronal membrane (Korpi et al., 2002; Sieghart et al., 1999). The overall structure of a GABA_AR consists of a large N-terminal domain followed by 5 transmembrane (TM) domains and a large cytoplasmic loop between TM3 and TM4 (Luscher & Keller, 2004; Tretter et al., 1997). Determined by subunit composition, GABA_A receptors can generate two major modes of inhibitory transmission: phasic and synaptic inhibition or tonic inhibition via extrasynaptic receptors.

GABA_ARs exhibit extensive structural heterogeneity as indicated by the 19 different polypeptide subunit genes that have been identified and cloned: α 1–6, β 1–3, γ 1–3, δ , ϵ , π , θ and ρ 1–2, (Korpi et al., 2002; Sieghart et al., 1999; Sieghart and Sperk, 2002). Whilst a large variety of GABA_AR subtypes could theoretically be formed, the total number of naturally occurring combinations is significantly less due to limitations on the subunit partners that can assemble together (Sieghart et al., 1999; Sieghart & Sperk,

2002). Co-expression of α and β subunits in heterologous cells is sufficient for the assembly of GABA-gated ion channels in the cell surface, however co-expression of γ 1-3, δ , ϵ , π , or θ subunits is required to fully mimic the electrophysiological and pharmacological properties of native receptors (Whiting, 1999).

1.5.1.1 Synaptic GABA_A receptors

GABAergic receptors exist in most inhibitory synapses of the vertebrate CNS and can be regulated by compounds such as benzodiazepines and barbiturates (Stephenson, 1988). Synaptic GABA_ARs underlie classical “phasic” GABA_A inhibition or inhibitory postsynaptic currents (IPSCs) (Fig. 1.11_{A1}).

The vast majority of GABA_ARs found in the brain contain diverse α and β subunit variant along with γ 2 subunit (Fig. 1.10). The first evidence of this came to light when Schofield et al (1987) discovered that whilst co-expression of different α and β subunits generated functional receptors, they lacked binding sites for benzodiazepines (Levitan et al., 1988; Pritchett et al., 1988). Importantly, co-expression of α and β subunits with the γ 2 subunits produced GABA_ARs with high-affinity binding for benzodiazepine ligands (Pritchett et al., 1989). Based on these findings and on the further analysis of recombinant receptors, $\alpha\beta\gamma$ pentamer receptors likely have a stoichiometry of $2\alpha:2\beta:1\gamma$ (Chang et al., 1996; Tretter et al., 1997) (Fig. 1.10).

1.5.1.2 Extrasynaptic GABA_A receptors

Whilst the synaptic $\alpha\beta\gamma$ combination is responsible for transient phasic IPSCs, extrasynaptic GABA_ARs receptors that typically contain a δ -subunit in place of γ 2, mediate a less conventional and persistent Cl⁻ influx called “tonic inhibition” i.e. a hyperpolarising current that is always “switched on” (Fig. 1.11_{B1}). Receptors containing the δ -subunit are typically located outside of the synapse (Nusser et al., 1998) and whilst it is believed that the δ -subunit substitutes the γ -subunit (Sieghart et al., 1999; Whiting, 1999); the stoichiometry of $\alpha\beta\delta$ receptors remains uncertain as δ can assume multiple positions in the receptor pentamer (Kaur et al., 2009). δ -subunits can localise with α 1 and several β -subunits (Pirker et al., 2000), but δ -subunit immunoreactivity was frequently co-distributed with α 4 immunoreactivity in the thalamus, striatum, cortex

and dentate gyrus molecular layer (Pirker et al., 2000; Wisden et al., 1992). In particular, immunoprecipitation studies show that antibodies to the δ -subunit precipitate the $\alpha 4$ subunit in TC cells of the VB (Jia et al., 2005), and that $\alpha 4$ and δ subunits colocalise with one another (Sur et al., 1999) predominantly at extrasynaptic sites (Jia et al., 2005). Indeed, $\alpha 4$ knockout mice have been shown to lose tonic inhibition both in the dentate gyrus and in TC neurons (Chandra et al., 2006).

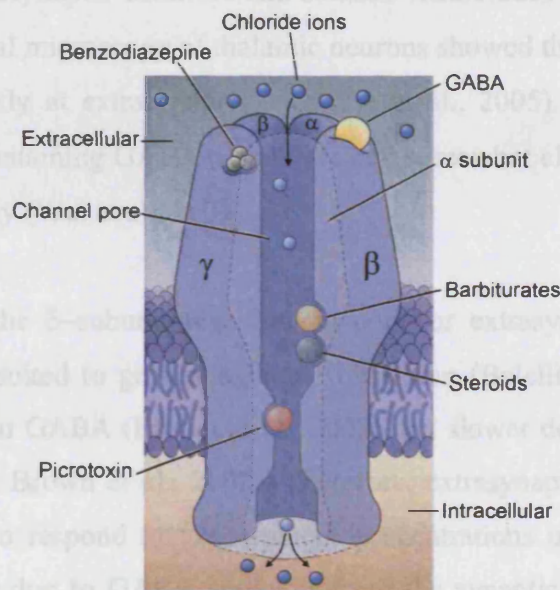


Figure 1.12

Schematic illustration of an ionotropic GABA_A receptor

GABA_A receptors contain two binding sites GABA and numerous sites at which drugs bind and modulate these receptors. Taken and modified from Purves et al., 2000.

Electrophysiological and anatomical evidence from the cerebellum suggests that phasic IPSCs are mediated by postsynaptic GABA_ARs that contain $\gamma 2$ subunits in a combination of diverse α and β (Brickley et al., 1999). In agreement, targeted deletion of the $\gamma 2$ subunit gene in mice results in a dramatic and selective reduction in IPSCs (Essrich et al., 1998). These changes occurred concomitantly with a deficit in postsynaptic clusters of GABA_ARs and the synaptic clustering molecule gephyrin (Essrich et al., 1998). Thus, although $\gamma 2$ subunit is not necessary for receptor assembly

and translocation to cell surface, it is critical to GABA_AR clustering at specific sites on the postsynaptic membrane and pharmacological specificity.

GABA_ARs containing the δ -subunit are thought to be exclusively extrasynaptic (Brickley et al., 2001; Nusser & Mody, 2002). The first indication of this particular subcellular localisation came from work in the cerebellum, where immunogold particles for the δ -subunit could not be detected in synaptic junctions but instead abundantly present in the extrasynaptic dendritic and somatic membranes (Nusser et al., 1998). In agreement, confocal microscopy of thalamic neurons showed that $\alpha 4$ and δ -subunits are found predominantly at extrasynaptic sites (Jia et al., 2005). In granule cells of the dentate gyrus, δ -containing GABA_ARs are located somewhat closer to the synapses, but still perisynaptically (Wei et al., 2003).

The presence of the δ -subunit receptors in peri- or extrasynaptic locations convey properties ideally suited to generating tonic inhibition (Belelli et al., 2009), namely a higher sensitivity to GABA (Brown et al., 2002) and slower desensitisation (Saxena & MacDonald, 1994; Brown et al., 2002). Therefore, extrasynaptic GABA_ARs appear to be “tailor-made” to respond to low ambient concentrations of GABA present in the extracellular space due to GABA spillover from the synaptic cleft (Semyanov et al., 2004; Farrant & Nusser, 2005; Glykys & Mody, 2007a & b).

Tonic GABA_A current was first identified in cerebellar granule cells (Brickley et al., 1996 & 2001; Hamann et al., 2002; Kaneda et al., 1995; Nusser et al., 1998) and later revealed in dentate gyrus granule cells (DGGCs) (Chandra et al., 2006; Nusser & Mody, 2002; Mtchedlishvili & Kapur, 2006) and CA1 pyramidal cells hippocampus (Caraiscos et al., 2004), somatosensory layer V cells (Yamada et al., 2007) and layer II/III pyramidal cells of the cerebral cortex (Drasbek & Jensen, 2006; Drasbek et al., 2007; Vardya et al., 2008), the hypothalamus (Park et al., 2006 & 2007), substantia gelatinosa neurons of the spinal cord (Takahashi et al., 2006) and thalamus (Belelli et al., 2005; Bright et al., 2007; Cope et al., 2005; Jia et al., 2005). In addition, tonic GABA_A inhibition has been identified in DGGCs and interneurons in layer V/VI of the temporal neocortex in human tissue (Scimemi et al., 2006).

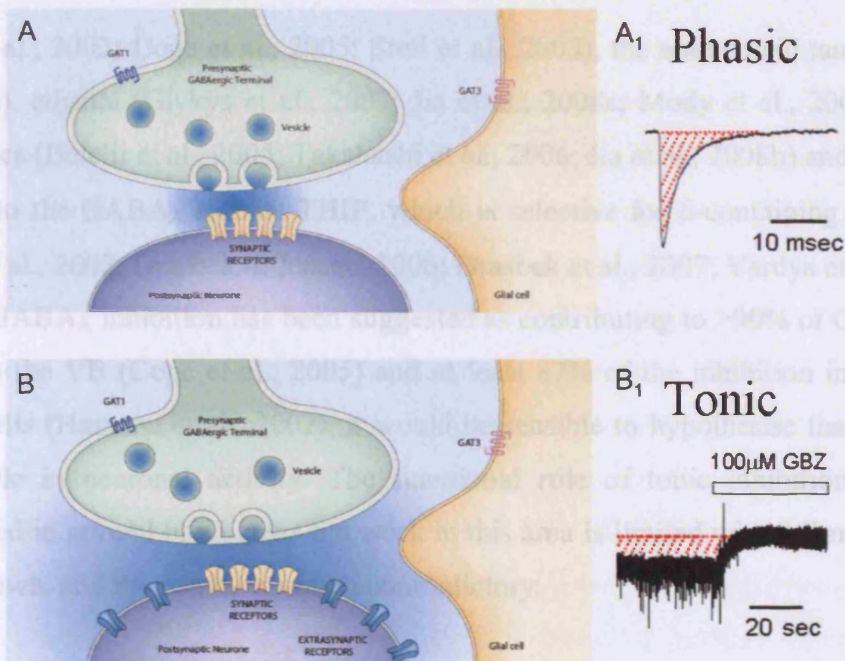


Figure 1.13

Phasic and tonic GABA_A inhibition

Schematic diagram of release of vesicles containing GABA from a presynaptic neuron which activates receptors located at the synapse (A), resulting in an IPSC (A₁). Diffuse low concentration of GABA (represented by blue shading) tonically activates the high-affinity extrasynaptic GABA_A (blue) receptors (B), despite action of GABA transporters removing the transmitter from the extracellular space. The activation of these extrasynaptic GABA_A receptors is revealed by application of the GABA_A antagonist gabazine (GBZ, SR95531) (B₁). Addition of this antagonist blocks phasic IPSCs mediated by synaptic receptors. In addition, the extrasynaptic receptors are blocked resulting in a shift in the holding baseline current of the cell. Red shading in A₁ and B₁ represents the charge transfer of both types of inhibition. Fig A and B modified from Farrant & Nusser (2005), A₁ and B₁ are unpublished recordings of a TC neuron of the VB made by Dr. David Cope.

Extrasynaptic GABA_ARs are pharmacologically distinct from synaptic receptors (Nusser & Mody, 2002). As well as being insensitive to benzodiazepine agonists (Brown et al., 2002; Cope et al., 2005; Nusser & Mody, 2002), δ-subunit containing extrasynaptic GABA_ARs have increased sensitivity to neurosteroids (Belelli et al., 2002;

Brown et al., 2002; Cope et al., 2005; Stell et al., 2003), the amino acid taurine (Jia et al., 2008c), ethanol (Glykys et al., 2007; Jia et al., 2008a; Mody et al., 2007), certain anaesthetics (Belelli et al., 2005; Takahashi et al., 2006; Jia et al., 2008b) and are highly sensitive to the GABA_A agonist THIP, which is selective for δ -containing GABA_ARs (Brown et al., 2002; Drasbek & Jensen, 2006; Drasbek et al., 2007; Vardya et al., 2008). As tonic GABA_A inhibition has been suggested as contributing to >90% of GABAergic activity in the VB (Cope et al., 2005) and at least 87% of the inhibition in cerebellar granule cells (Hamann et al., 2002), it would be sensible to hypothesise that it plays a crucial role in neuronal activity. The functional role of tonic inhibition has been investigated in several brain areas but work in this area is limited with full mechanisms still unknown, and the results are often contradictory:

- eGABA_ARs appear to play a role in regulating light input into the suprachiasmatic nucleus, inhibiting the ability of light to produce phase shifts which is important at night (Ehlen & Paul, 2009);
- In an attempt to clarify the impact of tonic inhibition on neuronal offset and gain and thus neuronal processing, Pavlov et al (2009) examined CA1 pyramidal cell properties. Neuronal offset is altered by shunting inhibition, and the gain of a neuronal response to an excitatory input can be modified by changing the level of "background" synaptic noise. They demonstrated that eGABA_ARs exhibit marked outward rectification, whereas IPSCs exhibit a linear I-V relationship. Tonic GABA_AR-mediated currents had minimal effect upon subthreshold membrane potential variation due to synaptic noise, but predominantly affected neurons at spiking threshold and had a greater modulatory effect on excitatory inputs close to threshold membrane potentials in hippocampal cells (Pavlov et al., 2009). Therefore eGABA_ARs modulated network excitability without altering the sensitivity of neurons to changing inputs i.e. exclusively affecting offset and not gain.
- eGABA_AR activation resulted in a clear increase in latency and variability of LTCP timing, presumably through shunting inhibition in the LGN (Bright et al., 2007). This shunting inhibition would have reduced the voltage change elicited by a stimulus, making it less likely de-inactivation of I_T occurs and possibly destabilising network oscillations (Bright et al., 2007), and

- Tonic current enhancement in TC cells of the VB promoted low-threshold burst firing and block of the tonic GABA_A inhibition led to a small depolarisation that encouraged tonic firing (Cope et al., 2005). This may provide a function to how endogenous agents that decrease tonic GABA_A current may promote wakefulness and those that enhance tonic inhibition can encourage sleep (Cope et al., 2005).

As well as its functional role starting to become clearer, tonic GABA_A inhibition has also been implicated in several pathophysiological conditions. Altered levels of neurosteroids in the CNS are associated with numerous neurological and psychiatric disorders (Herd et al., 2007) including enhanced anxiety during premenstrual dysphoric disorder (PMDD) and elevation of seizure frequency in catamenial epilepsy (Maguire et al., 2005). In DGGCs of hippocampal brain slices of normal mice, elevated progesterone in late diestrus enhanced the expression of δ -subunit containing GABA_ARs and exhibited increased tonic inhibition (Maguire et al., 2005). Reduced neuronal excitability was reflected by diminished anxiety in behavioural observations and seizure susceptibility in the EEG (Maguire et al., 2005).

After pilocarpine treatment, an agent used to elicit temporal lobe epilepsy, a decrease in δ -subunit immunogold labelling at perisynaptic locations and increased γ 2 subunit labelling on dentate gyrus granule cell dendrites was observed (Zhang et al., 2007). The lowered δ -subunit expression could lead to a decrease in tonic inhibition and an associated increase in excitatory activity in the region (Semyanov et al., 2004). Succinic semialdehyde dehydrogenase (SSADH) deficiency is an inherited disorder in which patients display neurodevelopmental retardation, ataxia and absence seizures which progress to tonic-clonic paroxysms (Pearl et al., 2003). Whilst synaptic GABAergic activity in SSADH knockout mice is normal, tonic GABA_A inhibition was strongly increased in layer II/III pyramidal cells of the cortex (Drasbeck et al., 2008), presumably via increased levels of extracellular GABA since its breakdown is impaired in this condition.

Therefore, tonic GABA_A inhibition not only has important implications in normal physiological neuronal networks, but has been implicated in several pathological conditions.

1.5.2 GABA_B receptors

Bowery et al (1980 & 1981) were the first to identify GABA_BRs. GABA application to peripheral nerve terminals exhibited a bicuculline insensitive reduction of evoked noradrenaline release in isolated rat heart and mouse vas deferens tissue (Bowery et al., 1980). This action was mimicked by baclofen, a compound that has no effect on Cl⁻ conductance (Bowery et al., 1981). Furthermore, high-affinity binding sites for ³H-baclofen were identified in crude synaptic membranes of the rat brain (Hill & Bowery, 1981).

Functional studies suggested the presence of distinct GABA_BR variants (Bonanno & Raiteri, 1992 & 1993), which were later confirmed by several autoradiological and molecular techniques. Pre- and postsynaptic GABA_BRs are reported to differ in their sensitivity towards different GABA_BR antagonists (Deisz et al., 1997). Furthermore, auto- and heteroreceptors in cortical presynaptic terminals have been shown to respond differently to various GABA_B antagonists with CGP52432 affecting GABA but not glutamatergic release, and CGP35348 doing the opposite (Bonanno et al., 1997).

1.5.2.1 G-protein coupled metabotropic receptors

Ionotropic receptors gate ions directly whereas metabotropic receptors gate ions indirectly: the receptor and effector functions of gating are carried out by separate molecules (Siegelbaum et al., 2000). G-protein coupled receptors (GPCRs) are metabotropic, contain seven transmembrane spanning domains and are coupled to an effector component by a guanine nucleotide protein (G-protein). The family of GPCRs includes the α - and β -adrenergic receptors, acetylcholine (ACh) receptors, metabotropic glutamate receptors (mGluRs), serotonin and GABA_B receptors (Siegelbaum et al., 2000).

When a neurotransmitter binds to the extracellular surface of the receptor molecule, the intracellular residues of the receptor molecule are phosphorylated, revealing a site for the nearby G-protein to dock (Hille et al., 1992). An activated G-protein results in a complex and long biological cascade that begins with the G-protein binding to the effector molecule of the receptor, which is often an enzyme e.g. adenylyl cyclase (Fig. 1.10). The enzyme can then produce a diffusible second messenger that can bind to its

specific target protein within the cell e.g. another receptor, an ion channel, mobilising Ca^{2+} or a protein kinase that can go on to phosphorylate a target protein.

Due to the motivation of such a complex biological cascade in the cellular cytoplasm, alongside the amplification of the signal at many stages of the cascade (Figure 1.11), the effect of a neurotransmitter-bound metabotropic receptor on a target protein can take tens of milliseconds to minutes (Siegelbaum et al., 2000; Purves et al., 2000). However, the lack of speed and inability to generate action potentials should not shadow the importance of GPCRs. They have the capacity to affect target proteins a great distance from the receptor itself, including other receptor types; therefore can have a profound effect on establishing the electrical and physiological properties of a neuron e.g. modulating resting membrane potential and input resistance of a neuron, the duration of action potentials, transmitter release and can even alter gene expression (Siegelbaum et al., 2000).

Coupling to $G_{i/o}$ protein appears to be the prevalent transduction pathway of native GABA_BRs (Bettler et al., 1998). Pertussis toxin is an exotoxin that catalyses the α subunit of $G_{i/o}$ leaving it in a GDP-bound inactive state (Fig 1.10), thus preventing the G-protein interacting with the GPCR. Intraventricular injection of pertussis toxin into the rat brain three days prior to cutting slices prevented baclofen induction of long-lasting IPSPs (see 1.4.2.4), whilst Cl^- conductance was unaffected (Thalmann et al., 1988). It is believed that the activated α -subunit of $G_{i/o}$ type G protein inhibits AC (Bettler et al., 1998), whilst the $\beta\gamma$ -subunits bind to and activate GIRK channels at postsynaptic sites (Luscher et al., 1997) and repress the opening of Ca^{2+} channels and transmitter release at presynaptic sites (Ikeda, 1996) (Fig. 1.12).

By activating the enzyme AC directly, forskolin can be used to artificially raise levels of cAMP in the cytoplasm of cells. When baclofen is applied alone to brain tissue *in vitro* and *in vivo*, no change in baseline cAMP concentration occurs, however baclofen dose-dependently inhibits forskolin-stimulated AC activity and GABA_BR antagonists counteract the baclofen effect on forskolin-stimulated cAMP (Hashimoto & Kuriyama, 1997; Knight & Bowery, 1996). Indeed the activation of GABA_BR_1 in transfected cells reduced forskolin-induced cAMP formation (Kaupmann et al., 1997).

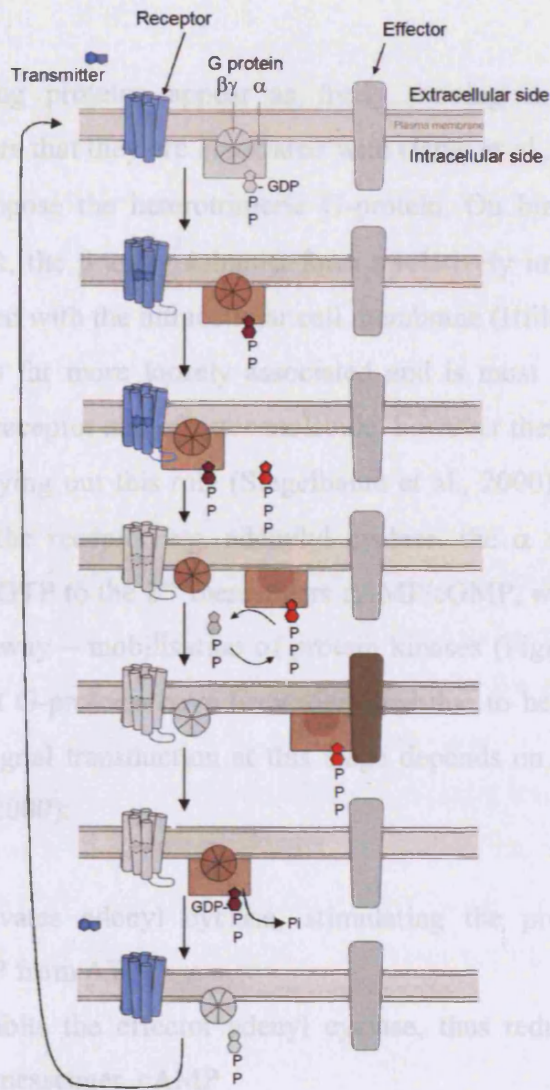


Figure 1.14 Metabotropic GPCR activation

The binding of a transmitter to the receptor allows the G-protein bearing GDP to bind to an intracellular domain of the receptor. This association causes GTP to exchange with GDP, which causes the α -subunit of G-protein, now bearing GTP, to dissociate from the $\beta\gamma$ -subunits. The α -subunit next associates with an intracellular domain of the effector, thereby activating the enzyme to produce 2nd messengers e.g. cAMP from ATP with adenylyl cyclase. Hydrolysis of GTP to GDP and inorganic phosphate (Pi) leads to the dissociation of the α -subunit from the effector and its re-association with the $\beta\gamma$ -subunits. The activation of the effector is repeated until the dissociation of the transmitter returns the receptor to its original conformation. Taken and modified from Kandel et al., 2000.

1.5.2.2 G-proteins

These essential linking proteins appear as freely moving in the cytoplasm and outnumber the receptors that they are associated with (Hille et al., 1992) (Fig. 1.10). α , β and γ subunits compose the heterotrimeric G-protein. On binding to the receptor molecule of the GPCR, the β and γ subunits form a relatively immobile, hydrophobic dimer closely associated with the intracellular cell membrane (Hille et al., 1992) (Figure 1.9). The α subunit is far more loosely associated and is most often responsible for coupling between the receptor and effector molecule, however there are some examples of the $\beta\gamma$ dimer carrying out this role (Siegelbaum et al., 2000). When bound to the effector molecule of the receptor e.g. adenylyl cyclase, the α subunit catalyses the conversion of ATP or GTP to the 2nd messengers cAMP/cGMP, which triggers the next step of the signal pathway – mobilisation of protein kinases (Figure 1.10). At present, more than 12 different G-proteins have been identified due to heterogeneity of the α -subunit, and further signal transduction at this stage depends on the nature of the G-protein (Purves et al., 2000):

- G_s directly activates adenylyl cyclase, stimulating the production of the 2nd messenger cAMP from ATP
- $G_{i/o}$ directly inhibits the effector adenylyl cyclase, thus reduces the intracellular levels of the 2nd messenger, cAMP
- G_q stimulates the effector phospholipase C_β , which cleaves PIP_2 into the 2nd messengers IP_3 and diacylglycerol (DAG)
- G_o mediates inhibition of voltage-dependent Ca^{2+} channels
- G_k activates K^+ channels

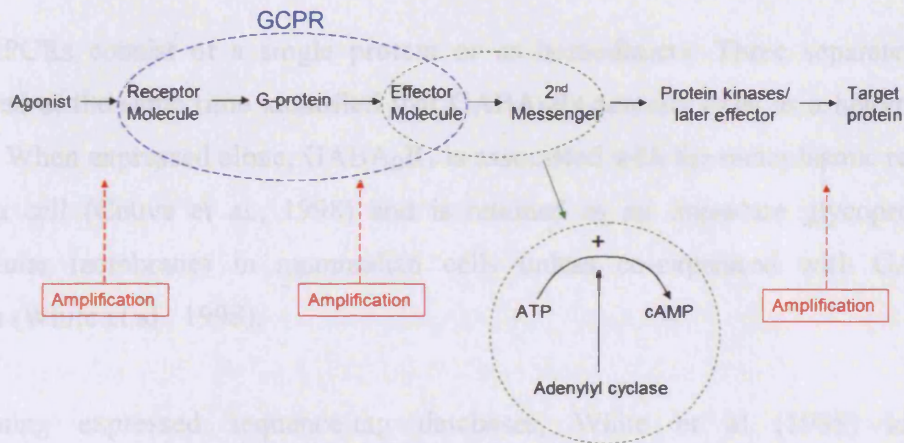


Figure 1.15 Amplification in signal transduction pathways

G-protein molecules outnumber the receptor molecules to which they are coupled. The activation of a single receptor by a single transmitter molecule, can therefore lead to the activation of numerous G-proteins. The G-proteins serve to amplify this small synaptic signal by binding with effector molecules which then synthesise an effective concentration of 2nd messenger within the cytoplasm. Further amplification occurs with the protein kinase reaction (Siegelbaum et al., 2000). While not every step of this signalling pathway involves amplification, the overall cascade results in a tremendous increase in the potency of the initial signal. Taken and modified from Purves et al., 2000.

1.5.2.3 Cellular localisation of GABA_B receptors

GABA_BRs were identified by expression cloning using a high affinity GABA_BR antagonist, CGP64213 (Kaupmann et al., 1997). This ligand allowed the identification of cDNAs encoding two GABA_BR proteins that were designated as GABA_BR_{1a} and GABA_BR_{1b}. Using a novel photo-affinity labelled derivative of [¹²⁵I] CGP71872, they detected two proteins at 130 and 100kDa in the cerebellum, cortex and spinal cord of the rat (Kaupmann et al., 1997). The amino acid sequences of these GABA_BR cDNAs were highly indicative of 7 transmembrane (TM) spanning G protein-coupled receptors (GPCRs) and indicated that these receptors belong to the same gene family as the metabotropic glutamate receptor (mGluR) (Kaupmann et al., 1997). Interestingly, they found that agonists had significantly lower binding at recombinant as opposed to native receptors (Kaupmann et al., 1997). A year later a vital discovery was made.

Most GPCRs consist of a single protein or as homodimers. Three separate studies conducted at the same time identified that GABA_BRs actually exist as a heterodimeric protein. When expressed alone, GABA_BR₁ is associated with the endoplasmic reticulum within a cell (Couve et al., 1998) and is retained as an immature glycoprotein on intracellular membranes in mammalian cells unless co-expressed with GABA_BR₂ subunits (White et al., 1998).

By mining expressed sequence-tag databases, White et al (1998) identified complimentary DNA to the GABA_BR₁, designated as GABA_BR₂. This GABA_BR₂ subunit showed similar homology to GABA_BR₁ subunits i.e. a molecular weight of 110kDa, 7 TM domains and a long extracellular N-terminus (Kaupmann et al., 1998; Jones et al., 1998; White et al., 1998) (Figure 1.12). Through two-hybrid screening, they showed that the GABA_BR₂ forms a heterodimer with GABA_BR₁ through an interaction at their intracellular carboxy-terminal tails (White et al., 1998; Benke et al., 1999; Margeta-Mitrovic et al., 2000). Co-expression of both receptors formed fully functional GABA_BRs at the cell surface that bound with high affinity to endogenous agonists, similarly to native receptors (Kaupmann et al., 1998; White et al., 1998) and conferred robust stimulation of coupled K⁺ channels in transfected cells (Jones et al., 1998).

The GABA_{B2} was later found to be solely responsible for the specific coupling of GABA_BRs to their physiological effectors i.e. G proteins, as GABA_BR₁ could be largely replaced with a random coil peptide without any functional consequences (Margeta-Mitrovic et al., 2001). Agonists bind to the extracellular amino-terminal of the GABA_BR₁ subunit (Kaupmann et al., 1998; White et al., 1998) (Figure 1.12). This produces a conformational change in the GABA_BR₂ subunit that reveals a site for the associated G protein to bind to and thus begin the cascade of events that follow (Bettler et al., 1998). Many splice variants of the GABA_BR₁ subunit have now been genetically identified in different species but not characterised *in vitro*, no evidence for variants of the GABA_BR₂ subunit exists so far but this should not shadow the possibility of currently unidentified GABA_BR₂ splice variants (Bowery et al., 2002).

In situ experiments found that whilst most GABA_BR₁ proteins are associated with GABA_BR₂, the GABA_BR_{1b} variant is located on both presynaptic terminals and postsynaptic sites, and GABA_BR_{1a} preferentially at post-synaptic membrane surfaces

(Benke et al., 1999). Using immunocytochemistry, this localisation was confirmed in the rat thalamus and cerebral cortex (Princivalle et al., 2000 & 2001), however was opposite in the cerebellum and spinal cord. In the monkey VB, GABA_BR labelling was largely associated with extrasynaptic and perisynaptic sites at axodendritic and axosomatic synapses (Villalba et al., 2006). In addition, electron microscopy of rat cerebellum and VB revealed an extrasynaptic localisation of GABA_BR_{1a/b} and GABA_BR₂ (Kulik et al., 2002). Using genetic and electrophysiological methods in wild-type, GABA_BR_{1a}^{-/-} and GABA_BR_{1b}^{-/-} mice, Ulrich et al (2007) found that the two receptor subtypes coexist to a similar degree at postsynaptic sites and GABAergic terminals in TC cells of the VB, but not at glutamatergic terminals. Specifically, GABA_BR_{1a} containing receptors inhibit the release of glutamate from corticothalamic fibres impinging onto TC cells, whereas both GABA_BR_{1a} and GABA_BR_{1b} appear to equally inhibit the release of GABA from NRT neurons onto VB cells (Ulrich et al., 2007).

1.5.2.4 Function of GABA_B receptors

GABA_BRs are metabotropic which means that they gate ions indirectly via coupled guanine nucleotide proteins (G protein) (Siegelbaum et al., 2000) (see Chapter 1.4.2.1). GABA_BRs modulate synaptic transmission by inhibition of transmitter release from presynaptic terminals, increasing a K⁺ conductance responsible for long-lasting IPSCs and by regulating intracellular AC levels (Bowery et al., 1993; Misgeld et al., 1995).

In hippocampal pyramidal cells the postsynaptic action of baclofen was found to involve an increase of potassium conductance (Newberry & Nicoll, 1984, 1985; Gahwiler & Brown, 1985; Inoue et al., 1985a, b). In agreement, synaptic activation of pathways converging on hippocampal pyramidal cells resulted in a slow inhibitory postsynaptic potential that involved an increase in potassium conductance (Newberry & Nicoll, 1985; Hablitz & Thalmann, 1987), and GABA_BRs were suggested as responsible for this phenomenon (Newberry & Nicoll, 1985). Using the selective GABA_BR antagonist phaclofen, Dutar & Nicoll (1988) convincingly established that GABA_BRs exhibit the slow postsynaptic IPSC that was dependent on K⁺ moving out of a cell. Activation of inwardly rectifying K⁺ channels influences membrane excitability by bringing the neuron closer to the equilibrium potential of K⁺ leading to hyperpolarisation (Dutar and Nicoll, 1988). Olsen & Avoli (1997) described the role of

GABA_A and GABA_BRs in the generation of a monosynaptic IPSP in human cortical neurons. An early and fast hyperpolarisation was blocked by bicuculline, a GABA_A antagonist, whereas a GABA_B inhibitor blocked the late portion of the IPSP (Olsen & Avoli, 1997). Both drugs given together abolished the entire IPSP.

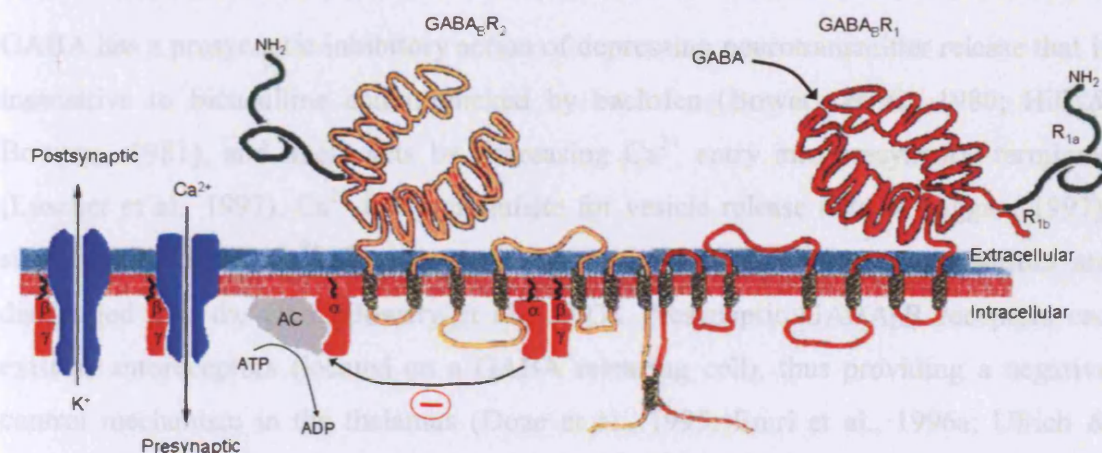


Figure 1.16

Schematic representation of the GABA_B receptor

GABA_BR_{1b} differs from GABA_BR_{1a} in that the amino-terminal 147 residues are replaced by 18 different residues in R_{1b}. The amino-terminal is predicted to consist of two globular lobes that trap GABA upon closure. Binding of the two receptor subtypes at the carboxy termini allows for recruitment of GABA_BRs into functional complexes and direct them to specific signal transduction machineries. Specificity for G protein coupling is likely to be provided by the 2nd intracellular loop. The activated α-subunit of G_{i0} type G protein inhibits AC. The βγ-subunits trigger opening of GIRKs at postsynaptic sites and Ca²⁺ channels at presynaptic sites. Taken and modified from Bowery & Enna (2000) and Bettler et al (1998).

Postsynaptic GABA_BR hyperpolarising action via activation of GIRKs (G protein-coupled inwardly rectifying K⁺ channels) is now a widely accepted phenomenon and has been described in numerous brain areas including the cerebral cortex (Howe & Zieglansberger, 1986) and thalamus (Soltesz et al., 1988; Crunelli et al., 1988). In mice lacking the Kir3.2 K⁺ channel (a GIRK channel isoform) the GABA_BR-mediated

postsynaptic K^+ conductance was abolished (Luscher et al., 1997; Slesinger et al., 1997). Presynaptic $GABA_B$ R-mediated inhibition was unaltered in these animals, demonstrating that GIRK channels do not mediate presynaptic $GABA_B$ R actions (Luscher et al., 1997). However, some data does suggest the presence of some presynaptic K^+ action (Thompson & Gahwiler, 1992).

GABA has a presynaptic inhibitory action of depressing neurotransmitter release that is insensitive to bicuculline and mimicked by baclofen (Bowery et al., 1980; Hill & Bowery., 1981), and likely acts by decreasing Ca^{2+} entry into presynaptic terminals (Luscher et al., 1997). Ca^{2+} is a prerequisite for vesicle release (Wu & Saggau, 1997), such diminution of Ca^{2+} flux means fewer vesicles containing neurotransmitter are discharged into the cleft (Bowery et al., 1993). Presynaptic $GABA_B$ R receptors can exist as autoreceptors (located on a GABA releasing cell), thus providing a negative control mechanism in the thalamus (Doze et al., 1995; Emri et al., 1996a; Ulrich & Huguenard, 1996); or as heteroreceptors on glutamate, serotonin, noradrenaline and acetylcholine releasing cells (Misgeld et al., 1995) mediating inhibition via reducing vesicular release of an excitatory neurotransmitter. $GABA_B$ Rs have been associated with P/Q-, N- and possibly L-type Ca^{2+} channels in various brain regions (Bettler et al., 1998).

In spinal cord neurons, $GABA_B$ R activation decreased the duration of action potentials and excitatory neurotransmitter release from afferent fibres (Curtis et al., 1997), and inhibited both evoked and spontaneous $GABA_A$ R-mediated IPSCs in rat hippocampal slices (Doze et al., 1995). Action-potential independent miniature IPSC (mIPSC) frequency was also reduced by both baclofen and voltage-dependent Ca^{2+} channel blocker, cadmium (Doze et al., 1995). Similarly, baclofen reduced monosynaptically evoked $GABA_A$ IPSCs in slices containing NRT and TC cells to just ~10% of control value (Ulrich & Huguenard, 1996). In addition, baclofen decreased mIPSC frequency by half without affecting the amplitude of the inhibitory currents (LeFeuvre et al., 1997). Such autoinhibition in NRT and TC neurons is also accompanied by presynaptic inhibition of EPSPs in VB and LGN cells (Emri et al., 1996a). Furthermore, the $GABA_B$ R antagonist CGP35348 prevented the occurrence of paired-pulse inhibition, clearly demonstrating the role of $GABA_B$ autoreceptors (Olsen & Avoli, 1997).

1.5.3 GABA and absence seizures

1.5.3.1 Human genetics

Awareness of the polygenic aetiology underlying CAE has led attempts to identify the molecular pathogenesis of mutations and the process of epileptogenesis. Problems stemming from the incomplete penetrance of mutations alongside inter- and intrafamilial phenotypic variations have hindered any great progress (MacDonald & Kang, 2009). Only a few GABA receptor mutations have been mentioned in Section 1.1.2.1, when in fact many more missense, nonsense and frameshift mutations of α_1 , β_3 , γ_2 and δ GABA_AR subunits have been revealed (MacDonald & Kang, 2009). However the majority of these mutations relate to other IGEs and/or FSs, therefore do not accurately represent CAE and typical absence seizures. The developmental aspect of CAE (see 1.1.2.1) alongside the fact that different GABA receptor subunit genes are active at different stages of brain development (Laurie et al., 1992; Snead, 1994) is likely to have great impact on the expression of absence seizures.

1.5.3.2 Interplay of GABA with absence seizures

GABA transmission plays a pivotal role in typical absence seizure expression. Many of the pharmacological agents used to induce SWDs are GABAergic agonists e.g. THIP and GHB (see Section 1.2.2), and interestingly these agents exacerbate SWDs further on (co)administration to other animal models (Aizawa et al., 1997; Depaulis et al., 1988; Snead et al., 1998) (see Tables 1.3, 1.4 and 1.5). Unlike the antiepileptic effect that GABA mimetics have on convulsive epilepsies, enhancement of GABAergic inhibition in the brain potentiates clinical (Ettinger et al., 1999; Perucca et al., 1998; Schachter, 1997; Schachter & Yerby, 1997) and experimental absence seizures (see below).

In the presence of muscimol, THIP, baclofen and γ -vinyl GABA (an irreversible inhibitor of GABA degradation), Vergnes et al (1984) found that SWD duration was increased in GAERS. In agreement, systemic administration of baclofen to GAERS increased duration of SWDs; however CGP35348 dose-dependently suppressed SWDs (Bernasconi et al., 1992; Marescaux et al., 1992a & d). These findings have been repeated in lethargic and stargazer mice (Aizawa et al., 1997; Hosford et al., 1992) and in the GHB model (Snead, 1990 & 1995). Moreover, systemic and thalamic administration of GABA_A and GABA_B agonists elicited SWD-like oscillations in non-

epileptic animals (Hosford et al., 1992 & 1997; Liu et al., 1991; Marescaux et al., 1992a, c, d).

In agreement, direct and bilateral injection of baclofen into NRT and VB of GAERS dose-dependently increased the spontaneous SWDs (Liu et al., 1992). Furthermore, direct application of GVG and muscimol to the ventral lateral thalamus of GAERS significantly increased SWDs whereas the same injection into the midline thalamus had little or no effect (Liu et al., 1991a & b). It is worth highlighting at this point that whilst GABA_A and GABA_B agonist administration will exacerbate a SWD (Liu et al., 1991a & b; Hosford & Wang, 1997; Vergnes et al., 1984), GABA_A antagonists do not suppress or block them (Danober et al., 1998; Snead, 1984). In addition, an irreversible inhibitor of GABA aminotransferase, vigabatrin and tiagabine which blocks GABA removal from the synaptic cleft via GAT-1 both intensify SWDs, but not by direct interaction at the GABA_{A/B} receptor itself (Manning et al., 2003).

Interestingly, synaptic GABAergic changes appear to be minor in experimental animal models of absence. In lethargic and tottering mouse models, excitatory transmission was reduced in thalamocortical neurons but synaptic inhibitory transmission remained intact (Caddick et al., 1999). In agreement, miniature GABA_A IPSCs and the baclofen reduction of IPSC frequency in VB and cortical neurons were no different in pre-seizure GAERS compared to NEC (Bessaih et al., 2006). The only differences observed were in NRT neurons, in which GAERS exhibited 25% larger amplitude and 40% faster mIPSC decay. In addition, baclofen was significantly less effective in decreasing mIPSC frequency in GAERS (Bessaih et al., 2006).

Transgenic mice over expressing the GABA_BR_{1a} subunit exhibit spontaneous and recurrent SWDs which were blocked by ETX and CGP35348 and exacerbated by baclofen (Wang et al., 2009; Wu et al., 2007). Whilst these animals are perhaps more representative of atypical absences (Wu et al., 2007), they still provide further evidence that enhanced GABA mediated inhibition is necessary to enhance or induce absence seizures.

1.6 Aims

Typical absence seizures are characteristic of many idiopathic generalised epilepsies and are the only seizure type in CAE. They appear in the EEG as synchronised, bilateral SWDs and are accompanied by impairment of consciousness and behavioural arrest. Through studies of patients and experimental animal models, we know that absence seizures arise in thalamocortical networks. Whilst SWD initiation takes place in the somatosensory cortex, the thalamus quickly becomes entrained. Several studies have advanced our understanding of the cellular mechanisms that underlie absence seizures; however they remain not fully understood.

Unlike convulsive epilepsies, systemic or intrathalamic administrations of GABAergic promoting agents exacerbate absence seizures in both patients and various experimental animal models. Several GABA_AR subunit mutations have been identified but mostly represent cohorts with more complex phenotypes than pure CAE. Furthermore, only minor changes in synaptic GABA_A inhibition have been revealed in animals with spontaneous SWDs.

Considering that augmented rather than impaired GABA transmission is a likely feature of absence seizures alongside the knowledge that only limited synaptic changes have been identified, it would be interesting to investigate the presence and role of tonic GABA_A inhibition in absence seizures. Therefore, the *first aim* of the work described in this thesis was to study the presence of tonic GABA_A inhibition in the VB thalamus of animals with spontaneous SWDs (GAERS) and with pharmacological agents that induce SWDs in otherwise normal animals. This was done using *in vitro* patch clamp technique in brain slices.

These data from these experiments revealed that enhanced tonic GABA_A inhibition was a common cellular phenomenon across all of the major animal models of absence epilepsy (Cope et al., 2009). Through further *in vitro* investigations Dr. Cope identified that aberrant GABA re-uptake via GAT-1 in the VB thalamus of GAERS was responsible for the increased tonic GABA_A current (Cope et al., 2009). The *second aim* of the work in this thesis was to further characterise the significance of this cellular pathology using *in vivo* methods. Indeed, direct thalamic block of GAT-1 was sufficient

to induce SWDs in normal animals and GAT-1 knockout mice were found to exhibit spontaneous seizures.

GHB enhanced tonic GABA_A current *in vitro* via postsynaptic GABA_BRs and GHB was unable to induce SWDs in extrasynaptic GABA_AR knockout mice, both suggesting a modulation of extrasynaptic GABA_A receptors by postsynaptic GABA_BRs and extrasynaptic GABA_ARs. Thus, the *third aim* of this thesis was to investigate this possibility further with the specific GABA_B agonist, baclofen.

Chapter 2

Methods

All experiments were performed in accordance with the United Kingdom Animal (Scientific Procedures) Act (1986). All procedures were approved by local ethical review and covered by appropriated project and personal licences. Every precaution was taken to minimise animal suffering and number of animals used.

2.1 In vitro experiments: whole-cell patch clamp recordings

2.1.1 Animals

Litters of Wistar rats were obtained from Harlan (UK) at postnatal (P) day 15. They remained housed with the mother until both male and females were used at P21-26. GAERS and NEC rats (P14–30) were bred and obtained from an established colony at the School of Biosciences, Cardiff University (UK). All animals had access to food and water *ad libitum*. The animal facility was maintained on a 12:12 hour light:dark cycle (8am:8pm), at a constant ambient temperature (19-21°C) with 45-65% relative humidity.

2.1.2 Slice preparation

Brain slices were prepared and maintained according to the methods described in Cope et al (2005). All solutions were prepared and oxygenated with carbogen (95% O₂ / 5% CO₂) prior to, throughout and after cutting slices (Table 2.1). Wistar, GAERS and NEC rats were anaesthetised using a mixture of isoflurane and oxygen (at 2.5l/min O₂ with 5% isoflurane) until loss of righting-reflex and then decapitated. The brain was rapidly removed from the cranium and placed in a small beaker containing ~75ml of ice-cold (≤ 4 °C) “cutting” aCSF (Table 2.1). After ~30 seconds, the brain was taken from the aCSF and placed on a cooled petri dish covered with filter paper. Sections of each brain were cut and discarded to isolate a block of tissue containing the region of interest, in the correct orientation. The tissue block was carefully glued to a cutting stage and rapidly transferred to the cutting chamber of a Microtome microslicer (Microm, Walldorf, Germany), where it was immediately re-submerged in the remaining ice-cold (≤ 4 °C) “cutting” aCSF (Table 2.1). 300µm thick slices were then cut. To avoid neuronal death as much as possible, the process of “blocking” and transferring the brain tissue took no longer than two minutes. A fiber-optic light (Microtec Fibre Optics) was

positioned over the cutting chamber that was kept at $\leq 4^{\circ}\text{C}$ throughout (Microm cooler, model: CU 65).

Thalamic slices (6-8 hemisections) containing the VB were cut in the horizontal plane, using the anterior commissure, internal capsule and fornix as landmarks (Paxinos & Watson, 1986). Hippocampal slices were cut in the horizontal plane and 7-8 pairs of slices were collected from each brain. Alternatively, a sagittal cut generated 6–8 cerebellar slices. Slices were immediately placed in an incubation chamber containing “cutting” aCSF, minus indomethacin or kynurenic acid at room temperature ($\sim 22^{\circ}\text{C}$) for initial storage (see Table 2.1).

After 20 minutes:

- “Storage” aCSF (Table 2.1) gradually replaced aCSF in the incubation chamber at 1.5 ml/min using a peristaltic pump (REGLO-Digital; Ismatec, Switzerland);
- A water bath (Grant, JB series) containing beaker(s) of “recording” aCSF was turned on to heat at $\sim 55^{\circ}\text{C}$, and
- A master-heating element (model: Badcontroller V; Luigs and Neumann, Germany) started warming the recording chamber on the microscope and the perfused recording aCSF (1.5 ml/min) to $33\pm 1^{\circ}\text{C}$

2.1.3 Whole-cell patch clamp recordings

An hour later, one slice was carefully moved to the recording chamber of the microscope where it was continuously perfused (1.5ml/min) with recording aCSF at $33\pm 1^{\circ}\text{C}$. The slice was anchored in place by a nylon grid glued onto a flattened, platinum U-shaped frame. The rest of the slices remained in the incubation chamber at room temperature, maintained in the storage aCSF until required. Whole-cell patch clamp recordings were then made from the soma of cells under voltage-clamp conditions. Experiments were performed on a single neuron within a single slice, after which the slice was discarded. The experimental setup was placed on a leveled air table (Technical Manufacturing Corporation; MA, USA), inflated by nitrogen.

aCSF	Concentration (mM)										Temp °C
	NaCl	Glucose	CaCl ₂	MgCl ₂	NaH ₂ PO ₄	KCl	NaHCO ₃	Sucrose	KA	Indo	
Cut	85	10	2	2	1.25	2.5	26	73.6	3	0.0045	≤ 4
Initial storage									0	0	~22
Storage	126	10	2	2	1.25	2.5	26	0	0	0	~22
Record	126	10	2	1	1.25	2.5	26	0	3	0	33±1

Table 2.1

Table showing the concentration of compounds in aCSF solutions

Stock (x 20) of all three aCSF solutions, minus glucose and NaHCO₃, were prepared every week. Dilution of each stock solution into 500ml of distilled H₂O, with addition of glucose and NaHCO₃, was done for each experiment prior to cutting slices. Compound concentration in each aCSF varied depending on the stage of slice preparation, however all three solutions had osmolarity of 300–305mOsm. All solutions were thoroughly oxygenated prior to, during and after cutting slices and throughout recording. The pH of normal aCSF is ~7.6, but when it is bubbled with carbogen, the high (95%) oxygen reacts with the bicarbonate (NaHCO₃) to form a weak carbonic acid. This brings the pH down to 7.3-7.4 which is physiological for CSF. Adding kynurenic acid (KA) to aCSF causes the pH to fall to ~7.0 so we add alkali (a few drops of 1M NaOH; no more than 0.5ml) to adjust aCSF to 7.6. This way, once the aCSF is bubbled with carbogen it acidifies once again and comes down into physiological range.

2.1.3.1 Cell identification

Cells were visualised using a microscope (Luigs and Neuman; Germany) with differential interference contrast-infrared optics (DIC-IR). Using a 10X air objective (Nikon; Japan) and normal wavelength light, the brain region of interest was moved into the field of view. A 40X-immersion objective (Nikon; Japan) and infrared-filtered light visualised individual neurons on a black and white monitor (LCD display monitor, JVC; Brian Reese Scientific, Newbury, UK) connected to a TV lens (Nikon; Japan) and CCD video camera (C7500-51, Hamamatsu; Hamamatsu Photonics Ltd, Welwyn Garden City, UK).

The healthiest cells were identified using specific visual criteria. Cells that had a visible nucleus or were swollen, shrunken and had outward blebs on the cellular membrane were presumed dead or dying and thus avoided. Those that had a clear, smooth and bright three-dimensional appearance were considered healthy (Molleman, 2003; Walz et al., 2002) and a patch attempt would be made on these cells. The healthiest cells were usually located and patched between 40–90µm deep in the slice, and each cell type varied in size and shape.

2.1.3.2 Pipettes

Pipettes were pulled from borosilicate glass capillaries (GC-120F-10; Harvard Apparatus, Kent, UK) using a Flaming/Brown micropipette puller (Model P-97, Sutter Instruments Co, USA). The micropipette puller was programmed to generate pipettes specifically for each cell-type, thus the open tip resistance of these pipettes was altered depending on the cell-type recorded. Pipettes used to patch thalamo-cortical (TC) cells of the VB had an open tip resistance (R_{pip}) between 2–5 MΩ when filled with an intracellular solution that contained the following (in mM): 130 CsCl, 2 MgCl₂, 4 Mg-ATP, 0.3 Na-GTP, 10 HEPES and 0.1 EGTA (pH 7.25– 7.30; 290-293 mOsm). Pipettes used to patch granule cells of the dentate gyrus had an open tip resistance of 3–5 MΩ, and 4–8 MΩ for cerebellar granule cells when filled with CsCl intracellular solution.

50ml stock of this CsCl intracellular solution was made when required. It was immediately frozen in 0.5ml aliquots after being filtered using a 0.2µm inorganic membrane syringe filter (25mm, Whatman International Ltd, Maidstone, UK). For each experiment, an aliquot was thawed and kept on ice in a 1ml syringe. The intracellular solution was filtered a second time (0.2µm, 4mm; Nalgene, CA, USA) whilst filling the pipette with a non-metallic syringe-needle (MicroFil; World Precision Instruments, FL, USA).

2.1.3.3 Obtaining whole-cell patch

Pipettes were fixed to a headstage of an Axopatch 200A amplifier (Axon Instruments, CA, USA) mounted on a manipulator and connected, via an analog-to-digital converter

(Digidata 1322A, Axon Instruments), to a personal computer. The oscilloscope mode of the pCLAMP 9.0 software (Molecular Devices) was used to observe current changes relayed by the amplifier and to record data.

Positive pressure was applied to the patch pipette via a plastic tube connected with the pipette holder. A stop-cock four-way tap was attached to the alternate end of the tube and pressure at the pipette tip could be controlled by opening or closing this tap. The pipette was moved into the aCSF being perfused through the recording chamber and the manipulator was locked tightly into position. When the pipette tip was initially in the recording chamber, offset was moved to zero. Both the microscope, via a Nikon F-2 focus unit, and the manipulator were connected to a keypad controller (Keypad SM-5, Luigs and Neumann, Germany). These two keypad controllers were connected to a master control box (SM-5 Master (10); Luigs and Neumann, Germany), permitting simultaneous but separate, coarse and fine movements of both the pipette and microscope in the X, Y and Z - axes.

With positive pressure clearing the cellular membrane of any “debris”, the pipette tip was manouvered near to the cell. By observing the current response to a 5mV voltage test pulse or “seal test”, it was possible to predict the status between pipette tip and cell membrane. On contact i.e. a small dimple becoming visible and a current drop in response to the seal test, the positive pressure was released. A high resistance seal between the tip of the pipette and cell soma membrane was obtained ($>1 \text{ G}\Omega$) and the holding potential lowered from 0 mV to -70 mV (see Section 2.1.4).

At this stage, fast and slow components of pipette capacitance (C_{pip}) were corrected appropriately. Whole-cell configuration was reached via breakthrough of the membrane by applying gentle suction via the stop-cock tap and a zap located on the amplifier (0.5–3 msec), aided by the difference in osmolarity between internal pipette solution and the cell. Series resistance (R_s) and whole-cell capacitance were estimated by cancelling the large capacitive transients revealed by the seal test. Series resistance was monitored throughout the recording period and was compensated by 75–80% in the presence of a lag value of 7 μsecs throughout all recordings. Data were kept if the R_s value was

between 5–15 M Ω at the beginning, and had not deviated >30% at the end of the recording. Whole cell capacitance (pF) was noted (see Section 2.1.7.1.3).

2.1.4 Isolation of GABA_A currents

At ~ -65 mV, the physiological reversal potential of Cl⁻ (E_{Cl}) is close to the resting membrane potential of the cell. Under physiological conditions, the extracellular concentration of Cl⁻ is higher than the intracellular concentration. When a Cl⁻ channel opens e.g. GABA_A receptor, Cl⁻ ions are driven by the concentration gradient and against the negative resting membrane potential, thus flow into the cell generating an outward current.

In these experiments, neurons were voltage-clamped at a holding potential of -70 mV and therefore, E_{Cl} was raised to ~ 0 mV. The high concentration of CsCl in the pipette “Cl⁻ loaded” the cell and the extracellular Cl⁻ concentration of the aCSF was lowered (1mM MgCl). As a result, the direction of ion movement was reversed and GABA_A-mediated Cl⁻ currents became inward.

Caesium in CsCl blocks outward K⁺ channels (Gahwiler & Brown, 1995; Spain et al., 1987). Therefore, when the patch status changed from “cell attached” to “whole-cell” there was a net inward current at -70 mV. With outward K⁺ channels blocked, the “leak” of the cell membrane was reduced i.e. the integrity of the membrane was heightened. A more electrically compact neuron meant that it was possible to observe smaller electrical signals and signals further from the soma.

Kynurenic acid (3mM) and tetrodotoxin (TTX, 500nM) were present in all recording aCSF to block ionotropic glutamate receptors and Na⁺ dependent action potentials, respectively. Thus, only action potential independent miniature inhibitory postsynaptic currents (mIPSCs) were present. TTX was omitted from the aCSF used for some recordings of GAERS and NEC. 5 μ M GABA was included in the recording aCSF for hippocampal slice experiments, in agreement with Glykys & Mody (2007). Tonic

current in these slices is dependent on vesicular release of GABA, thus TTX would significantly affect tonic current recordings.

2.1.5 Experimental Protocol

A recording commenced only when series resistance and baseline current were stable, usually 5-10 minutes after obtaining whole-cell configuration. Two different protocols were used: short (Fig. 2.1A) and long (Fig. 2.1B).

2.1.5.1 Short protocol

Under control conditions, a slice was continuously perfused with recording aCSF as described in Table 2.1. To investigate action of various drugs, each slice was placed into the recording chamber that contained aCSF the additional drug(s). Thus, a slice was in the continuous presence of any agent tested. The presence of a GABA_A receptor-mediated tonic current was exposed by focal application of the GABA_A antagonist 6-amino-3-(4-methoxyphenyl)-1-(6H)-pyridazinebutanoic acid hydrobromide [SR 95531, gabazine] (GBZ) into the recording chamber. After 55 seconds of stable baseline recording was obtained, 100 μ M GBZ was focally applied using a 100 μ l pipette (Gilson, France; 20 μ l of a 10mM stock solution).

GBZ blocked sIPSCs, mIPSCs and the tonic Cl⁻ conductance mediated by extrasynaptic GABA_A receptors therefore decreased current required to maintain a cell membrane at the -70mV holding potential. As a result, and due to the inward nature of the Cl⁻ current under these experimental conditions (see Section 2.1.4), an outward shift of baseline current occurred. This baseline shift corresponded to the presence of a GABA_A receptor-mediated tonic current (Fig. 2.1A).

2.1.5.2 Long protocol

Alternative to the chronic application of a drug as in the short protocol, drugs were acutely applied through the perfusion system of the experimental set-up in this protocol. After approximately 60 seconds of stable baseline recording had been obtained, aCSF containing the additional drug(s) was acutely perfused through the slice. Following at

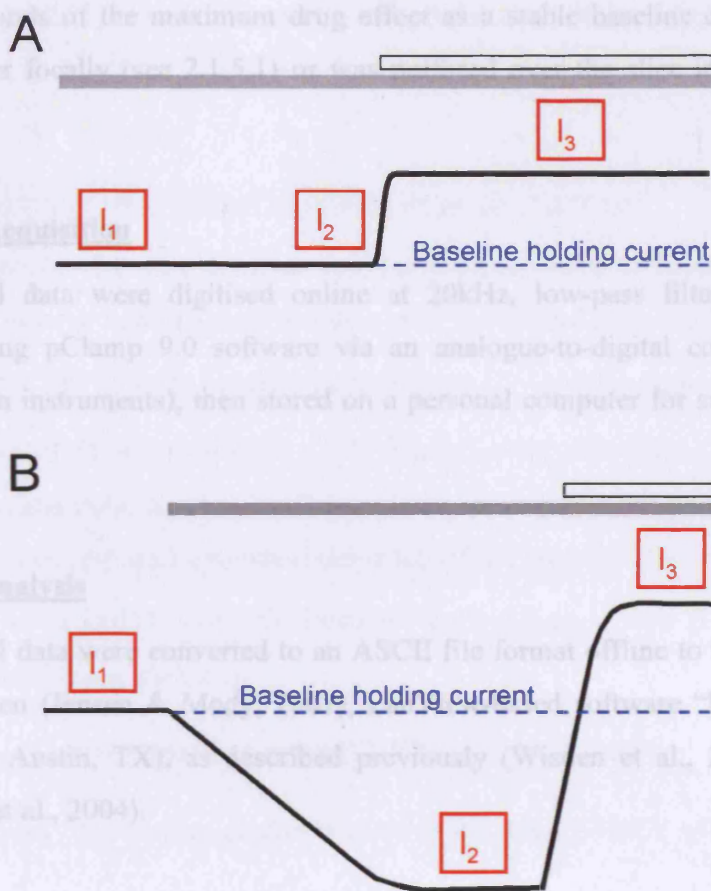


Figure 2.1

Schematic illustration of typical recordings under short (A) and long (B) protocols

The white bar indicates presence of GBZ. The grey bar indicates the presence of a drug either present from the start of the recording (A) or applied through the perfusion system of the setup following baseline recording (B). Red boxes represent the blocks selected for analysis (see Sections 2.1.7.1 and 2.1.7.2), I_1 and I_2 represent baseline holding current in A with I_1 representing baseline holding current in B. **A)** Application of GBZ blocks both synaptic and extrasynaptic GABA_ARs. This results with block of phasic events and tonic GABA_A current, resulting in an outward (upward) shift in holding current of the cell (I_3). **B)** As with in A, GBZ application results with an outward (upward) shift in holding current of the cell (I_3) in long protocol recordings. The effect of the drug(s) applied after 60 seconds of recording baseline holding current was observed. If the drug(s) enhanced tonic GABA_A current then an inward (downward) shift in baseline current was observed (I_2).

least 30 seconds of the maximum drug effect as a stable baseline current. GBZ was applied either focally (see 2.1.5.1) or was perfused over the slice in additional aCSF (Fig. 2.1B).

2.1.6 Data Acquisition

Experimental data were digitised online at 20kHz, low-pass filtered at 3kHz and acquired using pClamp 9.0 software via an analogue-to-digital converter (Digidata 1322A; Axon instruments), then stored on a personal computer for subsequent off-line analysis.

2.1.7 Data analysis

Experimental data were converted to an ASCII file format offline to be analysed using custom-written (Jensen & Mody, 2001), LabView-based software “EVAN” (National Instruments, Austin, TX), as described previously (Wisden et al., 2002; Stell et al., 2003; Cope et al., 2004).

2.1.7.1 Tonic GABA_A current

For analysis of GABA_A receptor-mediated tonic current, 3 blocks of the baseline value were required from each recorded cell, for both protocols. Using the detection software of EVAN, 5ms segments of the baseline were captured every 100ms for an entire trace. In both protocols, blocks of the baseline were selected and the 5ms segments contained within each block were subsequently imported into the analysis software.

In order to avoid IPSCs or small shifts of baseline holding current from skewing the current value of each block, a baseline standard deviation was applied to each group of 5ms segments as a limiting criterion. The baseline standard deviation was determined by visually inspecting the 5ms segments of the I₁ block of each cell and then applying a threshold. Any segments above this threshold e.g. segments that lay on IPSCs, were regarded as contaminated and removed from the group. A mean baseline value was calculated from the remaining “uncontaminated” group of 5ms segments in each block and this value was imported into Microsoft Excel (v. 2003) for statistical analysis. The

baseline standard deviation that was determined for I_1 was then applied to I_2 and I_3 for each cell.

2.1.7.1.1 Analysis of tonic current amplitude in the short protocol

Three 5 second blocks were selected: one immediately prior to focal GBZ application (I_2), and two more at equitemporal distance prior to (I_1) and after focal GBZ application (I_3) (Fig. 2.1A). The average baseline control value ($I_2 - I_1 = \Delta_{\text{CONTROL}}$) and the baseline shift post-GBZ application value ($I_3 - I_2 = \Delta_{\text{TONIC}}$), were calculated (Fig. 2.1A). Under each experimental condition i.e. a cell population recorded in the presence of the same drug(s), the mean amplitude, standard deviation of the mean (STDEV) and the standard error of the mean (SEM) was calculated for both Δ_{CONTROL} and Δ_{TONIC} . A cell was included in the cell population if:

- i) Δ_{TONIC} was larger than twice STDEV of I_1 and I_2 , and
- ii) Δ_{TONIC} was a value greater than twice the mean STDEV of Δ_{CONTROL} .

These two criteria ensured that the outward baseline shift following GBZ application was larger than any “drift” in baseline current prior to GBZ application.

- iii) Student’s paired t -test compared the mean amplitude of Δ_{TONIC} to Δ_{CONTROL} over each cell population. If significantly different, the presence of a tonic current was finally established.

This constituted the third criterion applied to the data, and due to its role as an “internal control”, the significance will not be stated for the duration of this thesis.

Student’s unpaired t -test was used to compare the mean amplitudes of GABA_A receptor-mediated tonic current (Δ_{TONIC}) under different experimental conditions. The mean Δ_{TONIC} value for each condition, SEM and significance are stated (see Chapters 3 & 5).

2.1.7.1.2 Analysis of tonic current amplitude in the long protocol

Unlike the short protocol, it was not possible to objectively determine 3 equitemporal blocks from these recordings. This was due to some variance in the speed of drug action which was dependent on the time the perfused aCSF reached the recording chamber, depth of the cell in the slice and affinity of drug for receptor type. Instead, a longer block was selected to ensure an accurate mean of baseline could be calculated. Three 20 second-periods were selected: first from the control (I_1), second at the maximum drug-induced change (I_2) and third, post-GBZ application (I_3) (Fig. 2.1B). For each cell, the post-GBZ baseline value (I_3) was used to calculate both control ($I_3 - I_1 = \Delta_{\text{CONTROL TONIC}}$; area above red dotted line in Fig. 2.1B), and drug-elicited changes to tonic current amplitudes ($I_3 - I_2 = \Delta_{\text{DRUG TONIC}}$; area below red dotted line in Fig. 2.1B). The drug induced change of tonic current amplitude was also calculated: $\Delta_{\text{DRUG TONIC}} - \Delta_{\text{CONTROL TONIC}} = \Delta_{\text{CHANGE}}$. Mean amplitude, STDEV of the mean and SEM was calculated for $\Delta_{\text{CONTROL TONIC}}$, $\Delta_{\text{DRUG TONIC}}$ and Δ_{CHANGE} . Student's paired *t*-test was used to determine significant effect of a drug, comparing $\Delta_{\text{CONTROL TONIC}}$ and $\Delta_{\text{DRUG TONIC}}$. Mean amplitude of Δ_{CHANGE} from each condition was used for comparison to other experimental conditions, using Student's unpaired *t*-test. Mean $\Delta_{\text{CONTROL TONIC}}$ and $\Delta_{\text{DRUG TONIC}}$ values for each condition, SEM and significance are stated (see Chapters 3 and 5).

2.1.7.1.3 Normalised tonic GABA_A current

For each cell, the tonic current amplitude (Δ_{TONIC} for short protocol; $\Delta_{\text{CONTROL TONIC}}$ and $\Delta_{\text{DRUG TONIC}}$ for long protocol) was divided by its whole-cell capacitance value. The mean, STDEV and SEM of the normalised tonic current amplitude was calculated for each experimental condition. Student's unpaired *t*-test was used to compare the mean value of normalised tonic current amplitude between different experimental conditions (for both long and short protocols) and Student's paired *t*-test was used to compare

these values within an experimental condition for the long protocol. The mean value (pA/pF), SEM and statistical significance are stated (see Chapters 3 and 5).

2.1.7.2 IPSC analysis

The first 55 seconds of a short-protocol recording were selected for IPSC analysis. The I_1 and I_2 blocks selected for tonic current analysis in long-protocol recordings were extended as close to 60 seconds as possible.

Again, using the detection software of EVAN, miniature (mIPSCs) and spontaneous (sIPSCs) IPSCs were distinguished by applying amplitude and kinetics-based thresholds. All detected events were imported into analysis software and individual IPSC events were visually inspected for validity, being segregated into either contaminated or uncontaminated events. Contamination involved other IPSCs occurring before the first had returned to baseline, or no smooth, clear peak present. Some events detected as below the threshold and included by the software were obviously baseline noise, and these were discarded.

The uncontaminated IPSCs were averaged and peak amplitude, rise time (10-90%), weighted decay time constant (the integral of the average IPSC from peak divided by peak amplitude) and the charge transfer (the integral of the average IPSC for each cell) were calculated. The frequency of IPSCs was taken as the total number of IPSCs (both contaminated and uncontaminated) divided by the number of seconds in the selected epoch of time. The properties of the averaged IPSCs between experimental conditions were compared using Student's unpaired *t*-test.

All Student's *t*-tests used for tonic GABA_A current analysis and IPSC analysis were 2 tailed.

2.2 In Vivo experiments: reverse microdialysis and EEG recordings

In vivo experimental procedures were similar to the methods described in Richards et al (2003) and Manning et al (2004).

2.2.1 Animals

All animals had access to food and water *ad libitum*. The animal facility was maintained on a 12:12 hour light:dark cycle (8am:8pm for rats, 6am:6pm for mice), at a constant ambient temperature (19-21°C) with 45-65% relative humidity.

2.2.1.1 Rats

Male Wistar rats (250–300g, >13 weeks of age) were obtained from Harlan (Bicester, UK), and then housed individually at Cardiff University (UK). Male and female GAERS and NEC (250-300g, 6–12 months of age) were obtained from an established colony at the School of Biosciences, Cardiff University (UK).

2.2.1.2 Mice

Breeding pairs of GABA_AR δ -subunit knockout (KO) mice were obtained from The Jackson Laboratory (Bar Harbor, Maine, USA) and a colony was initiated and bred in-house at the School of Biosciences, Cardiff University (UK). δ -KO mice and their wild-type (WT) littermates between 6 and 12 months of age (25–35g) were used for experiments. Breeding pairs of GAT-1 KO mice were obtained from the Mutant Mouse Regional Resource Center (University of California, Davis, USA). A colony of GAT-1 KO mice was established and both male and female KOs and WT littermates were used at 6-7 months of age (25–35g).

2.2.1.3 Genotyping mutant mice

Heterozygous breeding pairs of GAT-1 and δ -subunit GABA_A mice were used to generate WT, heterozygous and mutant offspring. Although GAT-1 mice have an identifiable phenotype that includes tremor and ataxia, δ -subunit KO mice exhibit no discernable phenotype. Therefore, it was necessary to use a genotyping protocol to identify offspring. Genotyping involved the polymerase chain reaction (PCR) which isolates and selectively amplifies a specific region of DNA.

Briefly, PCR relies on specific cycles of repeated heating and cooling which results in separation of DNA strands (denaturation step) at ~95°C, binding of primers to the single strands of DNA (annealing step) at 50-60°C and then enzymatic replication of the DNA (extension step) at 75-80°C. Primers are short DNA fragments containing sequences

complementary to the DNA target region i.e. GAT-1 or δ -subunit mutation. Specifically, two primers which are complimentary to the 3' (three prime) end of the sense and anti-sense strand of the DNA target are required. These primers along with DNA polymerase and deoxynucleoside triphosphates (dNTPs; the building blocks from which new DNA is assembled) were present in the PCR setup to enable selective and repeated DNA amplification; with primers essential for the initiation of DNA synthesis and DNA polymerase critical for assembling new DNA strands. As PCR progresses and the above steps are repeated, the DNA generated is itself used as a template for replication, setting in motion a chain reaction in which the DNA template is exponentially amplified. Finally, to ascertain whether PCR generated the anticipated DNA fragment, agarose gel electrophoresis was used to separate the DNA by size. The size of the DNA was compared to a molecular weight marker and a positive control. Assessment of the resulting DNA bands indicated if the successful amplification of the DNA had been achieved and thus, whether the animal was WT, heterozygote or mutant.

This genotyping protocol was carried out by Phillip Blanning at Cardiff University, and as I did not perform this technique I have not included the genotyping results in this thesis.

2.2.2 Anaesthesia and analgesia

Initially, rats and mice were anaesthetised using at 3l/min oxygen with 5% isoflurane. Once anaesthetised, animals were positioned on a stereotaxic frame. To maintain an appropriate degree of anaesthesia, rats received a combination of 1.5 l/min O₂, 0.5 l/min N₂O with 1.5-2.5 % isoflurane and mice received 2.5 l/min O₂ with 1.5-2.5% isoflurane. Anaesthesia was considered to be sufficient for surgery when there was absence of the pedal withdrawal reflex (assessed by extending the hind leg and pinching between digits of the foot), and tail pinch reflex (Flecknell, 1996). Responses to these reflexes and the breathing rate were monitored throughout the surgery, with anaesthesia levels altered if appropriate. Before the effects of isoflurane wore-off, all rats and mice received 1ml saline i.p. to help prevent dehydration.

2.2.3 Surgical procedures

2.2.3.1 Surgical procedure: Implanting EEG electrodes in rat

The rat was positioned on a stereotaxic frame such that the top, front teeth were placed over a horizontal bar, ear bars were positioned in both auditory canals and a further horizontal bar was clamped over the snout, through which maintenance anaesthesia was administered. Together, these ensured a fixed, horizontal position of the top of the skull. To maintain the body temperature of the rats, a heater (model, company) set to 37°C was placed beneath the animal.

Hair on the head was dampened and then clipped. Using a scalpel, a midline incision was made from above the snout to the back of the skull. Four clamps secured to connective tissue under the skin (2 anterior, 2 posterior) were used to open up the skull area and to keep the eyes of the rat closed. All muscle and connective tissue covering the skull was then scraped away and blood vessels in the surrounding skin were cauterised. Taking care to avoid the eyes, H₂O₂ was used to remove any debris that remained on the skull.

Six gold plated screw posts (1cm, Svenska Dentorama AB; UK) were used to record the EEG of each animal. Each screw post or “electrode” was carefully soldered to an exposed end of copper wire (~2cm long) prior to surgery. A dental drill was used to make six holes: bilaterally over the frontal cortex (anterior to bregma and lateral to midline), the parietal cortex (posterior to bregma and lateral to midline) and ground/reference screw electrodes over the cerebellum (posterior to lambda and lateral to midline). The screws were fixed permanently to the skull with methylacrylic cement. Whilst the first layer of cement was setting, the other end of the copper wire of each screw was soldered onto a pre-prepared 6-channel multiple connector. Additional cement was layered around the electrodes, wires and connector resulting in a smooth-sided headmount providing easy access to the connector. Skin at the front and at the back of the headmount was then sutured. Once the cement had set, the rat was moved off the stereotaxic frame and allowed to recover and was monitored closely.

2.2.3.2 Surgical procedure: Implanting reverse microdialysis probes in rat

At the same time as implanting the screw post electrodes, two guide cannulae (Fig. 2.2B) for CMA 12 microdialysis probes (Fig. 2.2A) (Carnegie Medicin, Stockholm, Sweden) were implanted over the ventrobasal (VB, mm, relative to bregma; AP -3.1; L 3.0; V 6, Paxinos and Watson, 1998) thalamus. For implantation of guide cannula, the ventral coordinate would be 4.0 as the tip of the infusion cannula extends beyond the guide cannula by 2mm. Both the screws and cannulae were fixed permanently to the skull with methylacrylic cement. Taking great care to avoid contact, copper wires attached to the screws were bent to manoeuvre around the implanted cannulae before final fixation to the skull.

2.2.3.3 Surgical procedure: Implanting EEG electrodes in mice

The mouse was placed in a stereotaxic frame (as in 2.2.3.1) and the skull surface was prepared as it was for the rat (using two clamps instead of four). Four gold plated screw posts (0.8cm, Retopin, Edenta, Switzerland) were used to record the EEG of each animal. Each electrode was carefully soldered to an exposed end of copper wire (~1.5cm long), prior to surgery. To avoid implanting the screw too deep into the brain tissue, the copper wire was positioned at ~2mm from the tip of the screw. A dental drill was used to make four holes: bilaterally over parietal cortex (posterior to bregma and lateral to midline) and ground/reference screw electrodes over the cerebellum (posterior to lambda and lateral to midline). The electrodes, wires and 4-channel multiple connectors were fixed permanently to the skull as it was for the rat (2.2.3.1).

2.2.4 Experimental protocols

Each animal was allowed to recover from surgery for at least 5 days prior to experiments. For the duration of recording, the animal was placed in a plexiglass box. The plexiglass box, leads and preamplifier were housed within a Faraday cage to reduce electrical interference from external sources. Each animal was acclimatised in this box for 30 minutes before an experiment commenced.

2.2.4.1 EEG recording

Once acclimatised, a 6-channel headstage of a Plexon amplifier (model REC/64; Dallas, Texas) was fastened to the connector cemented to the skull of the rat (a 4-channel connector was used for mice). The resulting signal was amplified (Plexon REC/64), processed through the associated Plexon software and then stored on a P.C.

2.2.4.1.1 EEG recording: GAERS and NEC

After being connected to the headstage of the Plexon amplifier and acclimatised, an EEG recording was made from each GAERS and NEC rat for 120 minutes.

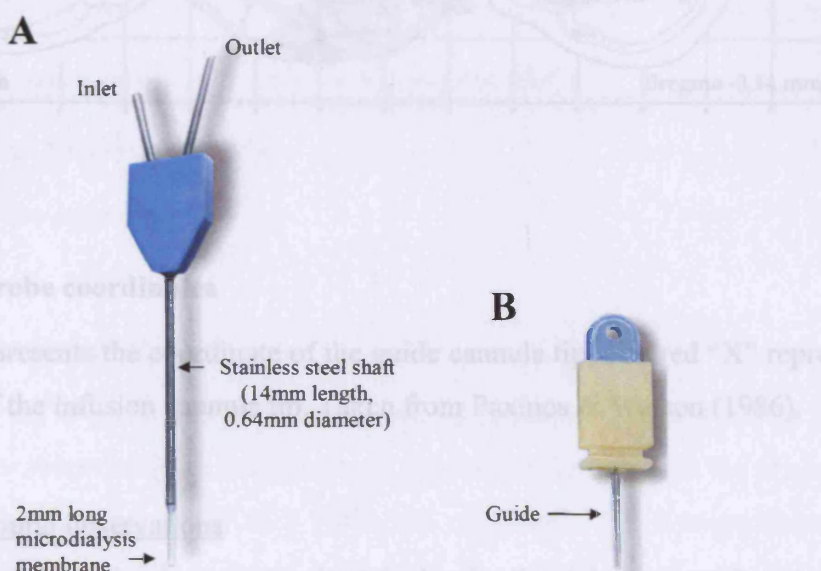


Figure 2.2

Microdialysis probe and guide cannula

The inside of a guide cannula (**B**) is coated with silicone. The CMA 12 microdialysis probe (**A**) sits tightly in the guide cannula (**B**) as it is mounted in a blue plastic body matched to the size of the cannula capsule. Figure taken and modified from www.microdialysis.com



et al., 2003). For this reason, all rats were gently stimulated by sight, sound or touch during my recordings and the data recorded throughout drug application were compared to data gathered in the presence of aCSF.

2.2.5 Data analysis

Data were filtered online: four channels, continuous lowpass Bessel filter of 60Hz, gain of 1000, at a sampling rate of 1 kHz. Spike 2 software (v. 5; Cambridge Electronic design Ltd., UK) was used for offline analysis of the EEG on a personal computer.

2.2.5.1 SWD identification

The start and end of a SWD was taken to be the first and last spike-wave complex. SWDs were classified as paroxysmal events on the EEG with the following properties:

- ≥ 2.5 times the peak-to-peak amplitude of the baseline EEG;
- Having an abrupt onset and end, and
- A spike-and-wave appearance.

2.2.5.2 SWD frequency analysis

The frequency of the seizures was calculated from 10 randomly selected SWDs taken from the EEG trace recorded from one animal. Using Spike 2.0 software, the frequency i.e. number of spikes per second, of each SWD was calculated. The average frequency of SWDs for each animal was then averaged. The SWD frequency for each experimental condition was reached by collating the average frequency of each animal and calculating the mean, STDEV and SEM of this data. The range of SWD frequency was determined by the lowest and highest frequency observed across all EEG traces.

2.2.5.3 Quantification of SWDs

For all experiments, seizures were quantified as the total number of SWDs; the average length of SWDs (seconds) and the total time spent in seizure (seconds) over the total recorded period and normalised to either 15 (mice) or 20 minute (rat) epochs. For all experimental conditions, except GAERS and NEC, the time spent in seizure per 15 or

20 minute epoch was plotted relative to the time of administration of the SWD-inducing agent. The latency of the first seizure and the time of the last seizure were also calculated. Drug effects were assessed by Student's unpaired *t*-test and statistical significance is stated (see Chapter 4).

2.3 Drugs

The concentration of drugs used in each experiment is stated in the relevant Chapter "Results" section.

2.3.1 Sources of drugs

Drugs were obtained from the following sources:

1-(2-[[[diphenylmethylene]imino]-oxy]ethyl)-1,2,5,6-tetrahydro-3-pyridinecarboxylic acid hydrochloride (NO711), kynurenic acid, 4,5,6,7-tetrahydroisoxazolo-[5,4-C]pyridine-3-ol (THIP), 2-ethyl-2-methylsuccinimide (ethosuximide, ETX), (\pm)- β -(aminomethyl)-4-chlorobenzenepropanoic acid (baclofen), tetraethylammonium chloride (TEA), 4-aminopyridine (4-AP), barium chloride dehydrate (Ba^{2+}), γ -butyrolactone (GBL) and γ -hydroxybutyric acid (GHB) from Sigma-Aldrich (Poole, Dorset; U.K); 6-imino-3-(4-methoxyphenyl)-1-(6H)-pyridazinebutanoic acid hydrobromide (SR 95531, gabazine, GBZ), tetrodotoxin (TTX), (2S)-3-[[3,4-dichlorophenyl]ethyl]amino-2-hydroxypropyl](phenylmethyl) phosphinic acid (CGP55845), (2S)-(+)-5,5-dimethyl-2-morpholineacetic acid (SCH50911) and 6,7,8,9-tetrahydro-5-hydroxy-5H-benzocyclohept-6-ylideneacetic acid (NCS382) from Tocris Bioscience (Bristol, U.K).

2.3.2 Drugs in solution

In vitro experiments:

All drugs were dissolved directly in aCSF (see Table 2.1), with the exception of CGP55845 which was initially dissolved in DMSO (100 μ l) before addition to aCSF. The final maximum concentration of DMSO was $\leq 0.1\%$, which has been shown to have no effect on IPSCs or tonic current (Belelli et al., 2005; Peden et al., 2008). A stock of TTX was made and frozen into 500 μ l aliquots which were thawed during preparation of aCSF and added to the recording aCSF.

In vivo experiments:

All drugs were dissolved directly in aCSF prior to reverse microdialysis experiments.

ETX was dissolved in saline prior to i.p injection.

Chapter 3

Tonic GABA_A current in models of typical absence epilepsy

3.1 Introduction

Although our understanding of thalamo-cortical (TC) networks that operate during SWDs has been advanced by previous *in vivo* and *in vitro* studies (Crunelli and Leresche, 2002), a cellular pathology common to all experimental models of typical absence epilepsy remains to be established. A wealth of experiments led to the concept that epileptogenesis reflects a simple imbalance between inhibitory and excitatory transmission (Bradford et al., 1995; Olsen & Avoli, 1997), however this notion is now being revised thanks to mounting evidence indicating that the role that inhibitory GABAergic transmission plays in various syndromes of epilepsy is more complex than originally perceived (Fritschy, 2008).

Several GABA_A receptor subunit mutations have been identified in humans that suffer with typical absences, albeit as part of more complex phenotypes (Urak et al., 2006; Baulac et al., 2001; Kananura et al., 2002; Macdonald & Kang, 2009; Wallace et al., 2001). Importantly, systemic or intrathalamic administration of agents that enhance GABAergic inhibition can either initiate or exacerbate seizures in both patients and animal models (Banerjee & Snead, 1995; Ettinger et al., 1999; Hosford et al., 1992; Manning et al., 2003; Perucca et al., 1998; Schacter et al., 1997; Snead, 1991; Vergnes et al., 1984). Furthermore, GABA_B antagonists terminate an absence seizure, a criterion that all experimental models should adhere to (Aizawa et al., 1997; Bernasconi et al., 1992; Hosford et al., 1992; Liu et al., 1992; Marescaux et al., 1992a & d). Thus it appears that enhanced GABAergic inhibition in the thalamus may be a characteristic of absence epilepsy.

Two types of inhibition result from activating GABA_ARs: transient synaptic GABA_AR mediated IPSCs, or “phasic” inhibition and the persistent peri- and/or extrasynaptic GABA_AR mediated current or “tonic” inhibition (Farrant & Nusser, 2005). Both phasic and tonic GABA_AR-mediated inhibition are present in the VB but by contributing to more than 90% of the overall GABAergic signal, tonic eGABA_AR-mediated current prevails (Cope et al., 2005).

To date, the contribution of tonic GABA_A inhibition in the VB thalamus to absence epilepsy has not been explored. Thus, I have investigated the presence of tonic

eGABA_AR-mediated currents in the VB thalamus of an established genetic model (GAERS) and pharmacological models of absence epilepsy (GHB, THIP and penicillin). My data implicate augmented tonic GABA_A current in the VB thalamus as a novel and a potentially cohesive cellular pathology of absence epilepsy.

3.2 Methods

Whole cell patch clamp recordings were performed using both short (see Chapter 2.1.5.1 and 2.1.7.1.1) and long protocols (see Chapter 2.1.5.2 and 2.1.7.1.2) in TC neurons of the VB of GAERS, non-epileptic control (NEC) and Wistar rats as described in Chapter 2.1.

3.3 Results

3.3.1 Enhanced tonic GABA_A current in GAERS

Tonic GABA_A current amplitude from TC neurons in slices containing the somatosensory VB thalamus of GAERS were measured from P14 to P30, and compared to age-matched NEC. No significant differences in tonic current amplitude were observed between either strains at P14-16 (P16 GAERS: 37.1 ± 6.1 pA; P16 NEC: 31.1 ± 5.3 pA) ($p > 0.05$) (Fig. 3.1 and 3.2A). However at P17, there was an approximate two-fold increase in tonic current amplitude in GAERS (72.4 ± 14.1 pA) compared to NEC (34.7 ± 5.9 pA) ($p < 0.05$; Fig. 3.1 and 3.2A). No significant differences in normalised tonic current amplitude were observed between strains at P14-16 (GAERS P16: 0.7 ± 0.1 pA/pF; NEC P16 0.5 ± 0.1 pA/pF) ($p > 0.05$), however at P17 there was a two-fold increase in normalised tonic current amplitude in GAERS (1.6 ± 0.4 pA/pF) compared to NEC (0.8 ± 0.1 pA/pF) ($p < 0.05$) (Fig. 3.2B). Therefore, the increase in tonic current amplitude occurred independently of whole-cell capacitance values.

The two-fold increase of tonic current amplitude in GAERS compared to NEC continued in the days after P17, despite an age-dependent gradual increase of tonic current amplitude for both strains (GAERS P29/30: 122.9 ± 21.7 pA; NEC P29/30: 60.6 ± 12.4 pA) ($p < 0.05$), independently of whole-cell capacitance (Fig. 3.2B).

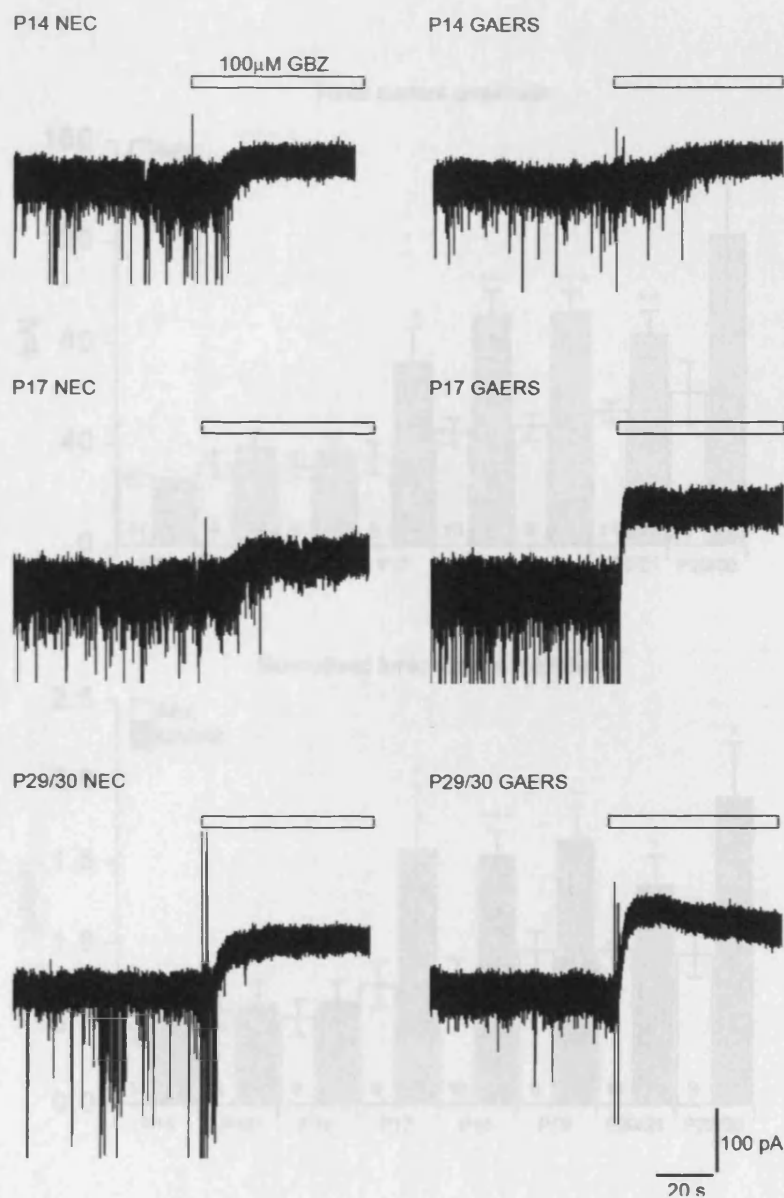


Figure 3.1

Increased tonic GABA_A current in GAERS

Representative current traces from six different TC neurons of P14 (upper panel), P17 (middle panel) and P29/30 (lower panel) NEC (left) and GAERS (right). The presence of a tonic GABA_A current was revealed by the focal application of gabazine (100μM; GBZ, white bars) and subsequent outward shift in baseline current. Note that the size of tonic current is similar between strains at P14, but is approximately two-fold larger in GAERS at P17, remaining larger in GAERS at P29/30. Scale bars are indicated.

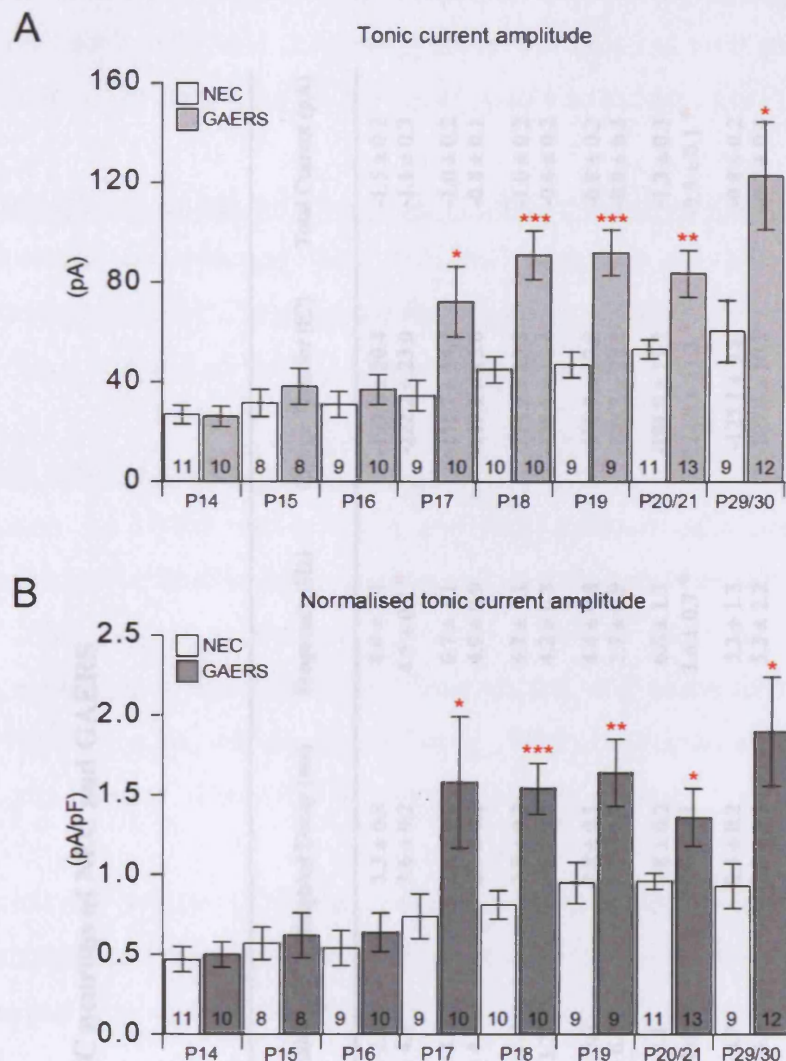


Figure 3.2

Developmental profile of tonic GABA_A current in NEC and GAERS

A) comparison of the tonic current amplitude in NEC (white columns) and GAERS (grey columns). **B)** comparison of the tonic current amplitude normalised to whole-cell capacitance in NEC (white columns) and GAERS (grey columns). **A + B:** * p < 0.05, ** p < 0.01, *** p < 0.001, compared to age-matched NEC. The number of recorded neurons for each strain and age are indicated at the base of each column in **A** and **B**.

Table 3.1

Comparison of sIPSC parameters in TC neurons of NEC and GAERS

		<i>sIPSC parameter</i>					
Rat strain and age		n	Peak amplitude (pA)	Weighted Decay (ms)	Frequency (Hz)	Charge Transfer (fC)	Total Current (pA)
P14	GAERS	14	-52.7 ± 2.5	3.3 ± 0.3	8.0 ± 1.1	-193.6 ± 20.4	-1.5 ± 0.2
	NEC	3	-53.6 ± 4.3	3.6 ± 0.2	4.5 ± 0.7 *	-222.2 ± 23.0	-1.1 ± 0.3
P15	GAERS	8	-49.8 ± 3.2	2.6 ± 0.2	6.7 ± 1.1	-151.7 ± 14.7	-1.0 ± 0.2
	NEC	8	-52.2 ± 4.3	2.5 ± 0.2	4.9 ± 0.9	-149.1 ± 15.6	-0.8 ± 0.1
P16	GAERS	10	-55.9 ± 5.0	2.8 ± 0.2	5.7 ± 1.1	-174.1 ± 13.3	-1.0 ± 0.2
	NEC	9	-42.1 ± 3.2 *	2.9 ± 0.2	4.2 ± 0.8	-138.8 ± 11.4	-0.6 ± 0.2
P17	GAERS	11	-48.0 ± 5.0	2.8 ± 0.1	4.4 ± 0.8	-150.8 ± 17.0	-0.8 ± 0.2
	NEC	9	-57.4 ± 6.1	3.2 ± 0.3	3.7 ± 0.9	-209.5 ± 28.8	-0.8 ± 0.3
P18	GAERS	9	-58.1 ± 5.1	2.8 ± 0.2	6.6 ± 1.3	-191.9 ± 19.2	-1.3 ± 0.3
	NEC	12	-42.5 ± 4.6 *	2.6 ± 0.1	3.6 ± 0.7 *	-124.6 ± 11.3 *	-0.5 ± 0.1 *
P19	GAERS	10	-45.0 ± 4.7	2.5 ± 0.2	5.3 ± 1.3	-125.1 ± 9.8	-0.8 ± 0.2
	NEC	9	-44.3 ± 3.9	2.1 ± 0.1	5.3 ± 2.2	-109.6 ± 10.2	-0.7 ± 0.4
P20/21	GAERS	13	-37.9 ± 4.0	2.2 ± 0.1	2.8 ± 0.8	-93.8 ± 10.3	-0.3 ± 0.2
	NEC	14	-41.6 ± 3.6	2.4 ± 0.2	3.8 ± 1.0	-117.8 ± 13.3	-0.5 ± 0.1
P29/30	GAERS	9	-42.1 ± 6.4	2.1 ± 0.2	3.2 ± 0.5	-106.3 ± 24.3	-0.4 ± 0.1
	NEC	12	-37.4 ± 2.8	2.7 ± 0.3	2.2 ± 0.7	-118.4 ± 19.0	-0.3 ± 0.1

* p < 0.05 compared to GAERS; n = number of cells recorded

Comparison of spontaneous IPSC (sIPSC) parameters in GAERS and NEC at the same ages revealed no consistent differences (Table 3.1). Interestingly, there was significantly smaller sIPSC peak amplitude, frequency, charge transfer and total current in GAERS than NEC at P18, but these changes were not maintained at later ages (Table 3.1).

3.3.2 SWD-inducing agents enhance tonic GABA_A current in VBTC neurons

Having observed an enhanced tonic GABA_A current in the VB thalamus of an established genetic model, I investigated the effects that pharmacological agents used to induce SWDs *in vivo* had on tonic GABA_A current *in vitro*.

3.3.2.1 GHB enhances tonic GABA_A current

The induction of SWDs via systemic and intra-thalamic administration of GHB constitutes the best established pharmacological model of absence seizures (Crunelli & Leresche, 2002). As the presynaptic inhibitory action of GHB and its postsynaptic inhibitory action via GABA_BRs in the thalamus are well characterised (Banerjee & Snead, 1995; Emri et al., 1996b; Gervasi et al., 2003; Le Feuvre et al., 1997), I have tested the post-synaptic effect of GHB on tonic GABA_A current.

In the presence of 500nM TTX, tonic GABA_A current amplitude from TC neurons in slices containing the somatosensory VB thalamus of P21–26 Wistar rats was measured both before and after 3mM GHB was administered via the perfusion system (Fig. 3.3A) and in the continuous presence of 0.3–3mM GHB (Fig. 3.4A-D). GHB dose-dependently increased tonic current amplitude compared to control (104.1 ± 5.4 pA) under the short protocol (300 μ M GHB: 141.3 ± 13.4 pA, $p < 0.01$; 1mM GHB: 142.6 ± 13.7 pA, $p < 0.01$; 3mM: 175.4 ± 10.9 pA, $p < 0.001$) (Fig. 3.4A-D, 3.5A) and under the long protocol (control: 75.9 ± 13.5 pA; 3mM GHB: 116.6 ± 14.2 pA; $p < 0.001$) (Fig. 3.3A-B). The GHB-induced increase of tonic current amplitude occurred independently of whole-cell capacitance values at all doses tested (Fig. 3.3C, 3.5B).

Comparison of mIPSC parameters revealed a significantly reduced frequency and total current in the presence of all concentrations of GHB except 300 μ M (Tables 3.2 and 3.3).

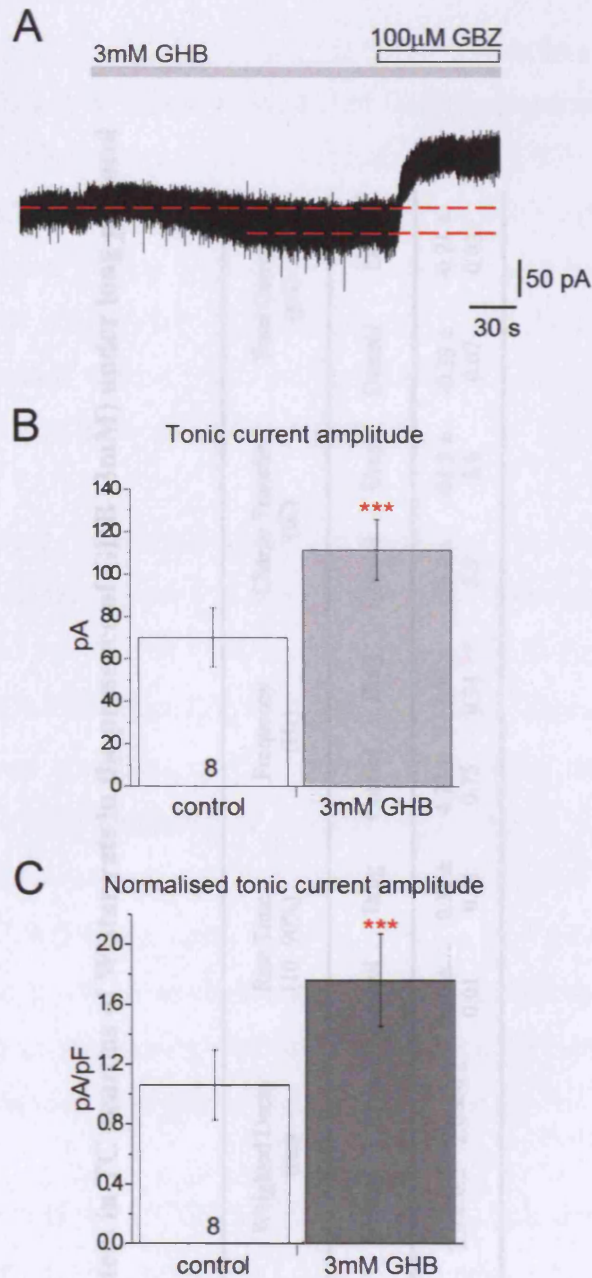


Figure 3.3

GHB enhances tonic GABA_A current in Wistar TC neurons

A) representative current trace from a Wistar rat TC neuron showing the effect of acute perfusion of 3mM GHB (grey bar) on baseline current. Note that GHB (3mM) induced an inward shift of the baseline current. **B)** comparison of the effects of 3mM GHB on tonic current amplitude to the paired control. **C)** comparison of the tonic current amplitude normalised to whole-cell capacitance in the presence of 3mM GHB to the paired control. **B + C** *** $p < 0.001$. Numbers of recorded neurons are indicated at the base columns in **B** and **C**. All recordings were done in the presence of TTX (500nM).

Table 3.2

Comparison of mIPSC parameters in TC neurons of Wistar rats in the presence of GHB (3mM) under long protocol

		<i>mIPSC parameter</i>											
		Peak amplitude (pA)		Weighted Decay (ms)		Rise Time (10-90%)		Frequency (Hz)		Charge Transfer (fC)		Total Current (pA)	
n		Control	Drug	Control	Drug	Control	Drug	Control	Drug	Control	Drug	Control	Drug
3mM GHB	8	-35.8 ± 2.1	-36.9 ± 2.3	2.0 ± 0.2	2.0 ± 0.2	0.30 ± 0.01	0.31 ± 0.01	4.77 ± 0.75	2.59 ± 0.31 **	-79.4 ± 5.9	-81.3 ± 5.6	-0.39 ± 0.07	-0.21 ± 0.03*

* p < 0.05, ** p < 0.01 compared to control; n = number of cells recorded

3.3.2.2 GHB enhances tonic GABA_A current via GABA_B receptors

Much controversy exists over the site-of-action of GHB, being described as both a weak agonist at GABA_BRs (Bernasconi et al., 1992; Emri et al., 1996b; Gervasi et al., 2003) and as a specific agonist at the putative GHB receptor (GHBR) (Banerjee et al., 1993; Maitre et al., 1990; Snead 1994a, b; Snead, 1996). Considering the current controversy over the receptor site at which GHB acts (see Chapter 1.2.2.1.1), I have investigated the effect of GHB co-applied with a GABA_BR antagonist (CGP55845) and the putative GHBR antagonist (NCS382) on tonic GABA_A current.

Tonic GABA_A current amplitude from TC neurons in slices containing the somatosensory VB thalamus of P21–26 Wistar rats, was measured during the continuous presence of 3mM GHB with CGP55845 (10μM), 3mM GHB with NCS 382 (1mM) and 1mM NCS 382 alone (Fig. 3.4E-G and 3.5A). The action of 3mM GHB (175.4 ± 10.9 pA) was abolished by the putative GHB antagonist 1mM NCS382 to 119.1 ± 5.4 pA ($p > 0.05$, compared to control) (Fig. 3.6E-G, 3.7A). No significant changes in tonic GABA_A current amplitude were observed in the presence of NCS382 (1mM) (control: 104.1 ± 5.4 pA; 1mM NCS382: 114.1 ± 10.4 pA; $p > 0.05$). Again, no significant differences ($p > 0.05$) were observed between control tonic current amplitude and the tonic current in the presence of 3mM GHB with NCS382 (1mM) and when normalised to the whole-cell capacitance values (Fig. 3.5B).

Interestingly, 3mM GHB with CGP55845 (10μM) not only blocked GHB-induced increase of tonic current, but reduced tonic GABA_A current to below that observed under control conditions (86.3 ± 6.9 pA) ($p < 0.05$) (Fig. 3.5A). However, the reduction of tonic GABA_A current below control amplitude was not apparent when the current amplitude was normalised to whole-cell capacitance (1.8 ± 0.2 pA/pF) ($p > 0.05$) (Fig. 3.5B).

Comparison of mIPSC parameters revealed a significantly higher frequency and total current in the presence of GHB (3mM) with CGP55845 (10μM) and with NCS382 (1mM) compared to the values observed for 3mM GHB alone (Table 3.3), consistent with previous data (Gervasi et al., 2003; Emri et al., 1996b).

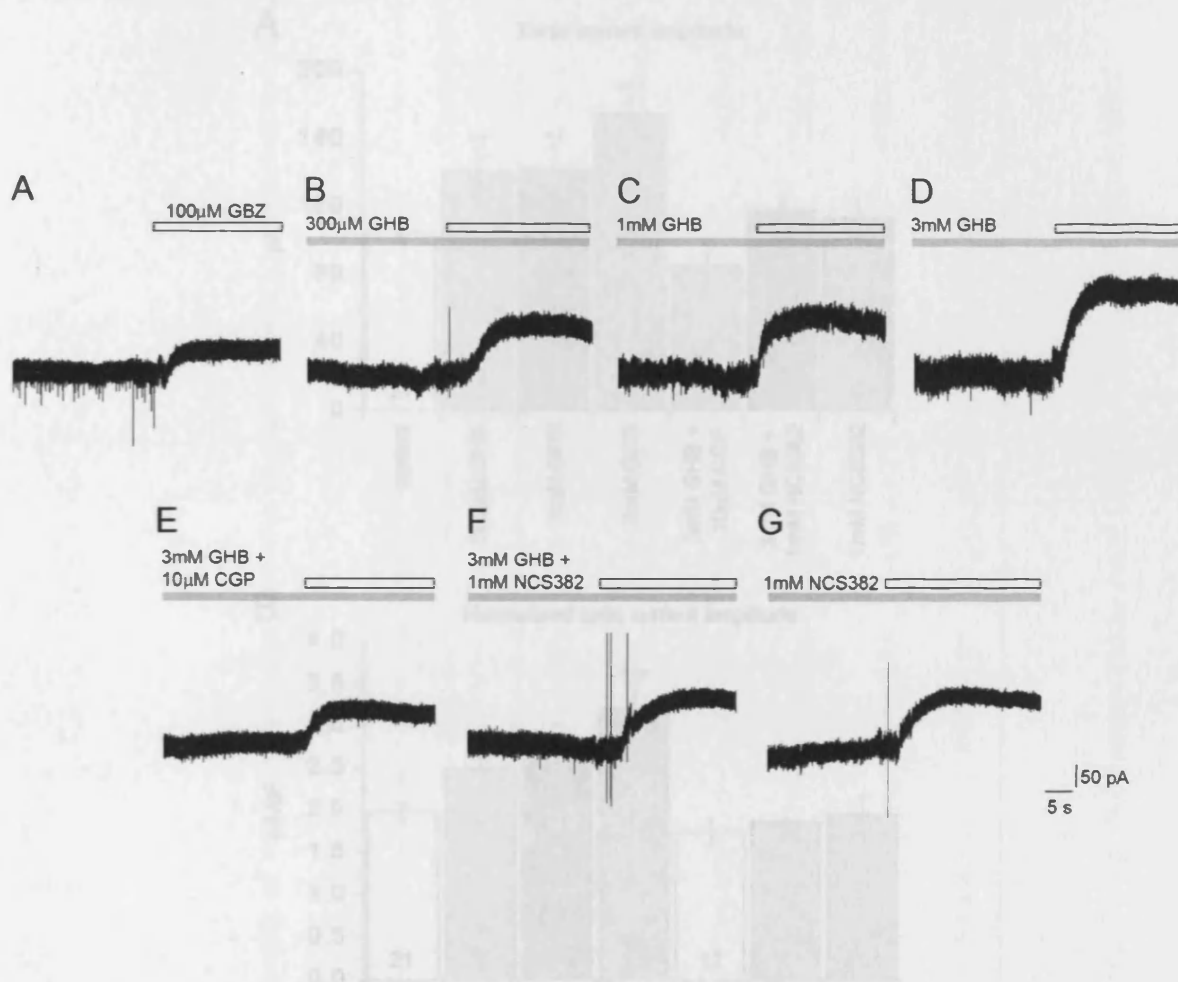


Figure 3.4

GHB dose-dependently enhances tonic GABA_A inhibition

Representative current traces from seven different Wistar rat TC neurons showing the effects of 300µM GHB (**B**; grey bar), 1mM GHB (**C**; grey bar), 3mM GHB (**D**; grey bar), 3mM GHB with 10µM CGP55845 (**E**; grey bar), 3mM GHB with 1mM NCS382 (**F**; grey bar) and 1mM NCS382 alone (**G**; grey bar). **A** is a representative current trace of a neuron under control conditions. Brain slices were in the continuous presence of varying concentrations of GHB (short protocol, see Chapter 2.1.5.1). Focal application of GBZ (100µM; white bars) revealed an outward shift in baseline current, indicating the presence of tonic current. Scale bars are indicated. All recordings were done in the presence of TTX (500nM).

Bar graph showing the normalized tonic current amplitude for the same neurons as in (A). A + B: * $p < 0.05$, ** $p < 0.01$, *** $p < 0.001$, compared to control. Numbers of recorded neurons are indicated at the base of each column in A and B.

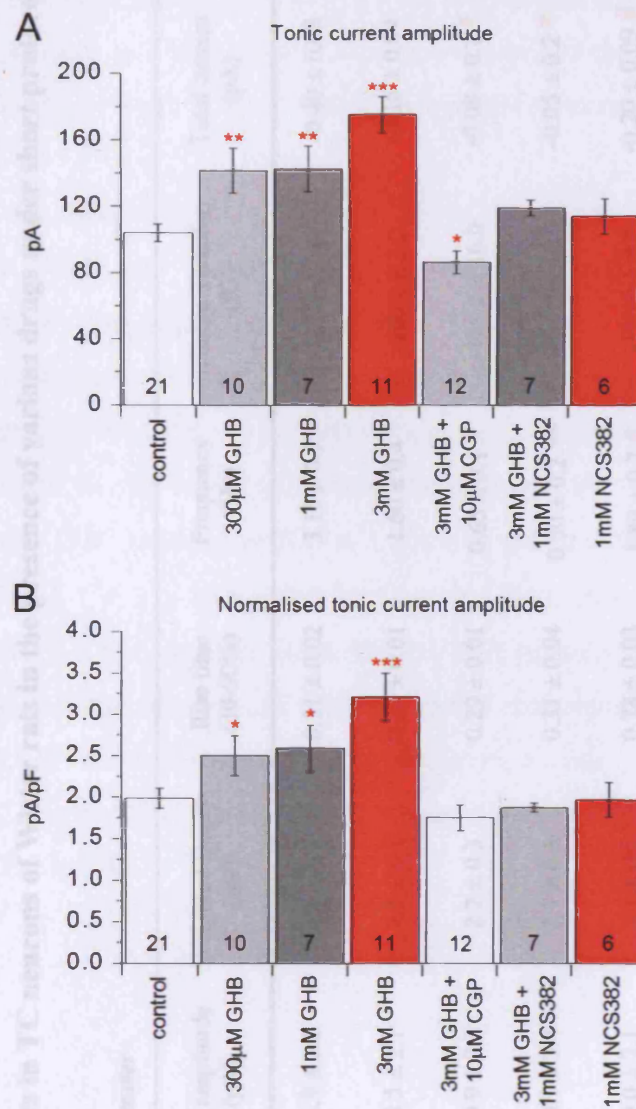


Figure 3.5

Comparison of tonic GABA_A current under varying concentrations of GHB, CGP55845 and NCS382

A) comparison of the effect of varying concentrations of GHB (300µM – 3mM), GHB with CGP55845 (10µM) and GHB with NCS382 (1mM) on tonic GABA_A current amplitude. **B)** comparison of the tonic GABA_A current amplitude normalised to whole-cell capacitance for the same neurons as in (A). **A + B:** * p < 0.05, ** p < 0.01, *** p < 0.001, compared to control. Numbers of recorded neurons are indicated at the base of each column in A and B.

Table 3.3

Comparison of mIPSC parameters in TC neurons of Wistar rats in the presence of various drugs under short protocol

	<i>mIPSC parameter</i>						
	n	Peak amplitude (pA)	Weighted Decay (ms)	Rise time (10-90%)	Frequency (Hz)	Charge Transfer (fC)	Total current (pA)
Control	21	-41.9 ± 2.2	2.7 ± 0.1	0.31 ± 0.02	3.15 ± 0.5	-122.8 ± 11.7	-0.40 ± 0.08
300µM GHB	10	-38.5 ± 2.7	2.5 ± 0.1	0.27 ± 0.01	1.60 ± 0.4	-100.8 ± 2.2	-0.16 ± 0.04
1mM GHB	7	-39.9 ± 2.3	2.7 ± 0.3	0.29 ± 0.01	0.65 ± 0.1 *	-121.2 ± 16.0	-0.08 ± 0.1 *
3mM GHB	11	-40.1 ± 3.4	2.7 ± 0.6	0.31 ± 0.04	0.50 ± 0.2 **	-103.5 ± 14.9	-0.05 ± 0.2 *
3mM GHB + 10uM CGP55845	12	-39.0 ± 2.1	3.1 ± 0.6	0.28 ± 0.03	1.89 ± 0.7 #	-110.0 ± 8.7	-0.20 ± 0.09 #
3mM GHB + 1mM NCS382	7	-40.1 ± 4.0	2.2 ± 0.5	0.28 ± 0.03	3.14 ± 0.4 ###	-100.4 ± 3.5	-0.31 ± 0.33 ###

* p < 0.05, ** p < 0.01 compared to control; # p < 0.05 ### p < 0.01 compared to 3mM GHB; n = number of cells recorded

3.3.2.3 The δ -subunit specific GABA_A agonist THIP enhances tonic GABA_A current

Another agent that has been shown to induce SWDs *in vivo* and is therefore a potential model of absence seizures is THIP. I have therefore examined the effect of THIP on tonic GABA_AR-mediated current in the somatosensory VB thalamus.

Tonic GABA_A current amplitude from TC neurons of the VB in P21–26 Wistar rats were recorded both before and during THIP (0.1–10 μ M) administration through the perfusion system. THIP dose-dependently increased tonic current amplitude compared to control (all concentrations: $p < 0.001$) (Fig. 3.6 and 3.7A). A concentration-dependent THIP-induced increase in the tonic current amplitude was also observed when the tonic current was normalised to the whole-cell capacitance values ($p < 0.001$) (Fig. 3.7B). Application of 100nM THIP induced an $80.3 \pm 1.8\%$ increase in tonic current amplitude from 83.3 ± 17.0 pA to 150.3 ± 19.8 pA (Fig. 3.6A & 3.7A), and application of 3 μ M THIP induced a $383.2 \pm 5.9\%$ increase, from 119.7 ± 19.7 pA to 578.4 ± 28.9 pA (Fig. 3.6B & 3.7A). Note that the control tonic current values measured for each respective concentration of THIP were not significantly different to one another ($p > 0.05$). Analysis of mIPSCs revealed no differences between control conditions and in the presence of THIP (Table 3.4).

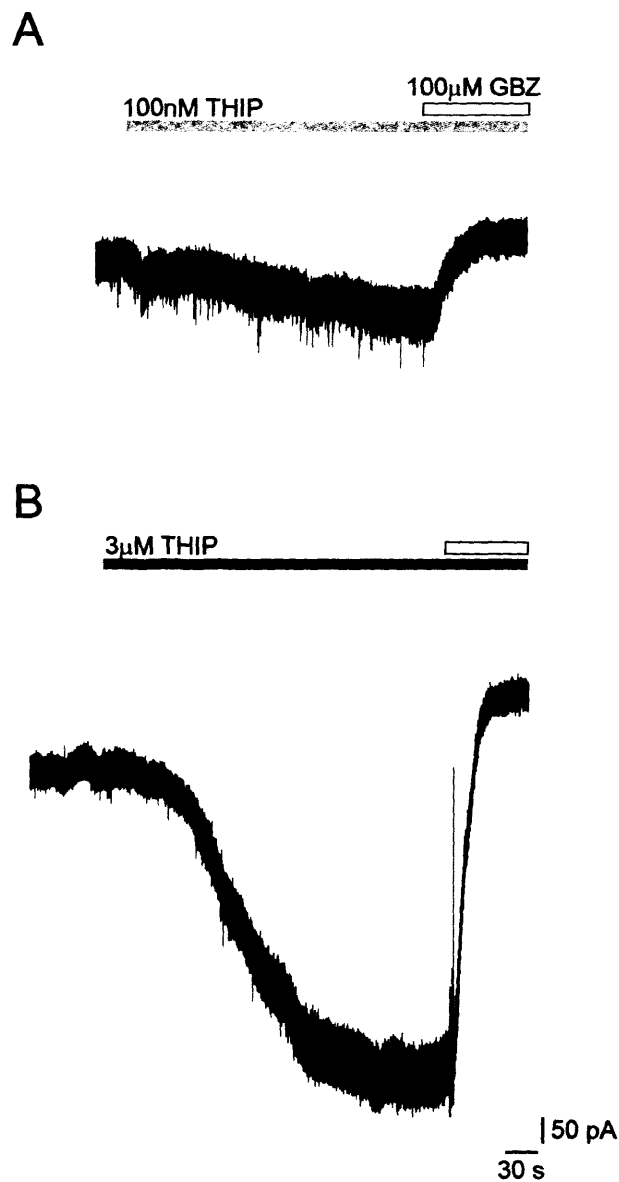


Figure 3.6

The δ -subunit GABA_A agonist THIP enhances tonic GABA_A current

Representative current traces from two different Wistar rat TC neurons, showing the effect of acute perfusion of 100nM (A; grey bar) and 3µM THIP (B; grey bar) on baseline current. The presence of THIP at both concentrations induces an inward shift of baseline current. Application of GBZ (100 µM; white bar) both via perfusion (A) and focally (B) blocks the THIP-induced increase of tonic current. The subsequent outward shift in baseline current by GBZ reveals the presence of the tonic current under both control conditions (compared to the original baseline current) and in the presence of THIP. Scale bars are indicated. All recordings were done in the presence of TTX (500nM).

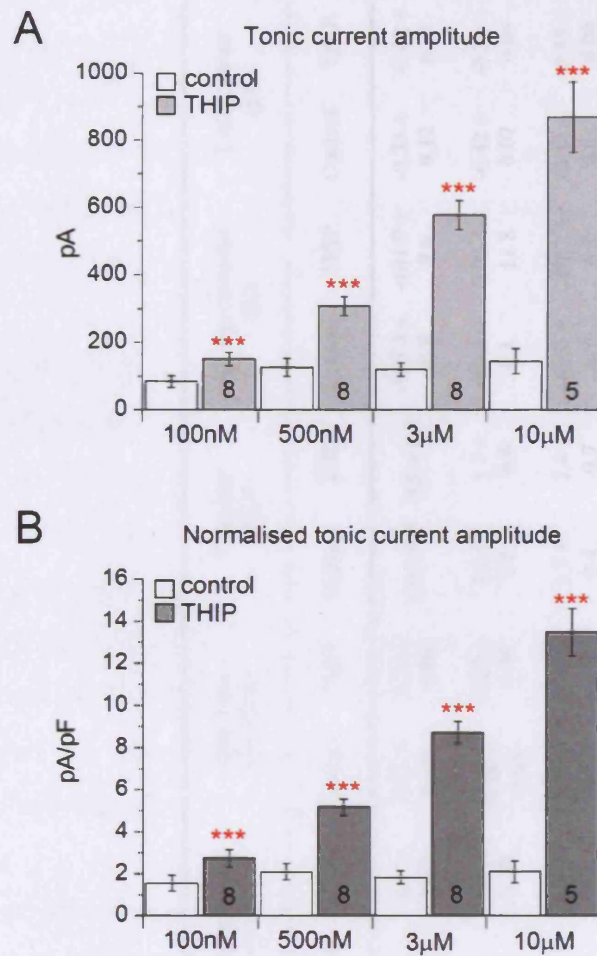


Figure 3.7

Comparison of tonic current with varying concentrations of THIP

A) comparison of tonic current amplitude in the presence of varying concentrations of THIP (grey columns) to their paired control (white columns). **B)** comparison of tonic current amplitude normalised to whole-cell capacitance for the same neurons as in (A). **A + B:** *** $p < 0.001$ compared to their respective controls. The numbers of recorded neurons for each concentration are as indicated at the base of each column in **A** and **B**.

Table 3.4

Comparison of mIPSC parameters in TC neurons of Wistar rats in the presence of different concentrations of THIP

		<i>mIPSC parameter</i>											
		Peak amplitude (pA)		Weighted Decay (ms)		Rise Time (10 -90%)		Frequency (Hz)		Charge Transfer (fC)		Total Current (pA)	
n		Control	THIP	Control	THIP	Control	THIP	Control	THIP	Control	THIP	Control	THIP
100nM THIP	8	-28.4 ± 3.5	-29.7 ± 3.3	2.1 ± 0.18	2.1 ± 0.23	0.35 ± 0.06	0.29 ± 0.06	3.0 ± 0.7	3.9 ± 0.7	-103.3 ± 10.8	-101.9 ± 9.6	-0.33 ± 0.12	-0.42 ± 0.11
500nM THIP	7	-33.8 ± 3.9	-36.4 ± 3.7	2.7 ± 0.27	2.4 ± 0.30	0.28 ± 0.03	0.29 ± 0.04	4.2 ± 0.8	3.7 ± 0.6	-99.3 ± 6.3	-100.4 ± 11.8	-0.42 ± 0.07	-0.33 ± 0.04
3µM THIP	4	-28.3 ± 1.9	-34.3 ± 4.5	2.4 ± 0.03	2.0 ± 0.3	0.36 ± 0.08	0.31 ± 0.1	1.7 ± 0.4	2.4 ± 0.7	-68.9 ± 6.7	-67.3 ± 6.7	-0.14 ± 0.04	-0.15 ± 0.04

n = number of cells recorded

3.3.3 A specific GABA_BR antagonist reduces tonic GABA_A current in GAERS

So far, enhanced tonic GABA_A current in TC cells of the VB appears to be a common feature of the genetic and pharmacological models tested. A defining criterion of a typical absence epilepsy model is that SWDs are suppressed by GABA_B antagonists (Danober et al., 1998). Having already observed the GABA_BR-specific antagonist reduction of the GHB-induced increase of tonic GABA_A current (see Section 3.3.2.2), I have investigated the effect of CGP55845 on the augmented tonic GABA_A current observe in GAERS animals (see Section 3.3.1).

Tonic GABA_A current amplitude from TC neurons in slices containing the somatosensory VB thalamus of P18–21 GAERS and NEC were measured under control conditions and in the continuous presence of CGP 55845 (10μM). There was approximately a two-fold increase of tonic current amplitude in GAERS and CGP55845 (10μM) significantly decreased tonic current amplitude in both GAERS (control: 158.4 ± 26.8 pA; CGP55845: 70.2 ± 8.2 pA, $p < 0.01$) compared to GAERS control) and NEC (control: 87.7 ± 4.8 pA; CGP55845: 55.9 ± 3.0 pA, $p < 0.05$) (Fig. 3.8A & B). In addition, the reduction of tonic GABA_A current amplitude caused by CGP55845 occurred in both strains independently of the whole-cell capacitance values (Fig. 3.8C).

There is no difference between the tonic GABA_A current amplitudes of GAERS and NEC in the presence of CGP55845 (10μM) (Fig. 3.8B and C), nor between GAERS with CGP55845 compared to the NEC control value ($p > 0.05$).

Comparison of mIPSC parameters in GAERS and NEC revealed no differences between control conditions and with 10μM CGP55845 (Table 3.5).

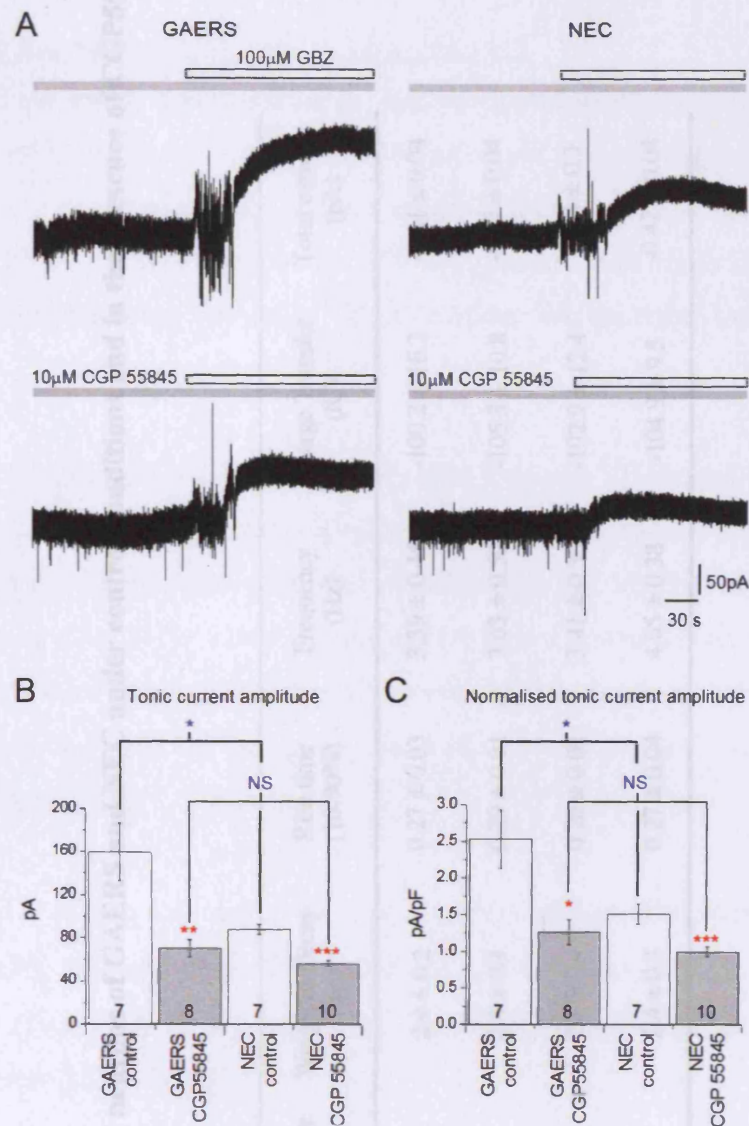


Figure 3.8

A specific GABA_B receptor antagonist reduces tonic GABA_A current in GAERS

A) representative current traces from four different TC neurons of P21-26 GAERS (left panel) and NEC (right panel) under control conditions (upper traces) and in the presence of CGP55845 (10 μ M; lower traces). Scale bars are indicated. B) comparison of tonic current amplitude between GAERS and NEC under control conditions and in the presence of CGP 55845. C) comparison of tonic GABA_A current amplitude normalised to whole-cell capacitance. B + C: * p < 0.05, ** p < 0.01, *** p < 0.001, compared to controls; * p < 0.05 GAERS compared to NEC; NS not significant. Numbers of recorded neurons are indicated at the base of each column in B and C. All recordings were done in the presence of 500nM TTX.

Table 3.5**Comparison of mIPSC parameters in TC neurons of GAERS and NEC under control conditions and in the presence of CGP55845**

<i>mIPSC parameter</i>							
	n	Peak amplitude (pA)	Weighted Decay (ms)	Rise time (10-90%)	Frequency (Hz)	Charge Transfer (fC)	Total current (pA)
GAERS control	7	-33.4 ± 3.2	2.4 ± 0.2	0.27 ± 0.03	3.39 ± 0.44	-100.2 ± 16.2	-0.31 ± 0.04
GAERS + 10 μM CGP 55845	8	-32.8 ± 3.8	2.4 ± 0.1	0.29 ± 0.01	3.63 ± 0.50	-105.3 ± 10.8	-0.37 ± 0.04
NEC control	7	-34.3 ± 3.9	2.8 ± 0.4	0.26 ± 0.01	3.41 ± 0.36	-102.9 ± 12.4	-0.34 ± 0.3
NEC + 10 μM CGP 55845	10	-33.7 ± 3.2	2.4 ± 0.3	0.27 ± 0.04	4.05 ± 0.38	-104.9 ± 9.5	-0.42 ± 0.04

n = number of cells recorded

3.3.4 Penicillin has no effect on tonic GABA_A current

Large doses of penicillin administered to cats via intramuscular injection have been shown to induce SWDs. In light of the fact that increased tonic GABA_A current appears to be a common phenomenon in various animal models of absence epilepsy (see Chapter 3.3.1-3.3.3), I have examined the effect of penicillin on tonic GABA_A current on tonic GABA_AR-mediated current in TC cells of the VB thalamus in P21-26 Wistar rats (Fig. 3.9).

Plasma and aCSF samples obtained from cats that received ¹⁴C-penicillin injection or focal application into the thalamus revealed penicillin distribution within the brain (Quesney & Gloor, 1978). From this data, I calculated the relative concentration of penicillin necessary for SWD induction and tested these concentrations in brain slices containing TC neurons of the VB. After intramuscular injection these analyses found a concentration of 58μM in the thalamus and 2.08mM was applied intrathalamically (Quesney & Gloor, 1978).

Penicillin failed to induce any change in tonic current amplitude (58μM penicillin: 44.2 ± 9.2 pA, p >0.05; 2.08mM penicillin: 42.3 ± 7.3 pA) compared to control (62.1 ± 6.2 pA) (p >0.05) (Fig. 3.9A & B), independently of whole-cell capacitance (p >0.05, compared to control) (Fig 3.9C).

Comparison of mIPSCs revealed significantly reduced peak amplitude, weighted decay and charge transfer, whereas no change in frequency or rise-time (10-90%) were noted (Table 3.6).

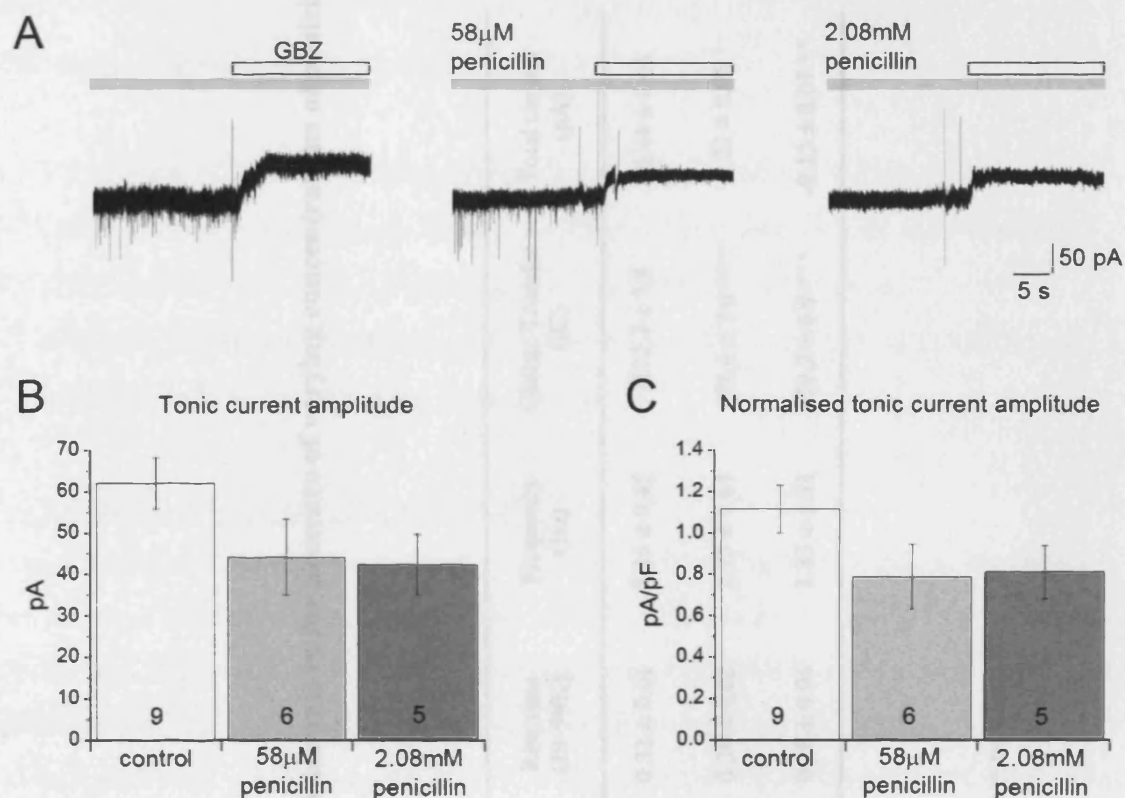


Figure 3.9

Tonic GABA_A current in the presence of penicillin

A) representative current traces from three different Wistar rat TC neurons showing the effect of 58 μ M penicillin (grey bar; middle trace) and 2.08mM penicillin (grey bar; right trace) on baseline current. Focal application of GBZ (100 μ M; white bars) revealed an outward shift in baseline current, indicating presence of tonic current. The left current trace is representative of a neuron under control conditions. **B**) comparison of the effect of 58 μ M penicillin and 2.08mM penicillin on the tonic current amplitude control. **C**) comparison of the tonic current amplitudes normalised to whole-cell capacitance to control. Numbers of recorded neurons are indicated at the base of each column in **B** + **C**. Scale bars are indicated. All recordings were done in the presence of TTX (500nM).

Table 3.6

Comparison of mIPSC parameters in TC neurons of Wistar rats in the presence of varying concentrations of penicillin

	<i>mIPSC parameter</i>						
	n	Peak amplitude (pA)	Weighted Decay (mS)	Rise time (10-90%)	Frequency (Hz)	Charge Transfer (fC)	Total current (pA)
Control	9	-44.0 ± 0.8	2.4 ± 0.14	0.32 ± 0.01	3.36 ± 0.45	-132.7 ± 3.8	-0.44 ± 0.06
58µM penicillin	7	-37.3 ± 2.4 **	1.8 ± 0.12 **	0.30 ± 0.02	2.73 ± 0.61	-78.6 ± 7.6 ***	-0.22 ± 0.06 *
2mM penicillin	5	-33.4 ± 4.5 **	1.2 ± 0.02 ***	0.28 ± 0.06	2.33 ± 1.31	-50.3 ± 6.9 ***	-0.15 ± 0.07 **

* p < 0.05, ** p < 0.01, *** p < 0.001 compared to control; n = number of

3.4 Discussion

The results described in this chapter show that:

- TC neurons of GAERS exhibit enhanced tonic but not phasic GABA_A current;
- GHB enhances tonic GABA_A current via direct postsynaptic action at GABA_BRs;
- THIP increases tonic but not phasic GABA_A current in TC neurons;
- A specific GABA_BR antagonist reduces the tonic GABA_A current in GAERS, and
- Penicillin fails to affect tonic GABA_A current

3.4.1 Enhanced tonic current in GAERS

Tonic GABA_A current is mediated by δ -subunit containing extrasynaptic receptors in the thalamus (Belelli et al., 2005; Cope et al., 2005; Jia et al., 2005; Porcello et al., 2003), and expression of these δ -subunit containing GABA_ARs reaches significant levels in the rat VB from approximately P12 (Laurie et al., 1992). Therefore, I investigated tonic GABA_A currents of TC neurons in the VB of GAERS and NEC from P14 onwards.

GAERS exhibit bilateral SWDs (7–11 Hz) concomitant with behavioural arrest from P30, reaching 100% incidence by P90 (Danober et al., 1998). In agreement with previous work done in younger GAERS (Bessaih et al., 2006), comparison of the sIPSCs of the VB revealed no consistent differences between GAERS and NEC. Conversely, I observed an approximate two-fold increase in tonic GABA_A current amplitude in GAERS animals at P17, which was maintained through to P30.

Interestingly, there appear to be brief modifications to the sIPSC parameters in GAERS at P18 where peak amplitude, frequency, charge transfer and thus total sIPSC current are reduced. It is possible that this is the result of some modulatory mechanism(s) responding to compensate for the rapidly enhanced tonic GABA_AR signal recorded at P17 i.e. a reduction of phasic, synaptically mediated GABA_A inhibition to offset the enhanced tonic, extrasynaptically mediated GABA_A inhibition. Of course, this is a purely speculative suggestion and further work would have to be carried out in order to properly investigate this phenomenon. As the alterations to sIPSC parameters do not

persist past P18 it seems that the compensatory action, if it took place, was temporary. In addition, it should be noted that the sIPSC parameters were deduced from a short baseline current (just 55 seconds) which is likely to affect the validity of these synaptic data.

During development neurons undergo dramatic changes as they progressively acquire and establish their adult synaptic connections and phenotype. Indeed throughout the first two postnatal weeks, the extensive extracellular space in the VB is filled with developing cytoplasmic organelles and neuropil of TC neurons (De Biasi et al., 1996). By the end of the 3rd postnatal week elaborate neuropil, synaptic terminals and the organisation of the VB becomes indistinguishable from that observed in adults (De Biasi et al., 1996). A similar time-course for postnatal development of GABAergic circuits in the VB thalamus was identified in 1997 by De Biasi et al., using a combination of immunohistochemistry and electron microscopy techniques. Specifically, the subcellular localisation of GABA at mature GABAergic terminals only reached an adult distribution between P16–20 despite an intense GABA immunoreactivity in the VB at birth.

The presence of such augmented tonic GABA_A current in the VB of GAERS at an age prior to SWD onset raises the possibility that this phenomenon may be a precondition for absence seizures. Considering the somewhat abrupt appearance at P17, specifically when adult synaptic organisation and GABAergic terminals are in final stages of maturation (De Biasi et al., 1996, 1997), supports the notion that augmented tonic GABA_A current is a result of some developmental malfunction(s).

Since TC neurons undergo major structural and morphological changes during the 1st three postnatal weeks, it is important to determine whether or not enlarged tonic GABA_A current is a result of such alterations to cell configuration. Measuring membrane capacitance of a cell under whole-cell patch conditions serves as a useful indicator of surface area (Walz et al., 2002), therefore I normalised tonic GABA_A current amplitude to the membrane capacitance for each cell. Even when normalised to membrane capacitance, tonic current amplitude remained significantly higher in GAERS from P17 onwards compared to age-matched NEC. This then verifies that

enhanced tonic GABA_A current is a result of eGABA_AR gain-of-function, and not due to any changes in basic cellular properties of the neurons.

Simultaneous experiments carried out by other members of Crunelli's group have shown that in pre-seizure mice (*stg* and *lh*), the tonic GABA_A current amplitude in TC neurons of the VB was similar to that of control littermates. However, it was significantly enhanced at post-seizure ages, again independently of whole cell capacitance values (Cope et al., 2009). Furthermore, comparison of sIPSC properties revealed no difference between mutant and control littermates at pre- or post-seizure age (Cope et al., 2009).

Together these results show that eGABA_AR function is enhanced in TC neurons of the VB thalamus across genetic models. The significance of augmented tonic GABA_A inhibition appearing prior and up to seizure onset in GAERS, strongly suggests that this cellular pathology is a prerequisite to SWDs. It would be interesting to investigate whether similar developmental profile is present in the mouse models also.

3.4.2 Processes underlying the augmented tonic GABA_A current in the VB of GAERS

Quantitative binding experiments with [³H]GABA in adult GAERS and NEC failed to demonstrate any variation of GABA_A and GABA_B binding between the two strains (Knight & Bowery, 1992). These findings concur with data obtained in similar experiments using the GABA_B antagonist [³H]CGP62349 (Richards et al., 1995). In addition, the specific binding of [³H]muscimol, [³H]flunitrazepam, [³⁵S]TBPS and [³H]SR95531 were also similar in GAERS and NEC (Snead et al., 1992a). Thus it is unlikely that augmented tonic GABA_A current is a result of heightened expression of eGABA_ARs in GAERS.

GABA is found in the extracellular space in the CNS at concentrations between 0.2 and 2.5 μM (Kuntz et al., 2004). Many sources of this extracellular GABA have been suggested, such as “spillover” from vesicular release at the synapse (Bright et al., 2007), reversal of GABA transporters (GATs) (Nusser & Mody, 2002) and non-vesicular release (Rossi et al., 2003).

Tonic GABA_A current in cerebellar granule cells is dependent on action-potential mediated GABA release early in development (Brickley et al., 1996; Kaneda et al., 1995), however becomes action-potential independent later in development (Rossi et al., 2003). This is most likely due to changes in the microstructure of cerebellum, where granule cell dendrites become ensheathed in a glial glomerulus (Jakab & Hamori, 1988), which prevents the diffusion of locally released GABA (Brickley et al., 1996; Rossi & Hamann, 1998).

Bright et al (2007) found that tonic GABA_A inhibition is almost abolished in TC neurons of the dorsal lateral geniculate nucleus (dLGN), when transmitter release probability is reduced – either by lowered Ca²⁺ concentrations (1mM extracellular Ca²⁺ = 93% reduction) or when action-potential evoked release is blocked by TTX (500nM = 87% reduction). Since tonic GABA_A current in TC neurons of the dLGN and pyramidal cells of the hippocampus is dependent on vesicular GABA release (Bright et al., 2007), the augmented tonic GABA_A conductance in the TC neurons of the VB of GAERS may be a result of increased vesicular GABA release. However, it seems that this is not the case.

My data show that both sIPSC frequency, which is a measure of action-potential dependent vesicular GABA release, and mIPSC frequency were no different between GAERS and NEC. Therefore, similar frequency values for both sIPSCs and mIPSCs in each strain indicate that the majority of vesicular GABA release is in fact quantal. Further support of this notion is that TTX had no effect of tonic current amplitude in either GAERS or NEC, nor did it impede the observation of a substantial tonic current in TC neurons of the VB in normal Wistar animals (see Section 3.4.3), in agreement with Belelli et al (2005) and Peden et al (2008).

Using microdialysis to determine extracellular GABA levels in adult behaving animals, Richards et al (1995) found that basal quantity of GABA was ~50% higher in the ventral thalamus of GAERS than NEC. Critically, they found that systemic i.p. administration of baclofen and CGP35348 produced no changes to the level of GABA, despite baclofen increasing the duration of SWDs. They also reached the conclusion

that any reduction of SWDs as a result of GABA_B antagonist applications is due to “GABA_BR blockade and thus independent of GABA level”.

From these findings it appears likely that augmented tonic current in the VB is due to a larger quantity of GABA in the extracellular space, which is not a result of an increased synaptic release from GABAergic fibres.

The neighbouring NRT gives rise to a strong GABAergic input into the VB. Indeed, Pinault et al (1997) discovered that bursting of the NRT during a SWD induced a small tonic hyperpolarisation of VB neurons. This NRT activity would have to be factored into any explanation for the initial experiments involving GAERS and NEC, however in the presence of TTX which essentially blocks surrounding circuitry input, an augmented tonic GABA_A current amplitude was sustained. Therefore, whilst the NRT undoubtedly plays a crucial role throughout SWDs *in vivo*, an additional pathological is likely to underlie enhanced tonic GABA_A inhibition in TC neurons of the VB.

Once released, GABA diffuses through the neuropil before its action is terminated by reuptake into presynaptic terminals and surrounding glia. Four GABA transporters (GATs) have been identified so far (GAT 1 – 4) (Borden et al., 1996), however GAT-1 and GAT-3 are predominant throughout the CNS (Nishimura et al., 1997; Ikegaki et al., 1994).

Subtype specific GABA reuptake inhibitors that block GATs such as tiagibine, NO711 and SNAP5114, will lead to increased concentrations of GABA in the extracellular space, thus enhancing GABAergic neurotransmission. Indeed, antagonising GAT-1 with NO711 selectively enhanced the tonic inhibition of cerebellar granule cells by over 300% without affecting phasic inhibitory transmission (Nusser & Mody, 2002). Similar findings have been made by blocking GAT-2/3 in the rat neocortex (Keros & Hablitz, 2005) and by antagonising GABA uptake in hippocampal brain slices, which induced the appearance of eGABA_AR-mediated tonic conductance in pyramidal cells (Semyanov et al., 2003).

In order to examine the origin of increased levels of extracellular GABA in the ventral thalamus in GAERS (Richards et al., 1995), Sutch et al (1999) measured GABA release

and uptake in crude synaptosomes from the thalamus of GAERS and control animals. Importantly, they found that uptake of [³H]GABA was reduced in GAERS compared to control animals, and that GAT reduced affinity for GABA appeared to underlie the increased extracellular level in epileptic animals. Thus it seems likely that the augmented tonic GABA_A current observed in the TC neurons of GAERS and monogenic mutant mouse models of absence may be caused by dysfunctional GABA uptake in the VB thalamus. Indeed this was the case, with GAT-1 dysfunction prevalent in GAERS (Cope et al., 2009). This issue is discussed further in Chapter 4.

3.4.3 GHB-induced increase of eGABA_AR-mediated inhibition

Systemic and intrathalamic administration of GHB in primates, rats and mice induces SWDs alongside behavioural arrest (Aizawa et al., 1997; Godshalk et al., 1977; Snead, 1978a; Snead, 1988) and constitutes the best characterised pharmacological model of typical absence seizures (Crunelli & Leresche, 2002). Furthermore, systemic and intrathalamic administration of GHB in GAERS exacerbates SWDs (Liu et al., 1991; Snead, 1988; Depaulis et al., 1988).

Previous electrophysiological studies have shown most GHB action to be either in part or fully mediated by GABA_BRs (Crunelli et al., 2006). For instance, Williams et al (1995) found that GHB caused a dose-dependent hyperpolarisation of TC neurons of cells in the LGN thalamus by acting directly at postsynaptic GABA_BRs. However, using autoradiographical techniques Snead (1994) revealed that GABA_B binding sites are present from birth but that GHB binding sites do not appear in the rat thalamus until P21. For this reason I used P21-26 Wistar rats throughout this study.

Interestingly, I observed that different concentrations of GHB significantly increased tonic GABA_A current in TC neurons of the VB, in particular 300µM GHB which is the threshold concentration for inducing absence seizures *in vivo* (Snead, 1991). These data provide further evidence in support of augmented eGABA_AR function in the VB as a characteristic of SWDs (see 3.4.1). Again, in agreement with data from GAERS, *Stg* and *lh* (Cope et al., 2009), the GHB-induced increase of tonic GABA_A current occurred independently of membrane capacitance values (see 3.4.1). Thus it is probable that other basic cellular properties did not contribute to GHB enhanced tonic GABA_A current.

The sensitivity of SWDs to GABA_BR modulation is a defining criterion of experimental models of typical absence epilepsy (Danober et al., 1998; Marescaux et al., 1992a; Snead, 1995). Indeed, the induction and exacerbation of seizures by GABA_A and GABA_B agonists alongside the block of SWDs by GABA_B antagonists has been well characterised across various genetic and pharmacological models (Aizawa et al., 1997; Bernasconi et al., 1992; Banerjee & Snead, 1995; Depaulis et al., 1988; Hosford et al., 1992; Liu et al., 1992 & 1995; Manning et al., 2003; Marescaux et al., 1992a & d; Snead, 1991; Vergnes et al., 1984; Vergnes et al., 1992). My data show that both a GABA_BR antagonist (CGP55845) and the putative GHB receptor antagonist, NCS382 attenuated the GHB-induced increase of tonic GABA_A current amplitude.

Usually, NCS382 is either ineffective as a GHB antagonist (Gervasi et al., 2003) or acts as a partial agonist (Emri et al., 1996b; Gervasi et al., 2003). My data one of the first examples to demonstrate GHB-antagonism by NCS382 using an electrophysiological technique in brain slices. Furthermore, these results may provide an explanation to the mechanism by which both GABA_B antagonists (Bernasconi et al., 1992; Marescaux et al., 1992a) and NCS382 (Snead, 1996a) terminate absence seizures *in vivo*.

It is well established that GHB mediates its inhibitory action at presynaptic terminals by reducing neurotransmitter release (Emri et al., 1996b; Gervasi et al., 2003), presumably via presynaptic GABA_BRs (Crunelli et al., 2006). A similar dose-dependent decrease in mIPSC frequency was observed here (see 3.4.3.1), thus the GHBR/GABA_BR augmentation of eGABA_AR function occurs despite a decreased GABA release.

Briefly, GABA_BRs are part of the metabotropic receptor family (Kaupmann et al., 1997 & 1998) that are coupled to inhibitory G-proteins (G_{i/o}) (Siegelbaum et al., 2000) which mediate their inhibitory effects either by opening postsynaptic K⁺ channels (GIRKs) (Dutar & Nicoll, 1988), decreasing Ca²⁺ influx into presynaptic terminals (Bowery et al., 1980; Hill & Bowery, 1981) or by reducing intracellular levels of cAMP (Bowery et al., 1993; Misgeld et al., 1995). Taking into account the controversy over GHB site-of-action it is worth noting that there is also evidence of the putative GHBR being a G-protein coupled receptor (Snead et al., 2000).

In my experiments, patch pipettes were filled with caesium chloride which has been shown to block GIRK channels (Maccaferri et al., 1995; Spain et al., 1987) and the postsynaptic action of baclofen (Gahwiler & Brown, 1995). Considering that both synaptic transmission and $G_{i/o}$ postsynaptic facilitation of GIRK channels were blocked under my experimental conditions, GHB may facilitate eGABA_AR function independently of K⁺ channels through the postsynaptic membrane. Therefore, GHB-induced increase of tonic GABA_A current may also give rise to a potential and novel metabotropic–ionotropic receptor relationship (see Chapter 5).

GHB action has been indirectly linked to GABA_AR function in the past. Because of its similarities to GABA action, in 1987 Snead & Nichols investigated whether the binding site for GHB was related to a chloride ion channel. They ascertained the effect of eight different anions on the binding of [³H]GHB to synaptosomal membranes of rat and human brain tissue and found chloride inhibited [³H]GHB binding in a dose-dependent manner and that picrotoxin strongly enhanced [³H]GHB binding in a Cl⁻-dependent manner (Snead & Nichols, 1987). However, where GABA has been shown to induce an increased rate of efflux of Cl⁻ from loaded hippocampal cells via GABA_ARs (Segal & Barker, 1984), GHB had no direct effect on Cl⁻ efflux under similar conditions (Snead, 1990). It appears that my data provide some of the first electrophysiological evidence in support for the GHB binding coupled GABA_AR activity, albeit via an indirect pathway as it has been established that GHB has no affinity for GABA_ARs itself (Snead & Liu, 1993).

3.4.3.1 Simultaneous GHB effects at presynaptic terminals

Evoked EPSP (eEPSP) amplitude (Emri et al., 1996a), evoked IPSP (eIPSP) amplitude (Urich & Huguenard, 1996; Le Feuvre et al., 1997) and mIPSC frequency (Le Feuvre et al., 1997) are reduced by the specific GABA_BR agonist, baclofen acting at presynaptic GABA_BRs in the VB. This negative control mechanism has also been identified in the presence of GHB, which produced similar dose-dependent results whereby eEPSP (Emri et al., 1996b; Gervasi et al., 2003) and eIPSP (Gervasi et al., 2003) amplitudes were reduced in the VB thalamus. In agreement, I detected a dose-dependent reduction of mIPSC frequency in the presence of GHB. Unlike previous work that detected GHB effects on eEPSP amplitude at concentrations as low as 100 – 250 μM GHB (Gervasi et

al., 2003; Emri et al., 1996b), the mIPSC frequency in my experiments remained unchanged in the presence of 300 μ M GHB.

It is important to note that the mIPSC data in this thesis were taken from just 55 seconds of baseline recording which is likely to affect the validity of these synaptic data. Other studies used an epoch of at least 3 minutes (LeFeuvre et al., 1997) and if I were to repeat these experiments I would extend the mIPSC recording period which may reveal a presynaptic effect of 300 μ M GHB.

3.4.3.2 GHB action and possible GABA_BR heterogeneity

GHB was found to be converted into GABA *in vitro* by GHB dehydrogenase in a crude synaptosomal preparation studying GABA_BR binding (Hechler et al., 1997). As brain-slice preparations maintain more of the intrinsic nature of tissue, it is reasonable to consider that GHB conversion to GABA is occurring in these experiments. Therefore, GHB may mediate some of its effect as both GHB at GHB_R/GABA_BRs and as GABA at GABA_BRs.

Unfortunately the mIPSC data are not strong enough to warrant discussion here (see above), but the block of GHB-mediated increase in tonic current by two pharmacologically distinct antagonists (CGP55845 and NCS382) alongside the possibility of GHB-mediated GABA in the slice, supports a suggested GHB site-specificity and/or GABA_BR heterogeneity.

Banerjee & Snead (1995) measured the release of GABA and GLU in the VB thalamus of behaving animals. Whilst baclofen dose-dependently decreased both basal and evoked extracellular output of GABA and GLU, GHB only reduced GABA release and had no effect on basal GLU discharge (Banerjee & Snead, 1995). Additionally, phaclofen antagonised baclofen-induced inhibition of GABA release without affecting glutamate release in cortical synaptosomes, whereas CGP35348 specifically blocked the effect of baclofen on glutamate release but had little effect on GABA release (Bonanno & Raiteri, 1992). An identical selective antagonism was observed in thalamic and cortical synaptosomes where the putative GHB antagonist NCS382 attenuated the GHB-induced reduction in presynaptic efflux (Snead et al., 1995).

As the thalamus is one of the brain regions with the highest density of GABA_B binding sites (Bowery et al., 1987), it seems reasonable to expect some pre- and postsynaptic receptor heterogeneity in the VB which may render a site specific for GHB action. A GHB binding specific site may include the much contested GHBR (Andriamampandry et al., 2003); however this cloned receptor requires a more precise characterisation (Crunelli et al., 2006).

It is possible that there are pre-synaptic GABA_B receptors in the VB more complex than the already established R_{1a} and R_{1b} splice variants where GHB preferentially binds and exhibits its weak agonistic action. Certainly R_{1c}, R_{1d} and R_{1e} splice variants have been identified as ubiquitously expressed, in forebrain, cerebellum and peripheral tissue, respectively (Isomoto et al., 1998; Pfaff et al., 1999; Schwarz et al., 2000). Distribution, ontogeny and the full physiological function of these isoforms has yet to be clarified (Bowery et al., 2002), but their existence proves them as appealing possibilities when considering that the ligand binding domain of a functional GABA_BR is located on the GABA_BR1 subunit, with the GABA_BR2 subunit escorting it to the cellular membrane (Couve et al., 1998; Calver et al., 2001; Kaupmann et al., 1998; White et al., 1998). It is feasible therefore, to propose that one of the above isoforms, or a yet unidentified variant of the GABA_BR, could constitute specific GHB binding sites.

3.4.4 THIP-induced increase of tonic GABA_A inhibition

δ-subunit containing receptors exhibit a high affinity for GABA (Brown et al., 2002; Saxena & Macdonald, 1994) and being located peri- and/or extra-synaptically, responding to ambient GABA levels these GABA_A receptors are ideally located to mediate tonic GABA_A current in the VB thalamus.

In 1987, Fariello and Golden systemically administered THIP in adult rats. They found that this δ-subunit selective GABA_A agonist THIP induced SWDs *in vivo*, and suggest that it could be a potential model of typical absence seizures. Thus I investigated the effect of THIP on tonic GABA_A current in TC neurons of the VB. Because Wistar rats at P21-26 were used for the GHB experiments, this age range was used for these experiments also.

Consistent with previous work involving mice (Belelli et al., 2005; Jia et al., 2005), I found that THIP induced a concentration-dependent increase of tonic GABA_A current that was independent of whole-cell capacitance.

Baseline current noise is typically an indicator of eGABA_AR activation (Porcello et al., 2003; Mtchedlishvili & Kapur, 2006), and I observed that the higher concentrations of this eGABA_AR specific agonist ultimately led to a larger baseline noise thus all but the largest mIPSCs were visible. To avoid distortion of the mIPSC data therefore, only current traces with clearly visible mIPSCs were analysed and for this reason there are fewer neurons included in the analysis population for mIPSC parameters than for tonic current. In fact, no mIPSCs were visible in the presence of 10 μ M THIP (Table 3.4). From the analysed mIPSCs it is apparent that THIP induces no differences in mIPSC parameters, at least up to 3 μ M and again in agreement with Belelli et al (2005). It seems therefore that all concentrations of THIP tested appear to act directly at extrasynaptic GABA_ARs. In agreement, IPSCs of cortical neurons remain unaltered in the presence of THIP at 20 μ M (Krook-Magnuson et al., 2008), as do recombinant receptors containing the γ 2 subunits with 10 μ M THIP (Storustovu and Ebert, 2006). It should be noted however that the mIPSCs were recorded from just 55 seconds of baseline recording which restricts further conclusions being made from this data.

3.4.5 GABA_B antagonist reduction of tonic GABA_A current in GAERS

The CGP55845 block of the GHB-induced increase of tonic GABA_A current raised the possibility of a mechanism by which GABA_BRs could modulate eGABA_ARs (Section 3.4.3). Therefore, I investigated whether augmented tonic current amplitude observed in GAERS was modulated in a similar way by a GABA_BR antagonist. I tested this at an age where enhanced tonic GABA_A current was observed in the VB of GAERS, P18 – 21.

Interestingly, I found that CGP55845 reduced tonic current to ~44% of the control value recorded in GAERS at P18-21. This suggests that the facilitation of eGABA_AR function by GABA_BR activation actually contributes to over half of the tonic current in GAERS. Furthermore, I found that CGP55845 reduced tonic GABA_A current in the NEC also, but to a lesser extent i.e. 64% of the control value originally recorded in NEC. These

changes to tonic GABA_A inhibition occurred independently of membrane capacitance in both strains.

Reduction of tonic GABA_A current in GAERS by CGP55845 may provide an explanation for the sensitivity of SWDs to GABA_B antagonists; however this explanation becomes less straightforward when considering the decrease of tonic current amplitude by CGP55845 in NEC.

At this point it is wise to look further at the absolute values of tonic GABA_A receptor current across the strains. Under control conditions tonic GABA_A current is 158.40 ± 26.77 pA and the CGP-reduction to 44% is to 70.20 ± 8.23 pA. NEC on the other hand, exhibits a control tonic current value of 87.68 ± 4.79 pA and then 55.99 ± 3.00 pA in the presence of CGP55845 (10 μ M). First of all this indicates that postsynaptic GABA_BR-facilitation of eGABA_ARs is occurring under control condition. This phenomenon is investigated and discussed further in Chapter 5. Secondly, comparison of these data revealed that the tonic current value in GAERS in the presence of CGP55845 is not statistically different to the tonic current value of NEC, both under control conditions and in presence of CGP55845. Thus, if enhanced tonic GABA_A current in TC neurons of the VB is a common phenomenon across models of absence, CGP55845 effects may provide a mechanism through which GABA_B antagonists can attenuate SWDS *in vivo*: reducing tonic GABA_A inhibition in GAERS to a similar level that is observed in NEC, that naturally do not exhibit SWDs. Moreover, the percentage reduction of tonic current amplitude in GAERS by CGP55845 is strikingly similar to the CGP55845-mediated decrease of tonic GABA_A current with 3mM GHB, ~49%.

The age of GAERS used for these experiments is when enhanced GABA_A current was measurable, but it is also prior to detectible GHB binding sites (Snead 1994). This suggests two things: firstly, that postsynaptic GABA_BR modulation of eGABA_ARs is present at P18-21 and secondly, strengthens the case for GHB action at GABA_BRs.

3.4.6 Penicillin failed to enhance tonic GABA_A current

Intramuscular injection of high doses of penicillin into the cat consistently produces both the EEG and behavioural correlates of absence seizures (Gloor et al., 1977;

Guberman et al., 1975; Fisher & Prince, 1977; Quesney et al., 1977; Quesney & Gloor et al., 1978). However, penicillin fails to induce SWDs in rats (Avoli, 1980) and all absence seizure model criteria have yet to be fully characterised with penicillin (Fariello, 1979) (see Table 1.4).

I found that penicillin reduced synaptic GABA_AR-mediated currents, in agreement with previous studies (Mtchedlishvili & Kapur, 2006; Twyman & Macdonald, 1992; Yeung et al., 2003). As expected from an open channel blocker (Twyman & Macdonald, 1992), penicillin dose-dependently accelerated the weighted decay of mIPSCs which decreased charge transfer, but the frequency and rise-time (10-90%) remained the same as control. However in contrast to previous work, mIPSC amplitude was also decreased in the presence of penicillin which contributed to decreased charge transfer. The overall affect of these changes was a reduction of synaptic GABA_A inhibition which would be expected from the non-competitive antagonism (Macdonald & Barker, 1977). Despite the clear changes in mIPSCs observed in the presence of penicillin, it is important to highlight that the mIPSCs were recorded from just 55 seconds of baseline recording.

In line with experiments in hippocampal neurons (Yeung et al., 2003; Mtchedlishvili & Kapur, 2006), penicillin did not affect the tonic GABA_A current. Whilst any changes in tonic current were not significant, there does appear to be a trend where cells have lower current amplitudes in the presence of penicillin, compared to control conditions. This trend may be resolved if the number of cells for of each concentration were increased. Interestingly however, both Mtchedlishvili & Kapur (2006) and Yeung et al (2003) observed that whilst penicillin did not antagonise eGABA_ARs, it did result with a reduction in baseline noise. Similarly, traces recorded in the presence of penicillin in my experiment do appear to have a more compact baseline current. As baseline current noise is an indicator of persistently open eGABA_ARs (Porcello et al., 2003; Mtchedlishvili & Kapur, 2006), it appears that penicillin does have a small effect at eGABA_ARs and this may be reflected in a trend for slightly smaller tonic current amplitudes. It is possible that penicillin failed to have full antagonistic action at eGABA_ARs because of their persistently open and slow desensitising properties (Brown et al., 2002; Saxena & Macdonald, 1994).

SWDs are induced in cats when penicillin was administered via IM injection (Gloor et al., 1977; Guberman et al., 1975; Fisher & Prince, 1977; Quesney et al., 1977; Quesney & Gloor et al., 1977) or applied diffusely to the cerebral cortex (Gloor et al., 1977; Quesney & Gloor, 1978), however direct intrathalamic microinjection failed to induce epileptiform activity (Gloor et al., 1966; Quesney & Gloor, 1978). Considering that enhanced tonic GABA_A current in thalamic cells of the VB is a prerequisite for SWDs (Cope et al., 2009) and that direct thalamic application of GABA_A and GABA_B agonists can exacerbate or induce SWDs (see Chapter 1.2), it is unsurprising that thalamic application of penicillin which failed to affect tonic GABA_A current in brain slices, also failed to induce SWDs in cortical or thalamic structures when focally applied to the thalamus *in vivo* (Quesney & Gloor, 1978). Furthermore, diffuse cortical application of weak penicillin solution induced bilateral synchronous epileptic activity in the EEG similar to those induced by IM injection of large doses, but was absent from thalamic neurons (Gloor et al., 1966; Quesney & Gloor, 1978).

Considering that the initiation site of SWD generation lies in the cortex (Meeren et al., 2002; Polack et al., 2007) and cells in this region were found to exhibit hyperactivity (Polack et al., 2007), it seems feasible to suggest that penicillin may induce SWDs via a cortical manifestation of the drug i.e. penicillin creating cortical hyperactivity through its antagonistic action at synaptic GABA_ARs. Seeing that a low concentration of penicillin can cause cortical SWDs (Gloor et al., 1966; Quesney & Gloor, 1978), it has been suggested that much larger doses of penicillin are required with intramuscular injection to counteract simultaneous cellular activation caused by penicillin in the thalamus (Quesney & Gloor, 1978).

It is important to note that stimulation of the thalamus and basal ganglia triggered SWDs in animals that received penicillin intramuscularly (Quesney et al., 1977) and via diffuse cortical application (Gloor et al., 1977). Therefore, the thalamus still plays an important role in penicillin-induced SWDs. Interestingly, no behavioural expression of SWDs were observed in GAERS when isolated cortical paroxysms were discharged unless the thalamus was entrained in the SWD of GAERS (Polack et al., 2007). Thus the behavioural correlates of an absence seizure appear to result from thalamic involvement.

Instead of enhanced tonic GABA_A current in the VB, SWDs induced by penicillin in cats may more closely represent the aberrant activity of the cortex seen in SWDs and thus, exist as an important tool for SWD investigation. Indeed, the inability of penicillin to elicit SWDs in rats (Avoli et al., 1980) supports the notion that hyperactivity in the more complex and convoluted cat cortex might more accurately represent the human cortical manifestation of SWDs.

3.5 Conclusion

The data in this chapter indicate that enhanced tonic GABA_A current in the VB is a common feature of absence seizures *in vitro*, across various established genetic models and in the presence of pharmacological agents that induce SWDs *in vivo*. Additionally, the data demonstrate that GHB augments tonic GABA_A current through post-synaptic GABA_B and/or GHB receptors. Whilst it seems that aberrant GAT-1 is initially responsible for the enhanced tonic current in genetic models of absence (Cope et al., 2009), GABA_B agonist/antagonist action on SWDs *in vivo* may be a result of postsynaptic GABA_BR enhancement of eGABA_AR function alongside the “classical” pre- and postsynaptic GABA_B actions. Not detracting from the involvement of other neurotransmitters, brain inputs and the classical postsynaptic GABA_B effects, this data has identified a novel phenomenon common to the majority of absence seizure models and mechanism whereby GABA_BR antagonists can suppress SWDs.

Chapter 4

Extrasynaptic GABA_A receptor gain-of-function in
the ventrobasal thalamus is crucial for SWD
generation *in vivo*

4.1 Introduction

A cortical “initiation site” within the peri-oral subregion of the primary somatosensory cortex has been found to lead the initiation of spontaneous SWDs in both the GAERS and WAG/Rij rat model of absence seizures (Meeren et al., 2002; Pinault et al., 2003; Polack et al., 2007 & 2009). The SWD quickly propagates and becomes generalised over the rest of the cortex and thalamus with cortical and thalamic sites interacting bidirectionally, after the first 500msecs (Meeren et al., 2002). It is clear that despite a cortical initiation, the occurrence of a SWD is dependent on an intact and reciprocally connected thalamocortical network as a lesion of the lateral thalamus in various models of absence epilepsy suppresses SWDs (Avanzini et al., 1992; Meeren et al., 2009; Pelligrini & Gloor, 1979; Vergnes & Marescaux, 1992). Polack et al (2007) observed short discharges at somatosensory cortical sites which would either entrain SWD or exist without propagation to the thalamus. No behavioural changes were present with the isolated cortical paroxysms, thus it seems the behavioural correlates of an absence seizure result from thalamic involvement (Polack et al., 2009).

In Chapter 3 I demonstrated that enhanced tonic GABA_A current in TC neurons in the VB is a common feature of several genetic and pharmacological models of absence seizures *in vitro*. Considering the importance of the thalamus to SWD generation and because the role of augmented tonic GABA_A current in TC neurons of the VB has not yet been established in behaving animals, I have carried out experiments to determine the epileptogenic significance of this common cellular pathology *in vivo*.

My data show that eGABA_AR gain-of-function is critical to the induction of SWDs, thus supporting the conclusions made in Chapter 3. Additionally, my data implicate an aberrant GABA transporter subtype 1 (GAT1) in the VB as a candidate responsible for the enhanced tonic current in TC neurons, and thus SWDs in animal models of absence seizures.

4.2 Methods

EEG recordings, reverse microdialysis and data analysis were carried out as described in Chapter 2.2. In order to carry out accurate reverse microdialysis there are several

methodological aspects that have to be considered prior to application of the technique, which are discussed below.

4.2.1 Principles and methodological considerations of reverse microdialysis

Traditionally, microdialysis is a technique that has been used to monitor and sample levels of endogenous compounds and drugs in interstitial fluid and the extracellular space of tissue (Hocht et al., 2007). Microdialysis sampling has proven advantageous in determining the chemistry of a tissue by providing frequent and direct sampling from a specific area. A more recent application of the microdialysis technique is the introduction of a substance into the extracellular space of a tissue via the microdialysis probe, also known as “reverse microdialysis” (Galvan et al., 2003).

A microdialysis probe is designed to mimic a blood capillary in function, through which a perfusion fluid or “perfusate” is slowly dialysed. The outer surface of the probe is made up of a porous membrane, and via this permeable there is a bidirectional exchange of molecules. The difference in concentration of a specific molecule determines diffusion direction. To minimise depletion of endogenous levels of molecules, the perfusate used in my experiments was aCSF which closely resembled CSF found in the brain of rats (Davson et al., 1987). Both THIP and NO711 were dissolved in this aCSF and delivered by following the concentration gradient across the probe membrane and out into the VB tissue. The contribution of other convective processes, such as osmotic and hydrostatic pressure, to the transport of exogenous substances during reverse microdialysis is believed to be minimal (Bungay et al., 1990), thus reverse microdialysis is largely limited to the diffusion process.

It is important to note that whilst the diffusion gradient, and thus molecular weight and hydrophobicity of a drug, are essential factors in the microdialysis process, the physical composition of the medium in which transport occurs is also important (Shippenberg & Thompson, 2001). Diffusion through brain tissue is typically slower than through an aqueous solution as impermeable cell membranes of neurons significantly increase resistance in tissue (Nicholson & Rice, 1986). Not only do neurons decrease the fluid volume available for diffusion but the complex geometry of extracellular space around neurons and fibres also obstruct the diffusional path, both increasing resistance to the movement of molecules through the tissue (Nicholson & Rice, 1986). Furthermore, it is

possible for diffusion through tissue to be slowed even further by molecules of the perfusate binding to cell surface proteins along the diffusion path (Rice et al., 1985).

As diffusion through tissue is a rate limiting step in reverse microdialysis, the choice of dialysis probe is essential in ensuring optimised drug delivery. The probe size and membrane type are two factors that require consideration. Most membranes have a molecular weight “cut-off” at 20kDa which enable small molecules to pass and block the movement of larger molecules, such as bacteria (Hocht et al., 2007; Shippenberg & Thompson, 2008). Both THIP (176.6 Da) and NO711 (386.87 Da) are below the 20kDa threshold and thus will move through the porous membrane with ease. The rate of perfusion across a membrane is proportional to the membrane area; therefore increasing the length of a probe will result in greater probe efficiency (Plock & Kloft, 2005). However, whilst it is important to maximise drug administration to the tissue, the probe membrane length must not exceed the size of the targeted tissue, else area-specificity is lost. In addition, compounds do not diffuse more than 1mm from the dialysis membrane surface in tissue i.e. 1mm radial distance around the probe (Westerink & de Vries, 2001; Hocht et al., 2007). In order to limit drug administration to the specific locus of the VB thalamus, I used probes that were 2mm long similar to the probes used by Richards et al (2003). Considering the radial penetration distance of the probe (1mm) alongside the length of the membrane (2mm), approximately 8mm³ of the surrounding tissue was reached by the perfusate fluid (Richards et al., 2003). At the coordinates used in my experiments (mm to bregma: AP -3.1, L 3.0, V 6.0; Paxinos & Watson, 1998), the probe would sit in the very centre of the VB complex and considering the diffusion distance from the probe surface, will probably diffuse to all of the VB. There is a possibility that perfusion at these coordinates may also extend beyond the vicinity of the VB, especially at the ventral position between 4–5mm which contains the laterodorsal thalamic nucleus.

Drug application via reverse microdialysis carries many advantages:

- by using a low flow rate (typically 1µM/min) it reduces depletion of endogenous compounds in extracellular fluid (Shippenberg & Thompson, 2008);

- can maintain a constant and low drug concentration at the target tissue (Hocht et al., 2007);
- the dialysis membrane acts as a physical barrier and prevents turbulent flow of the perfusate fluid, resulting in low levels of tissue disruption which is advantageous for chronic application experiments (Shippenberg & Thompson, 2008);
- it allows local application in specific regions of the brain and permits direct control over the duration of drug administration (Hocht et al., 2007);
- can deliver the drug without net gain of fluid over a sustained period of time (Hocht et al., 2007);
- the probe function can be monitored throughout the experiment by assessing probe output (Hocht et al., 2007), and
- can ascertain behavioural changes whilst applying drug.

It is important to note that after the probes are inserted for the first time, there can be a period of disturbed tissue function caused by lesion of the tissue displaced by the probe (Thompson & Shippenberg, 2001). This is characterised by increased glucose metabolism, decreased blood flow and disturbed neurotransmitter release which can last from 20 minutes to 24 hours (Thompson & Shippenberg, 2001). Considering this, after inserting the probes, rats were allowed to adjust and the EEG was observed during perfusion of aCSF for 20 minutes prior to the later recording. Behaviour and EEG of all animals appeared normal in the initial 20 minute period, thus I presumed that any disturbed tissue function was minimal and lasted a short time.

The concentration of drugs (THIP and NO711) in the perfusate was selected on the basis of the results of the *in vitro* experiments (Chapter 3 and Cope et al., 2009). It is important to note that reverse microdialysis reduces the effective concentration of an administered drug to $\leq 10\%$ i.e. only $\sim 10\%$ of the drug diffuses out of the probe (Juhász et al., 1990; Portas et al., 1996). Therefore, perfusion of $30\mu\text{M}$, $70\mu\text{M}$ and $100\mu\text{M}$ THIP would deliver approximately $3\mu\text{M}$, $7\mu\text{M}$, and $10\mu\text{M}$ THIP to the VB thalamus, respectively. Similarly, $200\mu\text{M}$ of NO711 delivered $20\mu\text{M}$ NO711 to the VB.

4.3 Results

4.3.1 Enhanced eGABA_AR function is sufficient for absence seizures

In 1987, Fariello and Golden discovered that systemic administration of THIP in normal adult rats provoked SWDs and is therefore a potential pharmacological model for typical absence seizures. I have shown that by acting directly at eGABA_ARs, THIP induced a concentration-dependent increase of tonic GABA_A current in TC cells of VB slices from Wistar rats (Chapter 3.3.2.3). To directly test the hypothesis that enhanced eGABA_AR function in TC neurons of the VB is critical to the generation of SWDs, varying concentrations of THIP were bilaterally administered via reverse microdialysis directly into the VB regions of adult, male Wistar rats. Subsequent EEG recordings and behavioural observations were made.

Simultaneous and bilateral EEG traces were recorded from a total of 15 adult, male Wistar rats under control conditions, i.e. no probes, then following bilateral reverse microdialysis injection into the VB thalamus of either aCSF (n=15) or varying concentrations of THIP (30µM, n=6; 70µM, n=5; 100µM, n=5). One animal was used to test both 30µM and 100µM THIP but recovered for 14 days between experiments.

No SWDs were observed in the EEG of Wistar rats under control conditions (no probes) or during the continuous microdialysis of aCSF (120 minutes) (Fig. 4.1 and Fig. 4.2). Only 1 out of the 6 animals exhibited SWDs in the presence of 30µM THIP (Fig. 4.2A), however 70µM and 100µM THIP robustly induced absence seizures i.e. SWDs and their behavioural correlates, in every animal tested (Fig. 4.1, Fig. 4.2B and C).

Seizures recorded during the administration of both 70µM and 100µM THIP had a clear spike-and-wave appearance (see extended traces in Fig. 4.1), started and finished abruptly, and occurred at a frequency of 5.7 ± 0.1 Hz (range 3.9 – 7.6 Hz, average of 10 SWDs from each rat dialysed with 70µM THIP) and 5.1 ± 0.1 Hz (range 3.2 – 6.8 Hz, average of 10 SWDs from each rat dialysed with 100µM THIP).

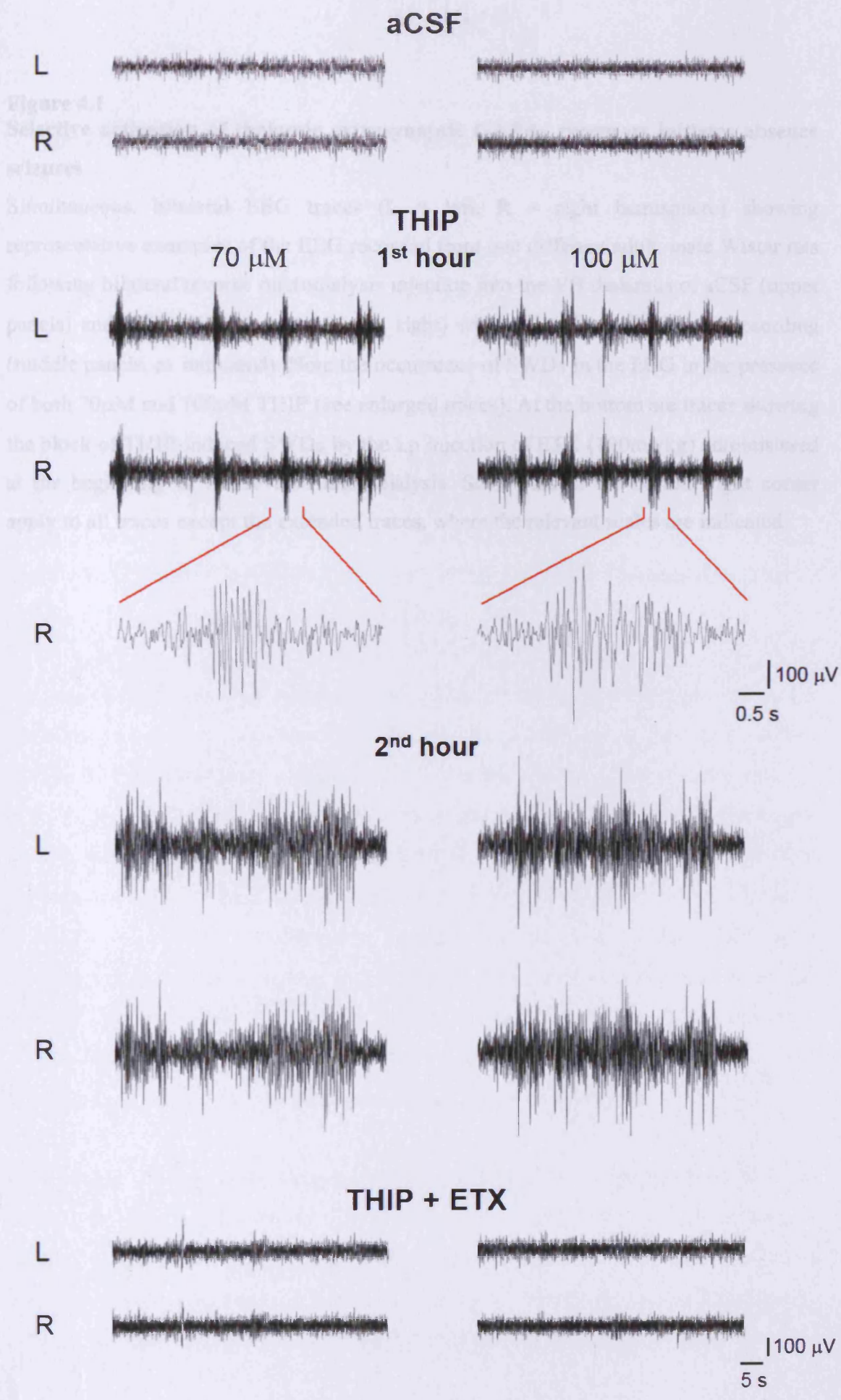


Figure 4.1

Figure 4.1**Selective activation of thalamic extrasynaptic GABA_A receptors initiates absence seizures**

Simultaneous, bilateral EEG traces (L = left, R = right hemisphere) showing representative examples of the EEG recorded from two different adult, male Wistar rats following bilateral reverse microdialysis injection into the VB thalamus of aCSF (upper panels) and THIP (70 μ M, left; 100 μ M, right) within the 1st or 2nd hour of recording (middle panels, as indicated). Note the occurrence of SWDs in the EEG in the presence of both 70 μ M and 100 μ M THIP (see enlarged traces). At the bottom are traces showing the block of THIP-induced SWDs by the i.p injection of ETX (100mg/kg) administered at the beginning of the reverse microdialysis. Scale-bars in the bottom right corner apply to all traces except the extended traces, where the relevant scales are indicated.

SWDs recorded on the EEG were accompanied by classic behavioural correlates of absence seizures, including cessation of movement and some vibrissal twitching lasting for the entire duration of a SWD (Video 1).

The time that the rats spent in seizure increased throughout the 2 hour recording period, which is demonstrated clearly by the upward gradient of the line representing bilateral reverse microdialysis of 70 μ M (Fig. 4.2B) and 100 μ M THIP (Fig. 4.2C).

Interestingly, in 2 out of 5 animals (70 μ M THIP) along with 3 out of 5 animals in the presence of 100 μ M THIP, SWD length increased in duration throughout the recording period (Fig. 4.1). However on average, the difference between the long seizures in the 2nd hour and the shorter SWDs in the 1st hour of recording did not reach statistical significance (70 μ M: 1st hour = 9.9 \pm 3.7 sec, 2nd hour = 11.9 \pm 5.8 sec, $p > 0.5$; 100 μ M: 1st hour = 7.7 \pm 2.2 sec, 2nd hour = 12.4 \pm 6.9 sec, $p > 0.5$).

Animals that received bilateral reverse microdialysis of 100 μ M THIP exhibited longer total time in seizure for the duration of the recording, compared to those that received 70 μ M THIP (70 μ M: 525.1 \pm 89.4 sec/2hrs, 100 μ M: 936.4 \pm 172.9 sec/2hrs; $p < 0.05$) (Fig. 4.2D), which might be explained by a different latency of SWD generation. Indeed, the 1st seizure observed after the start of reverse microdialysis of 70 μ M THIP occurred at 17.5 \pm 3.9 min, significantly later than that of 100 μ M THIP (3.8 \pm 1.6 min, $p < 0.01$) (Fig.4.3C). Concomitantly, animals that received 100 μ M THIP spent significantly more time in seizure for the first 40 minutes of recording than those that received 70 μ M THIP (20 minute epoch: 70 μ M = 21.9 \pm 9.3 sec/20mins, 100 μ M = 128.3 \pm 36.2 sec/20mins, $p < 0.05$; 40 minute epoch: 70 μ M = 33.5 \pm 4.5 sec/20mins, 100 μ M = 117.1 \pm 30.5 secs/20mins, $p < 0.05$) (Fig.4.2C).

Interestingly, the time that rats spent in seizure from the 60 minute epoch onwards are similar for both concentrations (e.g. 80 minute epoch: 70 μ M = 126.0 \pm 23.1 sec/20mins, 100 μ M = 132.3 \pm 16.7 sec/20mins, $p > 0.5$) (Fig. 4.2B and C). The number of seizures that occurred in the presence of both concentrations of THIP were similar (70 μ M: 68.3 \pm 21.5 SWD/2hrs, 100 μ M: 67.6 \pm 20.8 SWD/2hrs, $p > 0.5$) (Fig. 4.3A).

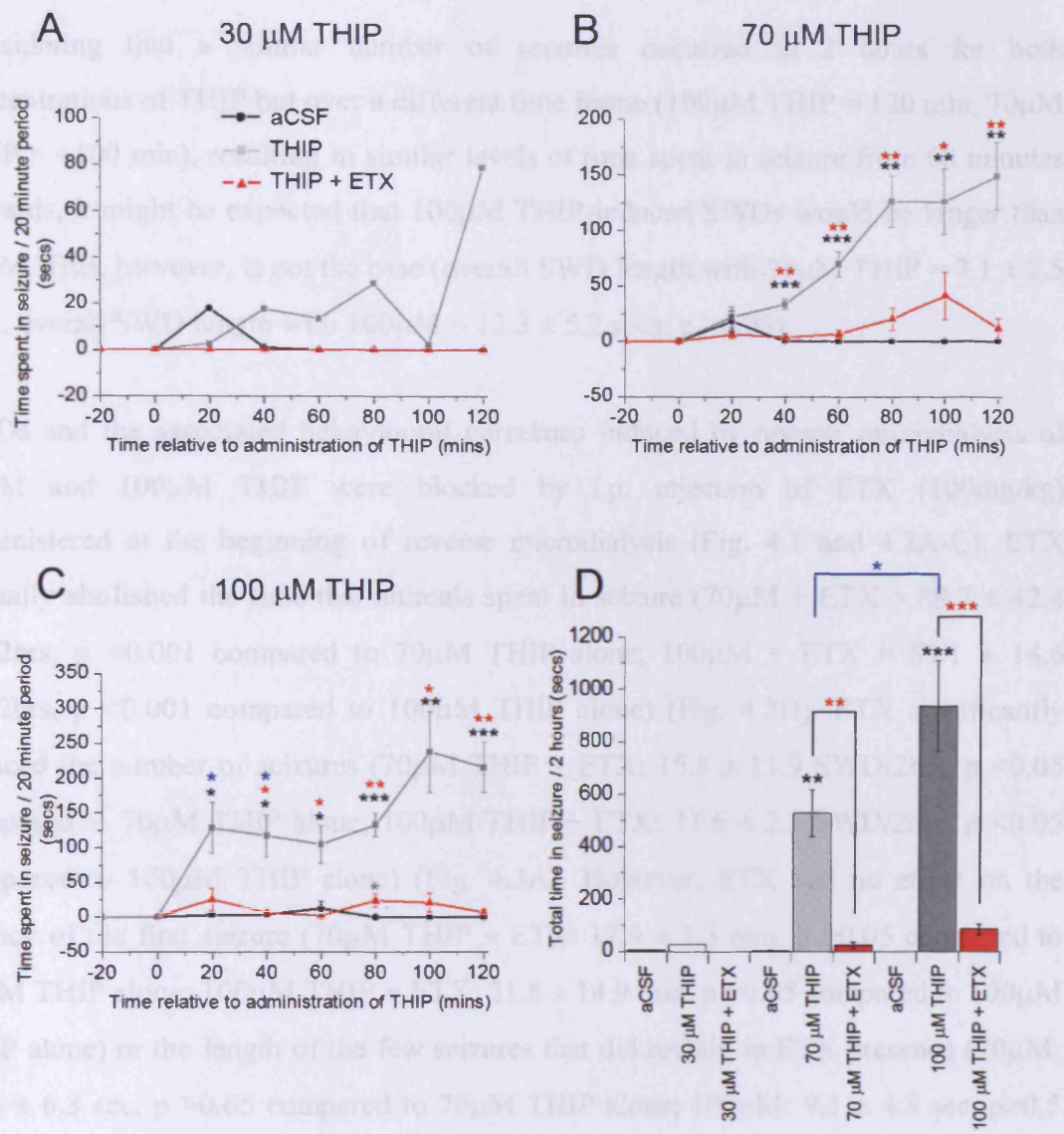


Figure 4.2

THIP elicits ETX-sensitive SWDs

A – C graphs showing the effects of bilateral reverse microdialysis of aCSF (black line); THIP (30μM, A; 70μM, B; 100μM, C; grey line) and THIP together with i.p injection of ETX (100 mg/kg, at time zero; red line) on the time spent in SWDs per 20 minute periods. D) comparison of the total time spent in seizure across 2 hours in the presence of varying concentrations of THIP (grey columns), aCSF and the block of THIP-induced SWDs along with systemic administration of ETX. B - D: * p < 0.05, ** p < 0.01 and *** p < 0.001, THIP vs. aCSF; * p < 0.05, ** p < 0.01 and *** p < 0.001, THIP vs. THIP + ETX; * p < 0.05, 70μM THIP vs. 100μM THIP. C: * p < 0.05, THIP + ETX vs. aCSF.

Considering that a similar number of seizures occurred in 2 hours for both concentrations of THIP but over a different time frame (100 μ M THIP = 120 min, 70 μ M THIP = \sim 100 min), resulting in similar levels of time spent in seizure from 60 minutes onwards, it might be expected that 100 μ M THIP-induced SWDs would be longer than 70 μ M. This, however, is not the case (overall SWD length with 70 μ M THIP = 7.1 ± 2.5 secs; overall SWD length with 100 μ M = 12.3 ± 5.2 secs; $p > 0.05$).

SWDs and the associated behavioural correlates induced by reverse microdialysis of 70 μ M and 100 μ M THIP were blocked by i.p. injection of ETX (100mg/kg) administered at the beginning of reverse microdialysis (Fig. 4.1 and 4.2A-C). ETX virtually abolished the time that animals spent in seizure (70 μ M + ETX = 88.7 ± 42.4 sec/2hrs, $p < 0.001$ compared to 70 μ M THIP alone; 100 μ M + ETX = 83.1 ± 14.6 sec/2hrs, $p < 0.001$ compared to 100 μ M THIP alone) (Fig. 4.2D). ETX significantly reduced the number of seizures (70 μ M THIP + ETX: 15.8 ± 11.9 SWD/2hrs, $p < 0.05$ compared to 70 μ M THIP alone; 100 μ M THIP + ETX: 11.6 ± 2.3 SWD/2hrs, $p < 0.05$ compared to 100 μ M THIP alone) (Fig. 4.3A). However, ETX had no effect on the latency of the first seizure (70 μ M THIP + ETX: 17.9 ± 3.3 min, $p > 0.05$ compared to 70 μ M THIP alone; 100 μ M THIP + ETX: 21.8 ± 14.9 min, $p > 0.05$ compared to 100 μ M THIP alone) or the length of the few seizures that did remain in ETX presence (70 μ M: 12.6 ± 6.3 sec, $p > 0.05$ compared to 70 μ M THIP alone; 100 μ M: 9.1 ± 4.8 sec, $p > 0.5$ compared to 100 μ M THIP alone) (Fig. 4.3B and C).

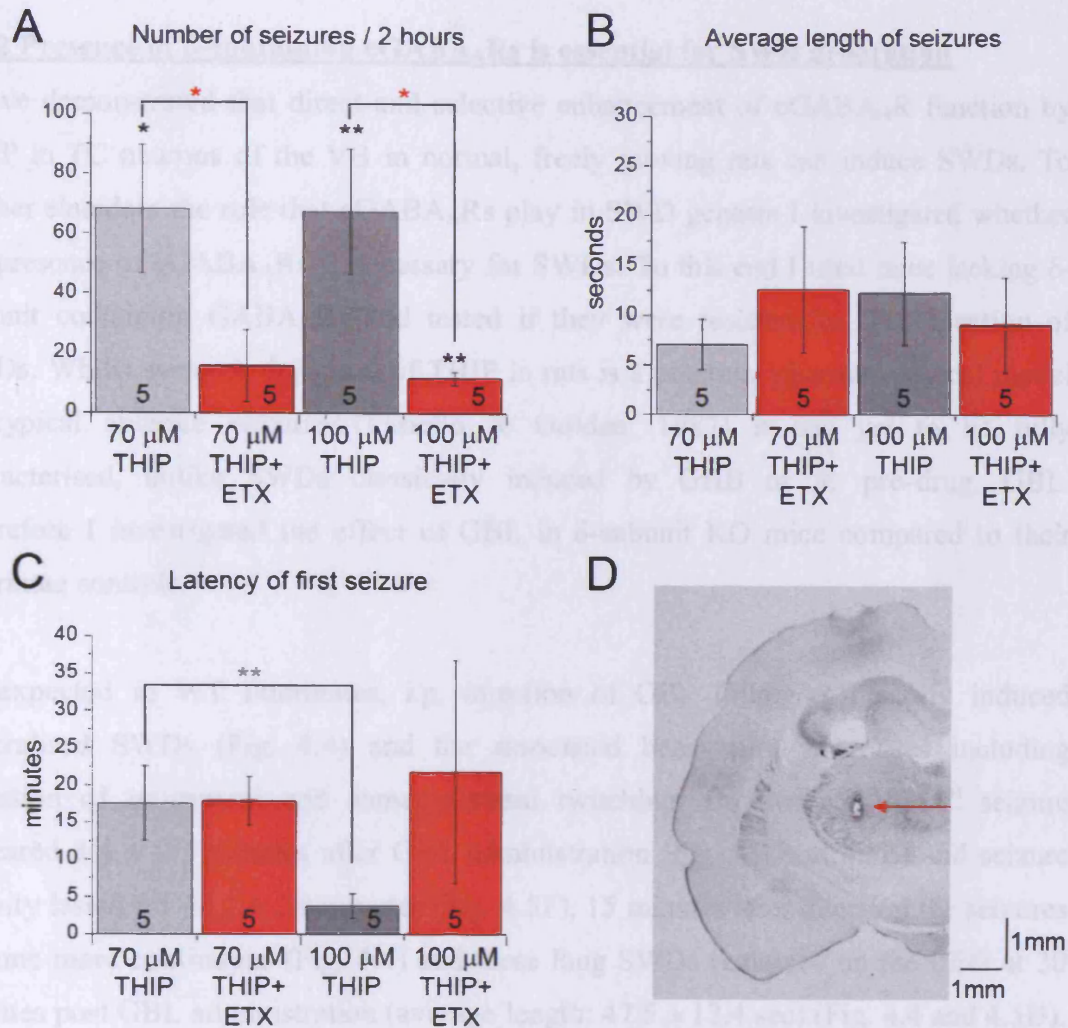


Figure 4.3

Properties of THIP-induced SWDs

Comparison of the effects of bilateral intrathalamic administration of varying concentrations of THIP (70 μ M, light grey columns; 100 μ M, dark grey columns) and THIP alongside i.p injection of ETX (100 mg/kg; red columns) in adult, male Wistar rats on the number of seizures (A), average length of seizures (B) and latency of the first seizure (C). 30 μ M THIP and aCSF data were not included here as there were no SWDs recorded in their presence. Numbers of animals recorded are shown in each column. **A:** * $p < 0.05$ and ** $p < 0.01$ THIP or THIP + ETX vs. aCSF; * $p < 0.05$, THIP vs. THIP + ETX. **C:** ** $p < 0.01$, 70 μ M THIP vs. 100 μ M THIP. **D)** Unilateral brain section showing the termination of the microdialysis probe (red arrow) in the left brain hemisphere of one of the recorded Wistar rats. Scale bars are indicated.

4.3.2 Presence of δ -containing eGABA_ARs is essential for SWD generation

I have demonstrated that direct and selective enhancement of eGABA_AR function by THIP in TC neurons of the VB in normal, freely moving rats can induce SWDs. To further elucidate the role that eGABA_ARs play in SWD genesis I investigated whether the presence of eGABA_ARs is necessary for SWDs. To this end I used mice lacking δ -subunit containing GABA_ARs and tested if they were resistant to the induction of SWDs. Whilst systemic injection of THIP in rats is a potential pharmacological model of typical absence seizures (Fariello & Golden, 1987) it has yet to be fully characterised, unlike SWDs classically induced by GHB or its pro-drug, GBL. Therefore I investigated the effect of GBL in δ -subunit KO mice compared to their littermate controls.

As expected in WT littermates, i.p. injection of GBL (50mg/kg) readily induced generalised SWDs (Fig. 4.4) and the associated behavioural correlates including cessation of movement and some vibrissal twitching. On average the 1st seizure appeared 3.4 ± 0.3 minutes after GBL administration (Fig. 4.4 and 4.5E) and seizure activity lasted for 48.1 ± 1.9 minutes (Fig. 4.5F). 15 minutes after injection the seizures became more continuous (Fig. 4.4) and these long SWDs remained on the EEG at 30 minutes post GBL administration (average length: 47.5 ± 12.4 sec) (Fig. 4.4 and 4.5D). Interestingly, GBL-induced SWDs in these mice (using 50mg/kg) had more similarities with the those induced by administration of 100mg/kg GBL in normal mice (Aizawa et al., 1997).

ETX (200 mg/kg) drastically reduced the time that WT mice spent in GBL-induced SWDs (GBL in WT = 1949.4 ± 151.6 sec/hr, GBL + ETX in WT = 8.5 ± 6.0 sec/hr; $p < 0.001$) (Fig. 4.4 and 4.5A and B), significantly decreasing the number of SWDs (GBL in WT: 44.0 ± 9.7 SWD/hr, GBL + ETX in WT: 3.4 ± 1.7 SWD/hr; $p < 0.001$) (Fig. 4.5C). Only 3 of 5 WT mice exhibited a few seizures in the presence of both GBL and ETX, having a longer latency to onset (GBL in WT = 3.4 ± 0.3 min, GBL + ETX in WT = 5.9 ± 1.5 min; $p < 0.05$) (Fig. 4.5E) and were significantly shorter than when GBL was administered alone (GBL = 47.5 ± 12.4 sec, GBL + ETX = 1.3 ± 0.8 sec, $p < 0.001$) (Fig. 4.5D). ETX brought forward the time of the last seizure to 32.52 ± 9.06 minutes in WT mice ($p < 0.05$, compared to GBL alone in WT) (Fig. 4.5F).

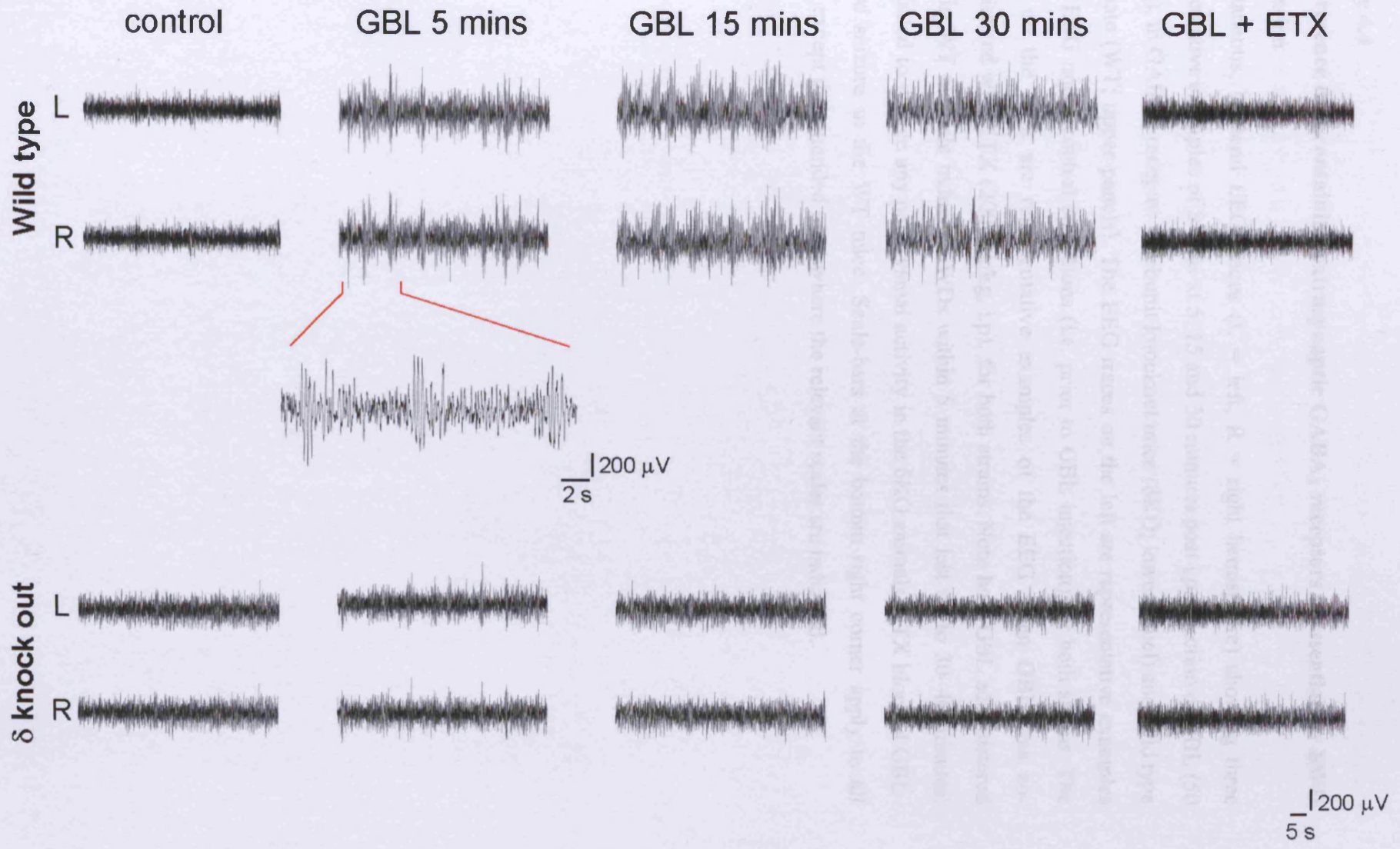


Figure 4.4

Figure 4.4

The presence of δ -containing extrasynaptic GABA_A receptors is essential for SWD generation

Simultaneous, bilateral EEG traces (L = left, R = right hemisphere) showing three representative examples of SWDs at 5, 15 and 30 minutes post i.p. injection of GBL (50 mg/kg), in GABA_A receptor δ -subunit knockout mice (δ KO; lower panel) and wild type littermate (WT; upper panels). The EEG traces on the left are representative examples of the EEG under control conditions (i.e. prior to GBL injection) for both strains. The traces on the right are representative examples of the EEG when GBL was co-administered with ETX (200 mg/kg, i.p), for both strains. Note how GBL administered alone in WT animals induces SWDs within 5 minutes that last up to 30–40 minutes. GBL failed to induce any paroxysmal activity in the δ KO animals. ETX blocked GBL-induced seizure in the WT mice. Scale-bars at the bottom right corner apply to all traces, except the extended trace where the relevant scales are indicated.

Injection of GBL (50mg/kg) failed to induce SWDs in δ -subunit GABA_AR KO mice (Fig. 4.4 and 4.5A and B), though elicited a few SWDs in 2 animals (13.6 ± 9.3 SWD/hr, $p < 0.05$ compared to GBL in WT) (Fig. 4.5C).

Overall, not only is selective augmentation of eGABA_AR function in TC cells sufficient to induce SWDs, but these receptors in the VB are actually essential to SWD induction.

Figure 4.5

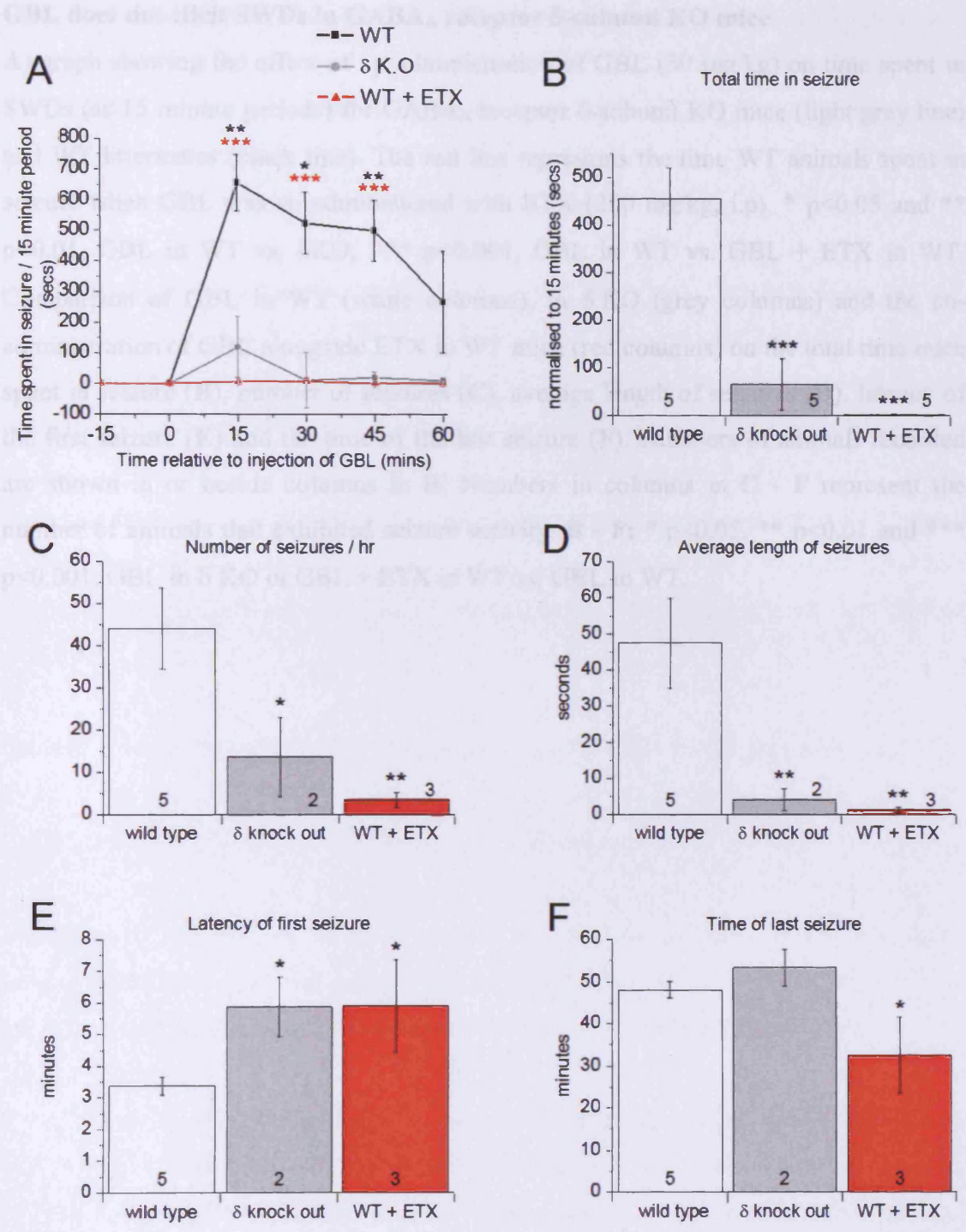


Figure 4.5

Figure 4.5

GBL does not elicit SWDs in GABA_A receptor δ -subunit KO mice

A) graph showing the effect of i.p administration of GBL (50 mg/kg) on time spent in SWDs (as 15 minute periods) for GABA_A receptor δ -subunit KO mice (light grey line) and WT littermates (black line). The red line represents the time WT animals spent in seizure when GBL was co-administered with ETX (200 mg/kg, i.p). * $p < 0.05$ and ** $p < 0.01$, GBL in WT vs. δ KO; *** $p < 0.001$, GBL in WT vs. GBL + ETX in WT. Comparison of GBL in WT (white columns), in δ KO (grey columns) and the co-administration of GBL alongside ETX in WT mice (red columns) on the total time mice spent in seizure (**B**), number of seizures (**C**), average length of seizures (**D**), latency of the first seizure (**E**) and the time of the last seizure (**F**). Numbers of animals recorded are shown in or beside columns in **B**. Numbers in columns in **C - F** represent the number of animals that exhibited seizure activity. **B - F**: * $p < 0.05$, ** $p < 0.01$ and *** $p < 0.001$, GBL in δ KO or GBL + ETX in WT vs. GBL in WT.

4.3.3 Blocking GABA uptake via GAT-1 in the VB provokes absence seizures

Using a well established pharmacological model of absence epilepsy I have shown that the presence of eGABA_ARs in the VB are critical to SWD generation and that selective activation of these receptors by intrathalamic injection of THIP in normal animals is sufficient to induce both the electrographic and behavioural correlates of absence seizures.

An important study carried out by Richards et al (1995) found that adult GAERS have an elevated level of GABA in the VB: ~50% higher than age-matched NEC. Aberrant GABA uptake by GAT-1 in GAERS has been identified in crude thalamic synaptosomes, suggesting it may be responsible for the elevated GABA levels in these epileptic animals (Sutch et al., 1999). Indeed, work carried out by Dr. David Cope in Professor Crunelli's laboratory concurrently to the experiments I completed for Chapter 3, identified that compromised GABA uptake via GAT-1 is responsible for the augmented tonic GABA_A current in TC neurons in the VB of GAERS *in vitro* (Cope et al., 2009).

Therefore, to directly test the role that thalamic GAT-1 plays in the generation of SWDs in behaving animals, I investigated the effect of reverse microdialysis of a selective GAT-1 inhibitor (NO711) in the VB of normal Wistar rats.

Simultaneous and bilateral EEG traces were recorded from 5 male Wistar rats under control conditions (i.e. no probes, 30 minutes), then following bilateral reverse microdialysis injection in the VB thalamus of either aCSF or NO 711 (200µM).

No SWDs were observed in the EEG under control conditions or in the presence of aCSF (Fig. 4.6 and Fig. 4.7A). However, bilateral intrathalamic administration of NO711 readily induced seizures in all 5 of the animals examined (Fig. 4.6 and Fig. 4.7A).

Paroxysmal activity on the EEG had a spike and wave appearance (see extended traces in Fig. 4.6), an abrupt start and finish and occurred at a mean frequency of 8.7 ± 1.3 Hz (range 5.05– 15.3 Hz, average of 10 SWDs taken from each of 5 rats). Importantly,

aCSF

L 

R 

NO 711

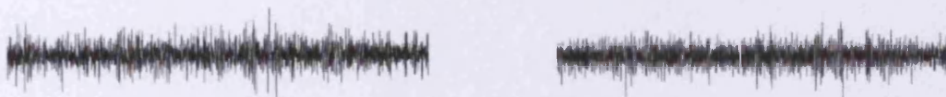
L 

R 

R 

200 μ V
1 s

NO 711 + ETX

L 

R 

200 μ V
5 s

Figure 4.6

Figure 4.6

Selective block of GAT-1 in the VB elicits absence seizures

Simultaneous, bilateral EEG traces (L = left, R = right hemisphere) showing representative EEG traces recorded from two different adult, male Wistar rats (left and right traces) following bilateral reverse microdialysis into the ventrobasal (VB) thalamus of aCSF (upper panels) and the selective GAT-1 blocker, NO711 (200 μ M; middle panels). Note the presence of SWDs in the EEG of both animals (see extended traces) upon microdialysis of NO711 into the VB. SWDs in the EEG occurred concomitantly with behavioural arrest typical of absence seizures (Video 2). The traces in the bottom panels show the block of NO711-induced SWDs by the i.p injection of ETX (100 mg/kg) administered at the beginning of the reverse microdialysis. Scale-bars at the bottom right corner apply to all traces except extended traces, where the relevant scales are indicated.

SWDs occurred concomitantly with the behavioural correlates of absence seizures i.e. cessation of movement, vibrissal twitching (Video 2).

On average, the 1st SWD appeared very soon after the start of the reverse microdialysis of NO711 (1.6 ± 0.5 minutes) and the time rats spent in seizure steadily increased until the 60 minute epoch (20 minute epoch = 241.8 ± 37.5 sec/20min; 40 minute epoch = 451.7 ± 148.6 sec/20min; 60 minute epoch = 521.5 ± 130.7 sec/20min) after which it reached a plateau (80 minute epoch = 419.2 ± 117.1 sec/20min; 100 minute epoch = 416.4 ± 118.4 sec/20min; 120 minute epoch = 398.9 ± 100.9 sec/20min).

A typical requirement of genetic and pharmacological models of absence seizures is that ETX blocks spontaneous or induced SWDs. Indeed, i.p. injection of ETX (100 mg/kg) at the start of NO711 administration, significantly reduced the total time the rats spent in SWDs (NO711 = 2449.5 ± 604.4 sec/2hrs; NO711 + ETX = 708.3 ± 512.5 sec/2hrs; $p < 0.001$) (Fig. 4.7B). ETX significantly reduced the number of seizures (NO711 = 352.8 ± 112.2 /2hrs; NO711 + ETX = 67.4 ± 33.2 /2hrs; $p < 0.05$) (Fig. 4.7C) and increased the latency of the 1st seizure (NO711 = 1.6 ± 0.5 minutes; NO711 + ETX = 13.8 ± 5.5 minutes; $p < 0.05$) (Fig. 4.7E), but had no effect on the length of the few remaining SWDs (NO711 = 14.9 ± 11.2 sec; NO711 + ETX = 5.4 ± 3.4 sec; $p > 0.05$) (Fig.4.7D).

From 80 minutes onwards, the time that animals spent in seizure with NO711 was no longer significantly different to NO711 administered alongside ETX (80 minute epoch NO711 + ETX = 151.6 ± 112.3 , $p > 0.05$ compared to NO711 alone at 80 minute epoch).

My data show that blockade of thalamic GAT-1 by NO711 induces ETX-sensitive SWDs in normal animals, probably by enhancing the tonic GABA_A current of TC neurons in the VB (Cope et al., 2009).

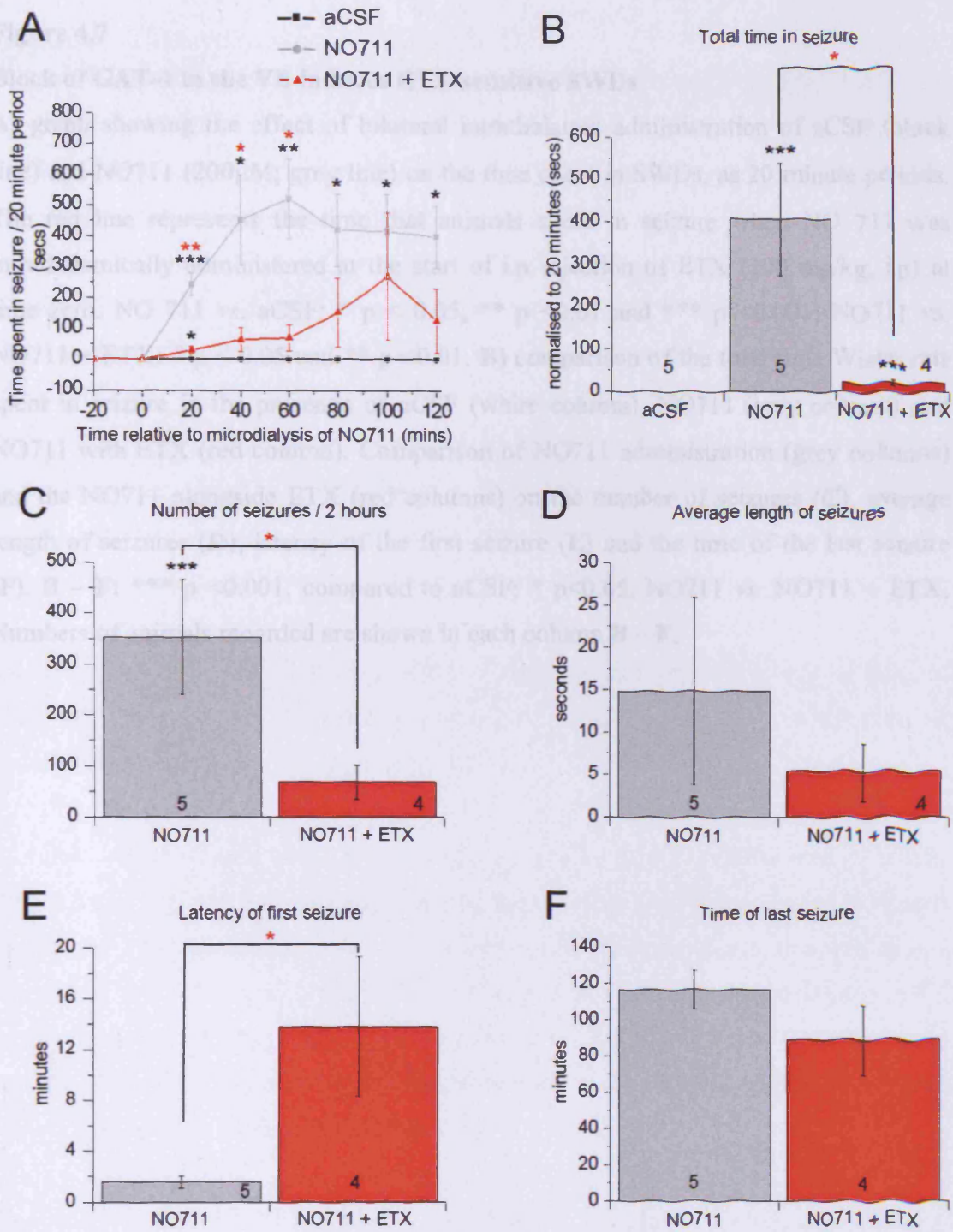


Figure 4.7

Figure 4.7

Block of GAT-1 in the VB induces ETX-sensitive SWDs

A) graph showing the effect of bilateral intrathalamic administration of aCSF (black line) and NO711 (200 μ M; grey line) on the time spent in SWDs, as 20 minute periods. The red line represents the time that animals spent in seizure when NO 711 was intrathalamically administered at the start of i.p injection of ETX (100 mg/kg, i.p) at time zero. NO 711 vs. aCSF: * $p < 0.05$, ** $p < 0.01$ and *** $p < 0.001$; NO711 vs. NO711 + ETX: * $p < 0.05$ and ** $p < 0.01$. **B)** comparison of the total time Wistar rats spent in seizure in the presence of aCSF (white column), NO711 (grey column) and NO711 with ETX (red column). Comparison of NO711 administration (grey columns) and the NO711 alongside ETX (red columns) on the number of seizures (**C**), average length of seizures (**D**), latency of the first seizure (**E**) and the time of the last seizure (**F**). **B – F**: *** $p < 0.001$, compared to aCSF; * $p < 0.05$, NO711 vs. NO711 + ETX. Numbers of animals recorded are shown in each column **B – F**.

4.3.4 GAT-1 KO mice exhibit spontaneous SWDs

Considering that blockade of thalamic GAT-1 by NO711 induces ETX-sensitive SWDs in normal Wistar rats, it could be predicted that GAT-1 KO mice would naturally exhibit SWDs. As the presence of spontaneous SWDs has not yet been determined, I investigated the EEG of adult, freely moving GAT-1 KO mice.

Simultaneous and bilateral EEG traces were recorded from 8 male and female GAT-1 KO mice and 8 control littermates (WTs). No SWDs were observed in WTs, however GAT-1 KO mice exhibited paroxysmal activity on the EEG (Fig. 4.8 and Fig. 4.9A) that had a spike-and-wave appearance (see extended traces in Fig. 4.8), abrupt onset and a mean frequency of 5.2 ± 0.1 Hz (range 4.7 – 5.7 Hz, $n = 10$ SWDs in each of eight mice). Importantly, these spontaneous SWDs occurred at the same time as behavioural correlates of absence seizures, such as behavioural arrest and vibrissal twitching.

On average GAT-1 KO mice spent 490.0 ± 38.75 seconds in SWD every 15 minutes (Fig. 4.9B) (1984.3 ± 225.9 sec/hr), 234 ± 20.2 SWD per hour (Fig. 4.9C) with an average length of 9.0 ± 1.2 seconds (Fig. 4.9D).

Systemic administration of ETX (200 mg/kg, i.p) abolished the appearance of SWDs (Fig. 4.8 and Fig. 4.9A), drastically reducing the time that GAT-1 mice spent in seizure to just 18.0 ± 7.5 seconds every 15 minutes ($p < 0.001$, compared to control conditions; Fig. 4.9B), just 70.1 ± 42.1 sec/hr ($p < 0.001$, compared to control conditions). ETX significantly lowered the number of seizures (13.0 ± 4.3 SWD/hr, $p < 0.001$ compared to control) (Fig. 4.9C) and reduced the length of GAT-1 KOs spontaneous SWDs to just 4.0 ± 1.6 seconds ($p < 0.05$) (Fig. 4.9D).

Therefore, it appears that GAT-1 KO mice exhibit ETX-sensitive spontaneous SWDs.

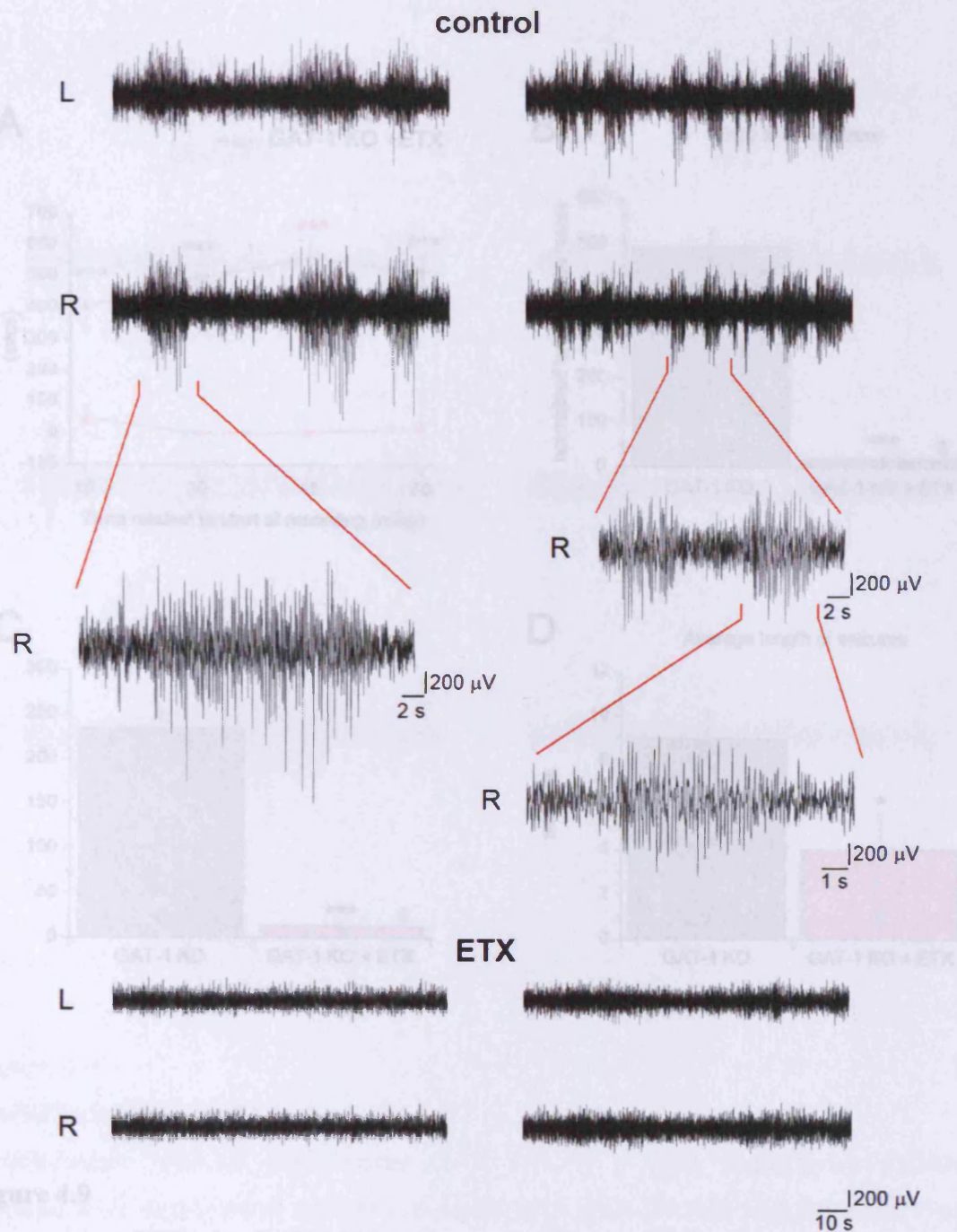


Figure 4.8

Spontaneous SWDs in GAT-1 KO mice are sensitive to ETX

A sample showing the time GAT-1 KO mice spent in SWDs under control conditions

and with an injection of ETX. Only mice that had control w. ETX. ***

GAT-1 knockout mice exhibit spontaneous absence seizures

Simultaneous, bilateral EEG traces (L = left, R = right hemisphere) showing representative examples of the EEG recorded from two different GAT-1 KO mice under control conditions (upper panels) and after systemic administration of ETX (200 mg/kg, i.p; lower panels). Scale-bars at the bottom right corner apply to all traces except the extended trace where the relevant scales are indicated.

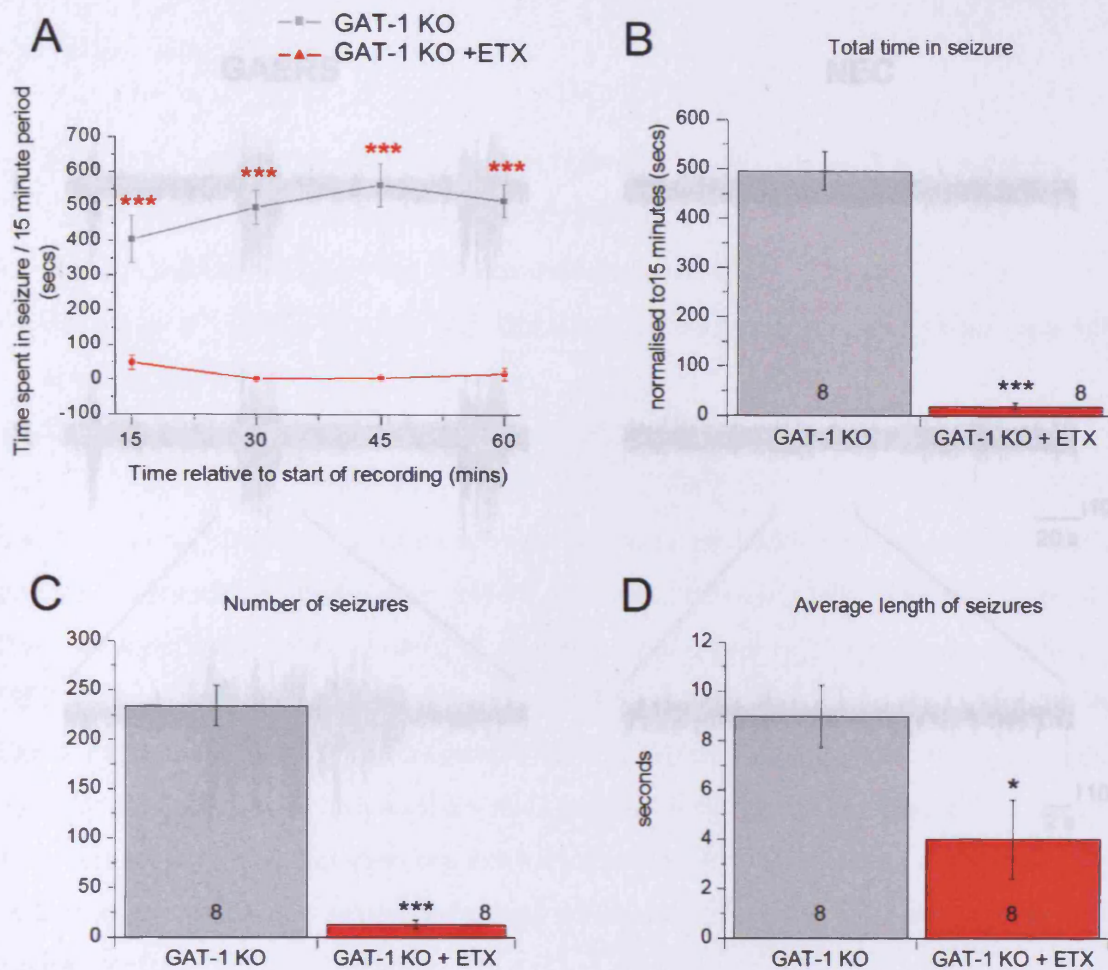


Figure 4.9

GAERS and NEC EEG

Simultaneous bilateral EEG traces (L/R = left/right hemisphere) showing

comparisons of the EEG recorded from wild GAERS and NEC mice. Note

Figure 4.9

Spontaneous SWDs in GAT-1 KO mice are sensitive to ETX

A) graph showing the time GAT-1 KO mice spent in SWDs under control conditions (grey line) and with i.p injection of ETX (200 mg/kg; red line). control vs. ETX: *** $p < 0.001$. Comparison of GAT-1 spontaneous seizures (grey columns) and the effect of ETX (red columns) on total time mice spent in seizure normalised to a 15 minute period (B), number of SWDs (C) and the average length of SWDs (D). Number of animals recorded is stated in columns. B – D: * $p < 0.05$, *** $p < 0.001$, GAT-1 KO vs. GAT-1 KO + ETX.

4.4 Discussion

The results of the present study are as follows:

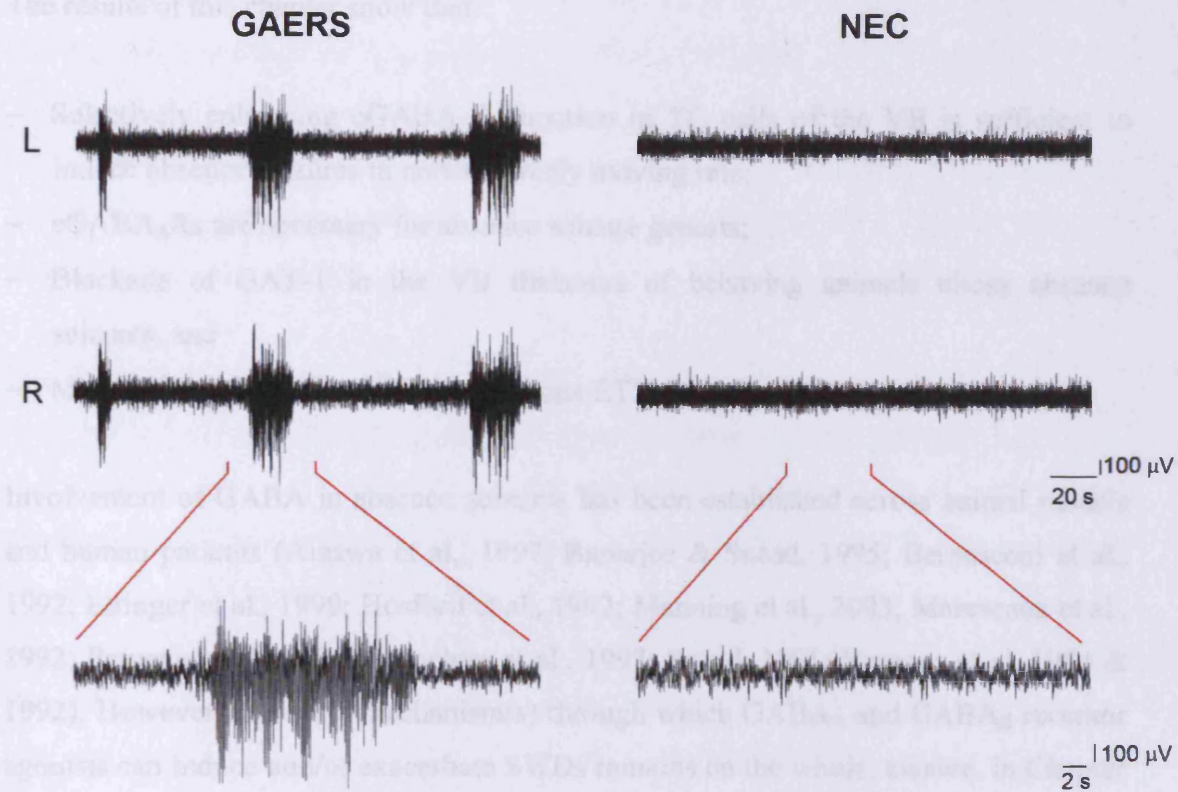


Figure 4.10

GAERS and NEC EEG

Simultaneous, bilateral EEG traces (L = left, R = right hemisphere) showing representative examples of the EEG recorded from adult GAERS and NEC rats. Note the presence of SWDs in GAERS and not in NEC. Relevant scale bars are indicated.

4.4.1 GABA_A RECEPTOR SENSITIVITY

Synaptic activation of GABA_A receptors in adult rats is a potential pharmacological model of absence seizures (Frye & Gloor, 1979; Vignier & Marescau, 1982) and that increase of short GABA_A current in TC neurons of the VB by acting directly at α GABA_ARs is being shown, without having an effect on the synaptic GABAergic events (Chapter 3.5.2.2), in agreement with Beffert et al (2005) and Na et al (2005).

4.4 Discussion

The results of this chapter show that:

- Selectively enhancing eGABA_AR function in TC cells of the VB is sufficient to induce absence seizures in normal, freely moving rats;
- eGABA_ARs are necessary for absence seizure genesis;
- Blockade of GAT-1 in the VB thalamus of behaving animals elicits absence seizures, and
- Mice lacking GAT-1 exhibit spontaneous ETX-sensitive absence seizures

Involvement of GABA in absence seizures has been established across animal models and human patients (Aizawa et al., 1997; Banerjee & Snead, 1995; Bernasconi et al., 1992; Ettinger et al., 1999; Hosford et al., 1992; Manning et al., 2003; Marescaux et al., 1992; Perucca et al., 1998; Schachter et al., 1997; Snead, 1991; Vergnes et al., 1984 & 1992). However, the exact mechanism(s) through which GABA_A and GABA_B receptor agonists can induce and/or exacerbate SWDs remains on the whole, elusive. In Chapter 3 I presented data that implicate augmented tonic GABA_A current in TC cells of the VB thalamus as a common cellular pathology across several genetic and pharmacological models *in vitro*.

Considering the importance of the thalamus in SWD genesis (Avanzini et al., 1992; Meeren et al., 2009; Pelligrini & Gloor, 1979; Vergnes & Marescaux, 1992) and that enhanced tonic GABA_A current is detected in TC cells of the VB across a range of absence models *in vitro*, it was important to investigate the function of eGABA_ARs and increased tonic GABA_A current under *in vivo* conditions.

4.4.1 eGABA_AR gain-of-function induces SWDs

Systemic administration of THIP in adult rats is a potential pharmacological model of absence seizures (Fariello & Golden, 1987). THIP caused a concentration-dependent increase of tonic GABA_A current in TC neurons of the VB by acting directly at eGABA_ARs in brain slices, whilst having no effect on the synaptic GABAergic events (Chapter 3.3.2.3), in agreement with Belelli et al (2005) and Jia et al (2005).

To ascertain the role of eGABA_AR gain-of-function in TC neurons of the VB in SWD genesis, I investigated the effect of direct administration of THIP into the thalamus of normal, behaving rats. The outcome of this bilateral intrathalamic THIP application was induction, and continued appearance, of absence seizures.

Application of 70µM and 100µM THIP robustly elicited both the electrographic and behavioural correlates of absence seizures, unlike 30µM THIP which failed to consistently produce SWDs.

It is likely that in order to induce a SWD, a sufficient number of neurons of the VB will have to exhibit sufficiently enhanced tonic GABA_A current. Whilst the spatial resolution of each probe has been established (Richards et al., 2003), brain tissue resistance to diffusion may result in a delay of THIP reaching all TC neurons in this 8mm³ space (Nicholson & Rice, 1986).

Supporting this notion is the disparity between the onset of SWDs in the presence of different concentrations of THIP. Animals spent more time in seizure for the 1st 40 minutes of recording and experienced a faster latency of SWDs with 100µM THIP than with 70µM.

Considering the low molecular weight of THIP, it is likely that the movement of perfused aCSF did not vary whether it contained 70µM or 100µM THIP. Instead, the variation of latency and time spent in seizure over the first 40 minutes of perfusion is perhaps a direct result of the extent to which tonic GABA_A current is enhanced by the two concentrations of THIP. Maybe SWDs are observed soon after perfusion of 100µM THIP as it augments tonic current in those neurons close to the probe surface to an extent sufficient to cause seizures. As THIP increases tonic GABA_A current in a concentration-dependent manner (Chapter 3.3.2.3), tonic GABA_A current would be increased to a lesser degree in the presence of 70µM THIP. Thus it is possible that SWDs are detected after 70µM THIP had diffused through more VB tissue and affected a greater number of TC cells to generate sufficient augmentation of tonic GABA_A current for the resulting SWDs. The time that it took for the aCSF to diffuse through the

tissue and affect this critical number of neurons could therefore explain the delayed appearance of SWDs.

When compared to the THIP-induced increases observed in TC neurons *in vitro* (Chapter 3.3.2.3), it is somewhat surprising that 3 μ M THIP, capable of inducing a 458.7 ± 29.9 pA tonic GABA_A current, is not sufficient for SWDs *in vivo*. The relative ease in which diffusion will occur through a brain slice compared to the resistance that intact brain tissue hinders aCSF movement (Nicholson & Rice, 1986) may provide an explanation to the lack of SWDs with intrathalamic administration of 30 μ M THIP. 10 μ M THIP induced a 725.7 ± 82.2 pA tonic GABA_A current i.e. a 502.4 ± 30.9 % increase *in vitro*. The whole-cell patch clamp technique is an invaluable tool when examining electrophysiological properties of individual neurons, and whilst it is advantageous in advancing our understanding of more minute changes in cellular physiology, isolating investigation to just one cell may magnify any observed phenomenon. Therefore a 725.68 ± 82.23 pA tonic GABA_A current recorded from individual neurons in brain slices may not be an accurate reflection of the size of tonic current that occurs in the cells throughout 8mm³ of dense brain tissue. It is possible that for this reason 30 μ M (~3 μ M actual) THIP was not able to induce SWDs in behaving animals. Bidirectional interaction between cortex and thalamus alongside cortical initiation (Avanzini et al., 1992; Meeren et al., 2002 & 2009; Pinault et al., 2003; Polack et al., 2007; Vergnes & Marescaux, 1992) should also be taken into consideration when discussing induction of absence seizures via intrathalamic drug administration. Thus may be possible that to generate SWDs in animals without an absence seizure phenotype i.e. lacking a cortical “focus”, greater THIP-induced tonic GABA_A inhibition of TC neurons than that observed in genetic models such as GAERS, is necessary for the VB thalamus to instigate the seizures.

Another interesting observation is that the time that animals spent in seizure in the presence of both concentrations of THIP did not reach a plateau within 2 hours of recording. The continued increase of time in seizure across 2 hours may represent slow diffusion of THIP i.e. THIP had not reached all neurons within this 8mm³ volume by the end of the recording. Alternatively, it is possible that THIP did reach all of the cells in the VB area within 2 hours and SWD time increased through some other

mechanism(s). For instance, an accumulation of THIP activating more eGABA_ARs, or it is a reflection of the non-desensitising property of the eGABA_ARs. To answer this question it would be interesting to extend the recording period. In half of animals SWDs appeared to get longer in the 2nd hour of recording and this may also be due to accumulation and/or diffusion of THIP.

The fact that only half of the rats showed lengthened seizures may be a result of small differences in probe localisation. It is generally assumed that SWDs develop in the same neuronal circuits that normally generate sleep spindles (Avanzini et al., 2000), however it has been shown that different intrathalamic subcircuits are involved in the two different types of oscillations (Meeren et al., 2009). Specifically, lesions that left the rostral pole of the RTN and part of the TCR nuclei intact in WAG/Rij rats resulted in an ipsilateral suppression of sleep spindles, but a large increase of bilateral SWDs (Meeren et al., 2009). So, if the rostral pole of the NRT is important to SWD genesis (Meeren et al., 2009), it seems feasible to suggest that some slight disparity between probe coordinates could result in a less comprehensive THIP dialysis through the rostral VB, thus preventing the lengthening of SWDs. However no obvious discrepancy was noted on looking at the brain sections of each rat.

The number of seizures that occurred over 2 hours of recording was almost identical in the presence of both 70µM and 100µM THIP. Considering this, alongside the fact that animals with 100µM exhibited seizures much sooner and for more time within the first 40 minutes of perfusion than with 70µM, it could be expected that 100µM-induced SWDs would be longer than those seizures exhibited by 70µM THIP. However, no statistical difference in seizure length was calculated between THIP concentrations. Variability of the SWDs exhibited by animals in both experimental conditions meant that half had longer seizures in the 2nd hour of the experiment. It is likely that this variation has masked any clear disparities between overall seizure length and the two concentrations of THIP. Increasing the number of animals recorded for each concentration of THIP would perhaps ascertain any differences in SWD length.

Ethosuximide (ETX) has a 70-80% success rate in removing absences in patients and thus is a drug of choice for a reliable block of SWDs in animal models (Richens et al.,

1995; Schachter et al., 1997). In order to clarify the paroxysmal activity elicited by THIP as characteristic absence seizures, the animals were treated with an i.p. injection of ETX at the same time as reverse microdialysis began. As expected, ETX blocked THIP-induced SWDs in all animals tested and thus by confirming the intrathalamic THIP-induced SWD analogy to human absences, this data strengthens the case for the THIP model of absence seizures.

Overall, since THIP is used at concentrations selective for the δ -subunit eGABA_ARs (Krook-Magnuson et al., 2008; Storustovu & Ebert, 2006), my findings show that enhanced eGABA_AR function in TC neurons of the VB can bring about the appearance of ETX-sensitive absence seizures in normal, freely moving rats.

4.4.2 eGABA_ARs are required for the appearance of absence seizures

I have already shown that eGABA_AR gain-of-function in TC neurons of the VB is sufficient to elicit SWDs *in vivo*; therefore I wanted to further elucidate the importance of eGABA_ARs in SWD generation.

Parenteral injection of GHB, or its pro-drug GBL, in mice and rats produces a well characterised, reliable animal mode of absence seizures that has specific ontogeny and a similar pharmacological profile to those of human patients (Godshalk et al., 1977; Snead, 1978a, b; Snead, 1988). Whereas i.p. injection of GBL readily elicited classic ETX-sensitive SWDs in wildtype littermates as expected (Aizawa et al., 1997), GBL administered to GABA_AR δ -subunit KO mice failed to induce seizures. This finding has great implications as these data show that the presence of eGABA_ARs is critical to SWD generation i.e. without δ -subunit containing GABA_ARs GBL cannot elicit absence seizures.

Not only does this data clearly demonstrate the necessity of eGABA_ARs and thus tonic GABA_A current to SWD genesis, but also strengthens my proposal of the existence of a postsynaptic GABA_BR-eGABA_AR link. In Chapter 3 I showed that GHB acts at postsynaptic GABA_BRs to enhance tonic GABA_A current in TC neurons *in vitro*.

GABA_B receptor agonists exacerbate (Bernasconi et al., 1992; Lui et al., 1992; Marescaux et al., 1992a & d; Vergnes et al., 1984) and antagonists block SWDs (Lui et

al., 1991b; Marescaux et al., 1992a; Snead, 1996; Vergnes et al., 1984), thus GABA_B receptor function plays an important role in seizure generation. Considering that enhanced tonic GABA_A current in is a common cellular pathology across genetic and pharmacological models (Chapter 3) and that increased eGABA_AR function in the VB of normal animals is sufficient to induce SWDs (4.4.2), it is possible that GHB mediates SWD induction by enhancing tonic GABA_A current in addition to its already established inhibitory activity at pre- (Emri et al., 1996b; Gervasi et al., 2003) and postsynaptic (Schweitzer et al., 2004) GABA_BRs.

Overall, these data provide further evidence that eGABA_AR presence is critical to absence seizure generation and support Chapter 3 findings that suggest a postsynaptic GABA_BR – eGABA_AR link in TC neurons of the VB.

4.4.3 Block of GABA uptake in the VB results in SWDs

It is now clear that augmented tonic GABA_A current is a coherent cellular pathology across models of absence epilepsy. A question then arises: what is the mechanism that underlies augmented tonic GABA_A current in absence epilepsy?

In Chapter 3, I discussed the possible candidates responsible for enhanced tonic GABA_A current in the VB and concluded it was most likely due to abnormal GABA reuptake. Cope et al (2009) carried out *in vitro* experiments to test the contribution of GABA reuptake by astrocytic GABA transporters (GAT-1 and GAT-3) on tonic current in GAERS and NEC *in vitro*. Block of GAT-1 or GAT-3 augmented tonic current in NEC. However, only block of GAT-3 and not GAT-1 increased tonic inhibition further in GAERS and Stg. These data imply that GABA reuptake into surrounding astrocytes via GAT-1 in the VB is compromised, resulting in high levels of ambient GABA and therefore augmented tonic GABA_A current in GAERS and Stg *in vitro* (Cope et al., 2009).

In light of the fact that aberrant GAT-1 activity underlies enhanced tonic GABA_A current in TC neurons in the VB of GAERS and Stg (Cope et al., 2009), I tested the role of thalamic GAT-1 in SWD generation *in vivo*. In support of the *in vitro* findings, my data demonstrate that block of GABA reuptake via GAT-1 by NO711 in the VB induces ETX-sensitive SWDs in normal, freely moving rats.

NO711-induced SWDs were dependent on blocking the reuptake of GABA that is naturally released over time by surrounding neurons and glia. Therefore, increase of tonic GABA_A current in cells of the VB was likely to take time while ambient GABA levels accumulated in the extracellular space. Indeed it took forty minutes for the time animals spent in seizure to reach near-maximum levels, from this point onwards maintaining a plateau. Additional to a gradual build-up of ambient GABA, it is possible that the resistance that dense brain tissue inflicts on aCSF diffusion delayed the full effect of NO711 (Sections 4.4.1 & 4.4.2), thus obstructing NO711 movement to all astrocytes. Only after forty minutes were all GAT-1 blocked and ambient GABA levels high enough to adequately increase the tonic GABA_A current in a sufficient number of TC cells of the VB to result in maximal SWD induction.

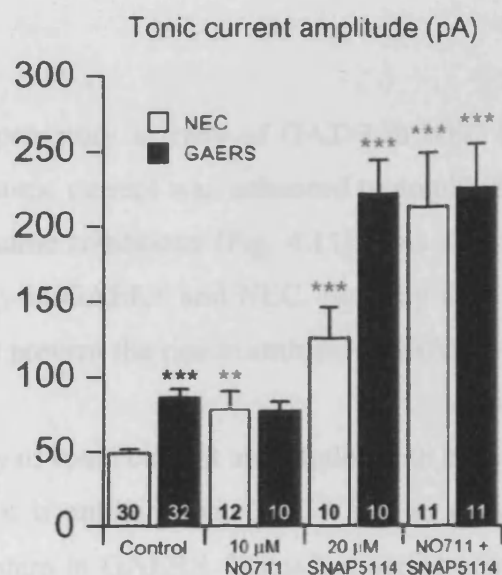


Figure 4.11

Tonic GABA_A current amplitudes in TC neurons of the VB of GAERS and NEC in the presence of GAT blockers

GAERS vs. NEC: *** P <0.001; Drug vs. no drug: ** p <0.01, *** p <0.001. Data presented as mean ± SEM. NO711 is GAT-1 blocker, SNAP5114 is a GAT-3 blocker. Figure taken from Cope et al., 2009.

Critical experiments revealed that whilst individually blocking GAT-1 (NO711) and GAT-3 (SNAP5114) increased tonic GABA_A current in NEC *in vitro* (Fig. 4.11), in

particular block of GAT-1 in NEC resulting in tonic current amplitude similar to those seen in GAERS; concurrent block of GAT-1 and GAT-3 enhanced tonic inhibition to a greater extent than summing the effect of applying NO711 and SNAP 5114 alone (Fig. 4.11) (Cope et al., 2009). This suggested that in NEC animals, block of GAT-1 in the VB causes a compensatory increase in GABA reuptake by GAT-3, and vice versa (Cope et al., 2009). In epileptic animals, application of NO711 had no effect on tonic current, but block of GAT-3 caused a large increase (Fig. 4.11) (Cope et al., 2009). When both NO711 and SNAP5114 were co-applied to thalamic brain slices of GAERS, the tonic GABA_A current was increased but the increase was similar to that observed after block of GAT-3 alone in GAERS and to the concurrent block of GAT-1 and GAT-3 in NEC animals. Therefore, irregular GABA reuptake via GAT-1 is responsible for the enhanced tonic GABA_A current observed in GAERS, and it seems that the compensatory increase in uptake by GAT-1 after blocking GAT-3 is lost in GAERS (Cope et al., 2009).

Removing the compensatory activity of GAT-3 in NEC by concurrent block of both GAT-1 and -3, the tonic current was enhanced to amplitude similar to that observed in GAERS under the same conditions (Fig. 4.11). This suggests that GAT-3 transporters perform equivalently in GAERS and NEC. So, why does GAT-3 not fully counteract aberrant GAT-1 and prevent the rise in ambient GABA?

Due to the similarity of tonic current amplitudes with concurrent block of GATs across GAERS and NEC, it is unlikely that GAT-3 acts as an additional abnormality in the GABA reuptake system in GAERS. Instead, it seems possible that the ability of both GABA transporters to remove GABA from extracellular space is restricted somehow. Cope et al (2009) found that block of GAT-3 in NEC enhanced tonic current and that GAT-1 compensated for this block. However the tonic GABA_A current did not return to normal amplitude through this GAT-1 compensation, so it is clear that GAT-1 failed to fully compensate for GAT-3 block in normal animals. Therefore it appears that both transporters have a maximum physiological limit to which they can remove GABA from extracellular space. Perhaps metabolism of GABA inside the astrocytes acts as a limiting factor to the amount of neurotransmitter the GAT-1 and -3 can take in over time. Hence, aberrant GAT-1 is responsible for the high levels of ambient GABA and thus enhanced tonic current and associated SWDs in GAERS (Cope et al., 2009);

however the compensatory increase in uptake of GABA via GAT-3 is not lost in GAERS, instead is restricted and thus could be argued that such “capped” GAT-3 function also contributes to absence seizures by maintaining rather than reducing the high ambient GABA caused by atypical GAT-1.

Whilst I have highlighted that the compensatory activity of GAT-3 is not sufficient to counteract the appearance of SWDs in GAERS, I also stated that this was likely to be a physiological limitation rather than a pathological manifestation. Therefore it is likely that comparable GAT-3 compensation would have occurred in my experiments using normal rats.

After peaking at forty minutes, the time animals spent in seizure declined slightly and then maintained a plateau. Considering at forty minutes the aCSF containing NO711 had presumably reached all of the astrocytes in the 8mm³ tissue, the plateau may represent the compensatory activity of GAT-3 i.e. GAT-3 acting sufficiently to maintain, rather than reduce the ambient level of GABA.

In agreement with data that there is a greater abundance of GAT-3 in the thalamus (De Biasi et al., 1998), application of GAT-3 blocker SNAP5114 to brain slices of NEC, increased the tonic current to a greater extent than NO711 (Cope et al., 2009). Therefore it would be interesting to investigate whether intrathalamic application of SNAP5114 in normal Wistar animals would result in more SWDs, acting accordingly with a greater tonic GABA_A current.

Another interesting observation was that from 80 minutes onwards, the time that animals spent in seizure on receiving simultaneous i.p injection of ETX and intrathalamic NO711 was not significantly different to that recorded for NO711 alone. This suggests that the effect of ETX diminished after the first hour of recording. As this was not observed under THIP co-application with ETX, this finding may have offered some clue to a yet unidentified mechanism by which ETX exhibits its anti-absence role e.g. stimulating GABA uptake. However, because ETX had no effect on tonic GABA_A current amplitude when applied to slices of GAERS, this notion is not likely. Instead, such diminished effects of ETX may be due to faster metabolism of ETX in these

animals, not revealed in animals when co-administered with THIP due to differences in drug affinities.

Since reverse microdialysis has the advantage of serving as both an administration and sampling technique, it would be interesting to ascertain levels of ETX in the output perfusate and establish if ETX is metabolised. Additionally, examination of the extracellular level of GABA in the output perfusate throughout the perfusion of NO711 would permit analysis of exact levels of GABA caused by block of reuptake, and thus advance knowledge of the degree to which tonic GABA_A current is enhanced *in vivo*.

Overall, I have shown that aberrant astrocytic GAT-1 identified *in vitro* is critical to absence seizure genesis *in vivo*. In addition to providing a potential therapeutic target, administration of NO711 may represent a novel model of absence seizures. However, further experiments are required to establish whether the physiological effects of NO711 in animals accurately reflect the characteristics of human absences.

To become a valid animal model of absence seizures it would be important to first ascertain whether NO711 administered via more accessible means e.g. intraperitoneally, consistently induced both the electrographic and behavioural correlates of SWDs in a dose-dependent, quantifiable and reproducible manner (see Chapter 1.2). Although an aspect of the pharmacological profile has been revealed through the ETX-mediated block of NO711-induced SWDs in my experiments, further characterisation is required through examining the effect of GABAergic and antiabsence drugs alongside i.p. NO711 application. Additional lines of investigation that would also strengthen NO711-induced SWDs as a valid absence model would involve: testing the effect of NO711 across different species i.e. rat, mouse, cat and monkey, and establishing whether a developmental profile exists.

4.4.4 Spontaneous absence seizures observed in GAT-1 KO mice

Considering the fact that aberrant GAT-1 underlies enhanced tonic GABA current in TC neurons of the VB in GAERS *in vitro* (Cope et al., 2009) and that block of GAT-1 in normal animals can induce SWDs after intrathalamic administration *in vivo* (Section 4.4.4), one would expect GAT-1 KO mice to spontaneously exhibit SWDs.

No study had tested the appearance of absence seizures, yet GAT-1 knockout mice show an enhanced tonic GABA_A current in TC neurons of the VB (Cope et al., 2009). As expected, I found that these mice not only exhibit SWDs naturally, but the seizures are sensitive to ETX. These findings mean that GAT-1 KO mice may represent, after further characterisation, another genetic model of absence seizures.

Considering suggestions made in Section 4.4.4 regarding the compensatory action of GAT-3, it would be interesting to establish the extent to which GAT-3 functions in these mice. For instance, examining the tonic current of TC cells of the VB in GAT-1 KO brain slices in the presence of NO711 and/or SNAP5114 then comparing these results with that of wildtype mice would establish the extent to which GAT-3 compensates for loss of GAT-1.

4.4.5 Parameters of SWDs vary across strains and pharmacological induction

Comparisons between the properties of the SWDs recorded in all of the experimental conditions for this chapter to ascertain any differences between pharmacological agents used to prompt seizures or strains would have been very interesting. However, the use of different species and the lack of a full dose-response for GBL, THIP and NO711 would make such comparisons complex and difficult to interpret. Furthermore, the experimental protocol used for mice and rats differed in length of recording which would make comparing “time in SWD” and the number of SWDs particularly difficult considering differences in SWD ontogeny across the range of pharmacological agents used.

4.5 Conclusion

The findings presented in this Chapter not only show that selective enhancement of eGABA_ARs function in the VB is sufficient to induce SWDs in normal rats *in vivo*, but also demonstrate that eGABA_ARs are necessary for SWD generation. Moreover, the inability of GBL to induce SWDs in eGABA_AR KO mice supports the proposed postsynaptic GABA_BR – eGABA_AR link detected *in vitro* (Chapter 3).

In addition, my data confirm that abnormal GABA reuptake in the VB via GAT-1, identified in brain slices of GAERS (Cope et al., 2009), is sufficient to induce SWDs in normal animals and underlies spontaneous seizures observed in GAT-1 KO mice.

Furthermore, my findings also reveal two potential new models of absence epilepsy and strengthen the partially established THIP model. Both the spontaneous SWDs observed in GAT-1 KO mice and the seizures induced by intrathalamic administration of NO711 could provide another opportunity for the investigation of absence seizures, though more experiments and further characterisation is required to establish full validity as models.

Taking into consideration the *in vitro* identification (Chapter 3) and the subsequent critical *in vivo* verification presented in this Chapter, I can conclude that enhanced tonic GABA_A current in TC neurons of the VB is critical to absence epilepsy. Together these novel data provide evidence for the first cohesive pathological cellular phenomenon for absence seizures across animal models. These also highlight the potential therapeutic targets in GABA reuptake and eGABA_ARs for the treatment of this type of epilepsy.

Chapter 5

Postsynaptic GABA_B receptors facilitate eGABA_AR function

5.1 Introduction

GABA can act at ionotropic GABA_ARs or metabotropic GABA_BRs, and the movement of ions caused by such receptor activation is well characterised (see Chapter 1.4).

Data from Chapter 3 suggested that the GHB acted at postsynaptic GABA_BRs to augment eGABA_AR-mediated tonic current in TC neurons. Furthermore, failure of GBL to induce SWDs in GABA_AR δ -subunit knockout mice supports the hypothesis that enhanced tonic GABA_A inhibition in the VB, a necessity to absence seizure generation (Cope et al., 2009), could be a result of some postsynaptic GABA_BR modulation of eGABA_AR function.

Immunolabelling techniques in monkey and rat have revealed that postsynaptic GABA_BRs are located at peri- or extrasynaptic sites in the thalamus (Kulik et al., 2002; Villalba et al., 2006), and this co-localisation with eGABA_ARs raises the possibility of interaction between the two receptor-types. Moreover, GABA_A and GABA_BRs have both been implicated in alternative receptor-receptor crosstalk within cells (Deng et al., 2009; Hirono et al., 2002; Huidobro-Toro et al., 1996). Taken together, such a relationship between eGABA_A and GABA_BRs appears to be a feasible suggestion.

In order to evaluate the role of postsynaptic GABA_BRs on tonic GABA_A current I have tested the specific GABA_BR agonist, baclofen. My data are the first electrophysiological evidence to clearly demonstrate a dose-dependent postsynaptic GABA_BR modulation of eGABA_AR activity in several brain areas that is independent of GIRK channel activity.

5.2 Methods

Whole cell patch clamp recordings were performed using both short (see 2.1.5.1 and 2.1.7.1.1) and long protocols (see 2.1.5.2 and 2.1.7.1.2) in brain slices containing granule cells of the dentate gyrus (DGGC) and cerebellum (CGC) and TC neurons of the VB from Wistar rats, as described in Chapter 2.1.

5.3 Results

5.3.1 Baclofen dose-dependently enhances tonic GABA_A current

In the presence of 500nM TTX, tonic GABA_A current amplitude from TC neurons in slices containing the somatosensory VB thalamus of P21–26 Wistar rats was measured both before and after 10μM baclofen was administered via the perfusion system (Fig. 5.1) and in the continuous presence of 0.3–10μM baclofen (Fig. 5.2). Baclofen dose-dependently increased tonic current amplitude (0.3μM baclofen: 62.7 ± 7.6 pA, $p > 0.05$; 1μM baclofen: 78.1 ± 4.2 pA, $p < 0.05$; 3μM baclofen: 95.1 ± 7.3 pA, $p < 0.01$; 10μM baclofen: 125.2 ± 12.0 pA, $p < 0.001$; 30μM baclofen: 135.5 ± 14.5 pA, $p < 0.001$) compared to control (62.1 ± 6.2 pA), under the short experimental protocol (Fig. 5.2A + C). The EC₅₀ of baclofen effect, calculated from the dose-response curve, was 3.1μM (Fig. 5.2B). Baclofen also increased tonic current amplitude under the long experimental protocol (control: 43.7 ± 8.9 pA; 10μM baclofen: 106.4 ± 6.8 pA, $p < 0.001$) (Fig. 5.1A+B). Baclofen-induced increase of tonic current amplitude occurred independently of whole-cell capacitance values at all doses ($p < 0.05$, $p < 0.01$ and $p < 0.001$) (Fig. 5.1C and 5.2C) except for 0.3μM and 1μM baclofen ($p > 0.05$) (Fig. 5.2C).

Comparison of mIPSC parameters revealed a significantly reduced frequency and total current in the presence of all concentrations of baclofen except 0.3μM baclofen (Tables 5.1 and 5.2), with all other parameters remaining unaffected.

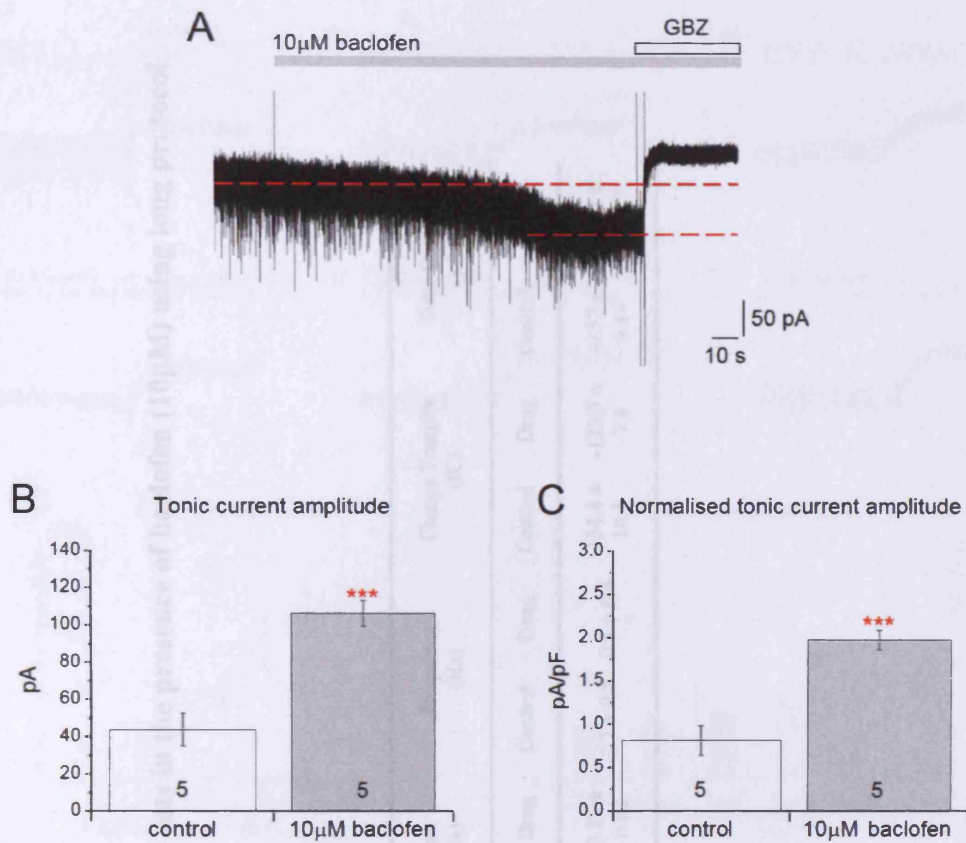


Figure 5.1

Baclofen enhances tonic GABA_A current in Wistar TC neurons of the VB

A) representative current trace recorded from a Wistar rat TC neuron showing the effect of acute perfusion of 10µM baclofen (grey bar) on baseline current. Focal application of GBZ (100µM; white bars) revealed an outward shift in baseline current, indicating presence of tonic current. Note how baclofen induced an inward shift in baseline current when administered to the brain slice. Red dotted lines represent the baseline current under control conditions and in the presence of baclofen. **B)** comparison of the effect of baclofen (10µM) on the tonic current amplitude to the paired control. **C)** comparison of the tonic current amplitudes normalised to whole-cell capacitance in the presence of 10µM baclofen to the paired control. **B + C: ***** $p < 0.001$. Number of recorded neurons are indicated at the base of each column in **B + C**. Scale bars are indicated. All recordings were done in the presence of TTX (500nM).

Table 5.1

Comparison of mIPSC parameters in TC neurons of Wistar rats in the presence of baclofen (10 μ M) using long protocol

	n	<i>mIPSC parameter</i>											
		Peak amplitude (pA)		Weighted Decay (mS)		Rise Time (10-90%)		Frequency (Hz)		Charge Transfer (fC)		Total Current (pA)	
		Control	Drug	Control	Drug	Control	Drug	Control	Drug	Control	Drug	Control	Drug
10 μ M baclofen	5	-43.9 \pm 3.8	-41.3 \pm 4.4	2.6 \pm 0.1	2.8 \pm 0.2	0.31 \pm 0.02	0.28 \pm 0.02	2.7 \pm 0.8	0.8 \pm 0.4 *	-134.4 \pm 10.1	-123.9 \pm 7.6	-0.37 \pm 0.14	-0.11 \pm 0.06 *

* p < 0.05 compared to control; n = number of cells recorded

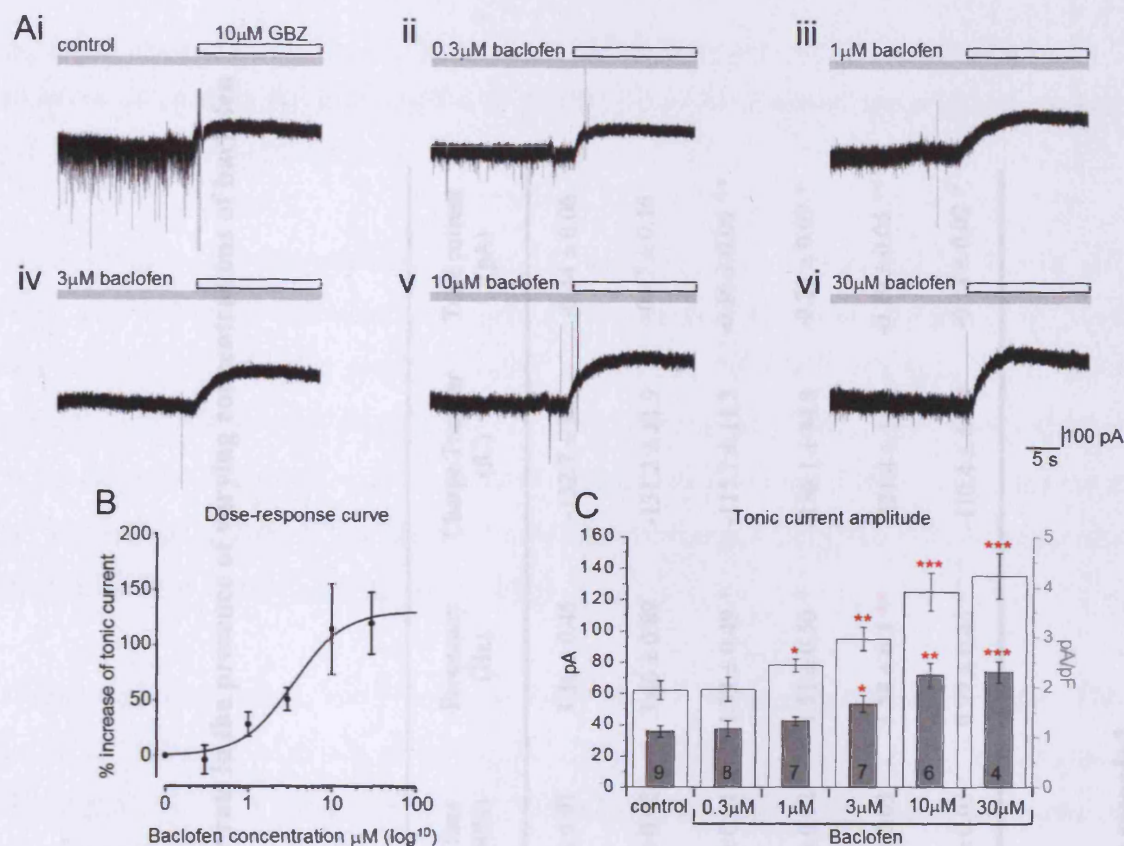


Figure 5.2

Baclofen dose-dependently increases tonic GABA_A current

A) representative current traces from six different Wistar rat TC neurons showing the effects of 0.3µM baclofen (**ii**; grey bar), 1µM baclofen (**iii**; grey bar), 3 µM baclofen (**iv**; grey bar), 10µM baclofen (**v**; grey bar) and 30µM baclofen (**vi**; grey bar). **Ai** is a representative current trace of a neuron under control conditions. Brain slices were in the continuous presence of varying concentrations of baclofen (short protocol, see Chapter 2.1.5.1). Focal application of GBZ (100µM; white bars) revealed an outward shift in baseline current, indicating the presence of tonic current. **B)** dose-response curve of baclofen on tonic GABA_A current amplitude. **C)** comparison of the effects of the various concentrations of baclofen on the tonic current amplitude (white bars; left Y-axis) and tonic current amplitude normalised to whole-cell capacitance (grey bars; right Y-axis). * $p < 0.05$, ** $p < 0.01$, *** $p < 0.001$, compared to controls. Numbers of recorded neurons are indicated at the base of each column in C. Scale bars are indicated. All recordings were done in the presence of TTX (500nM).

Table 5.2

Comparison of mIPSC parameters in TC neurons of Wistar rats in the presence of varying concentrations of baclofen

<i>mIPSC parameter</i>							
	n	Peak amplitude (pA)	Weighted Decay (mS)	Rise time (10-90%)	Frequency (Hz)	Charge Transfer (fC)	Total current (pA)
Control	9	-44.0 ± 0.8	2.4 ± 0.14	0.32 ± 0.01	3.36 ± 0.45	-132.7 ± 3.8	-0.44 ± 0.06
0.3µM baclofen	8	-42.5 ± 2.5	2.5 ± 0.17	0.31 ± 0.02	3.46 ± 0.89	-131.2 ± 11.9	-0.47 ± 0.16
1µM baclofen	7	-43.5 ± 1.8	2.5 ± 0.21	0.29 ± 0.01	1.33 ± 0.49 *	-115.7 ± 11.7	-0.16 ± 0.06 **
3µM baclofen	7	-43.5 ± 1.9	2.5 ± 0.27	0.29 ± 0.02	1.51 ± 0.50 *	-136.1 ± 34.8	-0.21 ± 0.09 *
10µM baclofen	6	-44.7 ± 1.3	2.3 ± 0.17	0.29 ± 0.03	1.58 ± 0.3 **	-121.4 ± 11.4	-0.19 ± 0.05 **
30µM baclofen	4	-44.8 ± 6.2	2.2 ± 0.21	0.27 ± 0.03	0.99 ± 0.43 *	-110.4 ± 6.8 *	-0.14 ± 0.02 *

* p < 0.05, ** p < 0.01 compared to control; n = number of cells recorded

5.3.2 Postsynaptic GABA_BRs modulate eGABA_AR under control conditions

In order to confirm baclofen action at GABA_BRs, I have tested the effect of various GABA_B antagonists on tonic GABA_A current.

Tonic GABA_A current amplitude from TC neurons of the VB in P21-26 Wistar rats were recorded in the continued presence of the specific GABA_B antagonists CGP55845 and SCH50911, and the putative GHB antagonist, NCS382. All antagonists were compared to control and 10μM baclofen tonic current amplitudes and were recorded either alone or co-applied with baclofen (10μM). Data in Figure 5.3B + C are expressed as “percentage of control” because the results were merged from two different data sets that had different controls (Fig. 5.3Ai & Bi).

10μM baclofen elicited, on average, a 220.5 ± 8.7 % increase in tonic current. The action of 10μM baclofen was abolished by 10μM CGP55845, 10μM SCH50911 but not by the putative GHB antagonist 1mM NCS382 (213.2 ± 8.0 %) ($p < 0.001$ compared to control and $p > 0.05$ compared to 10μM baclofen) (Fig. 5.3C). Not only was the effect of 10μM baclofen fully antagonised, but co-application of baclofen with the GABA_BR antagonists significantly lowered tonic current amplitude below control: 10μM CGP55845 with 10μM baclofen = 66.5 ± 9.7 % of control, $p < 0.001$; 10μM SCH50911 with 10μM baclofen = 69.0 ± 12.9 % of control, $p < 0.001$ (Fig. 5.3Ai, ii + iii, 5.3Bi, ii + iii & 5.3C). Interestingly, both 10μM CGP55845 (66.9 ± 5.7 % of control, $p < 0.01$) and 10μM SCH50911 (50.1 ± 18.1 % of control, $p < 0.01$) alone decreased tonic current to below control levels; whereas 1mM NCS382 had no effect (109.6 ± 9.2 % of control, $p > 0.05$) (Fig. 5.3Ai + iv, 5.3Bi + iv, 5.3C). All of these effects occurred independently of whole-cell capacitance (Fig. 5.3D).

Comparison of the mIPSC data revealed no difference in peak amplitude, weighted decay or rise-time (10-90%) between all drugs tested and their respective controls (Table 5.3). However all antagonists, applied alone or in conjunction with 10μM baclofen reversed the 10μM baclofen-induced frequency and total current reduction. When 10μM SCH50911 was present alone it significantly increased mIPSC frequency above control level (Table 5.3).

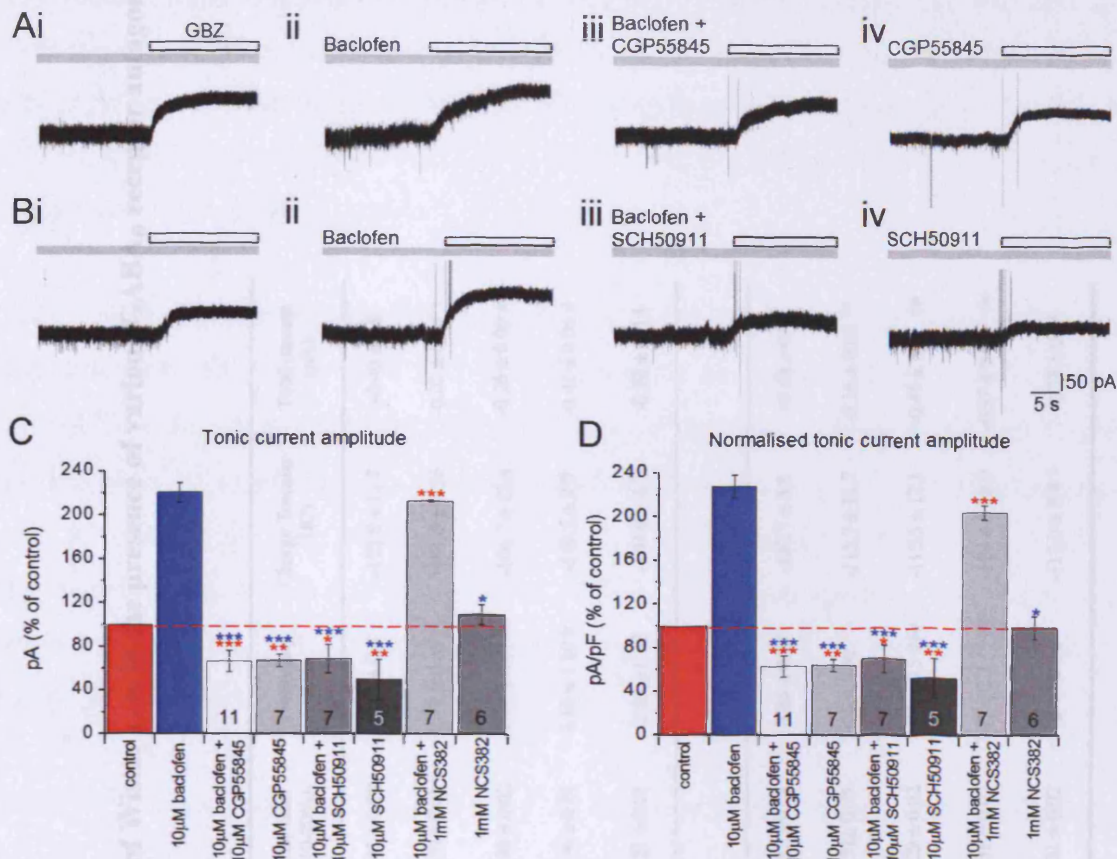


Figure 5.3
Baclofen increases tonic GABA_A current through GABA_BRs

A + B) representative current traces from eight different Wistar rat TC neurons showing the effect of 10 μ M CGP55845 (**Aiv**; grey bar) and 10 μ M SCH50911 (**Biv**; grey bar) alone and co-applied with 10 μ M baclofen (**Aiii + Biii**; grey bars), relative to 10 μ M baclofen (**Aii + Bii**; grey bars). **Ai + Bi** are traces representative of tonic current amplitudes under control conditions. **C)** comparison of the effect of various GABA_B antagonists with and without baclofen on tonic current amplitude as percentage of their respective controls. **D)** comparison of the tonic current amplitudes normalised to whole-cell capacitance as percentage of their respective controls. **C + D:** * $p < 0.05$, ** $p < 0.01$, *** $p < 0.001$, compared to control; * $p < 0.05$, *** $p < 0.001$, compared to 10 μ M baclofen. Numbers of recorded neurons are indicated at the base of each column in **C + D**. Scale bars are indicated. All recordings were done in the presence of TTX (500nM).

Table 5.3

Comparison of mIPSC parameters in TC neurons of Wistar rats in the presence of various GABA_B receptor antagonists

1 st Data set	<i>mIPSC parameter</i>						
	n	Peak amplitude (pA)	Weighted Decay (ms)	Rise time (10-90%)	Frequency (Hz)	Charge Transfer (fC)	Total current (pA)
Control	21	-41.9 ± 2.2	2.7 ± 0.1	0.31 ± 0.02	3.15 ± 0.5	-122.8 ± 11.7	-0.40 ± 0.8
10µM baclofen	10	-39.4 ± 2.3	2.5 ± 0.1	0.31 ± 0.01	0.78 ± 0.45 *	-101.3 ± 6.26	-0.07 ± 0.04 *
10µM baclofen + 10µM CGP55845	11	-38.7 ± 1.8	2.9 ± 0.4	0.30 ± 0.02	2.38 ± 0.61 #	-106.7 ± 13.4	-0.26 ± 0.09 #
10µM CGP55845	7	-39.9 ± 1.5	2.6 ± 0.1	0.30 ± 0.01	3.16 ± 1.10 #	-108.5 ± 9.9	-0.41 ± 0.06 #
1mM NCS382	6	-39.4 ± 1.7	2.6 ± 0.2	0.27 ± 0.01	2.85 ± 1.22	-104.8 ± 4.7	-0.30 ± 0.014
2nd Data set							
Control	9	-44.0 ± 0.8	2.4 ± 0.1	0.32 ± 0.01	3.36 ± 0.45	-132.7 ± 3.8	-0.44 ± 0.06
10µM baclofen	6	-44.7 ± 1.3	2.3 ± 0.2	0.31 ± 0.03	1.51 ± 0.50 **	-115.7 ± 11.7	-0.16 ± 0.06 **
10µM baclofen + 10µM SCH50911	7	-43.3 ± 2.6	2.2 ± 0.2	0.29 ± 0.02	4.06 ± 0.5 ###	-112.3 ± 17.1	-0.45 ± 0.07 ##
10µM SCH50911	5	-47.9 ± 4.2	2.3 ± 0.1	0.31 ± 0.02	7.61 ± 2.2 ** ##	-124.4 ± 13.9	-0.97 ± 0.51 * ##
10µM baclofen + 1mM NCS382	7	-44.9 ± 1.8	2.6 ± 0.2	0.31 ± 0.02	2.40 ± 0.6	-117.0 ± 5.4 *	-0.23 ± 0.05

* p < 0.05, ** p < 0.01 compared to control; # p < 0.05, ## p < 0.01, ### p < 0.001 compared to 10µM baclofen;

n = number of cells recorded

5.3.3 Baclofen increases tonic GABA_A current independently of K⁺ channels

The metabotropic GABA_BR produces its inhibitory effects through G_{i/o} coupled K⁺ channels on the postsynaptic membrane (Dutar & Nicoll, 1988; Olsen & Avoli, 1997). Although intracellular caesium has been shown to block GIRK channels (Gahwiler & Brown, 1995; Spain et al., 1987), I have also tested the effect of various K⁺ channel blockers on tonic GABA_A current.

Tonic GABA_A current amplitude from TC neurons in slices containing the somatosensory VB thalamus of P21–26 Wistar rats, was measured in the presence of 500nM TTX and during the continuous presence of 2mM Ba²⁺, 2mM 4-AP and 10mM TEA to block K⁺ channels, with and without 10μM baclofen (Fig. 5.4). The inclusion of such K⁺ channel blockers induced spontaneous mIPSC bursting activity (Fig. 5.4A + Bi), as previously shown (Le Feuvre et al., 1997). The bursts appeared to consist of a single large amplitude IPSC (Fig. 5.4Bii) with many smaller IPSCs superimposed on its decay (Fig. 5.4Biii).

2mM Ba²⁺, 2mM 4-AP and 10mM TEA (“K⁺ blockers”) alone increased tonic GABA_A current amplitude compared to those cells recorded in the absence of these blockers i.e. control (125.1 ± 13.3 pA, p <0.001) (Fig. 5.4C), independently of whole-cell capacitance (p <0.01) (Fig. 5.4D). 10μM baclofen, co-administered with K⁺ channel blockers, increased the tonic current amplitude further (203.6 ± 28.8 pA) compared to control (p <0.001) and K⁺ blockers alone (p <0.05) (Fig. 5.4A+C), independently of whole-cell capacitance (p <0.001 compared to control; p <0.05 compared to K⁺ blockers alone) (Fig. 5.4D).

Comparison of the mIPSC data unsurprisingly revealed significantly higher frequencies with K⁺ blockers alone and K⁺ blockers co-applied with 10μM baclofen compared to control (Table 5.4). The mIPSC peak amplitude was significantly larger in the presence of K⁺ blockers with baclofen which may reflect the inclusion of the large amplitude IPSC from each burst.

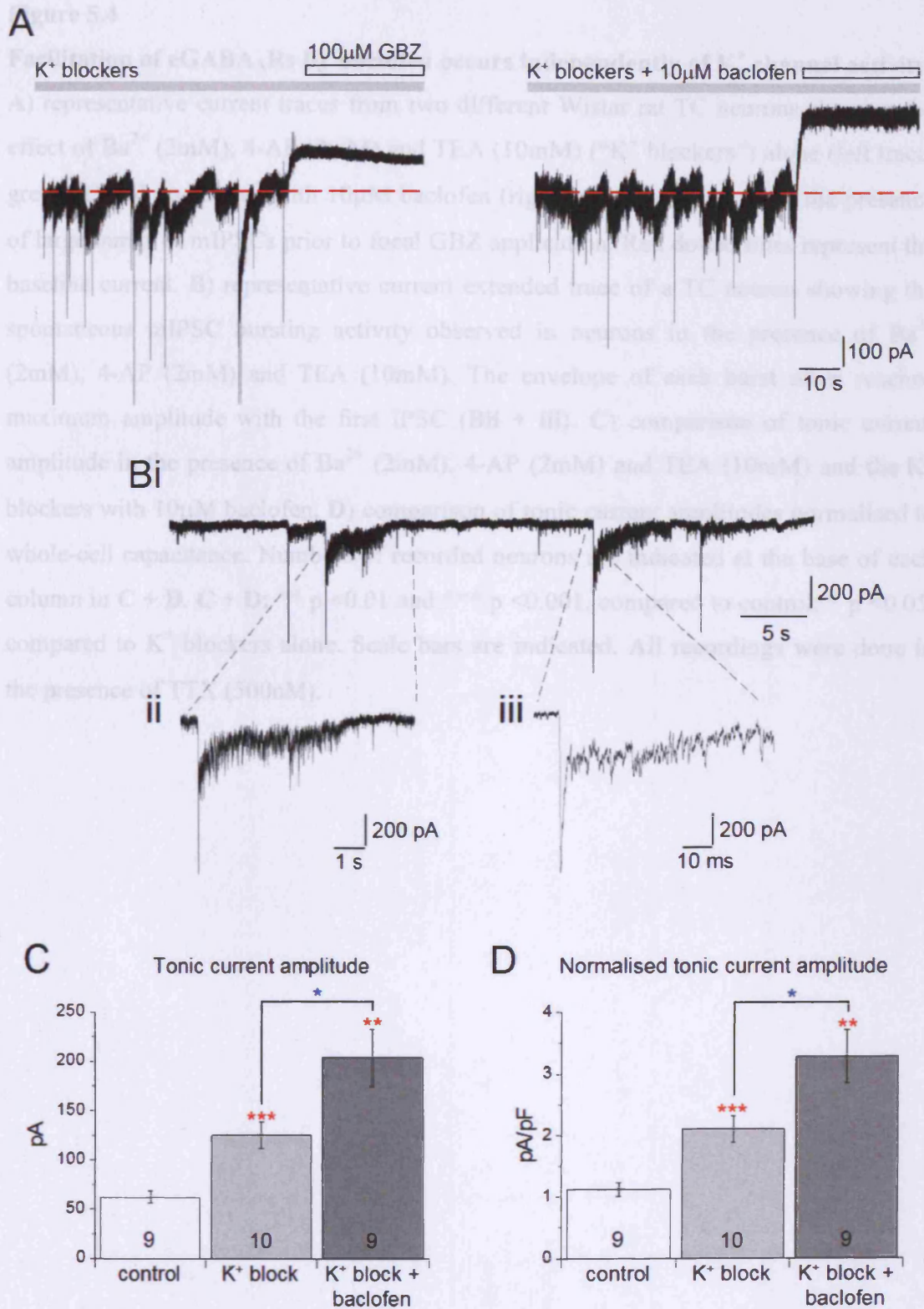


Figure 5.4

Figure 5.4

Facilitation of eGABA_ARs by baclofen occurs independently of K⁺ channel activity

A) representative current traces from two different Wistar rat TC neurons showing the effect of Ba²⁺ (2mM), 4-AP (2mM) and TEA (10mM) (“K⁺ blockers”) alone (left trace; grey bar) and co-applied with 10μM baclofen (right trace; grey bar). Note the presence of large bursts of mIPSCs prior to focal GBZ application. Red dotted lines represent the baseline current. **B)** representative current extended trace of a TC neuron showing the spontaneous mIPSC bursting activity observed in neurons in the presence of Ba²⁺ (2mM), 4-AP (2mM) and TEA (10mM). The envelope of each burst often reached maximum amplitude with the first IPSC (**Bii + iii**). **C)** comparison of tonic current amplitude in the presence of Ba²⁺ (2mM), 4-AP (2mM) and TEA (10mM) and the K⁺ blockers with 10μM baclofen. **D)** comparison of tonic current amplitudes normalised to whole-cell capacitance. Numbers of recorded neurons are indicated at the base of each column in **C + D**. **C + D:** ** p < 0.01 and *** p < 0.001, compared to control; * p < 0.05, compared to K⁺ blockers alone. Scale bars are indicated. All recordings were done in the presence of TTX (500nM).

Table 5.4
Comparison of mIPSC parameters in TC neurons of Wistar-Kyoto rats

mIPSC parameters	K ⁺ blockers		K ⁺ blockers + 10 μM baclofen	
	n	Weighted Discrepancy (SD)	n	Weighted Discrepancy (SD)
Control	10	2.4 ± 0.14	10	1.7 ± 0.01
K ⁺ blockers	10	2.4 ± 0.15	10	2.3 ± 0.01
K ⁺ blockers + 10 μM baclofen	10	2.4 ± 0.25	10	2.3 ± 0.01

** p < 0.01, *** p < 0.001 compared to control; * p < 0.05, compared to K⁺ blockers alone

Table 5.4

Comparison of mIPSC parameters in TC neurons of Wistar rats with K⁺ channels blocked

	<i>mIPSC parameter</i>						
	n	Peak amplitude (pA)	Weighted Decay (mS)	Rise time (10-90%)	Frequency (Hz)	Charge Transfer (fC)	Total current (pA)
Control	9	-44.0 ± 0.8	2.4 ± 0.14	0.32 ± 0.01	3.36 ± 0.45	-132.7 ± 3.8	-0.44 ± 0.06
K ⁺ blockers	10	-55.1 ± 5.9	2.4 ± 0.23	0.31 ± 0.01	13.41 ± 2.40 ***	-149.8 ± 18.3	-1.99 ± 0.42 **
K ⁺ blockers + 10µM baclofen	9	-59.8 ± 5.1 **	2.0 ± 0.20	0.31 ± 0.01	13.87 ± 2.52 ***	-137.7 ± 14.9	-2.06 ± 0.29 ***

** p < 0.01, *** p < 0.001 compared to control; n = number of cells recorded

5.3.4 GABA_B receptors modulate tonic GABA_A current in several brain regions

I have demonstrated a GABA_BR modulation of tonic GABA current in TC neurons of the VB. Tonic GABA_A current has been identified in cells of various brain regions, namely cerebellar granule cells (CGCs) (Brickley et al., 1996 & 2001; Hamann et al., 2002; Kaneda et al., 1995; Nusser et al., 1998) and dentate gyrus granule cells (DGGCs) (Chandra et al., 2006; Nusser & Mody, 2002; Mtchedlishvili & Kapur, 2006). Due to the wide array of studies investigating characteristics of tonic GABA_A current in these two brain areas, alongside the similarity in eGABA_AR subunit composition to TC cells of the VB ($\alpha 4\beta\delta$; Jia et al., 2005), I decided to ascertain the effect of baclofen and CGP55845 on CGC ($\alpha 6\beta\delta$; Brickley et al., 2001) and DGGC ($\alpha 4\beta\delta$; Wei et al., 2003) cells.

In the presence of 500nM TTX, tonic GABA_A current amplitude from CGC (Fig. 5.5A+B) and DGGC (Fig. 5.5C+D) neurons of P21–26 Wistar rats was measured in the continuous presence of 10 μ M baclofen and baclofen with 10 μ M CGP55845 (Fig. 5.5). Baclofen increased tonic current amplitude in CGCs compared to control (control: 13.7 ± 2.6 pA; 10 μ M baclofen: 25.3 ± 3.8 pA, $p < 0.05$) and 10 μ M CGP55845 not only blocked the baclofen-induced increase, but reduced the tonic current to below control (10 μ M baclofen & 10 μ M CGP55845: 6.4 ± 1.5 pA, $p < 0.05$) (Fig. 5.5A+Bi). All of these effects occurred independently of whole-cell capacitance (Fig. 5.5Bii).

Similar results were observed in DGGCs: control = 14.7 ± 2.7 pA; 10 μ M baclofen = 21.7 ± 1.6 pA, $p < 0.05$ compared to control; 10 μ M baclofen with 10 μ M CGP55845 = 6.1 ± 2.1 pA, $p < 0.05$ compared to control (Fig. 5.5C + Di). CGP55845-induced reduction of tonic current amplitude occurred independently of whole-cell capacitance, however baclofen mediated increase was not significantly different to control ($p > 0.05$) (Fig. 5.5Dii).

Comparison of mIPSC parameters revealed a significantly reduced frequency and total current in the presence of baclofen (Table 5.5), with all other parameters remaining unchanged in CGC and DGGCs. The GABA_BR antagonist reversed the 10 μ M baclofen-induced reduction in frequency and total current in both cell types.

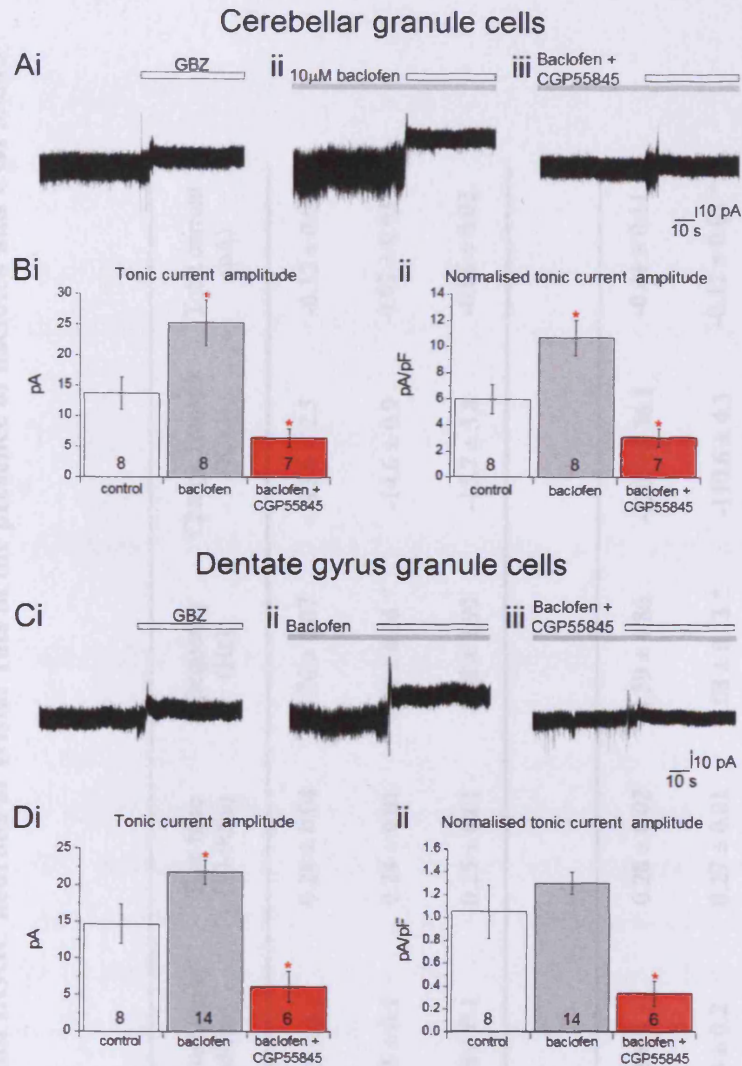


Figure 5.5

GABA_BR modulation of tonic GABA_A current occurs in several brain regions

A) representative current traces from three different Wistar rat CGC neurons showing the effect of 10 μ M baclofen (**Aii**; grey bar) and baclofen with 10 μ M CGP55845 (**Aiii**; grey bar). **Ai** is a representative current trace of a CGC neuron under control conditions. **C)** comparison of the effect of 10 μ M baclofen (**Cii**; grey bar) and baclofen with 10 μ M CGP55845 (**Ciii**; grey bar) on tonic current amplitude. **Ci** is a representative current trace of a CGC neuron under control conditions. **Bi + Di)** comparison of the effect of 10 μ M baclofen and baclofen with 10 μ M CGP55845 on tonic current amplitude. **Bii + Dii)** tonic current amplitudes normalised to whole-cell capacitance. **B + D:** * $p < 0.05$. Numbers of recorded neurons are indicated at the base of each column in **B + D**. Scale bars are indicated. All recordings were done in the presence of TTX (500nM).

Table 5.5

Comparison of mIPSC parameters in CGC and DGGC neurons of Wistar rats in the presence of baclofen and CGP55845

CGC	<i>mIPSC parameter</i>						
	n	Peak amplitude (pA)	Weighted Decay (mSecs)	Rise time (10-90%)	Frequency (Hz)	Charge Transfer (fC)	Total current (pA)
Control	8	-15.9 ± 1.1	0.72 ± 0.1	0.28 ± 0.04	7.76 ± 2.07	-13.6 ± 2.5	-0.12 ± 0.04
10µM baclofen	8	-15.5 ± 0.9	0.75 ± 0.1	0.24 ± 0.01	1.79 ± 0.16 *	-14.6 ± 0.9	-0.02 ± 0.01 *
10µM baclofen + 10µM CGP55845	7	-15.4 ± 2.2	0.78 ± 0.1	0.25 ± 0.01	4.88 ± 1.90	-15.7 ± 3.8	-0.06 ± 0.02
DGGC							
Control	8	-32.8 ± 6.6	3.2 ± 0.3	0.28 ± 0.02	4.59 ± 0.86	-120.9 ± 36.1	-0.41 ± 0.11
10µM baclofen	14	-39.5 ± 4.1	3.3 ± 0.2	0.27 ± 0.01	1.08 ± 0.13 *	-110.6 ± 4.3	-0.12 ± 0.01 *
10µM baclofen + 10µM CGP55845	6	-37.4 ± 0.4	3.6 ± 0.1	0.27 ± 0.01	2.26 ± 0.19	-138.3 ± 4.5	-0.31 ± 0.03

* p < 0.05 compared to control; n = number of cells recorded

5.4 Discussion

The results in this chapter show that:

- Baclofen dose-dependently enhances tonic GABA_A current in TC neurons;
- Baclofen modulation of tonic GABA_A current is independent of GIRK and other K⁺ channels;
- Postsynaptic GABA_B receptors tonically modulate eGABA_ARs under control conditions, and
- Postsynaptic GABA_BR-eGABA_AR interaction is ubiquitous in the brain.

5.4.1 Baclofen effects on mIPSCs and tonic GABA_A current

Raised tonic GABA_A current in TC neurons of the VB was shown to be a phenomenon present across different models of absence epilepsy (Chapter 3), both necessary and sufficient for SWD induction (Chapter 4). It was unsurprising that the eGABA_AR-specific agonist, THIP, enhanced tonic GABA_A current, but somewhat unexpected that the weak GABA_B agonist, GHB, also augmented tonic GABA_A current. Considering the controversy over the site-of-action of GHB, together with the possibility that the GHB effect may be partially mediated via GHB-derived GABA, I tested the effect of a specific GABA_B agonist on tonic GABA_A current.

In agreement with previous work (Ulrich & Huguenard, 1996; Emri et al., 1996a; Le Feuvre et al., 1997), baclofen dose-dependently decreased mIPSC frequency. At $\geq 1\mu\text{M}$, baclofen decreased the mIPSC frequency by about half without affecting the amplitude, similarly to Ulrich & Huguenard (1996) and Le Feuvre et al (1997). However, $0.3\mu\text{M}$ baclofen failed to significantly alter mIPSC frequency unlike the 22% decrease observed in the presence of $0.5\mu\text{M}$ baclofen by Le Feuvre et al (1997). As mentioned in Chapter 3, synaptic events were analysed from just 55 seconds of control baseline current prior to GBZ application whereas other studies used at least 3 minutes (Le Feuvre et al., 1997). This restricted time may have masked any subtle mIPSC changes that likely occur with $0.3\mu\text{M}$ baclofen.

Again, in line with preceding work, specific GABA_B antagonists reversed the presynaptic baclofen action (Ulrich & Huguenard, 1996; Le Feuvre et al., 1997). Earlier work showed GABA_B antagonists not only reversing baclofen-induced reduction in mIPSC frequency but an increase in mIPSC frequency (Le Feuvre et al., 1997) and eEPSP amplitude in TC cells (Emri et al., 1996a). From this, these two papers conclude that GABA_B auto- and heteroreceptors on presynaptic terminals provide a negative control mechanism by which excitatory and inhibitory transmission can be controlled, and that these receptors are tonically activated by ambient GABA levels. Interestingly, I did not consistently observe such increases in mIPSC frequency. Indeed the 52% increase in mIPSC frequency observed in Le Feuvre et al (1997) was present in only 3 out of 7 TC neurons. Considering this, it is possible that such activity may have been masked in my data which pooled results from individual cells and was taken from a short baseline current. Only when the highly specific GABA_B antagonist SCH50911 was applied to the cells alone, was tonic activation of presynaptic GABA_BRs removed to an extent enough to become visible in my results.

Simultaneous to the presynaptic action and similarly to GHB, baclofen dose-dependently increased tonic GABA_A current. At $\geq 1\mu\text{M}$, baclofen enhanced tonic GABA_A current however no effect was observed with $0.3\mu\text{M}$, similar to the lack of effect at presynaptic receptors at this concentration (see above). In addition, specific GABA_B antagonists and the putative GHB antagonist reversed the baclofen-induced augmentation of tonic GABA_A current. These results ascertain the receptor site where GHB mediates enhancement of eGABA_AR activity and further show that baclofen-induced augmented tonic GABA_A current is via GABA_BRs.

5.4.2 Baclofen augments tonic GABA_A current at the postsynaptic membrane and independently from K⁺ conductance through GIRK channels

I have already deduced that the majority of GABA release into the VB is quantal (see Chapter 3.4.2) and demonstrated that baclofen acts at presynaptic terminals to inhibit GABA release (see Chapter 5.4.1). Considering this presynaptic action therefore, one might expect baclofen to elicit a decrease of tonic GABA_A current through a reduction of GABA released into the extracellular space. Somewhat counter-intuitively, this was not the case. All of the *in vitro* experiments in this Chapter and Chapter 3 were carried

out in the presence of TTX. The inclusion of this toxin meant that each neuron was patched in a slice where synaptic transmission was essentially blocked. This strongly suggests that the baclofen-induced enhancement of tonic GABA_A current is via GABA_BRs in postsynaptic membranes, independent of baclofen presynaptic action.

Metabotropic GABA_BRs are coupled in the postsynaptic membrane to GIRK channels (Luscher et al., 1997; Slesinger et al., 1997) that leads to increased K⁺ conductance (Newberry & Nicoll, 1984, 1985; Gahwiler & Brown, 1985; Inoue et al., 1985a, b), resulting in a long-lasting and slow IPSP (Dutar & Nicoll, 1988; Olsen & Avoli, 1997). Caesium chloride was the major constituent of the intracellular solution and was used to help isolate the tonic GABA_A current (see Chapter 2.1.4).

Intracellular and extracellular application of caesium blocks inwardly-rectifying potassium channels (Maccaferri et al., 1993; Spain et al., 1987) and the postsynaptic action of baclofen (Gahwiler & Brown, 1995). Whilst it is widely accepted that GABA_BRs are coupled with GIRK channels, one example has shown GABA_BR inhibition to be mediated via activation of a TREK-2 K⁺ channel, that is not related to GIRK, in the entorhinal cortex (Deng et al., 2009). Considering this, alongside the possibility of caesium failing to penetrate small, distal dendrites, it was important to establish that enhanced tonic GABA_A current was not a manifestation of GABA_B-coupled K⁺ conductances.

Three major families of K⁺ channels exist: voltage-gated K⁺ channels (K_v) that are activated by depolarisation; inward rectifier K⁺ channels which are activated by hyperpolarisation and two-pore domains K⁺ channels which may also contribute to resting K⁺ conductance (Miller et al., 2000). TEA and 4-AP are classic K_v channel blockers (Camerino et al., 2000). These agents affect different K_v channel subtypes thus were both included in the aCSF and at high concentrations to ensure that all subtypes were blocked (Camerino et al., 2000). Barium (Ba²⁺) ions have similar crystal radius compared to K⁺ ions, but blocks rather than permeates the selective conducting pore (Gibor et al., 2004; Jiang & MacKinnon, 2000). Applied both intra- and extracellularly, Ba²⁺ blocks inwardly rectifying channels (Harris et al., 1998; Armstrong & Taylor, 1980) and the voltage-gated K⁺ channel family KCNQ (Gibor et al., 2004), which are

insensitive to TEA and 4-AP. The inclusion of these blockers ensured that no K^+ channels were active in the slice.

Caesium applied alone (Xiong & Stringer, 1999), TEA and 4-AP (Xiong & Stringer, 2001) induce spontaneous hyperactivity in hippocampal slices by increasing neuronal excitability. In agreement with Le Feuvre et al (1997) where TEA was tested on sIPSCs of VB neurons, block of K^+ channels elicited rhythmic, large amplitude bursts of mIPSCs, presumably by increasing the excitability of NRT neurons.

Considering that the NRT is the primary source of GABA for TC cells of the VB (Groeneweg & Witter, 2004; Prince, 1995), this bursting activity would have led to a greatly raised level of extracellular GABA which would predictably augment tonic $GABA_A$ current. Indeed this was the case, with an approximate two-fold increase in tonic $GABA_A$ current. Importantly, baclofen-mediated increase of tonic $GABA_A$ current remained in the presence of these K^+ blockers. This finding therefore strongly supports that the proposed postsynaptic $GABA_B$ modulation of e $GABA_A$ R function occurs independently of GIRK channels and other K^+ channels, and possibly through a $G_{i/o}$ -protein coupled pathway.

10 μ M baclofen increased tonic $GABA_A$ current by 201.7 ± 9.6 % and the K^+ blockers elicited a similar percentage increase (201.5 ± 10.6 %). If baclofen and the elevated extracellular GABA levels caused by K^+ blockers were via independent mechanisms/pathways, one would expect an additive increase to ~400% when baclofen and K^+ blockers were co-applied. Interestingly, only a 327.9 ± 14.1 % increase was elicited by co-application of baclofen and K^+ channel blockers, showing that the effects are not supplementary to one another.

It is clear from my data that baclofen acts directly at postsynaptic $GABA_B$ Rs to enhance tonic $GABA_A$ current. The increase of tonic $GABA_A$ current elicited by K^+ channel blockers may be less clear. It is possible that elevated extracellular GABA levels released by K^+ channel blockers activate not only the high-affinity e $GABA_A$ Rs, but postsynaptic $GABA_B$ Rs also which would lead to additional augmentation of tonic $GABA_A$ current. Therefore, elevated GABA resulting from NRT burst firing may

mediate increase of tonic GABA_A current via direct activation of eGABA_ARs and through indirect action at postsynaptic GABA_BRs.

5.4.3 Postsynaptic GABA_BRs tonically modulate eGABA_ARs

One very interesting finding from these experiments was how GABA_BR antagonists appeared to not only reverse baclofen-induced enhancement of tonic GABA_A current, but actually reduce current amplitudes below the control value. This phenomenon was also observed with GABA_B antagonists applied alone but not in the presence of the putative GHB antagonist. Not only do these data provide evidence that NCS382 is either a weak GABA_B antagonist or acting at an alternative receptor (see Chapter 3.4.3.1), but they are the first electrophysiological evidence of a postsynaptic GABA_BR modulation of eGABA_ARs under control conditions in the postsynaptic membrane.

A negative control mechanism of GABA_BRs on neurotransmitter release has already been well characterised on the presynaptic membrane in thalamic slices (Emri et al., 1996a & b; Le Feuvre et al., 1997). GABA_BRs act to reduce neurotransmitter release and antagonism results in the removal of their tonic activation and a larger synaptic output, albeit glutamatergic or GABAergic (Emri et al., 1996a & b; Le Feuvre et al., 1997). Alternatively, I have shown baclofen enhancing tonic GABA_A current and that removal of GABA_BR activation, either by baclofen or by ambient GABA, leads to a reduced tonic GABA_A current, suggesting a positive control mechanism between the two receptor subtypes on the postsynaptic membrane.

Together these two phenomena highlight the complexity of GABAergic inhibitory transmission. Not only does GABA mediate inhibition through well characterised ion movement at GABA_A and GABA_BRs, but mediates inhibitory transmission at a secondary stage whereby GABA_BRs reduce vesicular release and simultaneously enhance tonic GABA_A current acting postsynaptically.

5.4.4 Postsynaptic GABA_BR facilitation of eGABA_AR function is ubiquitous

Tonic GABA_A current and the associated GABA_AR subunits have been identified in cells from many brain regions (see Chapter 1.4.1.2). Considering that GABA_BRs are ubiquitously expressed throughout that brain, I investigated whether the postsynaptic GABA_BR-eGABA_AR link existed in two brain areas where tonic current was well

established: the cerebellum (Brickley et al., 1996 & 2001; Hamann et al., 2002; Kaneda et al., 1995; Nusser et al., 1998) and hippocampus (Chandra et al., 2006; Nusser & Mody, 2002; Mtchedlishvili & Kapur, 2006).

In both CGC and DGGCs, baclofen augmented tonic GABA_A current. Similarly, co-application with the specific GABA_B antagonist, CGP55845, reversed the GABA_B-mediated increase in eGABA_AR function and reduced tonic GABA_A current below control. These data clearly show that the postsynaptic GABA_BR increase of eGABA_AR function, that is present under control conditions, is present in many brain regions and strongly suggests that this phenomenon is ubiquitously present when GABA_B and GABA_ARs containing the δ -subunit are co-expressed in a membrane.

It should be noted that tonic current normalised to whole-cell capacitance was not significantly different in DGGCs in the presence of baclofen (10 μ M), presumably because small changes in tonic GABA_A currents are likely to be more easily skewed by variation in cell size.

5.4.5 Potential intracellular pathways of postsynaptic GABA_B-eGABA_AR interaction

Both GABA_A and GABA_B receptors have been implicated in receptor-receptor crosstalk relationships. For example, metabotropic 5-HT_{2C} receptors inhibit GABA_ARs by a Ca²⁺-dependent mechanism in *Xenopus oocytes* (Huidobro-Toro et al., 1996) and GABA_BRs enhance mGluR1-mediated excitatory transmission at parallel fibre-Purkinje cell synapses in the cerebellum (Hirono et al., 2001).

Whilst it is not uncommon for metabotropic and ionotropic receptors of different neurotransmitters to interact, my data provide one of the first electrophysiological cases whereby two different receptor-types for the same neurotransmitter are functionally connected within a cell. My findings strongly suggest that this GABA_B-eGABA_AR link occurs via an intracellular pathway that does not involve GIRK channels or any other K⁺ conductance.

Metabotropic receptors activate coupled G-proteins; subunits of which then bind to and activate effector molecule(s) of the receptor. G-protein activity often motivates a long

and complex biological cascade within a cell. Considering that K^+ conductance is not involved in the GABA_B-eGABA_AR link, it is feasible to assume that GABA_B effects are mediated by the alternative effector molecule coupled with GABA_BRs that is the precursor for protein kinase A (PKA), adenylyl cyclase (AC) (Fig. 5.6). Indeed this pathway has been recently exposed where TREK-2 channels are activated by GABA_BRs via the inhibitory G-protein ($G_{i/o}$) and PKA pathway (Deng et al., 2009).

Immunolabelling techniques in both monkey and rat brains have revealed that postsynaptic GABA_BRs are predominantly associated with peri- or extrasynaptic sites in the thalamus (Kulik et al., 2002; Vilallba et al., 2006). Intracellular cascades resulting from G-protein activation can overcome great distances to reach target molecules in cells (Hille et al., 1992; Purves et al., 2000), however colocalisation of the two receptors not only provides a physical link that raises the possibility of receptor interaction, but will allow a faster link between the two receptor subtypes.

GABA_B receptor modulation of GABA_A receptors has been suggested in a previous study. Hahner et al (1991) established that baclofen inhibited muscimol-stimulated uptake of $^{36}Cl^-$ by membrane vesicles from mouse cerebellum. They ascertained that baclofen action was not only concentration-dependent and antagonised by GABA_BRs, but mediated through G-protein action, speculating phosphorylation of GABA_ARs by PKC (Hahner et al., 1991). Indeed protein kinases modulate GABA_AR function and cell surface expression (Kittler & Moss, 2003), with most studies focusing on synaptic receptor subtypes in cultured neurons, often yielding conflicting results (Brandon et al., 2002). The distribution of an isoform of protein kinase C (PKC δ) was found to closely overlap with GABA_A δ -subunit in thalamic and hippocampal neurons (Choi et al., 2008). PKC $\delta^{-/-}$ mice exhibited reduced intoxication and an insensitivity of tonic GABA_A current to ethanol (Choi et al., 2008), an agent known to increase tonic current (Glykys et al., 2007; Jia et al., 2008b; Mody et al., 2007). A more recent study has highlighted a functional importance of eGABA_AR phosphorylation. Tang et al (2010) found that PKA phosphorylation of eGABA_ARs increased tonic current by increasing single-channel open frequency. This action was only observed in low GABA concentrations, because with increasing extracellular GABA the tonic GABA_A currents were more GABA dependent and less PKA dependent (Tang et al., 2010).

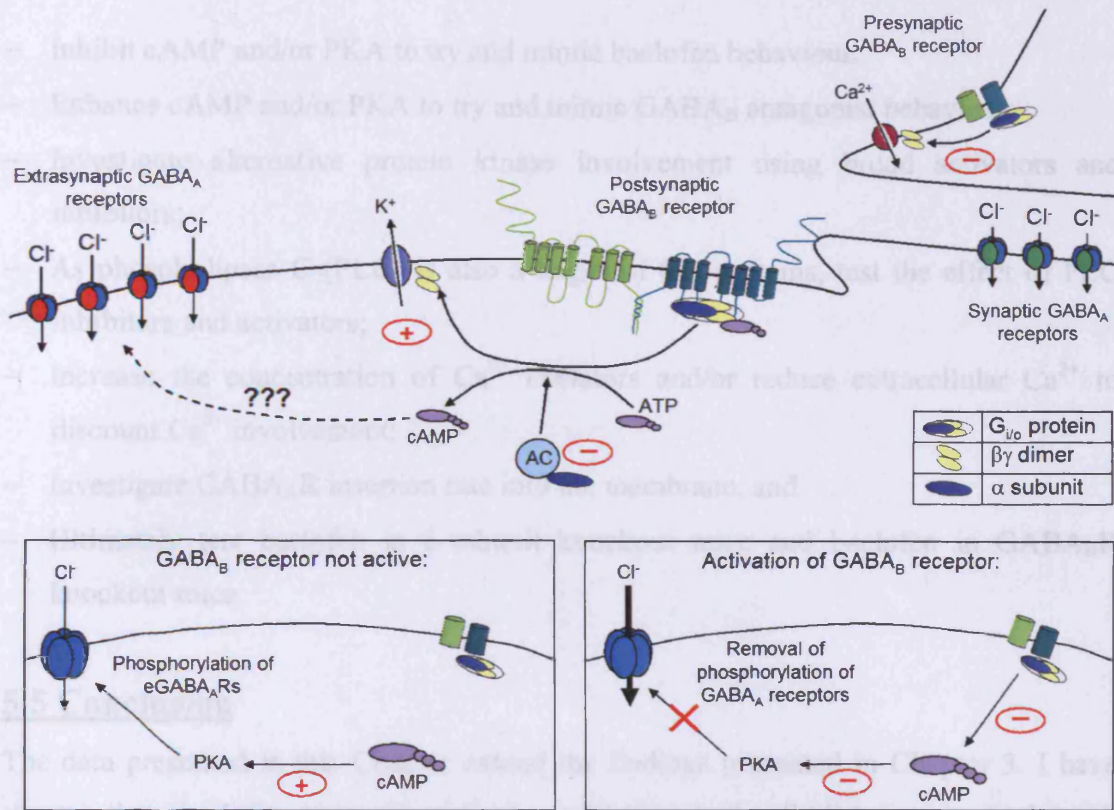


Figure 5.6

Schematic illustration of the potential signalling cascade leading to activation of eGABA_ARs by GABA_BRs

Minus marks indicates inhibition, whereas plus mark denotes facilitation. GABA_BR activation results in activation of inhibitory G-proteins (G_{i/o}). Activation of G_{i/o} inhibits the activity of AC, leading to a reduction in the production of cAMP from ATP and an inhibition of PKA. It is possible that PKA exerts a tonic inhibition of eGABA_ARs via phosphorylation, just as it does on TREK-2 channels (Deng et al., 2009). GABA_BR activation would then annul PKA-mediated tonic inhibition of eGABA_ARs, resulting in an increase in the function of eGABA_ARs.

The following experiments would confirm G_{i/o} protein involvement in the postsynaptic GABA_B-eGABA_AR link (speculated in Fig. 5.6) and perhaps reveal the role of adenylyl cyclase and associated protein kinase cascades on tonic GABA_A current:

- Block G_{i/o} protein using intracellularly applied pertussis toxin (PTx; a specific G_{i/o} blocker) or GDP-β-s (a non-hydrolysable GDP analogue that competitively inhibits G-protein activation by GTP) and test the cellular response to baclofen;

- Inhibit cAMP and/or PKA to try and mimic baclofen behaviour;
- Enhance cAMP and/or PKA to try and mimic GABA_B antagonist behaviour;
- Investigate alternative protein kinase involvement using broad activators and inhibitors;
- As phospholipase C (PLC) is also a target of G_{i/o} proteins, test the effect of PLC inhibitors and activators;
- Increase the concentration of Ca²⁺ chelators and/or reduce extracellular Ca²⁺ to discount Ca²⁺ involvement;
- Investigate GABA_AR insertion rate into the membrane, and
- Ultimately test baclofen in δ -subunit knockout mice and baclofen in GABA_BR knockout mice.

5.5 Conclusion

The data presented in this Chapter extend the findings presented in Chapter 3. I have shown that baclofen dose-dependently enhances tonic GABA_A current through postsynaptic GABA_BRs independently from K⁺ conductance. Not only do these results ascertain the receptor-site where GHB likely mediates an increase in tonic GABA_A current, but are the first electrophysiological data to show a metabotropic GABA_B and ionotropic GABA_AR link that exists in several brain regions. Furthermore, my data suggest that postsynaptic GABA_BRs tonically modulate eGABA_ARs under control conditions.

Chapter 6

General discussion

6.1 Summary of findings

I have shown that enhanced tonic GABA_A current in TC neurons of the VB is a common phenomenon in a genetic model and across pharmacological models of absence seizures, except penicillin (see Chapter 3.4.6). This is in agreement with similar findings from mice models (Cope et al., 2009). Furthermore, my data show that increased eGABA_AR function in the VB is both sufficient and necessary to induce SWDs. This is supported by the fact that focal intrathalamic application of a selective agonist for eGABA_ARs, THIP, was sufficient to elicit SWDs in normal animals and that mice lacking eGABA_ARs were resistant to absence seizure induction by GBL.

Moreover, I have presented data that directly implicate aberrant GAT-1 in SWD generation *in vivo*, with GAT-1 knockout mice exhibiting spontaneous SWDs and focal thalamic administration of the GAT-1 blocker, NO711, inducing SWDs in normal rats; a potential new model of absence epilepsy. This is in agreement with work carried out in brain slices of GAERS, which revealed that enhanced tonic GABA_A current in TC cells of the VB is due to compromised uptake via astrocytic GAT-1 (Cope et al., 2009).

In addition, my data indicate that activation of postsynaptic GABA_BRs enhances tonic GABA_A current, presumably via the G_{i/o} protein coupled adenylyl cyclase pathway, which was present under control conditions and occurred in several brain areas. This postsynaptic GABA_B-eGABA_AR link is further supported by the fact that GBL failed to induce SWDs in δ -subunit knockout mice.

Thus, one of the cellular thalamic pathologies that characterises absence seizures is an astrocyte-specific aberrant GAT-1 with the resulting elevated extracellular GABA level enhancing tonic GABA_A current through two mechanisms: direct activation of high affinity eGABA_ARs and indirect increase in eGABA_AR function due to activation of postsynaptic GABA_BRs.

6.2 Role of enhanced tonic GABA_A current in the pathophysiological mechanisms of absence seizures

Considering what we already know about the cellular activity of components of the somatosensory thalamocortical loop during a SWD, I suggest the following role of increased tonic GABA_A current in TC neurons of the VB in GAERS. I have not discussed the possible role in the mouse models as that data is not presented in this thesis.

Layer V/VI of the facial region of the somatosensory cortex, regarded as the initiation site of a SWD (Meeren et al., 2002; Polack et al., 2009), display distinct hyperactivity during and in between SWDs (Polack et al., 2007). These leading neurons exhibit periods of oscillatory activity that instigate seizures (Polack et al., 2007) (Fig. 1.6). Action potentials from these cortical cyclical depolarisations arrive at, and strongly excite, GABAergic neurons of the NRT, which respond by switching from a tonic firing mode to generating low-threshold Ca²⁺ potentials (Slaght et al., 2002) (Fig. 1.7). These large LTCPs are tightly linked to each spike-wave complex in the EEG (Seidenbecher et al., 1998; Slaght et al., 2002) and are crowned by prolonged bursts of action potentials (Slaght et al., 2002). The cyclical burst firing of NRT cells leads to barrages of IPSPs in TC cells of the neighbouring VB, which override the simultaneous cortical excitatory input (Charpier et al., 1999; Pinault et al., 1998; Steriade & Contreras, 1995) (Fig. 1.5) and concurrently raises the level of GABA in the VB extracellular space. Due to abnormal GABA uptake through GAT-1, ambient GABA levels then increase. This causes activation of eGABA_ARs and thus increases tonic GABA_A current in TC cells and membrane hyperpolarisation.

Such augmented tonic GABA_A current manifests itself in rendering between ~60% (Steriade & Contreras 1995) and ~93% (Pinault et al., 1998) of neurons in a state that prevents cellular discharge (Fig. 1.8). Persistent tonic GABA_A current not only hyperpolarises the cell, but also increases membrane conductance (Cope et al., 2005), reducing the action potential output. Increased membrane conductance has greater impact than membrane hyperpolarisation on the responsiveness of TC neurons (Cope et al., 2009), thus preventing the generation of LTCPs that one would expect from TC

neurons at more hyperpolarised potentials and instead, shunting cellular responses to synaptic inputs.

Importantly, the rare occurrence of TC cell firing is adequate to maintain the thalamocortical loop, converging onto reticular and cortical neurons to facilitate and sustain rhythmic oscillatory activity.

It is likely that the facial myoclonus observed in patients and vibrissal twitching in animal models result from hyperactivity of neurons in the associated perioral somatosensory cortex. Moreover, as the majority of cellular responses to synaptic input are essentially nullified by the enhanced tonic GABA_A current, processing of sensory inputs is likely to be reduced therefore causing loss of consciousness and behavioural arrest, the typical phenotypic manifestation of absence seizures.

Additionally, this hypothesis may explain how GABAergic agents exacerbate, or in fact induce, SWDs and further highlights the importance of an intact thalamocortical loop for absence seizure expression. Furthermore, it may provide an explanation for the previously reported long-lasting hyperpolarisation of TC cells of the VB of GAERS during SWDs (Pinault et al., 1998; Charpier et al., 1999).

6.3 GABA transporters and absence seizures

It would be interesting to investigate the properties of both astrocytic GABA transporters in GAERS.

Considering the developmental profile of CAE, it is interesting that both GAT-1 and GAT-3 achieve an adult-like pattern of expression by the third postnatal week in the cortex and the second week in the thalamus (Vitellaro-Zuccavello et al., 2003). This timing coincides with the developmental profile of increased tonic GABA_A current observed in GAERS (Cope et al., 2009).

As GAT-1 transporters are also found in the cerebral cortex, it would be interesting to study the properties of GATs at the initiation site of SWDs i.e. layer V/VI of the perioral somatosensory cortex (Meeren et al., 2002; Polack et al., 2007 & 2009). These

cells are more depolarised in epileptic animals, but exhibit a tonic hyperpolarisation on SWD initiation (Polack et al., 2007). In contrast to the VB, GAT-1 is the most highly expressed GAT in the cortex (Conti et al., 2004; De Biasi et al., 1998) and is mostly situated in neurons instead of astrocytes (Minelli et al., 1995), whereas GAT-3 is still located on astrocytes (Minelli et al., 1996). In S1 of adult rats, GAT-1 is densest in layer IV (Minelli et al., 1995); however the specific cell types that express GAT-1 have not been determined (Conti et al., 2004). GABA uptake at the synapse is responsible for terminating GABA synaptic action, thus shaping inhibitory responses (Conti et al., 2004). If we make an assumption that GAT-1 is located solely at GABAergic interneurons in the cortex, then these cells would be inhibited. Thus, a lack of GABAergic input from these interneurons may explain the cellular hyperactivity in the S1. The tonic hyperpolarisation at SWD onset may then be a result of aberrant GAT-1 located on astrocytes, similarly to the VB.

Neurotransporters, like receptors, can be regulated by phosphorylation however not much is known about how phosphorylation regulates their function. Sutch et al (1999) has already suggested that the raised extracellular GABA in the VB of GAERS (Richards et al., 1995) is a result of GATs having a lower affinity for GABA in the VB. A recent study has identified a complex pathway where adenosine receptors, via the adenylate cyclase/cAMP/PKA pathway, facilitate GAT-1 transport by restraining PKC-mediated inhibition in hippocampal synaptosomes (Cristovao-Ferreira et al., 2009). It is possible that changes to phosphorylation state of the GAT-1 in the VB may underlie the aberrant GABA uptake. This could be investigated through whole-cell patch clamp of astrocytes in the VB of GAERS and NEC.

Whilst it is clear that GAT-1 is aberrant, it is also interesting that GAT-3 is unable to fully compensate for the GAT-1 abnormality (Fig. 4.11) (Cope et al., 2009). A recent study has shown that a membrane permeable agent called roscovitin induced a tonic GABA current in hippocampal slices through action at GATs on interneurons, independently of Ca^{2+} , K^{+} , protein kinases and in the presence of TTX (Ivanov et al., 2009). By binding to proteins that catalyse cofactors involved in GABA breakdown, roscovitin increases cytosolic GABA concentration within the interneuron thus causing GABA efflux through GATs and increases in extracellular GABA (Ivanov et al., 2009). It is possible that the underlying reason for the limited compensation for GAT-1

dysfunction by GAT-3 is an associated limited GABA breakdown within the astrocytes, leading to a restricted GABA uptake by the GABA-gradient sensitive GAT-3.

6.4 Sensitivity of absence seizures to GABA_B antagonists

My findings demonstrate a novel role of thalamic GABA_BRs in absence seizures. Whilst it is clear that direct activation of eGABA_ARs through raised extracellular GABA levels resulting from aberrant GAT-1 is a prerequisite for SWDs, postsynaptic GABA_BR facilitation of eGABA_AR function also contributes to tonic GABA_A current in the VB.

It seems that in an absence seizure scenario i.e. excessive VB extracellular GABA, the novel postsynaptic GABA_BR-eGABA_AR interaction would not detract from the classic pre- and postsynaptic GABA_BR effects. Indeed, my data show GABA_BR augmentation of tonic GABA_A current occurred despite a simultaneous reduction of GABA release. Furthermore, activation of GIRK channels on the postsynaptic membrane would probably further increase the conductance of the cell (Williams et al., 1995), supplementing the shunting effect already caused by direct eGABA_AR action and postsynaptic GABA_BR facilitation of eGABA_ARs.

The importance of this novel receptor-receptor interaction was highlighted by data showing that GBL failed to elicit SWDs in mice lacking δ -subunit containing eGABA_ARs. Not only does this finding further confirm the necessity of tonic GABA_A current to SWD induction, but demonstrates that facilitation of eGABA_ARs via postsynaptic GABA_BRs is not some passive modulatory phenomenon, but a critical mechanism used by GBL and GHB to generate absence seizures.

Investigations into the effects of the specific G_{i/o} protein blocker, PTx, on SWDs have further implicated the importance of GABA_B-coupled intracellular mechanisms in absence seizures. Intracerebroventricular administration of PTx suppressed the occurrence of SWDs in the GHB and PTZ experimental rat models within 3 days of application (Snead, 1992a). Moreover, a single bilateral injection of PTx into thalamic nuclei of adult GAERS resulted in complete cessation of SWDs within 6 days of

administration, via localised action in the VB and crucially, alongside a decrease in GABA_B binding in this nucleus (Bowerly et al., 1999).

Furthermore, whilst raised extracellular GABA levels were determined in the VB of GAERS, Richards et al (1995) found that systemic administration of CGP35348 produced no changes in levels of GABA thus GABA blockade of SWDs was due to direct GABA_B action.

Interestingly, a study into absence seizure induced alterations of GABA_AR subunit expression suggested a similar GABA_B-eGABA_A receptor link. Banerjee et al (1998) studied $\alpha 1$, $\alpha 4$, $\beta 2$ and $\gamma 2$ subunit gene expression in the rat GHB model. They found that 2-4 hours after the onset of GHB-induced absence seizures there was a significant rise in the levels of $\alpha 1$ and a significant decrease of $\alpha 4$ mRNA in the VB, with $\beta 2$ and $\gamma 2$ staying the same. Upon blocking seizures with pre-treatment of CGP35348, no changes were seen in GABA_AR subunit expression, nor were any changes observed in the NRT or hippocampus with GHB alone (Banerjee et al., 1998), therefore the altered GABA_A subunit expression was mediated through GABA_BRs and isolated to the VB. Because these changes developed when the seizures were terminating, it is likely that the subunit alterations are a result of some compensatory mechanism. Indeed, on re-administration of GHB 6 hours later, when $\alpha 4$ expression was reduced, the total duration of absence seizures significantly decreased (Banerjee et al., 1998). Considering that we now know $\alpha 4$ subunits are co-expressed with δ -subunits to form functional receptors in the thalamus (Belelli et al., 2005; Chandra et al., 2006; Cope et al., 2005; Jia et al., 2005; Sur et al., 1999), these findings support the hypothesis that GHB acts at GABA_BRs to enhance tonic current, without which, GHB cannot induce absence seizures.

Many different GABAergic agents exacerbate both clinical and experimental absence seizures and this sensitivity to GABA_A and GABA_B agonists is a defining characteristic of SWDs (Danober et al., 1998; Marescaux et al., 1992a; Snead, 1995). As augmented tonic GABA_A current is a common cellular pathology across models of absence (Chapter 3), GABAergic agents may exhibit their SWD-enhancing effects by directly activating eGABA_ARs (GABA_A agonists), increasing facilitation of eGABA_AR function

via GABA_BRs (GABA_B agonists) or through both mechanisms (GABAmimetics). Interestingly, unlike GABA_AR antagonists (Danober et al., 1998; Snead, 1994), GABA_BR antagonists are capable of suppressing SWDs (Liu et al., 1991b; Vergnes et al., 1984). Considering that increased tonic GABA_A current is both sufficient and necessary for absence seizure induction (Chapter 4) and that CGP55845 significantly reduced tonic inhibition in GAERS and that elicited by GHB (Chapter 3), it is reasonable to suggest that GABA_BR antagonists suppress SWDs through decreasing tonic GABA_A current by reduction or removal of GABA_BR facilitation of eGABA_AR function, in addition to block of GIRKs. This of course should not detract from the already established and “classical” pre- and postsynaptic GABA_AR and GABA_BR activity.

Together, these findings raise the significance of GABA_BR facilitation of eGABA_AR function: whilst it is clear that increased tonic GABA_A current is vital to SWD genesis, postsynaptic GABA_BRs are also critical to controlling this eGABA_AR functionality. A crucial experiment for the future would be to ascertain the proposed G_{i/o}-protein link between the two receptor types by using intracellularly applied PTx *in vitro* (see Chapter 5.4.5).

6.5 Physiological role of the postsynaptic GABA_BR-eGABA_AR link

My data show that the novel GABA_B-eGABA_AR interaction is present in several brain areas which strongly suggests a ubiquitous expression and as a result, indicates that this positive modulatory mechanism plays an important role in synaptic transmission.

GABA_ARs that mediate tonic GABA_A current are “designed” to do so, with extrasynaptic location, high affinity for GABA (Brown et al., 2002), specific pharmacology (Nusser & Mody, 2002) and slow desensitisation (Saxena & MacDonald, 1994; Brown et al., 2002). It is clear from my *in vitro* THIP data that eGABA_ARs are capable of mediating infinite tonic GABA_A currents and this capability may become pathological. I suggest that postsynaptic GABA_BR facilitation of eGABA_AR function is just one part of a control system that is in place to constrain eGABA_ARs, and that alternative metabotropic receptor types might interact with eGABA_ARs. For instance, excitatory receptors on the postsynaptic membrane e.g. mGluRs, concurrent to

mediating EPSPs, may increase PKA phosphorylation proposed to reduce eGABA_AR function (Fig. 5.6), thereby elevating cellular excitation. This would provide dynamic control over eGABA_AR function: This, however, is a speculative suggestion which would require further investigation. Interestingly, preliminary experiments in our laboratory have indicated that several other neurotransmitters are capable of affecting tonic GABA_A current in the dLGN (DiGiovanni et al., 2008), however primarily through changes in vesicular GABA release.

A dynamic range of tonic GABA_A current was set by PKA phosphorylation of eGABA_ARs in transfected HEK 293 cells, whereby tonic currents became less PKA-dependent and more dependent on GABA with increasing extracellular GABA (Tang et al., 2010). The presence of GABA_BR facilitation of eGABA_AR function under control conditions suggests that GABA_BR interaction may play a similar dynamic role. I suggest that eGABA_AR tonic current is differently influenced by GABA_B facilitation in ambient and high levels of GABA. Application of GABA_B antagonists revealed that in ambient GABA, the tonic modulation by GABA_BRs constitutes ~35% of tonic GABA_A current (Chapter 5.3.2). Changes of just a few millivolts can alter the firing mode of thalamic cells, thus GABA_B facilitation may play a “priming” role in ambient GABA i.e. maintaining a switch between firing thresholds. When extracellular GABA increases, the high-affinity and slow desensitisation properties of eGABA_ARs could play a dominant role whereby tonic GABA_A current becomes more GABA dependent, as in Tang et al (2010). However, due to the nature of intracellular cascades associated with metabotropic receptors, it is possible that increasing levels of extracellular GABA will simultaneously amplify the GABA_BR facilitation of eGABA_ARs. Such signal amplification from GABA_B facilitation may act to “boost” tonic GABA_A current in high GABA levels.

In order to determine whether the GABA_B link to eGABA_ARs is fixed or whether facilitation of eGABA_AR function is enhanced by increases in extracellular GABA, one could measure the contribution of GABA_BRs in the presence of GABA_B antagonists and baclofen with varying additional quantities of GABA. This was touched upon in my *in vitro* experiments with K⁺ channel blockers increasing extracellular GABA levels in Chapter 5. On measuring the percentage contribution of GABA_B facilitation to overall tonic GABA_A current, it would be interesting to establish the functional implications of

this receptor-receptor modulation. One method that may aid this investigation is to measure spontaneous cellular activity on injection of the calculated GABA_B-mediated tonic GABA_A current value in voltage clamp or dynamic clamp. If the GABA_B facilitatory link to eGABA_ARs was affected by extracellular GABA then this GABA_B-eGABA_AR relationship would act as a dynamic positive feedback inhibitory mechanism that would accommodate small changes of membrane potential under ambient GABA levels, but enhance shunting inhibition when extracellular GABA levels increase. A dynamic nature of this novel receptor-receptor interaction would have great implications for control of cellular firing, and thus implications in sensory processing and sleep stages.

Interestingly, Ren & Mody (2006) found that GHB increased phosphorylation of the cAMP dependent nuclear transcription factor CREB, via GABA_BRs and PKA in the hippocampus. Whilst they highlighted the importance of this phenomenon in drug tolerance, this activity may also have implications here as activation of intracellular cascades by metabotropic receptors can alter gene and receptor expression (Siegelbaum et al., 2000). Thus, it is possible that GABA_BRs may increase tonic GABA_A current by raising the number of eGABA_ARs expressed by a cell in the extrasynaptic membrane in addition to or instead of increasing eGABA_AR activity. This may be elucidated by immunohistochemical techniques or through mathematical approaches as in Wisden et al (2002).

6.6 The future direction of investigations

This thesis presents several novel findings that may have implications for the fields of absence epilepsy research and that of GABA receptor physiology. My data are both interesting and comprehensive, and inevitably several avenues for future investigation have been revealed. Specific experimental suggestions have been made throughout the thesis, in particular the discussion sections of each Chapter.

Overall, I believe that further investigation of astrocytic GABA transporter properties in thalami of absence models; in-depth examination of the proposed G protein link between eGABA_ARs and postsynaptic GABA_BRs in all brain areas and an extension of

research into the (electro)physiological consequences of the tonic GABA_A current, present very exciting opportunities to advance our understanding of cellular physiology.

References

- AIZAWA, M., ITO, Y. & FUKUDA, H. 1997. Pharmacological profiles of generalized absence seizures in lethargic, stargazer and gamma-hydroxybutyrate-treated model mice. *Neurosci Res*, 29, 17-25.
- AMARAL, D. 2000. The Functional Organisation of Perception and Movement. In: KANDEL, E., SCHWARTZ, J. & JESSELL, T. (eds.) *Principles of Neural Science*. Fourth Edition ed.: McGraw-Hill.
- ANDRIAMAMPANDRY, C., TALEB, O., VIRY, S., MULLER, C., HUMBERT, J. P., GOBAILLE, S., AUNIS, D. & MAITRE, M. 2003. Cloning and characterization of a rat brain receptor that binds the endogenous neuromodulator gamma-hydroxybutyrate (GHB). *Faseb J*, 17, 1691-3.
- ARMSTRONG, C. M. & TAYLOR, S. R. 1980. Interaction of barium ions with potassium channels in squid giant axons. *Biophys J*, 30, 473-88.
- AVANZINI, G., DE CURTIS, M., MARESCAUX, C., PANZICA, F., SPREAFICO, R. & VERGNES, M. 1992. Role of the thalamic reticular nucleus in the generation of rhythmic thalamo-cortical activities subserving spike and waves. *J Neural Transm Suppl*, 35, 85-95.
- AVANZINI, G., DE CURTIS, M., PANZICA, F. & SPREAFICO, R. 1989. Intrinsic properties of nucleus reticularis thalami neurones of the rat studied in vitro. *J Physiol*, 416, 111-22.
- AVANZINI, G., PANZICA, F. & DE CURTIS, M. 2000. The role of the thalamus in vigilance and epileptogenic mechanisms. *Clin Neurophysiol*, 111 Suppl 2, S19-26.
- AVOLI, M. 1980. Electroencephalographic and pathophysiologic features of rat parenteral penicillin epilepsy. *Exp Neurol*, 69, 373-82.
- AVOLI, M. & GLOOR, P. 1981. The effects of transient functional depression of the thalamus on spindles and on bilateral synchronous epileptic discharges of feline generalized penicillin epilepsy. *Epilepsia*, 22, 443-52.
- AVOLI, M. & GLOOR, P. 1982a. Interaction of cortex and thalamus in spike and wave discharges of feline generalized penicillin epilepsy. *Exp Neurol*, 76, 196-217.
- AVOLI, M. & GLOOR, P. 1982b. Role of the thalamus in generalized penicillin epilepsy: observations on decorticated cats. *Exp Neurol*, 77, 386-402.
- AVOLI, M., GLOOR, P., KOSTOPOULOS, G. & GOTMAN, J. 1983. An analysis of penicillin-induced generalized spike and wave discharges using simultaneous recordings of cortical and thalamic single neurons. *J Neurophysiol*, 50, 819-37.
- AVOLI, M., ROGAWSKI, M. A. & AVANZINI, G. 2001. Generalized epileptic disorders: an update. *Epilepsia*, 42, 445-57.
- BAL, T. & MCCORMICK, D. A. 1993. Mechanisms of oscillatory activity in guinea-pig nucleus reticularis thalami in vitro: a mammalian pacemaker. *J Physiol*, 468, 669-91.
- BANERJEE, P. K., HIRSCH, E. & SNEAD, O. C., 3RD 1993. gamma-Hydroxybutyric acid induced spike and wave discharges in rats: relation to high-affinity [3H]gamma-hydroxybutyric acid binding sites in the thalamus and cortex. *Neuroscience*, 56, 11-21.
- BANERJEE, P. K. & SNEAD, O. C., 3RD 1995. Presynaptic gamma-hydroxybutyric acid (GHB) and gamma-aminobutyric acidB (GABAB) receptor-mediated release of GABA and glutamate (GLU) in rat thalamic ventrobasal nucleus (VB): a possible mechanism for the generation of absence-like seizures induced by GHB. *J Pharmacol Exp Ther*, 273, 1534-43.

- BANERJEE, P. K., TILLAKARATNE, N. J., BRAILOWSKY, S., OLSEN, R. W., TOBIN, A. J. & SNEAD, O. C., 3RD 1998. Alterations in GABA_A receptor α 1 and α 4 subunit mRNA levels in thalamic relay nuclei following absence-like seizures in rats. *Exp Neurol*, 154, 213-23.
- BARE, M. A., GLAUSER, T. A. & STRAWSBURG, R. H. 1998. Need for electroencephalogram video confirmation of atypical absence seizures in children with Lennox-Gastaut syndrome. *J Child Neurol*, 13, 498-500.
- BAULAC, S., HUBERFELD, G., GOURFINKEL-AN, I., MITROPOULOU, G., BERANGER, A., PRUD'HOMME, J. F., BAULAC, M., BRICE, A., BRUZZONE, R. & LEGUERN, E. 2001. First genetic evidence of GABA_A receptor dysfunction in epilepsy: a mutation in the γ 2-subunit gene. *Nat Genet*, 28, 46-8.
- BEARDEN, L. J., SNEAD, O. C., HEALEY, C. T. & PEGRAM, G. V. 1980. Antagonism of gamma-hydroxybutyric acid-induced frequency shifts in the cortical EEG of rats by dipropylacetate. *Electroencephalogr Clin Neurophysiol*, 49, 181-3.
- BELELLI, D., CASULA, A., LING, A. & LAMBERT, J. J. 2002. The influence of subunit composition on the interaction of neurosteroids with GABA_A receptors. *Neuropharmacology*, 43, 651-61.
- BELELLI, D., HARRISON, N. L., MAGUIRE, J., MACDONALD, R. L., WALKER, M. C. & COPE, D. W. 2009. Extrasynaptic GABA_A receptors: form, pharmacology, and function. *J Neurosci*, 29, 12757-63.
- BELELLI, D., PEDEN, D. R., ROSAHL, T. W., WAFFORD, K. A. & LAMBERT, J. J. 2005. Extrasynaptic GABA_A receptors of thalamocortical neurons: a molecular target for hypnotics. *J Neurosci*, 25, 11513-20.
- BENKE, D., HONER, M., MICHEL, C., BETTLER, B. & MOHLER, H. 1999. gamma-aminobutyric acid type B receptor splice variant proteins GBR1a and GBR1b are both associated with GBR2 in situ and display differential regional and subcellular distribution. *J Biol Chem*, 274, 27323-30.
- BERKOVIC, S., HOWELL, R., HAY, D. & HOPPER, J. 1994. Epilepsies in twins. In: WOLF, P. (ed.) *Epileptic Seizures and Syndromes*. London: John Libbey.
- BERNASCONI, R., LAUBER, J., MARESCAUX, C., VERGNES, M., MARTIN, P., RUBIO, V., LEONHARDT, T., REYMANN, N. & BITTIGER, H. 1992. Experimental absence seizures: potential role of gamma-hydroxybutyric acid and GABAB receptors. *J Neural Transm Suppl*, 35, 155-77.
- BESSAIH, T., BOURGEGAS, L., BADIU, C. I., CARTER, D. A., TOTH, T. I., RUANO, D., LAMBOLEZ, B., CRUNELLI, V. & LERESCHE, N. 2006. Nucleus-specific abnormalities of GABAergic synaptic transmission in a genetic model of absence seizures. *J Neurophysiol*, 96, 3074-81.
- BESSMAN, S. P. & FISHBEIN, W. N. 1963. Gamma-Hydroxybutyrate, a Normal Brain Metabolite. *Nature*, 200, 1207-8.
- BETTLER, B., KAUPMANN, K. & BOWERY, N. 1998. GABA_B receptors: drugs meet clones. *Curr Opin Neurobiol*, 8, 345-50.
- BIANCHI, A. & GROUP, I. C. 1995. Study of concordance of symptoms in families with absence epilepsies. In: DUNCAN, J. & PANAYIOTOPOULOS, C. P. (eds.) *Typical Absences and Related Epileptic Syndromes*. London: Churchill Livingstone.
- BLUME, W. T., LUDERS, H. O., MIZRAHI, E., TASSINARI, C., VAN EMDE BOAS, W. & ENGEL, J., JR. 2001. Glossary of descriptive terminology for ictal

- semiology: report of the ILAE task force on classification and terminology. *Epilepsia*, 42, 1212-8.
- BO, G. P., FONZARI, M., SCOTTO, P. A. & BENASSI, E. 1984. Parenteral penicillin epilepsy: tolerance to subsequent treatments. *Exp Neurol*, 85, 229-32.
- BONANNO, G., FASSIO, A., SCHMID, G., SEVERI, P., SALA, R. & RAITERI, M. 1997. Pharmacologically distinct GABA_B receptors that mediate inhibition of GABA and glutamate release in human neocortex. *Br J Pharmacol*, 120, 60-4.
- BONANNO, G. & RAITERI, M. 1992. Functional evidence for multiple gamma-aminobutyric acid_B receptor subtypes in the rat cerebral cortex. *J Pharmacol Exp Ther*, 262, 114-8.
- BONANNO, G. & RAITERI, M. 1993. Multiple GABA_B receptors. *Trends Pharmacol Sci*, 14, 259-61.
- BORDEN, L. A. 1996. GABA transporter heterogeneity: pharmacology and cellular localization. *Neurochem Int*, 29, 335-56.
- BORMANN, J., HAMILL, O. P. & SAKMANN, B. 1987. Mechanism of anion permeation through channels gated by glycine and gamma-aminobutyric acid in mouse cultured spinal neurones. *J Physiol*, 385, 243-86.
- BOUE-GRABOT, E., ROUDBARAKI, M., BASCLES, L., TRAMU, G., BLOCH, B. & GARRET, M. 1998. Expression of GABA receptor rho subunits in rat brain. *J Neurochem*, 70, 899-907.
- BOUMA, P. A., WESTENDORP, R. G., VAN DIJK, J. G., PETERS, A. C. & BROUWER, O. F. 1996. The outcome of absence epilepsy: a meta-analysis. *Neurology*, 47, 802-8.
- BOWERY, N. G. 1993. GABA_B receptor pharmacology. *Annu Rev Pharmacol Toxicol*, 33, 109-47.
- BOWERY, N. G., BETTLER, B., FROESTL, W., GALLAGHER, J. P., MARSHALL, F., RAITERI, M., BONNER, T. I. & ENNA, S. J. 2002. International Union of Pharmacology. XXXIII. Mammalian gamma-aminobutyric acid (B) receptors: structure and function. *Pharmacol Rev*, 54, 247-64.
- BOWERY, N. G., DOBLE, A., HILL, D. R., HUDSON, A. L., SHAW, J. S., TURNBULL, M. J. & WARRINGTON, R. 1981. Bicuculline-insensitive GABA receptors on peripheral autonomic nerve terminals. *Eur J Pharmacol*, 71, 53-70.
- BOWERY, N. G. & ENNA, S. J. 2000. gamma-aminobutyric acid(B) receptors: first of the functional metabotropic heterodimers. *J Pharmacol Exp Ther*, 292, 2-7.
- BOWERY, N. G., HILL, D. R., HUDSON, A. L., DOBLE, A., MIDDLEMISS, D. N., SHAW, J. & TURNBULL, M. 1980. (-)Baclofen decreases neurotransmitter release in the mammalian CNS by an action at a novel GABA receptor. *Nature*, 283, 92-4.
- BOWERY, N. G., HUDSON, A. L. & PRICE, G. W. 1987. GABA_A and GABA_B receptor site distribution in the rat central nervous system. *Neuroscience*, 20, 365-83.
- BOWERY, N. G., PARRY, K., BOEHRER, A., MATHIVET, P., MARESCAUX, C. & BERNASCONI, R. 1999. Pertussis toxin decreases absence seizures and GABA_B receptor binding in thalamus of a genetically prone rat (GAERS). *Neuropharmacology*, 38, 1691-7.
- BRADFORD, H. F. 1995. Glutamate, GABA and epilepsy. *Prog Neurobiol*, 47, 477-511.

- BRANDON, N., JOVANOVIĆ, J. & MOSS, S. 2002. Multiple roles of protein kinases in the modulation of gamma-aminobutyric acid(A) receptor function and cell surface expression. *Pharmacol Ther*, 94, 113-22.
- BRICKLEY, S. G., CULL-CANDY, S. G. & FARRANT, M. 1996. Development of a tonic form of synaptic inhibition in rat cerebellar granule cells resulting from persistent activation of GABA_A receptors. *J Physiol*, 497 (Pt 3), 753-9.
- BRICKLEY, S. G., CULL-CANDY, S. G. & FARRANT, M. 1999. Single-channel properties of synaptic and extrasynaptic GABA_A receptors suggest differential targeting of receptor subtypes. *J Neurosci*, 19, 2960-73.
- BRICKLEY, S. G., REVILLA, V., CULL-CANDY, S. G., WISDEN, W. & FARRANT, M. 2001. Adaptive regulation of neuronal excitability by a voltage-independent potassium conductance. *Nature*, 409, 88-92.
- BRIGHT, D. P., ALLER, M. I. & BRICKLEY, S. G. 2007. Synaptic release generates a tonic GABA_A receptor-mediated conductance that modulates burst precision in thalamic relay neurons. *J Neurosci*, 27, 2560-9.
- BROWN, N., KERBY, J., BONNERT, T. P., WHITING, P. J. & WAFFORD, K. A. 2002. Pharmacological characterization of a novel cell line expressing human $\alpha 4\beta 3\delta$ GABA_A receptors. *Br J Pharmacol*, 136, 965-74.
- BUNGAY, P. M., MORRISON, P. F. & DEDRICK, R. L. 1990. Steady-state theory for quantitative microdialysis of solutes and water in vivo and in vitro. *Life Sci*, 46, 105-19.
- BURGESS, D. L., JONES, J. M., MEISLER, M. H. & NOEBELS, J. L. 1997. Mutation of the Ca²⁺ channel beta subunit gene Cchb4 is associated with ataxia and seizures in the lethargic (*lh*) mouse. *Cell*, 88, 385-92.
- BURGESS, D. L. & NOEBELS, J. L. 1999. Single gene defects in mice: the role of voltage-dependent calcium channels in absence models. *Epilepsy Res*, 36, 111-22.
- CADDICK, S. J., WANG, C., FLETCHER, C. F., JENKINS, N. A., COPELAND, N. G. & HOSFORD, D. A. 1999. Excitatory but not inhibitory synaptic transmission is reduced in lethargic (Cacnb4(lh)) and tottering (Cacnalatg) mouse thalami. *J Neurophysiol*, 81, 2066-74.
- CALLENBACH, P. M., BOUMA, P. A., GEERTS, A. T., ARTS, W. F., STROINK, H., PEETERS, E. A., VAN DONSELAAR, C. A., PETERS, A. C. & BROUWER, O. F. 2009. Long-term outcome of childhood absence epilepsy: Dutch Study of Epilepsy in Childhood. *Epilepsy Res*, 83, 249-56.
- CALVER, A. R., ROBBINS, M. J., COSIO, C., RICE, S. Q., BABBS, A. J., HIRST, W. D., BOYFIELD, I., WOOD, M. D., RUSSELL, R. B., PRICE, G. W., COUVE, A., MOSS, S. J. & PANGALOS, M. N. 2001. The C-terminal domains of the GABA_B receptor subunits mediate intracellular trafficking but are not required for receptor signaling. *J Neurosci*, 21, 1203-10.
- CAMERINO, D. C., TRICARICO, D. & DESAPHY, J. F. 2007. Ion channel pharmacology. *Neurotherapeutics*, 4, 184-98.
- CARAISCOS, V. B., ELLIOTT, E. M., YOU-TEN, K. E., CHENG, V. Y., BELELLI, D., NEWELL, J. G., JACKSON, M. F., LAMBERT, J. J., ROSAHL, T. W., WAFFORD, K. A., MACDONALD, J. F. & ORSER, B. A. 2004. Tonic inhibition in mouse hippocampal CA1 pyramidal neurons is mediated by alpha5 subunit-containing gamma-aminobutyric acid type A receptors. *Proc Natl Acad Sci U S A*, 101, 3662-7.

- CARMANT, L., KRAMER, U., HOLMES, G. L., MIKATI, M. A., RIVIELLO, J. J. & HELMERS, S. L. 1996. Differential diagnosis of staring spells in children: a video-EEG study. *Pediatr Neurol*, 14, 199-202.
- CASTELLI, M. P., MOCCI, I., LANGLOIS, X., GOMMERENDAGGER, W., LUYTEN, W. H., LEYSEN, J. E. & GESSA, G. L. 2000. Quantitative autoradiographic distribution of gamma-hydroxybutyric acid binding sites in human and monkey brain. *Brain Res Mol Brain Res*, 78, 91-9.
- CASTELLI, M. P., PIBIRI, F., CARBONI, G. & PIRAS, A. P. 2004. A review of pharmacology of NCS-382, a putative antagonist of gamma-hydroxybutyric acid (GHB) receptor. *CNS Drug Rev*, 10, 243-60.
- CHAHBOUNE, H., MISHRA, A. M., DESALVO, M. N., STAIB, L. H., PURCARO, M., SCHEINOST, D., PAPADEMETRIS, X., FYSON, S. J., LORINCZ, M. L., CRUNELLI, V., HYDER, F. & BLUMENFELD, H. 2009. DTI abnormalities in anterior corpus callosum of rats with spike-wave epilepsy. *Neuroimage*, 47, 459-66.
- CHANDRA, D., JIA, F., LIANG, J., PENG, Z., SURYANARAYANAN, A., WERNER, D. F., SPIGELMAN, I., HOUSER, C. R., OLSEN, R. W., HARRISON, N. L. & HOMANICS, G. E. 2006. GABA_A receptor $\alpha 4$ subunits mediate extrasynaptic inhibition in thalamus and dentate gyrus and the action of gaboxadol. *Proc Natl Acad Sci U S A*, 103, 15230-5.
- CHANG, Y., WANG, R., BAROT, S. & WEISS, D. S. 1996. Stoichiometry of a recombinant GABA_A receptor. *J Neurosci*, 16, 5415-24.
- CHARPIER, S., LERESCHE, N., DENIAU, J. M., MAHON, S., HUGHES, S. W. & CRUNELLI, V. 1999. On the putative contribution of GABA_B receptors to the electrical events occurring during spontaneous spike and wave discharges. *Neuropharmacology*, 38, 1699-706.
- CHEN, L., CHETKOVICH, D. M., PETRALIA, R. S., SWEENEY, N. T., KAWASAKI, Y., WENTHOLD, R. J., BREDDT, D. S. & NICOLL, R. A. 2000. Stargazin regulates synaptic targeting of AMPA receptors by two distinct mechanisms. *Nature*, 408, 936-43.
- CHEUNG, H., KAMP, D. & HARRIS, E. 1992. An in vitro investigation of the action of lamotrigine on neuronal voltage-activated sodium channels. *Epilepsy Res*, 13, 107-12.
- CHOI, D. S., WEI, W., DEITCHMAN, J. K., KHARAZIA, V. N., LESSCHER, H. M., MCMAHON, T., WANG, D., QI, Z. H., SIEGHART, W., ZHANG, C., SHOKAT, K. M., MODY, I. & MESSING, R. O. 2008. Protein kinase C δ regulates ethanol intoxication and enhancement of GABA-stimulated tonic current. *J Neurosci*, 28, 11890-9.
- COENEN, A. M., BLEZER, E. H. & VAN LUIJTELAAR, E. L. 1995. Effects of the GABA-uptake inhibitor tiagabine on electroencephalogram, spike-wave discharges and behaviour of rats. *Epilepsy Res*, 21, 89-94.
- COENEN, A. M., DRINKENBURG, W. H., INOUE, M. & VAN LUIJTELAAR, E. L. 1992. Genetic models of absence epilepsy, with emphasis on the WAG/Rij strain of rats. *Epilepsy Res*, 12, 75-86.
- COENEN, A. M., DRINKENBURG, W. H., PEETERS, B. W., VOSSSEN, J. M. & VAN LUIJTELAAR, E. L. 1991. Absence epilepsy and the level of vigilance in rats of the WAG/Rij strain. *Neurosci Biobehav Rev*, 15, 259-63.
- COENEN, A. M. & VAN LUIJTELAAR, E. L. 1987. The WAG/Rij rat model for absence epilepsy: age and sex factors. *Epilepsy Res*, 1, 297-301.

- COENEN, A. M. & VAN LUIJTELAAR, E. L. 2003. Genetic animal models for absence epilepsy: a review of the WAG/Rij strain of rats. *Behav Genet*, 33, 635-55.
- CONTI, F., MINELLI, A. & MELONE, M. 2004. GABA transporters in the mammalian cerebral cortex: localization, development and pathological implications. *Brain Res Brain Res Rev*, 45, 196-212.
- CONTRERAS, D. & STERIADE, M. 1995. Cellular basis of EEG slow rhythms: a study of dynamic corticothalamic relationships. *J Neurosci*, 15, 604-22.
- COPE, D. W., DI GIOVANNI, G., FYSON, S. J., ORBAN, G., ERRINGTON, A. C., LORINCZ, M. L., GOULD, T. M., CARTER, D. A. & CRUNELLI, V. 2009. Enhanced tonic GABA_A inhibition in typical absence epilepsy. *Nat Med*, 15, 1392-8.
- COPE, D. W., HUGHES, S. W. & CRUNELLI, V. 2005. GABA_A receptor-mediated tonic inhibition in thalamic neurons. *J Neurosci*, 25, 11553-63.
- CORTEZ, M. A., MCKERLIE, C. & SNEAD, O. C., 3RD 2001. A model of atypical absence seizures: EEG, pharmacology, and developmental characterization. *Neurology*, 56, 341-9.
- COULTER, D. A., HUGUENARD, J. R. & PRINCE, D. A. 1989a. Characterization of ethosuximide reduction of low-threshold calcium current in thalamic neurons. *Ann Neurol*, 25, 582-93.
- COULTER, D. A., HUGUENARD, J. R. & PRINCE, D. A. 1989b. Specific petit mal anticonvulsants reduce calcium currents in thalamic neurons. *Neurosci Lett*, 98, 74-8.
- COULTER, D. A., HUGUENARD, J. R. & PRINCE, D. A. 1990. Differential effects of petit mal anticonvulsants and convulsants on thalamic neurones: calcium current reduction. *Br J Pharmacol*, 100, 800-6.
- COUVE, A., FILIPPOV, A. K., CONNOLLY, C. N., BETTLER, B., BROWN, D. A. & MOSS, S. J. 1998. Intracellular retention of recombinant GABA_B receptors. *J Biol Chem*, 273, 26361-7.
- CRISTOVAO-FERREIRA, S., VAZ, S. H., RIBEIRO, J. A. & SEBASTIAO, A. M. 2009. Adenosine A2A receptors enhance GABA transport into nerve terminals by restraining PKC inhibition of GAT-1. *J Neurochem*, 109, 336-47.
- CRUNELLI, V., EMRI, Z. & LERESCHE, N. 2006. Unravelling the brain targets of gamma-hydroxybutyric acid. *Curr Opin Pharmacol*, 6, 44-52.
- CRUNELLI, V., HABY, M., JASSIK-GERSCHENFELD, D., LERESCHE, N. & PIRCHIO, M. 1988. Cl⁻ and K⁺-dependent inhibitory postsynaptic potentials evoked by interneurons of the rat lateral geniculate nucleus. *J Physiol*, 399, 153-76.
- CRUNELLI, V. & LERESCHE, N. 2002b. Block of Thalamic T-Type Ca²⁺ Channels by Ethosuximide Is Not the Whole Story. *Epilepsy Curr*, 2, 53-56.
- CRUNELLI, V. & LERESCHE, N. 2002a. Childhood absence epilepsy: genes, channels, neurons and networks. *Nat Rev Neurosci*, 3, 371-82.
- CRUNELLI, V., LIGHTOWLER, S. & POLLARD, C. E. 1989. A T-type Ca²⁺ current underlies low-threshold Ca²⁺ potentials in cells of the cat and rat lateral geniculate nucleus. *J Physiol*, 413, 543-61.
- CURTIS, D. R., GYNTHNER, B. D., LACEY, G. & BEATTIE, D. T. 1997. Baclofen: reduction of presynaptic calcium influx in the cat spinal cord in vivo. *Exp Brain Res*, 113, 520-33.

- DANOBER, L., DERANSART, C., DEPAULIS, A., VERGNES, M. & MARESCAUX, C. 1998. Pathophysiological mechanisms of genetic absence epilepsy in the rat. *Prog Neurobiol*, 55, 27-57.
- DAVSON, H., WELCH, K. & SEGAL, M. 1987. *Physiology and Pathophysiology of the Cerebrospinal Fluid*, Churchill Livingstone.
- DE BIASI, S., AMADEO, A., ARCELLI, P., FRASSONI, C., MERONI, A. & SPREAFICO, R. 1996. Ultrastructural characterization of the postnatal development of the thalamic ventrobasal and reticular nuclei in the rat. *Anat Embryol (Berl)*, 193, 341-53.
- DE BIASI, S., AMADEO, A., ARCELLI, P., FRASSONI, C. & SPREAFICO, R. 1997. Postnatal development of GABA-immunoreactive terminals in the reticular and ventrobasal nuclei of the rat thalamus: a light and electron microscopic study. *Neuroscience*, 76, 503-15.
- DE BIASI, S. & RUSTIONI, A. 1990. Ultrastructural immunocytochemical localization of excitatory amino acids in the somatosensory system. *J Histochem Cytochem*, 38, 1745-54.
- DE BIASI, S., VITELLARO-ZUCCARELLO, L. & BRECHA, N. C. 1998. Immunoreactivity for the GABA transporter-1 and GABA transporter-3 is restricted to astrocytes in the rat thalamus. A light and electron-microscopic immunolocalization. *Neuroscience*, 83, 815-28.
- DEISZ, R. A., BILLARD, J. M. & ZIEGLGANSBERGER, W. 1997. Presynaptic and postsynaptic GABA_B receptors of neocortical neurons of the rat in vitro: differences in pharmacology and ionic mechanisms. *Synapse*, 25, 62-72.
- DELANTY, N. & FRENCH, J. 1988. Treatment of Lennox-Gastaut Syndrome: Current Recommendations. *CNS Drugs*, 10, 181-188.
- DENG, P. Y., XIAO, Z., YANG, C., ROJANATHAMMANEE, L., GRISANTI, L., WATT, J., GEIGER, J. D., LIU, R., PORTER, J. E. & LEI, S. 2009. GABA_B receptor activation inhibits neuronal excitability and spatial learning in the entorhinal cortex by activating TREK-2 K⁺ channels. *Neuron*, 63, 230-43.
- DEPAULIS, A., BOURGUIGNON, J. J., MARESCAUX, C., VERGNES, M., SCHMITT, M., MICHELETTI, G. & WARTER, J. M. 1988. Effects of gamma-hydroxybutyrate and gamma-butyrolactone derivatives on spontaneous generalized non-convulsive seizures in the rat. *Neuropharmacology*, 27, 683-9.
- DESCHENES, M., VEINANTE, P. & ZHANG, Z. W. 1998. The organization of corticothalamic projections: reciprocity versus parity. *Brain Res Brain Res Rev*, 28, 286-308.
- DI GIOVANNI, G., COPE, D. & CRUNELLI, V. 2008. Cholinergic and monoaminergic modulation of tonic GABA_A inhibition in the rat dorsal lateral geniculate nucleus. *Society for Neuroscience: Abstract*. Washington DC.
- DOMICH, L., OAKSON, G. & STERIADE, M. 1986. Thalamic burst patterns in the naturally sleeping cat: a comparison between cortically projecting and reticularis neurones. *J Physiol*, 379, 429-49.
- DOZE, V. A., COHEN, G. A. & MADISON, D. V. 1995. Calcium channel involvement in GABA_B receptor-mediated inhibition of GABA release in area CA1 of the rat hippocampus. *J Neurophysiol*, 74, 43-53.
- DRASBEK, K. R., CHRISTENSEN, J. & JENSEN, K. 2006. γ -hydroxybutyrate - a drug of abuse. *Acta Neurol Scand*, 114, 145-56.
- DRASBEK, K. R., HOESTGAARD-JENSEN, K. & JENSEN, K. 2007. Modulation of extrasynaptic THIP conductances by GABA_A-receptor modulators in mouse neocortex. *J Neurophysiol*, 97, 2293-300.

- DRASBEK, K. R. & JENSEN, K. 2006. THIP, a hypnotic and antinociceptive drug, enhances an extrasynaptic GABA_A receptor-mediated conductance in mouse neocortex. *Cereb Cortex*, 16, 1134-41.
- DRASBEK, K. R., VARDYA, I., DELENCLOS, M., GIBSON, K. M. & JENSEN, K. 2008. SSADH deficiency leads to elevated extracellular GABA levels and increased GABAergic neurotransmission in the mouse cerebral cortex. *J Inherit Metab Dis*, 31, 662-8.
- DRINKENBURG, W. H., COENEN, A. M., VOSSSEN, J. M. & VAN LUIJTELAAR, E. L. 1991. Spike-wave discharges and sleep-wake states in rats with absence epilepsy. *Epilepsy Res*, 9, 218-24.
- DRINKENBURG, W. H., VAN LUIJTELAAR, E. L., VAN SCHAIJK, W. J. & COENEN, A. M. 1993. Aberrant transients in the EEG of epileptic rats: a spectral analytical approach. *Physiol Behav*, 54, 779-83.
- DUNCAN, J. S. 1997. Idiopathic generalized epilepsies with typical absences. *J Neurol*, 244, 403-11.
- DUNG, H. C. 1977. Deficiency in the thymus-dependent immunity in "lethargic" mutant mice. *Transplantation*, 23, 39-43.
- DUNG, H. C., LAWSON, R. L. & STEVENS, M. 1977. A study of the increased serum level of IgG1 in 'lethargic' mice combined with a depressed thymus-dependent lymphoid system. *J Immunogenet*, 4, 287-93.
- DUNG, H. C. & SWIGART, R. H. 1972. Histo-pathologic observations of the nervous and lymphoid tissues of "lethargic" mutant mice. *Tex Rep Biol Med*, 30, 23-39.
- DUTAR, P. & NICOLL, R. A. 1988. A physiological role for GABA_B receptors in the central nervous system. *Nature*, 332, 156-8.
- EHLEN, J. C. & PAUL, K. N. 2009. Regulation of light's action in the mammalian circadian clock: role of the extrasynaptic GABA_A receptor. *Am J Physiol Regul Integr Comp Physiol*, 296, R1606-12.
- EMRI, Z., ANTAL, K. & CRUNELLI, V. 1996b. γ -hydroxybutyric acid decreases thalamic sensory excitatory postsynaptic potentials by an action on presynaptic GABA_B receptors. *Neurosci Lett*, 216, 121-4.
- EMRI, Z., TURNER, J. P. & CRUNELLI, V. 1996. Tonic activation of presynaptic GABA_B receptors on thalamic sensory afferents. *Neuroscience*, 72, 689-98.
- ENGEL, J., JR. 2001. A proposed diagnostic scheme for people with epileptic seizures and with epilepsy: report of the ILAE Task Force on Classification and Terminology. *Epilepsia*, 42, 796-803.
- ENGEL, J., JR. 2006a. ILAE classification of epilepsy syndromes. *Epilepsy Res*, 70 Suppl 1, S5-10.
- ENGEL, J., JR. 2006b. Report of the ILAE classification core group. *Epilepsia*, 47, 1558-68.
- ESSRICH, C., LOREZ, M., BENSON, J. A., FRITSCHY, J. M. & LUSCHER, B. 1998. Postsynaptic clustering of major GABA_A receptor subtypes requires the γ 2 subunit and gephyrin. *Nat Neurosci*, 1, 563-71.
- ETTINGER, A. B., BERNAL, O. G., ANDRIOLA, M. R., BAGCHI, S., FLORES, P., JUST, C., PITOCCHIO, C., ROONEY, T., TUOMINEN, J. & DEVINSKY, O. 1999. Two cases of nonconvulsive status epilepticus in association with tiagabine therapy. *Epilepsia*, 40, 1159-62.
- FARIELLO, R. G. 1979. Action of inhibitory amino acids on acute epileptic foci: an electrographic study. *Exp Neurol*, 66, 55-63.
- FARIELLO, R. G. & GOLDEN, G. T. Year. Chronic administration of THIP: An experimental model of bilaterally synchronous spikes and waves in rats. *In:*

- EPILEPSIA, ed. Annual Meeting of the American Epilepsy Society, 1983 Phoenix, Arizona. Raven Press, New York, 245 - 262.
- FARIELLO, R. G. & GOLDEN, G. T. 1987. The THIP-induced model of bilateral synchronous spike and wave in rodents. *Neuropharmacology*, 26, 161-5.
- FARRANT, M. & NUSSER, Z. 2005. Variations on an inhibitory theme: phasic and tonic activation of GABA_A receptors. *Nat Rev Neurosci*, 6, 215-29.
- FARWELL, J. R., DODRILL, C. B. & BATZEL, L. W. 1985. Neuropsychological abilities of children with epilepsy. *Epilepsia*, 26, 395-400.
- FEUCHT, M., FUCHS, K., PICHLBAUER, E., HORNIK, K., SCHARFETTER, J., GOESSLER, R., FUREDOR, T., CVETKOVIC, N., SIEGHART, W., KASPER, S. & ASCHAUER, H. 1999. Possible association between childhood absence epilepsy and the gene encoding GABRB3. *Biol Psychiatry*, 46, 997-1002.
- FISHER, R. S. & PRINCE, D. A. 1977. Spike-wave rhythms in cat cortex induced by parenteral penicillin. II. Cellular features. *Electroencephalogr Clin Neurophysiol*, 42, 625-39.
- FISHER, R. S., VAN EMDE BOAS, W., BLUME, W., ELGER, C., GENTON, P., LEE, P. & ENGEL, J., JR. 2005. Epileptic seizures and epilepsy: definitions proposed by the International League Against Epilepsy (ILAE) and the International Bureau for Epilepsy (IBE). *Epilepsia*, 46, 470-2.
- FITZPATRICK, D., PENNY, G. R. & SCHMECHEL, D. E. 1984. Glutamic acid decarboxylase-immunoreactive neurons and terminals in the lateral geniculate nucleus of the cat. *J Neurosci*, 4, 1809-29.
- FLETCHER, C. F., LUTZ, C. M., O'SULLIVAN, T. N., SHAUGHNESSY, J. D., JR., HAWKES, R., FRANKEL, W. N., COPELAND, N. G. & JENKINS, N. A. 1996. Absence epilepsy in tottering mutant mice is associated with calcium channel defects. *Cell*, 87, 607-17.
- FOJTIKOVA, D., BRAZDIL, M., HORKY, J., MIKL, M., KUBA, R., KRUPA, P. & REKTOR, I. 2006. Magnetic resonance spectroscopy of the thalamus in patients with typical absence epilepsy. *Seizure*, 15, 533-40.
- FRITSCHY, J. M. 2008. Epilepsy, E/I Balance and GABA_A Receptor Plasticity. *Front Mol Neurosci*, 1, 5.
- FRITSCHY, J. M., MESKENAITE, V., WEINMANN, O., HONER, M., BENKE, D. & MOHLER, H. 1999. GABA_B receptor splice variants GB_{1a} and GB_{1b} in rat brain: developmental regulation, cellular distribution and extrasynaptic localization. *Eur J Neurosci*, 11, 761-8.
- GABBOTT, P. L., SOMOGYI, J., STEWART, M. G. & HAMORI, J. 1986. A quantitative investigation of the neuronal composition of the rat dorsal lateral geniculate nucleus using GABA-immunocytochemistry. *Neuroscience*, 19, 101-11.
- GAHWILER, B. H. & BROWN, D. A. 1985. GABA_B receptor-activated K⁺ current in voltage-clamped CA3 pyramidal cells in hippocampal cultures. *Proc Natl Acad Sci U S A*, 82, 1558-62.
- GALVAN, A., SMITH, Y. & WICHMANN, T. 2003. Continuous monitoring of intracerebral glutamate levels in awake monkeys using microdialysis and enzyme fluorometric detection. *J Neurosci Methods*, 126, 175-85.
- GERVASI, N., MONNIER, Z., VINCENT, P., PAUPARDIN-TRITSCH, D., HUGHES, S. W., CRUNELLI, V. & LERESCHE, N. 2003. Pathway-specific action of gamma-hydroxybutyric acid in sensory thalamus and its relevance to absence seizures. *J Neurosci*, 23, 11469-78.

- GIBOR, G., YAKUBOVICH, D., PERETZ, A. & ATTALI, B. 2004. External barium affects the gating of KCNQ1 potassium channels and produces a pore block via two discrete sites. *J Gen Physiol*, 124, 83-102.
- GLAUSER, T. A., CNAAN, A., SHINNAR, S., HIRTZ, D. G., DLUGOS, D., MASUR, D., CLARK, P. O., CAPPARELLI, E. V. & ADAMSON, P. C. 2010. Ethosuximide, valproic acid, and lamotrigine in childhood absence epilepsy. *N Engl J Med*, 362, 790-9.
- GLOOR, P. & FARIELLO, R. G. 1988. Generalized epilepsy: some of its cellular mechanisms differ from those of focal epilepsy. *Trends Neurosci*, 11, 63-8.
- GLOOR, P., QUESNEY, L. F. & ZUMSTEIN, H. 1977. Pathophysiology of generalized penicillin epilepsy in the cat: the role of cortical and subcortical structures. II. Topical application of penicillin to the cerebral cortex and to subcortical structures. *Electroencephalogr Clin Neurophysiol*, 43, 79-94.
- GLYKYS, J. & MODY, I. 2007a. Activation of GABA_A receptors: views from outside the synaptic cleft. *Neuron*, 56, 763-70.
- GLYKYS, J. & MODY, I. 2007b. The main source of ambient GABA responsible for tonic inhibition in the mouse hippocampus. *J Physiol*, 582, 1163-78.
- GLYKYS, J., PENG, Z., CHANDRA, D., HOMANICS, G. E., HOUSER, C. R. & MODY, I. 2007. A new naturally occurring GABA_A receptor subunit partnership with high sensitivity to ethanol. *Nat Neurosci*, 10, 40-8.
- GODSCHALK, M., DZOLJIC, M. R. & BONTA, I. L. 1976. Antagonism of γ -hydroxybutyrate-induced hypersynchronization in the ECoG of the rat by anti-petit mal drugs. *Neurosci Lett*, 3, 145-50.
- GODSCHALK, M., DZOLJIC, M. R. & BONTA, I. L. 1977. Slow wave sleep and a state resembling absence epilepsy induced in the rat by gamma-hydroxybutyrate. *Eur J Pharmacol*, 44, 105-11.
- GOLSHANI, P., LIU, X. B. & JONES, E. G. 2001. Differences in quantal amplitude reflect GluR4- subunit number at corticothalamic synapses on two populations of thalamic neurons. *Proc Natl Acad Sci U S A*, 98, 4172-7.
- GROENEWEGEN, H. & WITTER, M. 2004. Thalamus. In: PAXINOS, G. (ed.) *The Rat Nervous System Third Edition*. San Diego: Elsevier Academic Press.
- GUBERMAN, A., GLOOR, P. & SHERWIN, A. L. 1975. Response of generalized penicillin epilepsy in the cat to ethosuximide and diphenylhydantoin. *Neurology*, 25, 785-64.
- HABLITZ, J. J. & THALMANN, R. H. 1987. Conductance changes underlying a late synaptic hyperpolarization in hippocampal CA3 neurons. *J Neurophysiol*, 58, 160-79.
- HAHNER, L., MCQUILKIN, S. & HARRIS, R. A. 1991. Cerebellar GABA_B receptors modulate function of GABA_A receptors. *Faseb J*, 5, 2466-72.
- HAINSWORTH, A. H., MCNAUGHTON, N. C., PEREVERZEV, A., SCHNEIDER, T. & RANDALL, A. D. 2003. Actions of sipatrigine, 202W92 and lamotrigine on R-type and T-type Ca²⁺ channel currents. *Eur J Pharmacol*, 467, 77-80.
- HAMANN, M., ROSSI, D. J. & ATTWELL, D. 2002. Tonic and spillover inhibition of granule cells control information flow through cerebellar cortex. *Neuron*, 33, 625-33.
- HARRIS, R. E., LARSSON, H. P. & ISACOFF, E. Y. 1998. A permanent ion binding site located between two gates of the Shaker K⁺ channel. *Biophys J*, 74, 1808-20.

- HASHIMOTO, K., FUKAYA, M., QIAO, X., SAKIMURA, K., WATANABE, M. & KANO, M. 1999. Impairment of AMPA receptor function in cerebellar granule cells of ataxic mutant mouse stargazer. *J Neurosci*, 19, 6027-36.
- HASHIMOTO, T. & KURIYAMA, K. 1997. In vivo evidence that GABA_B receptors are negatively coupled to adenylate cyclase in rat striatum. *J Neurochem*, 69, 365-70.
- HECHLER, V., RATOMPONIRINA, C. & MAITRE, M. 1997. γ -Hydroxybutyrate conversion into GABA induces displacement of GABA_B binding that is blocked by valproate and ethosuximide. *J Pharmacol Exp Ther*, 281, 753-60.
- HELLER, A. H., DICHTER, M. A. & SIDMAN, R. L. 1983. Anticonvulsant sensitivity of absence seizures in the tottering mutant mouse. *Epilepsia*, 24, 25-34.
- HERD, M. B., BELELLI, D. & LAMBERT, J. J. 2007. Neurosteroid modulation of synaptic and extrasynaptic GABA_A receptors. *Pharmacol Ther*, 116, 20-34.
- HILL, D. R. & BOWERY, N. G. 1981. ³H-baclofen and ³H-GABA bind to bicuculline-insensitive GABA_B sites in rat brain. *Nature*, 290, 149-52.
- HILLE, B. 1992. G protein-coupled mechanisms and nervous signaling. *Neuron*, 9, 187-95.
- HIRONO, M., YOSHIOKA, T. & KONISHI, S. 2001. GABA_B receptor activation enhances mGluR-mediated responses at cerebellar excitatory synapses. *Nat Neurosci*, 4, 1207-16.
- HOCHT, C., OPEZZO, J. A. & TAIRA, C. A. 2007. Applicability of reverse microdialysis in pharmacological and toxicological studies. *J Pharmacol Toxicol Methods*, 55, 3-15.
- HOLMES, G. L., MCKEEVER, M. & ADAMSON, M. 1987. Absence seizures in children: clinical and electroencephalographic features. *Ann Neurol*, 21, 268-73.
- HOSFORD, D. A., CLARK, S., CAO, Z., WILSON, W. A., JR., LIN, F. H., MORRISETT, R. A. & HUIN, A. 1992. The role of GABA_B receptor activation in absence seizures of lethargic (*lh/lh*) mice. *Science*, 257, 398-401.
- HOSFORD, D. A., LIN, F. H., KRAEMER, D. L., CAO, Z., WANG, Y. & WILSON, J. T., JR. 1995. Neural network of structures in which GABA_B receptors regulate absence seizures in the lethargic (*lh/lh*) mouse model. *J Neurosci*, 15, 7367-76.
- HOSFORD, D. A. & WANG, Y. 1997. Utility of the lethargic (*lh/lh*) mouse model of absence seizures in predicting the effects of lamotrigine, vigabatrin, tiagabine, gabapentin, and topiramate against human absence seizures. *Epilepsia*, 38, 408-14.
- HOSFORD, D. A., WANG, Y. & CAO, Z. 1997. Differential effects mediated by GABA_A receptors in thalamic nuclei in *lh/lh* model of absence seizures. *Epilepsy Res*, 27, 55-65.
- HOWE, J. R. & ZIEGLGANSBERGER, W. 1986. D-baclofen does not antagonize the actions of L-baclofen on rat neocortical neurons in vitro. *Neurosci Lett*, 72, 99-104.
- HUGUENARD, J. R., COULTER, D. A. & PRINCE, D. A. 1991. A fast transient potassium current in thalamic relay neurons: kinetics of activation and inactivation. *J Neurophysiol*, 66, 1304-15.
- HUGUENARD, J. R. & PRINCE, D. A. 1991. Slow inactivation of a TEA-sensitive K current in acutely isolated rat thalamic relay neurons. *J Neurophysiol*, 66, 1316-28.
- HUGUENARD, J. R. & PRINCE, D. A. 1992. A novel T-type current underlies prolonged Ca(2+)-dependent burst firing in GABAergic neurons of rat thalamic reticular nucleus. *J Neurosci*, 12, 3804-17.

- HUGUENARD, J. R. & PRINCE, D. A. 1994. Intrathalamic rhythmicity studied in vitro: nominal T-current modulation causes robust antioscillatory effects. *J Neurosci*, 14, 5485-502.
- HUIDOBRO-TORO, J. P., VALENZUELA, C. F. & HARRIS, R. A. 1996. Modulation of GABA_A receptor function by G protein-coupled 5-HT_{2C} receptors. *Neuropharmacology*, 35, 1355-63.
- IKEDA, S. R. 1996. Voltage-dependent modulation of N-type calcium channels by G-protein $\beta\gamma$ subunits. *Nature*, 380, 255-8.
- IKEGAKI, N., SAITO, N., HASHIMA, M. & TANAKA, C. 1994. Production of specific antibodies against GABA transporter subtypes (GAT1, GAT2, GAT3) and their application to immunocytochemistry. *Brain Res Mol Brain Res*, 26, 47-54.
- ILAE 1981. Proposal for revised clinical and electroencephalographic classification of epileptic seizures. From the Commission on Classification and Terminology of the International League Against Epilepsy. *Epilepsia*, 22, 489-501.
- ILAE 1989. Proposal for revised classification of epilepsies and epileptic syndromes. Commission on Classification and Terminology of the International League Against Epilepsy. *Epilepsia*, 30, 389-99.
- INOUE, M., DUYSSENS, J., VOSSEN, J. M. & COENEN, A. M. 1993. Thalamic multiple-unit activity underlying spike-wave discharges in anesthetized rats. *Brain Res*, 612, 35-40.
- INOUE, M., MATSUO, T. & OGATA, N. 1985a. Baclofen activates voltage-dependent and 4-aminopyridine sensitive K⁺ conductance in guinea-pig hippocampal pyramidal cells maintained *in vitro*. *Br J Pharmacol*, 84, 833-41.
- INOUE, M., MATSUO, T. & OGATA, N. 1985b. Possible involvement of K⁺-conductance in the action of gamma-aminobutyric acid in the guinea-pig hippocampus. *Br J Pharmacol*, 86, 515-24.
- ISOMOTO, S., KAIBARA, M., SAKURAI-YAMASHITA, Y., NAGAYAMA, Y., UEZONO, Y., YANO, K. & TANIYAMA, K. 1998. Cloning and tissue distribution of novel splice variants of the rat GABA_B receptor. *Biochem Biophys Res Commun*, 253, 10-5.
- IVANOV, A., TYZIO, R., ZILBERTER, Y. & BEN-ARI, Y. 2008. (R)-roscovitine, a cyclin-dependent kinase inhibitor, enhances tonic GABA inhibition in rat hippocampus. *Neuroscience*, 156, 277-88.
- JAHNSEN, H. & LLINAS, R. 1984a. Electrophysiological properties of guinea-pig thalamic neurones: an *in vitro* study. *J Physiol*, 349, 205-26.
- JAHNSEN, H. & LLINAS, R. 1984b. Ionic basis for the electro-responsiveness and oscillatory properties of guinea-pig thalamic neurones *in vitro*. *J Physiol*, 349, 227-47.
- JAKAB, R. L. & HAMORI, J. 1988. Quantitative morphology and synaptology of cerebellar glomeruli in the rat. *Anat Embryol (Berl)*, 179, 81-8.
- JIA, F., CHANDRA, D., HOMANICS, G. E. & HARRISON, N. L. 2008a. Ethanol modulates synaptic and extrasynaptic GABA_A receptors in the thalamus. *J Pharmacol Exp Ther*, 326, 475-82.
- JIA, F., GOLDSTEIN, P. A. & HARRISON, N. L. 2009. The modulation of synaptic GABA_A receptors in the thalamus by eszopiclone and zolpidem. *J Pharmacol Exp Ther*, 328, 1000-6.
- JIA, F., PIGNATARO, L., SCHOFIELD, C. M., YUE, M., HARRISON, N. L. & GOLDSTEIN, P. A. 2005. An extrasynaptic GABA_A receptor mediates tonic inhibition in thalamic VB neurons. *J Neurophysiol*, 94, 4491-501.

- JIA, F., YUE, M., CHANDRA, D., HOMANICS, G. E., GOLDSTEIN, P. A. & HARRISON, N. L. 2008b. Isoflurane is a potent modulator of extrasynaptic GABA_A receptors in the thalamus. *J Pharmacol Exp Ther*, 324, 1127-35.
- JIA, F., YUE, M., CHANDRA, D., KERAMIDAS, A., GOLDSTEIN, P. A., HOMANICS, G. E. & HARRISON, N. L. 2008c. Taurine is a potent activator of extrasynaptic GABA_A receptors in the thalamus. *J Neurosci*, 28, 106-15.
- JIANG, Y. & MACKINNON, R. 2000. The barium site in a potassium channel by x-ray crystallography. *J Gen Physiol*, 115, 269-72.
- JOHNSTON, G. A. 1996. GABA_C receptors: relatively simple transmitter-gated ion channels? *Trends Pharmacol Sci*, 17, 319-23.
- JONES, E. 1985. *The Thalamus*, New York & London, Plenum Press.
- JONES, K. A., BOROWSKY, B., TAMM, J. A., CRAIG, D. A., DURKIN, M. M., DAI, M., YAO, W. J., JOHNSON, M., GUNWALDSEN, C., HUANG, L. Y., TANG, C., SHEN, Q., SALON, J. A., MORSE, K., LAZ, T., SMITH, K. E., NAGARATHNAM, D., NOBLE, S. A., BRANCHEK, T. A. & GERALD, C. 1998. GABA_B receptors function as a heteromeric assembly of the subunits GABA_BR₁ and GABA_BR₂. *Nature*, 396, 674-9.
- JUHASZ, G., KEKESI, K., EMRI, Z., SOLTESZ, I. & CRUNELLI, V. 1990. Sleep-promoting action of excitatory amino acid antagonists: a different role for thalamic NMDA and non-NMDA receptors. *Neurosci Lett*, 114, 333-8.
- KAILA, K. & VOIPIO, J. 1987. Postsynaptic fall in intracellular pH induced by GABA-activated bicarbonate conductance. *Nature*, 330, 163-5.
- KAMINSKA, A., ICKOWICZ, A., PLOUIN, P., BRU, M. F., DELLATOLAS, G. & DULAC, O. 1999. Delineation of cryptogenic Lennox-Gastaut syndrome and myoclonic astatic epilepsy using multiple correspondence analysis. *Epilepsy Res*, 36, 15-29.
- KAMINSKI, R. M., VAN RIJN, C. M., TURSKI, W. A., CZUCZWAR, S. J. & VAN LUIJTELAAR, G. 2001. AMPA and GABA_B receptor antagonists and their interaction in rats with a genetic form of absence epilepsy. *Eur J Pharmacol*, 430, 251-9.
- KANANURA, C., HAUG, K., SANDER, T., RUNGE, U., GU, W., HALLMANN, K., REBSTOCK, J., HEILS, A. & STEINLEIN, O. K. 2002. A splice-site mutation in GABA_AR γ 2 associated with childhood absence epilepsy and febrile convulsions. *Arch Neurol*, 59, 1137-41.
- KANEDA, M., FARRANT, M. & CULL-CANDY, S. G. 1995. Whole-cell and single-channel currents activated by GABA and glycine in granule cells of the rat cerebellum. *J Physiol*, 485 (Pt 2), 419-35.
- KAUPMANN, K., CRYAN, J. F., WELLENDORPH, P., MOMBEBEAU, C., SANSIG, G., KLEBS, K., SCHMUTZ, M., FROESTL, W., VAN DER PUTTEN, H., MOSBACHER, J., BRAUNER-OSBORNE, H., WALDMEIER, P. & BETTLER, B. 2003. Specific gamma-hydroxybutyrate-binding sites but loss of pharmacological effects of gamma-hydroxybutyrate in GABA_BR₁-deficient mice. *Eur J Neurosci*, 18, 2722-30.
- KAUPMANN, K., HUGGEL, K., HEID, J., FLOR, P. J., BISCHOFF, S., MICKEL, S. J., MCMASTER, G., ANGST, C., BITTIGER, H., FROESTL, W. & BETTLER, B. 1997. Expression cloning of GABA_B receptors uncovers similarity to metabotropic glutamate receptors. *Nature*, 386, 239-46.
- KAUPMANN, K., MALITSCHKE, B., SCHULER, V., HEID, J., FROESTL, W., BECK, P., MOSBACHER, J., BISCHOFF, S., KULIK, A., SHIGEMOTO, R.,

- KARSCHIN, A. & BETTLER, B. 1998. GABA_B-receptor subtypes assemble into functional heteromeric complexes. *Nature*, 396, 683-7.
- KAUR, K. H., BAUR, R. & SIGEL, E. 2009. Unanticipated structural and functional properties of δ -subunit-containing GABA_A receptors. *J Biol Chem*, 284, 7889-96.
- KELLER, C. A., YUAN, X., PANZANELLI, P., MARTIN, M. L., ALLDRED, M., SASSOE-POGNETTO, M. & LUSCHER, B. 2004. The γ 2 subunit of GABA_A receptors is a substrate for palmitoylation by GODZ. *J Neurosci*, 24, 5881-91.
- KELLY, K. M., GROSS, R. A. & MACDONALD, R. L. 1990. Valproic acid selectively reduces the low-threshold (T) calcium current in rat nodose neurons. *Neurosci Lett*, 116, 233-8.
- KEROS, S. & HABLITZ, J. J. 2005. Subtype-specific GABA transporter antagonists synergistically modulate phasic and tonic GABA_A conductances in rat neocortex. *J Neurophysiol*, 94, 2073-85.
- KITTLER, J. T. & MOSS, S. J. 2003. Modulation of GABA_A receptor activity by phosphorylation and receptor trafficking: implications for the efficacy of synaptic inhibition. *Curr Opin Neurobiol*, 13, 341-7.
- KNIGHT, A. R. & BOWERY, N. G. 1996. The pharmacology of adenylyl cyclase modulation by GABA_B receptors in rat brain slices. *Neuropharmacology*, 35, 703-12.
- KORPI, E. R., GRUNDER, G. & LUDDENS, H. 2002. Drug interactions at GABA_A receptors. *Prog Neurobiol*, 67, 113-59.
- KROOK-MAGNUSON, E. I., LI, P., PALUSZKIEWICZ, S. M. & HUNTSMAN, M. M. 2008. Tonic active inhibition selectively controls feedforward circuits in mouse barrel cortex. *J Neurophysiol*, 100, 932-44.
- KULIK, A., NAKADATE, K., NYIRI, G., NOTOMI, T., MALITSCHKEK, B., BETTLER, B. & SHIGEMOTO, R. 2002. Distinct localization of GABA_B receptors relative to synaptic sites in the rat cerebellum and ventrobasal thalamus. *Eur J Neurosci*, 15, 291-307.
- KUMARESAN, S., DAVID, J. & JOSEPH, T. 2000. Comparative profiles of sodium valproate and ethosuximide on electro-behavioural correlates in gamma-hydroxybutyrate and pentylenetetrazol induced absence seizures in rats. *Indian J Physiol Pharmacol*, 44, 411-8.
- KUNTZ, A., CLEMENT, H. W., LEHNERT, W., VAN CALKER, D., HENNIGHAUSEN, K., GERLACH, M. & SCHULZ, E. 2004. Effects of secretin on extracellular amino acid concentrations in rat hippocampus. *J Neural Transm*, 111, 931-9.
- LABATE, A., BRIELLMANN, R. S., ABBOTT, D. F., WAITES, A. B. & JACKSON, G. D. 2005. Typical childhood absence seizures are associated with thalamic activation. *Epileptic Disord*, 7, 373-7.
- LANNES, B., MICHELETTI, G., VERGNES, M., MARESCAUX, C., DEPAULIS, A. & WARTER, J. M. 1988. Relationship between spike-wave discharges and vigilance levels in rats with spontaneous petit mal-like epilepsy. *Neurosci Lett*, 94, 187-91.
- LAUFS, H., LENGELER, U., HAMANDI, K., KLEINSCHMIDT, A. & KRAKOW, K. 2006. Linking generalized spike-and-wave discharges and resting state brain activity by using EEG/fMRI in a patient with absence seizures. *Epilepsia*, 47, 444-8.

- LAURIE, D. J., SEEBURG, P. H. & WISDEN, W. 1992. The distribution of 13 GABA_A receptor subunit mRNAs in the rat brain. II. Olfactory bulb and cerebellum. *J Neurosci*, 12, 1063-76.
- LE FEUVRE, Y., FRICKER, D. & LERESCHE, N. 1997. GABA_A receptor-mediated IPSCs in rat thalamic sensory nuclei: patterns of discharge and tonic modulation by GABA_B autoreceptors. *J Physiol*, 502 (Pt 1), 91-104.
- LEES, G. & LEACH, M. J. 1993. Studies on the mechanism of action of the novel anticonvulsant lamotrigine (Lamictal) using primary neurological cultures from rat cortex. *Brain Res*, 612, 190-9.
- LERESCHE, N., LIGHTOWLER, S., SOLTESZ, I., JASSIK-GERSCHENFELD, D. & CRUNELLI, V. 1991. Low-frequency oscillatory activities intrinsic to rat and cat thalamocortical cells. *J Physiol*, 441, 155-74.
- LERESCHE, N., PARRI, H. R., ERDEMLI, G., GUYON, A., TURNER, J. P., WILLIAMS, S. R., ASPRODINI, E. & CRUNELLI, V. 1998. On the action of the anti-absence drug ethosuximide in the rat and cat thalamus. *J Neurosci*, 18, 4842-53.
- LETTS, V. A., FELIX, R., BIDDLECOME, G. H., ARIKKATH, J., MAHAFFEY, C. L., VALENZUELA, A., BARTLETT, F. S., 2ND, MORI, Y., CAMPBELL, K. P. & FRANKEL, W. N. 1998. The mouse stargazer gene encodes a neuronal Ca²⁺-channel γ -subunit. *Nat Genet*, 19, 340-7.
- LETTS, V. A., VALENZUELA, A., KIRLEY, J. P., SWEET, H. O., DAVISSON, M. T. & FRANKEL, W. N. 1997. Genetic and physical maps of the stargazer locus on mouse chromosome 15. *Genomics*, 43, 62-8.
- LEUTMEZER, F., LURGER, S. & BAUMGARTNER, C. 2002. Focal features in patients with idiopathic generalized epilepsy. *Epilepsy Res*, 50, 293-300.
- LEVITAN, E. S., SCHOFIELD, P. R., BURT, D. R., RHEE, L. M., WISDEN, W., KOHLER, M., FUJITA, N., RODRIGUEZ, H. F., STEPHENSON, A., DARLISON, M. G. & ET AL. 1988. Structural and functional basis for GABA_A receptor heterogeneity. *Nature*, 335, 76-9.
- LIU, X. B., COBLE, J., VAN LUIJTELAAR, G. & JONES, E. G. 2007. Reticular nucleus-specific changes in $\alpha 3$ subunit protein at GABA synapses in genetically epilepsy-prone rats. *Proc Natl Acad Sci U S A*, 104, 12512-7.
- LIU, X. B. & JONES, E. G. 2003. Fine structural localization of connexin-36 immunoreactivity in mouse cerebral cortex and thalamus. *J Comp Neurol*, 466, 457-67.
- LIU, Z., SNEAD, O. C., 3RD, VERGNES, M., DEPAULIS, A. & MARESCAUX, C. 1991a. Intrathalamic injections of gamma-hydroxybutyric acid increase genetic absence seizures in rats. *Neurosci Lett*, 125, 19-21.
- LIU, Z., VERGNES, M., DEPAULIS, A. & MARESCAUX, C. 1991b. Evidence for a critical role of GABAergic transmission within the thalamus in the genesis and control of absence seizures in the rat. *Brain Res*, 545, 1-7.
- LIU, Z., VERGNES, M., DEPAULIS, A. & MARESCAUX, C. 1992. Involvement of intrathalamic GABA_B neurotransmission in the control of absence seizures in the rat. *Neuroscience*, 48, 87-93.
- LLINAS, R. R. & STERIADE, M. 2006. Bursting of thalamic neurons and states of vigilance. *J Neurophysiol*, 95, 3297-308.
- LOISEAU, J., LOISEAU, P., GUYOT, M., DUCHE, B., DARTIGUES, J. F. & AUBLET, B. 1990. Survey of seizure disorders in the French southwest. I. Incidence of epileptic syndromes. *Epilepsia*, 31, 391-6.
- LOISEAU, P. 1992. Human absence epilepsies. *J Neural Transm Suppl*, 35, 1-6.

- LOISEAU, P., DUCHE, B. & PEDESPAN, J. M. 1995. Absence epilepsies. *Epilepsia*, 36, 1182-6.
- LONG, C. W., BRUSZEWSKI, J. A. & SNEAD, R. M. 1980. Analysis of transcription during type C viral induction using cell permeabilization techniques. *Cancer Res*, 40, 22-5.
- LUSCHER, B. & KELLER, C. A. 2004. Regulation of GABA_A receptor trafficking, channel activity, and functional plasticity of inhibitory synapses. *Pharmacol Ther*, 102, 195-221.
- LUSCHER, C., JAN, L. Y., STOFFEL, M., MALENKA, R. C. & NICOLL, R. A. 1997. G protein-coupled inwardly rectifying K⁺ channels (GIRKs) mediate postsynaptic but not presynaptic transmitter actions in hippocampal neurons. *Neuron*, 19, 687-95.
- MACCAFERRI, G., MANGONI, M., LAZZARI, A. & DIFRANCESCO, D. 1993. Properties of the hyperpolarization-activated current in rat hippocampal CA1 pyramidal cells. *J Neurophysiol*, 69, 2129-36.
- MACDONALD, R. L. & BARKER, J. L. 1977. Pentylentetrazol and penicillin are selective antagonists of GABA-mediated post-synaptic inhibition in cultured mammalian neurones. *Nature*, 267, 720-1.
- MACDONALD, R. L. & KANG, J. Q. 2009. Molecular Pathology of Genetic Epilepsies Associated with GABA_A Receptor Subunit Mutations. *Epilepsy Curr*, 9, 18-23.
- MAGUIRE, J. L., STELL, B. M., RAFIZADEH, M. & MODY, I. 2005. Ovarian cycle-linked changes in GABA_A receptors mediating tonic inhibition alter seizure susceptibility and anxiety. *Nat Neurosci*, 8, 797-804.
- MAITRE, M. 1997. The γ -hydroxybutyrate signalling system in brain: organization and functional implications. *Prog Neurobiol*, 51, 337-61.
- MAITRE, M., HECHLER, V., VAYER, P., GOBAILLE, S., CASH, C. D., SCHMITT, M. & BOURGUIGNON, J. J. 1990. A specific γ -hydroxybutyrate receptor ligand possesses both antagonistic and anticonvulsant properties. *J Pharmacol Exp Ther*, 255, 657-63.
- MANNING, J. P., RICHARDS, D. A. & BOWERY, N. G. 2003. Pharmacology of absence epilepsy. *Trends Pharmacol Sci*, 24, 542-9.
- MANNING, J. P., RICHARDS, D. A., LERESCHE, N., CRUNELLI, V. & BOWERY, N. G. 2004. Cortical-area specific block of genetically determined absence seizures by ethosuximide. *Neuroscience*, 123, 5-9.
- MARESCAUX, C., MICHELETTI, G., VERGNES, M., DEPAULIS, A., RUMBACH, L. & WARTER, J. M. 1984. A model of chronic spontaneous petit mal-like seizures in the rat: comparison with pentylentetrazol-induced seizures. *Epilepsia*, 25, 326-31.
- MARESCAUX, C., MICHELETTI, G., VERGNES, M., RUMBACH, L. & WARTER, J. M. 1985. Diazepam antagonizes GABA_{mimetics} in rats with spontaneous petit mal-like epilepsy. *Eur J Pharmacol*, 113, 19-24.
- MARESCAUX, C., VERGNES, M. & BERNASCONI, R. 1992a. GABA_B receptor antagonists: potential new anti-absence drugs. *J Neural Transm Suppl*, 35, 179-88.
- MARESCAUX, C., VERGNES, M. & DEPAULIS, A. 1992b. Genetic absence epilepsy in rats from Strasbourg--a review. *J Neural Transm Suppl*, 35, 37-69.
- MARESCAUX, C., VERGNES, M. & DEPAULIS, A. 1992c. Neurotransmission in rats' spontaneous generalized nonconvulsive epilepsy. *Epilepsy Res Suppl*, 8, 335-43.

- MARESCAUX, C., VERGNES, M., LIU, Z., DEPAULIS, A. & BERNASCONI, R. 1992d. GABA_B receptor involvement in the control of genetic absence seizures in rats. *Epilepsy Res Suppl*, 9, 131-8; discussion 138-9.
- MARGETA-MITROVIC, M., JAN, Y. N. & JAN, L. Y. 2000. A trafficking checkpoint controls GABA_B receptor heterodimerization. *Neuron*, 27, 97-106.
- MARGETA-MITROVIC, M., JAN, Y. N. & JAN, L. Y. 2001. Function of GABA_BR₁ and GABA_BR₂ subunits in G protein-coupling of GABA_B receptors. *Proc Natl Acad Sci U S A*, 98, 14649-54.
- MCCORMICK, D. A. 1992. Neurotransmitter actions in the thalamus and cerebral cortex and their role in neuromodulation of thalamocortical activity. *Prog Neurobiol*, 39, 337-88.
- MCCORMICK, D. A. & PAPE, H. C. 1990. Properties of a hyperpolarization-activated cation current and its role in rhythmic oscillation in thalamic relay neurones. *J Physiol*, 431, 291-318.
- MCCORMICK, D. A. & PRINCE, D. A. 1987. Actions of acetylcholine in the guinea-pig and cat medial and lateral geniculate nuclei, in vitro. *J Physiol*, 392, 147-65.
- MCLEAN, M. J. & MACDONALD, R. L. 1986. Sodium valproate, but not ethosuximide, produces use- and voltage-dependent limitation of high frequency repetitive firing of action potentials of mouse central neurons in cell culture. *J Pharmacol Exp Ther*, 237, 1001-11.
- MEEREN, H. K., PIJN, J. P., VAN LUIJTELAAR, E. L., COENEN, A. M. & LOPES DA SILVA, F. H. 2002. Cortical focus drives widespread corticothalamic networks during spontaneous absence seizures in rats. *J Neurosci*, 22, 1480-95.
- MEEREN, H. K., VAN LUIJTELAAR, E. L. & COENEN, A. M. 1998. Cortical and thalamic visual evoked potentials during sleep-wake states and spike-wave discharges in the rat. *Electroencephalogr Clin Neurophysiol*, 108, 306-19.
- MEEREN, H. K., VEENING, J. G., MODERSCHEIM, T. A., COENEN, A. M. & VAN LUIJTELAAR, G. 2009. Thalamic lesions in a genetic rat model of absence epilepsy: dissociation between spike-wave discharges and sleep spindles. *Exp Neurol*, 217, 25-37.
- MIDZIANOVSKAIA, I. S., KUZNETSOVA, G. D., COENEN, A. M., SPIRIDONOV, A. M. & VAN LUIJTELAAR, E. L. 2001. Electrophysiological and pharmacological characteristics of two types of spike-wave discharges in WAG/Rij rats. *Brain Res*, 911, 62-70.
- MILLER, C. 2000. An overview of the potassium channel family. *Genome Biol*, 1, REVIEWS0004.
- MINELLI, A., BRECHA, N. C., KARSCHIN, C., DEBIASI, S. & CONTI, F. 1995. GAT-1, a high-affinity GABA plasma membrane transporter, is localized to neurons and astroglia in the cerebral cortex. *J Neurosci*, 15, 7734-46.
- MINELLI, A., DEBIASI, S., BRECHA, N. C., ZUCCARELLO, L. V. & CONTI, F. 1996. GAT-3, a high-affinity GABA plasma membrane transporter, is localized to astrocytic processes, and it is not confined to the vicinity of GABAergic synapses in the cerebral cortex. *J Neurosci*, 16, 6255-64.
- MISGELD, U., BIJAK, M. & JAROLIMEK, W. 1995. A physiological role for GABA_B receptors and the effects of baclofen in the mammalian central nervous system. *Prog Neurobiol*, 46, 423-62.
- MODY, I., GLYKYS, J. & WEI, W. 2007. A new meaning for "Gin & Tonic": tonic inhibition as the target for ethanol action in the brain. *Alcohol*, 41, 145-53.
- MOELLER, F., SIEBNER, H. R., WOLFF, S., MUHLE, H., BOOR, R., GRANERT, O., JANSEN, O., STEPHANI, U. & SINIATCHKIN, M. 2008a. Changes in

- activity of striato-thalamo-cortical network precede generalized spike wave discharges. *Neuroimage*, 39, 1839-49.
- MOELLER, F., SIEBNER, H. R., WOLFF, S., MUHLE, H., GRANERT, O., JANSEN, O., STEPHANI, U. & SINIATCHKIN, M. 2008b. Simultaneous EEG-fMRI in drug-naive children with newly diagnosed absence epilepsy. *Epilepsia*, 49, 1510-9.
- MOLLEMAN, A. 2003. *Patch Clamping: An introductory guide to patch clamp electrophysiology*, John Wiley & Sons, Inc.
- MORRISON, J. H. & FOOTE, S. L. 1986. Noradrenergic and serotonergic innervation of cortical, thalamic, and tectal visual structures in Old and New World monkeys. *J Comp Neurol*, 243, 117-38.
- MTCHEDLISHVILI, Z. & KAPUR, J. 2006. High-affinity, slowly desensitizing GABA_A receptors mediate tonic inhibition in hippocampal dentate granule cells. *Mol Pharmacol*, 69, 564-75.
- NEWBERRY, N. R. & NICOLL, R. A. 1984. Direct hyperpolarizing action of baclofen on hippocampal pyramidal cells. *Nature*, 308, 450-2.
- NEWBERRY, N. R. & NICOLL, R. A. 1985. Comparison of the action of baclofen with gamma-aminobutyric acid on rat hippocampal pyramidal cells in vitro. *J Physiol*, 360, 161-85.
- NICHOLSON, C. & RICE, M. E. 1986. The migration of substances in the neuronal microenvironment. *Ann N Y Acad Sci*, 481, 55-71.
- NISHIMURA, M., SATO, K., MIZUNO, M., YOSHIYA, I., SHIMADA, S., SAITO, N. & TOHYAMA, M. 1997. Differential expression patterns of GABA transporters (GAT1-3) in the rat olfactory bulb. *Brain Res Mol Brain Res*, 45, 268-74.
- NOBILI, L., BAGLIETTO, M. G., BEELKE, M., DE CARLI, F., VENESELLI, E. & FERRILLO, F. 2001. Temporal relationship of generalized epileptiform discharges to spindle frequency activity in childhood absence epilepsy. *Clin Neurophysiol*, 112, 1912-6.
- NOEBELS, J. L., QIAO, X., BRONSON, R. T., SPENCER, C. & DAVISSON, M. T. 1990. Stargazer: a new neurological mutant on chromosome 15 in the mouse with prolonged cortical seizures. *Epilepsy Res*, 7, 129-35.
- NOEBELS, J. L. & SIDMAN, R. L. 1979. Inherited epilepsy: spike-wave and focal motor seizures in the mutant mouse tottering. *Science*, 204, 1334-6.
- NUSSER, Z. & MODY, I. 2002. Selective modulation of tonic and phasic inhibitions in dentate gyrus granule cells. *J Neurophysiol*, 87, 2624-8.
- NUSSER, Z., SIEGHART, W. & SOMOGYI, P. 1998. Segregation of different GABA_A receptors to synaptic and extrasynaptic membranes of cerebellar granule cells. *J Neurosci*, 18, 1693-703.
- OHARA, P. T. & LIEBERMAN, A. R. 1993. Some aspects of the synaptic circuitry underlying inhibition in the ventrobasal thalamus. *J Neurocytol*, 22, 815-25.
- OLSEN, R. W. & AVOLI, M. 1997. GABA and epileptogenesis. *Epilepsia*, 38, 399-407.
- PANAYIOTOPOULOS, C. P. 1997. Absence Epilepsies. In: ENGEL, J., JR. & PEDLEY, T. (eds.) *Epilepsy: a Comprehensive Textbook*. Philadelphia: Lippincott-Raven Publishers.
- PANAYIOTOPOULOS, C. P., FERRIE, C. D., KNOTT, C. & ROBINSON, R. O. 1993. Interaction of lamotrigine with sodium valproate. *Lancet*, 341, 445.

- PANAYIOTOPOULOS, C. P., OBEID, T. & WAHEED, G. 1989. Differentiation of typical absence seizures in epileptic syndromes. A video EEG study of 224 seizures in 20 patients. *Brain*, 112 (Pt 4), 1039-56.
- PARK, J. B., SKALSKA, S., SON, S. & STERN, J. E. 2007. Dual GABA_A receptor-mediated inhibition in rat presympathetic paraventricular nucleus neurons. *J Physiol*, 582, 539-51.
- PARK, J. B., SKALSKA, S. & STERN, J. E. 2006. Characterization of a novel tonic GABA_A receptor-mediated inhibition in magnocellular neurosecretory neurons and its modulation by glia. *Endocrinology*, 147, 3746-60.
- PARRI, H. R. & CRUNELLI, V. 1998. Sodium current in rat and cat thalamocortical neurons: role of a non-inactivating component in tonic and burst firing. *J Neurosci*, 18, 854-67.
- PAVLOV, I., SAVTCHENKO, L. P., KULLMANN, D. M., SEMYANOV, A. & WALKER, M. C. 2009. Outwardly rectifying tonically active GABA_A receptors in pyramidal cells modulate neuronal offset, not gain. *J Neurosci*, 29, 15341-50.
- PAXINOS, G. & WATSON, C. 1986. *The Rat Brain: In Stereotaxic Coordinates* Academic Press
- PAYNE, H. L., CONNELLY, W. M., IVES, J. H., LEHNER, R., FURTMULLER, B., SIEGHART, W., TIWARI, P., LUCOCQ, J. M., LEES, G. & THOMPSON, C. L. 2007. GABA_A $\alpha 6$ -containing receptors are selectively compromised in cerebellar granule cells of the ataxic mouse, stargazer. *J Biol Chem*, 282, 29130-43.
- PEARL, P. L., GIBSON, K. M., ACOSTA, M. T., VEZINA, L. G., THEODORE, W. H., ROGAWSKI, M. A., NOVOTNY, E. J., GROPMAN, A., CONRY, J. A., BERRY, G. T. & TUCHMAN, M. 2003. Clinical spectrum of succinic semialdehyde dehydrogenase deficiency. *Neurology*, 60, 1413-7.
- PEDEN, D. R., PETITJEAN, C. M., HERD, M. B., DURAKOGLUGIL, M. S., ROSAHL, T. W., WAFFORD, K., HOMANICS, G. E., BELELLI, D., FRITSCHY, J. M. & LAMBERT, J. J. 2008. Developmental maturation of synaptic and extrasynaptic GABA_A receptors in mouse thalamic ventrobasal neurones. *J Physiol*, 586, 965-87.
- PEDROARENA, C. & LLINAS, R. 1997. Dendritic calcium conductances generate high-frequency oscillation in thalamocortical neurons. *Proc Natl Acad Sci U S A*, 94, 724-8.
- PEETERS, B., SPOOREN, W., VAN LUIJTELAAR, E. L. M. & COENEN, A. M. L. 1988. The WAG/Rij model for absence epilepsy: anticonvulsant drug evaluation. *Neurosci. Res. Comm*, 2, 93-97.
- PEETERS, B. W., KERBUSCH, J. M., VAN LUIJTELAAR, E. L., VOSSSEN, J. M. & COENEN, A. M. 1990. Genetics of absence epilepsy in rats. *Behav Genet*, 20, 453-60.
- PEETERS, B. W., VAN RIJN, C. M., VOSSSEN, J. M. & COENEN, A. M. 1989. Effects of GABA-ergic agents on spontaneous non-convulsive epilepsy, EEG and behaviour, in the WAG/RIJ inbred strain of rats. *Life Sci*, 45, 1171-6.
- PELLEGRINI, A. & GLOOR, P. 1979. Effects of bilateral partial diencephalic lesions on cortical epileptic activity in generalized penicillin epilepsy in the cat. *Exp Neurol*, 66, 285-308.
- PELLEGRINI, A., GLOOR, P. & SHERWIN, A. L. 1978. Effect of valproate sodium on generalized penicillin epilepsy in the cat. *Epilepsia*, 19, 351-60.
- PELLOCK, J. M. 1994. The clinical efficacy of lamotrigine as an antiepileptic drug. *Neurology*, 44, S29-35.

- PEREZ-REYES, E. 2003. Molecular physiology of low-voltage-activated t-type calcium channels. *Physiol Rev*, 83, 117-61.
- PERUCCA, E., GRAM, L., AVANZINI, G. & DULAC, O. 1998. Antiepileptic drugs as a cause of worsening seizures. *Epilepsia*, 39, 5-17.
- PFAFF, T., MALITSCHKEK, B., KAUPMANN, K., PREZEAU, L., PIN, J. P., BETTLER, B. & KARSCHIN, A. 1999. Alternative splicing generates a novel isoform of the rat metabotropic GABA_BR₁ receptor. *Eur J Neurosci*, 11, 2874-82.
- PFRIEGER, F. W., VESELOVSKY, N. S., GOTTMANN, K. & LUX, H. D. 1992. Pharmacological characterization of calcium currents and synaptic transmission between thalamic neurons in vitro. *J Neurosci*, 12, 4347-57.
- PINAULT, D. 2003. Cellular interactions in the rat somatosensory thalamocortical system during normal and epileptic 5-9 Hz oscillations. *J Physiol*, 552, 881-905.
- PINAULT, D., LERESCHE, N., CHARPIER, S., DENIAU, J. M., MARESCAUX, C., VERGNES, M. & CRUNELLI, V. 1998. Intracellular recordings in thalamic neurones during spontaneous spike and wave discharges in rats with absence epilepsy. *J Physiol*, 509 (Pt 2), 449-56.
- PINAULT, D., SMITH, Y. & DESCHENES, M. 1997. Dendrodendritic and axoaxonic synapses in the thalamic reticular nucleus of the adult rat. *J Neurosci*, 17, 3215-33.
- PIRKER, S., SCHWARZER, C., WIESELTHALER, A., SIEGHART, W. & SPERK, G. 2000. GABA_A receptors: immunocytochemical distribution of 13 subunits in the adult rat brain. *Neuroscience*, 101, 815-50.
- PLOCK, N. & KLOFT, C. 2005. Microdialysis -theoretical background and recent implementation in applied life-sciences. *Eur J Pharm Sci*, 25, 1-24.
- POLACK, P. O., GUILLEMAIN, I., HU, E., DERANSART, C., DEPAULIS, A. & CHARPIER, S. 2007. Deep layer somatosensory cortical neurons initiate spike-and-wave discharges in a genetic model of absence seizures. *J Neurosci*, 27, 6590-9.
- POLACK, P. O., MAHON, S., CHAVEZ, M. & CHARPIER, S. 2009. Inactivation of the somatosensory cortex prevents paroxysmal oscillations in cortical and related thalamic neurons in a genetic model of absence epilepsy. *Cereb Cortex*, 19, 2078-91.
- POLDRUGO, F. & ADDOLORATO, G. 1999. The role of gamma-hydroxybutyric acid in the treatment of alcoholism: from animal to clinical studies. *Alcohol Alcohol*, 34, 15-24.
- PORCELLO, D. M., HUNTSMAN, M. M., MIHALEK, R. M., HOMANICS, G. E. & HUGUENARD, J. R. 2003. Intact synaptic GABAergic inhibition and altered neurosteroid modulation of thalamic relay neurons in mice lacking δ -subunit. *J Neurophysiol*, 89, 1378-86.
- PORTAS, C. M., THAKKAR, M., RAINNIE, D. & MCCARLEY, R. W. 1996. Microdialysis perfusion of 8-hydroxy-2-(di-n-propylamino)tetralin (8-OH-DPAT) in the dorsal raphe nucleus decreases serotonin release and increases rapid eye movement sleep in the freely moving cat. *J Neurosci*, 16, 2820-8.
- POWELL, K. L., CAIN, S. M., NG, C., SIRDESAI, S., DAVID, L. S., KYI, M., GARCIA, E., TYSON, J. R., REID, C. A., BAHLO, M., FOOTE, S. J., SNUTCH, T. P. & O'BRIEN, T. J. 2009. A Ca_v3.2 T-type calcium channel point mutation has splice-variant-specific effects on function and segregates with seizure expression in a polygenic rat model of absence epilepsy. *J Neurosci*, 29, 371-80.

- PREVETT, M. C., DUNCAN, J. S., JONES, T., FISH, D. R. & BROOKS, D. J. 1995. Demonstration of thalamic activation during typical absence seizures using H2(15)O and PET. *Neurology*, 45, 1396-402.
- PRINCE, J. 1995. Thalamus. In: PAXINOS, G. (ed.) *The Rat Nervous System Second Edition*. Second Edition ed. San Diego: Elsevier Academic Press.
- PRINCIVALLE, A., REGONDI, M. C., FRASSONI, C., BOWERY, N. G. & SPREAFICO, R. 2000. Distribution of GABA_B receptor protein in somatosensory cortex and thalamus of adult rats and during postnatal development. *Brain Res Bull*, 52, 397-405.
- PRINCIVALLE, A. P., PANGALOS, M. N., BOWERY, N. G. & SPREAFICO, R. 2001. Distribution of GABA_BR_{1a}, GABA_BR_{1b} and GABA_BR₂ receptor protein in cerebral cortex and thalamus of adult rats. *Neuroreport*, 12, 591-5.
- PRINCIVALLE, A. P., RICHARDS, D. A., DUNCAN, J. S., SPREAFICO, R. & BOWERY, N. G. 2003. Modification of GABA_BR₁ and GABA_BR₂ receptor subunits in the somatosensory cerebral cortex and thalamus of rats with absence seizures (GAERS). *Epilepsy Res*, 55, 39-51.
- PRITCHETT, D. B., SONTHEIMER, H., GORMAN, C. M., KETTENMANN, H., SEEBURG, P. H. & SCHOFIELD, P. R. 1988. Transient expression shows ligand gating and allosteric potentiation of GABA_A receptor subunits. *Science*, 242, 1306-8.
- PRITCHETT, D. B., SONTHEIMER, H., SHIVERS, B. D., YMER, S., KETTENMANN, H., SCHOFIELD, P. R. & SEEBURG, P. H. 1989. Importance of a novel GABA_A receptor subunit for benzodiazepine pharmacology. *Nature*, 338, 582-5.
- PURVES, D., AUGUSTINE, G., FITZPATRICK, D., KATZ, L., LAMANTIA, A., MCNAMARA, J. & WILLIAMS, M. 2000. Neurotransmitters. In: AUGUSTINE, G. (ed.) *Neuroscience*. II ed. Sunderland, Massachusetts: Sinauer Associates, Inc.
- QIAO, X., CHEN, L., GAO, H., BAO, S., HEFTI, F., THOMPSON, R. F. & KNUSEL, B. 1998. Cerebellar brain-derived neurotrophic factor-TrkB defect associated with impairment of eyeblink conditioning in Stargazer mutant mice. *J Neurosci*, 18, 6990-9.
- QUESNEY, L. F. & GLOOR, P. 1978. Generalized penicillin epilepsy in the cat: correlation between electrophysiological data and distribution of 14C-penicillin in the brain. *Epilepsia*, 19, 35-45.
- QUESNEY, L. F., GLOOR, P., KRATZENBERG, E. & ZUMSTEIN, H. 1977. Pathophysiology of generalized penicillin epilepsy in the cat: the role of cortical and subcortical structures. I. Systemic application of penicillin. *Electroencephalogr Clin Neurophysiol*, 42, 640-55.
- REN, X. & MODY, I. 2006. γ -Hydroxybutyrate induces cyclic AMP-responsive element-binding protein phosphorylation in mouse hippocampus: an involvement of GABA_B receptors and cAMP-dependent protein kinase activation. *Neuroscience*, 141, 269-75.
- RICE, M. E., GERHARDT, G. A., HIERL, P. M., NAGY, G. & ADAMS, R. N. 1985. Diffusion coefficients of neurotransmitters and their metabolites in brain extracellular fluid space. *Neuroscience*, 15, 891-902.
- RICHARDS, D. A., LEMOS, T., WHITTON, P. S. & BOWERY, N. G. 1995. Extracellular GABA in the ventrolateral thalamus of rats exhibiting spontaneous absence epilepsy: a microdialysis study. *J Neurochem*, 65, 1674-80.

- RICHARDS, D. A., MANNING, J. P., BARNES, D., ROMBOLA, L., BOWERY, N. G., CACCIA, S., LERESCHE, N. & CRUNELLI, V. 2003. Targeting thalamic nuclei is not sufficient for the full anti-absence action of ethosuximide in a rat model of absence epilepsy. *Epilepsy Res*, 54, 97-107.
- RICHENS, A. 1995. Ethosuximide and valproate. In: DUNCAN, J. S. & PANAYIOTOPOULOS, C. P. (eds.) *Typical Absences and Related Epileptic Syndromes*. London: Churchill Livingstone.
- ROCCA, W. A., SHARBROUGH, F. W., HAUSER, W. A., ANNEGERS, J. F. & SCHOENBERG, B. S. 1987. Risk factors for absence seizures: a population-based case-control study in Rochester, Minnesota. *Neurology*, 37, 1309-14.
- ROSSI, D. J. & HAMANN, M. 1998. Spillover-mediated transmission at inhibitory synapses promoted by high affinity alpha6 subunit GABA(A) receptors and glomerular geometry. *Neuron*, 20, 783-95.
- ROSSI, D. J., HAMANN, M. & ATTWELL, D. 2003. Multiple modes of GABAergic inhibition of rat cerebellar granule cells. *J Physiol*, 548, 97-110.
- SADLEIR, L. G., FARRELL, K., SMITH, S., CONNOLLY, M. B. & SCHEFFER, I. E. 2006. Electroclinical features of absence seizures in childhood absence epilepsy. *Neurology*, 67, 413-8.
- SALEK-HADDADI, A., LEMIEUX, L., MERSCHHEMKE, M., FRISTON, K. J., DUNCAN, J. S. & FISH, D. R. 2003. Functional magnetic resonance imaging of human absence seizures. *Ann Neurol*, 53, 663-7.
- SALT, T. E., EATON, S. A. & TURNER, J. P. 1996. Characterization of the metabotropic glutamate receptors (mGluRs) which modulate GABA-mediated inhibition in the ventrobasal thalamus. *Neurochem Int*, 29, 317-22.
- SAPER, C. 2000. Brain Stem Modulation of Sensation, Movement and Consciousness. In: KANDEL, E., SCHWARTZ, J. & JESSELL, T. (eds.) *Principles of Neural Science*. Fourth Edition ed.: McGraw-Hill.
- SAXENA, N. C. & MACDONALD, R. L. 1994. Assembly of GABA_A receptor subunits: role of the δ -subunit. *J Neurosci*, 14, 7077-86.
- SCHACHTER, S. 1997. Treatment of Seizures. In: SCHACHTER, S. & SCHOMER, D. (eds.) *The Comprehensive Evaluation and Treatment of Epilepsy*. Academic Press.
- SCHACHTER, S. C. & YERBY, M. S. 1997. Management of epilepsy: pharmacologic therapy and quality-of-life issues. *Postgrad Med*, 101, 133-8, 141-4, 150-3.
- SCHEIBEL, M. E. & SCHEIBEL, A. B. 1966. The organization of the nucleus reticularis thalami: a Golgi study. *Brain Res*, 1, 43-62.
- SCHEIBEL, M. E. & SCHEIBEL, A. B. 1972. Specialized organizational patterns within the nucleus reticularis thalami of the cat. *Exp Neurol*, 34, 316-22.
- SCHLUMBERGER, E., CHAVEZ, F., PALACIOS, L., REY, E., PAJOT, N. & DULAC, O. 1994. Lamotrigine in treatment of 120 children with epilepsy. *Epilepsia*, 35, 359-67.
- SCHOFIELD, P. R., DARLISON, M. G., FUJITA, N., BURT, D. R., STEPHENSON, F. A., RODRIGUEZ, H., RHEE, L. M., RAMACHANDRAN, J., REALE, V., GLENCORSE, T. A. & ET AL. 1987. Sequence and functional expression of the GABA_A receptor shows a ligand-gated receptor super-family. *Nature*, 328, 221-7.
- SCHWARZ, D. A., BARRY, G., ELIASOF, S. D., PETROSKI, R. E., CONLON, P. J. & MAKI, R. A. 2000. Characterization of gamma-aminobutyric acid receptor GABA_BR_{1e}, a GABA_BR₁ splice variant encoding a truncated receptor. *J Biol Chem*, 275, 32174-81.

- SCHWEITZER, P., ROBERTO, M., MADAMBA, S. G. & SIGGINS, G. R. 2004. γ -hydroxybutyrate increases a potassium current and decreases the H-current in hippocampal neurons via GABA_B receptors. *J Pharmacol Exp Ther*, 311, 172-9.
- SCIMEMI, A., ANDERSSON, A., HEEROMA, J. H., STRANDBERG, J., RYDENHAG, B., MCEVOY, A. W., THOM, M., ASZTELY, F. & WALKER, M. C. 2006. Tonic GABA_A receptor-mediated currents in human brain. *Eur J Neurosci*, 24, 1157-60.
- SEGAL, M. & BARKER, J. L. 1984. Rat hippocampal neurons in culture: properties of GABA-activated Cl⁻ ion conductance. *J Neurophysiol*, 51, 500-15.
- SEIDENBECHER, T., STAAK, R. & PAPE, H. C. 1998. Relations between cortical and thalamic cellular activities during absence seizures in rats. *Eur J Neurosci*, 10, 1103-12.
- SEMYANOV, A., WALKER, M. C., KULLMANN, D. M. & SILVER, R. A. 2004. Tonically active GABA_A receptors: modulating gain and maintaining the tone. *Trends Neurosci*, 27, 262-9.
- SHERMAN, S. M. 2001. Tonic and burst firing: dual modes of thalamocortical relay. *Trends Neurosci*, 24, 122-6.
- SHERMAN, S. M. & GUILLERY, R. W. 1996. Functional organization of thalamocortical relays. *J Neurophysiol*, 76, 1367-95.
- SHIPPENBERG, T. S. & THOMPSON, A. C. 2001. Overview of microdialysis. *Curr Protoc Neurosci*, Chapter 7, Unit 7 1.
- SHOUSE, M. N. & DA SILVA, A. M. 1997. Chronobiology. In: ENGEL, J., JR. & PEDLEY, T. (eds.) *Epilepsy: a Comprehensive textbook* Philadelphia: Lippincott-Raven Publishers.
- SHOUSE, M. N., DA SILVA, A. M. & SAMMARITANO, M. 1996. Circadian rhythm, sleep, and epilepsy. *J Clin Neurophysiol*, 13, 32-50.
- SIEGELBAUM, S., SCHWARTZ, J. & KANDEL, E. 2000. Modulation of Synaptic Transmission: Second Messengers. In: KANDEL, E., SCHWARTZ, J. & JESSEL, T. (eds.) *Principles of Neural Science*. 4th ed.: McGraw-Hill.
- SIEGHART, W., FUCHS, K., TRETTER, V., EBERT, V., JECHLINGER, M., HOGER, H. & ADAMIKER, D. 1999. Structure and subunit composition of GABA_A receptors. *Neurochem Int*, 34, 379-85.
- SIEGHART, W. & SPERK, G. 2002. Subunit composition, distribution and function of GABA_A receptor subtypes. *Curr Top Med Chem*, 2, 795-816.
- SLAGHT, S. J., LERESCHE, N., DENIAU, J. M., CRUNELLI, V. & CHARPIER, S. 2002. Activity of thalamic reticular neurons during spontaneous genetically determined spike and wave discharges. *J Neurosci*, 22, 2323-34.
- SLESINGER, P. A., STOFFEL, M., JAN, Y. N. & JAN, L. Y. 1997. Defective GABA_BR-activated inwardly rectifying K⁺ currents in cerebellar granule cells isolated from weaver and Girk2 null mutant mice. *Proc Natl Acad Sci U S A*, 94, 12210-7.
- SNEAD, O. 1984a. γ -Hydroxybutyric acid, γ -aminobutyric acid, and petit mal epilepsy. In: FARIELLO, R., MORSELI, P. & LLOYD, K. (eds.) *Neurotransmitters, seizures and epilepsy*. New York: Raven.
- SNEAD, O. C., 3RD 1978a. Gamma hydroxybutyrate in the monkey. I. Electroencephalographic, behavioral, and pharmacokinetic studies. *Neurology*, 28, 636-42.
- SNEAD, O. C., 3RD 1978b. Gamma hydroxybutyrate in the monkey. II. Effect of chronic oral anticonvulsant drugs. *Neurology*, 28, 643-8.

- SNEAD, O. C., 3RD 1978c. Gamma hydroxybutyrate in the monkey. III. Effect of intravenous anticonvulsant drugs. *Neurology*, 28, 1173-8.
- SNEAD, O. C., 3RD 1984b. Ontogeny of gamma-hydroxybutyric acid. II. Electroencephalographic effects. *Brain Res*, 317, 89-96.
- SNEAD, O. C., 3RD 1988. γ -Hydroxybutyrate model of generalized absence seizures: further characterization and comparison with other absence models. *Epilepsia*, 29, 361-8.
- SNEAD, O. C., 3RD 1990. The ontogeny of GABAergic enhancement of the gamma-hydroxybutyrate model of generalized absence seizures. *Epilepsia*, 31, 363-8.
- SNEAD, O. C., 3RD 1991. The gamma-hydroxybutyrate model of absence seizures: correlation of regional brain levels of gamma-hydroxybutyric acid and gamma-butyrolactone with spike wave discharges. *Neuropharmacology*, 30, 161-7.
- SNEAD, O. C., 3RD 1992a. Evidence for GABA_B-mediated mechanisms in experimental generalized absence seizures. *Eur J Pharmacol*, 213, 343-9.
- SNEAD, O. C., 3RD 1992b. Pharmacological models of generalized absence seizures in rodents. *J Neural Transm Suppl*, 35, 7-19.
- SNEAD, O. C., 3RD 1994. The ontogeny of [³H] γ -hydroxybutyrate and [³H]GABA_B binding sites: relation to the development of experimental absence seizures. *Brain Res*, 659, 147-56.
- SNEAD, O. C., 3RD 1995. Basic mechanisms of generalized absence seizures. *Ann Neurol*, 37, 146-57.
- SNEAD, O. C., 3RD 1996a. Antiabsence seizure activity of specific GABA_B and γ -Hydroxybutyric acid receptor antagonists. *Pharmacol Biochem Behav*, 53, 73-9.
- SNEAD, O. C., 3RD 1996b. Relation of the [³H] γ -hydroxybutyric acid (GHB) binding site to the gamma-aminobutyric acidB (GABA_B) receptor in rat brain. *Biochem Pharmacol*, 52, 1235-43.
- SNEAD, O. C., 3RD 1998. Ganaxolone, a selective, high-affinity steroid modulator of the gamma-aminobutyric acid-A receptor, exacerbates seizures in animal models of absence. *Ann Neurol*, 44, 688-91.
- SNEAD, O. C., 3RD 2000. Evidence for a G protein-coupled γ -hydroxybutyric acid receptor. *J Neurochem*, 75, 1986-96.
- SNEAD, O. C., 3RD, BEARDEN, L. J. & PEGRAM, V. 1980. Effect of acute and chronic anticonvulsant administration on endogenous gamma-hydroxybutyrate in rat brain. *Neuropharmacology*, 19, 47-52.
- SNEAD, O. C., 3RD, DEPAULIS, A., BANERJEE, P. K., HECHLER, V. & VERGNES, M. 1992a. The GABA_A receptor complex in experimental absence seizures in rat: an autoradiographic study. *Neurosci Lett*, 140, 9-12.
- SNEAD, O. C., 3RD, DEPAULIS, A., VERGNES, M. & MARESCAUX, C. 1992b. Effect of intranigral muscimol on animal models of generalized absence seizures. *Epilepsy Res Suppl*, 8, 345-9; discussion 349-50.
- SNEAD, O. C., 3RD & LIU, C. C. 1993. GABA_A receptor function in the γ -hydroxybutyrate model of generalized absence seizures. *Neuropharmacology*, 32, 401-9.
- SNEAD, O. C., 3RD & NICHOLS, A. C. 1987. γ -Hydroxybutyric acid binding sites: evidence for coupling to a chloride anion channel. *Neuropharmacology*, 26, 1519-23.
- SNEAD, O. C., 3RD, YU, R. K. & HUTTENLOCHER, P. R. 1976. Gamma hydroxybutyrate. Correlation of serum and cerebrospinal fluid levels with electroencephalographic and behavioral effects. *Neurology*, 26, 51-6.

- SOLTESZ, I., HABY, M., LERESCHE, N. & CRUNELLI, V. 1988. The GABA_B antagonist phaclofen inhibits the late K⁺-dependent IPSP in cat and rat thalamic and hippocampal neurones. *Brain Res*, 448, 351-4.
- SOLTESZ, I., LIGHTOWLER, S., LERESCHE, N., JASSIK-GERSCHENFELD, D., POLLARD, C. E. & CRUNELLI, V. 1991. Two inward currents and the transformation of low-frequency oscillations of rat and cat thalamocortical cells. *J Physiol*, 441, 175-97.
- SPAIN, W. J., SCHWINDT, P. C. & CRILL, W. E. 1987. Anomalous rectification in neurons from cat sensorimotor cortex in vitro. *J Neurophysiol*, 57, 1555-76.
- STEFANI, A., SPADONI, F. & BERNARDI, G. 1997. Voltage-activated calcium channels: targets of antiepileptic drug therapy? *Epilepsia*, 38, 959-65.
- STEFANI, A., SPADONI, F., SINISCALCHI, A. & BERNARDI, G. 1996. Lamotrigine inhibits Ca²⁺ currents in cortical neurons: functional implications. *Eur J Pharmacol*, 307, 113-6.
- STELL, B. M., BRICKLEY, S. G., TANG, C. Y., FARRANT, M. & MODY, I. 2003. Neuroactive steroids reduce neuronal excitability by selectively enhancing tonic inhibition mediated by δ subunit-containing GABA_A receptors. *Proc Natl Acad Sci U S A*, 100, 14439-44.
- STEPHENSON, F. A. 1988. Understanding the GABA_A receptor: a chemically gated ion channel. *Biochem J*, 249, 21-32.
- STERIADE, M. & CONTRERAS, D. 1995. Relations between cortical and thalamic cellular events during transition from sleep patterns to paroxysmal activity. *J Neurosci*, 15, 623-42.
- STERIADE, M., DOSSI, R. C. & NUNEZ, A. 1991. Network modulation of a slow intrinsic oscillation of cat thalamocortical neurons implicated in sleep delta waves: cortically induced synchronization and brainstem cholinergic suppression. *J Neurosci*, 11, 3200-17.
- STERIADE, M. & LLINAS, R. R. 1988. The functional states of the thalamus and the associated neuronal interplay. *Physiol Rev*, 68, 649-742.
- STERIADE, M., MCCORMICK, D. A. & SEJNOWSKI, T. J. 1993. Thalamocortical oscillations in the sleeping and aroused brain. *Science*, 262, 679-85.
- STERIADE, M., PARE, D., PARENT, A. & SMITH, Y. 1988. Projections of cholinergic and non-cholinergic neurons of the brainstem core to relay and associational thalamic nuclei in the cat and macaque monkey. *Neuroscience*, 25, 47-67.
- STORUSTOVU, S. I. & EBERT, B. 2006. Pharmacological characterization of agonists at δ -containing GABA_A receptors: Functional selectivity for extrasynaptic receptors is dependent on the absence of γ 2. *J Pharmacol Exp Ther*, 316, 1351-9.
- SUBRAMANYAM, K., DAVID, J. & JOSEPH, T. 2001. Interaction of flunarizine with sodium valproate or ethosuximide in γ -hydroxybutyrate induced absence seizures in rats. *Indian J Exp Biol*, 39, 998-1001.
- SUR, C., FARRAR, S. J., KERBY, J., WHITING, P. J., ATTACK, J. R. & MCKERNAN, R. M. 1999. Preferential coassembly of α 4 and δ -subunits of the GABA_A receptor in rat thalamus. *Mol Pharmacol*, 56, 110-5.
- SUTCH, R. J., DAVIES, C. C. & BOWERY, N. G. 1999. GABA release and uptake measured in crude synaptosomes from Genetic Absence Epilepsy Rats from Strasbourg (GAERS). *Neurochem Int*, 34, 415-25.
- TAKAHASHI, A., MASHIMO, T. & UCHIDA, I. 2006. GABAergic tonic inhibition of substantia gelatinosa neurons in mouse spinal cord. *Neuroreport*, 17, 1331-5.

- TANG, X., HERNANDEZ, C. C. & MACDONALD, R. L. 2010. Modulation of spontaneous and GABA-evoked tonic $\alpha 4\beta 3\delta$ and $\alpha 4\beta 3\gamma 2L$ GABA_A receptor currents by protein kinase A. *J Neurophysiol*, 103, 1007-19.
- TEHRANI, M. H., BAUMGARTNER, B. J., LIU, S. C. & BARNES, E. M., JR. 1997. Aberrant expression of GABA_A receptor subunits in the tottering mouse: an animal model for absence seizures. *Epilepsy Res*, 28, 213-23.
- THALMANN, R. H. 1988. Evidence that guanosine triphosphate (GTP)-binding proteins control a synaptic response in brain: effect of pertussis toxin and GTP gamma S on the late inhibitory postsynaptic potential of hippocampal CA3 neurons. *J Neurosci*, 8, 4589-602.
- THOMPSON, A. C. & SHIPPENBERG, T. S. 2001. Microdialysis in rodents. *Curr Protoc Neurosci*, Chapter 7, Unit 7 2.
- THOMPSON, S. M. & GAHWILER, B. H. 1992. Comparison of the actions of baclofen at pre- and postsynaptic receptors in the rat hippocampus in vitro. *J Physiol*, 451, 329-45.
- TOTH, T. & CRUNELLI, V. 1992. Computer simulation of the pacemaker oscillations of thalamocortical cells. *Neuroreport*, 3, 65-8.
- TRACEY, D. 2004. Somatosensory System. In: PAXINOS, G. (ed.) *The Rat Nervous System Third Edition*. San Diego: Elsevier Academic Press.
- TREIMAN, D. M. 2001. GABAergic mechanisms in epilepsy. *Epilepsia*, 42 Suppl 3, 8-12.
- TRETTER, V., EHYA, N., FUCHS, K. & SIEGHART, W. 1997. Stoichiometry and assembly of a recombinant GABA_A receptor subtype. *J Neurosci*, 17, 2728-37.
- TWYMAN, R. E. & MACDONALD, R. L. 1992. Neurosteroid regulation of GABA_A receptor single-channel kinetic properties of mouse spinal cord neurons in culture. *J Physiol*, 456, 215-45.
- ULRICH, D., BESSEYRIAS, V. & BETTLER, B. 2007. Functional mapping of GABA_B-receptor subtypes in the thalamus. *J Neurophysiol*, 98, 3791-5.
- ULRICH, D. & HUGUENARD, J. R. 1996. GABA_B receptor-mediated responses in GABAergic projection neurones of rat nucleus reticularis thalami in vitro. *J Physiol*, 493 (Pt 3), 845-54.
- ULRICH, D. & HUGUENARD, J. R. 1997. GABA_A-receptor-mediated rebound burst firing and burst shunting in thalamus. *J Neurophysiol*, 78, 1748-51.
- URAK, L., FEUCHT, M., FATHI, N., HORNIK, K. & FUCHS, K. 2006. A GABA_A $\beta 3$ promoter haplotype associated with childhood absence epilepsy impairs transcriptional activity. *Hum Mol Genet*, 15, 2533-41.
- VAN LUIJTELAAR, E. L. & COENEN, A. M. 1986. Two types of electrocortical paroxysms in an inbred strain of rats. *Neurosci Lett*, 70, 393-7.
- VAN LUIJTELAAR, E. L. & COENEN, A. M. 1988. Circadian rhythmicity in absence epilepsy in rats. *Epilepsy Res*, 2, 331-6.
- VAN RIJN, C. M., WEYN BANNINGH, E. W. & COENEN, A. M. 1994. Effects of lamotrigine on absence seizures in rats. *Pol J Pharmacol*, 46, 467-70.
- VARDYA, I., DRASBEK, K. R., DOSA, Z. & JENSEN, K. 2008. Cell type-specific GABA_A receptor-mediated tonic inhibition in mouse neocortex. *J Neurophysiol*, 100, 526-32.
- VARGA, C., SIK, A., LAVALLEE, P. & DESCHENES, M. 2002. Dendroarchitecture of relay cells in thalamic barreloids: a substrate for cross-whisker modulation. *J Neurosci*, 22, 6186-94.

- VELAZQUEZ, J. L., HUO, J. Z., DOMINGUEZ, L. G., LESHCHENKO, Y. & SNEAD, O. C., 3RD 2007. Typical versus atypical absence seizures: network mechanisms of the spread of paroxysms. *Epilepsia*, 48, 1585-93.
- VERGNES, M. & MARESCAUX, C. 1992. Cortical and thalamic lesions in rats with genetic absence epilepsy. *J Neural Transm Suppl*, 35, 71-83.
- VERGNES, M., MARESCAUX, C., BOEHRER, A. & DEPAULIS, A. 1991. Are rats with genetic absence epilepsy behaviorally impaired? *Epilepsy Res*, 9, 97-104.
- VERGNES, M., MARESCAUX, C. & DEPAULIS, A. 1990. Mapping of spontaneous spike and wave discharges in Wistar rats with genetic generalized non-convulsive epilepsy. *Brain Res*, 523, 87-91.
- VERGNES, M., MARESCAUX, C., DEPAULIS, A., MICHELETTI, G. & WARTER, J. M. 1986. Ontogeny of spontaneous petit mal-like seizures in Wistar rats. *Brain Res*, 395, 85-7.
- VERGNES, M., MARESCAUX, C., DEPAULIS, A., MICHELETTI, G. & WARTER, J. M. 1987. Spontaneous spike and wave discharges in thalamus and cortex in a rat model of genetic petit mal-like seizures. *Exp Neurol*, 96, 127-36.
- VERGNES, M., MARESCAUX, C., LANNES, B., DEPAULIS, A., MICHELETTI, G. & WARTER, J. M. 1989. Interhemispheric desynchronization of spontaneous spike-wave discharges by corpus callosum transection in rats with petit mal-like epilepsy. *Epilepsy Res*, 4, 8-13.
- VERGNES, M., MARESCAUX, C., MICHELETTI, G., DEPAULIS, A., RUMBACH, L. & WARTER, J. M. 1984. Enhancement of spike and wave discharges by GABA_{mimetic} drugs in rats with spontaneous petit-mal-like epilepsy. *Neurosci Lett*, 44, 91-4.
- VERGNES, M., MARESCAUX, C., MICHELETTI, G., REIS, J., DEPAULIS, A., RUMBACH, L. & WARTER, J. M. 1982. Spontaneous paroxysmal electroclinical patterns in rat: a model of generalized non-convulsive epilepsy. *Neurosci Lett*, 33, 97-101.
- VERGNES, M., MARESCAUX, C., MICHELETTI, G., RUMBACH, L. & WARTER, J. M. 1985. Blockade of "antiabsence" activity of sodium valproate by THIP in rats with petit mal-like seizures. Comparison with ethosuximide. *J Neural Transm*, 63, 133-41.
- VILLALBA, R. M., RAJU, D. V., HALL, R. A. & SMITH, Y. 2006. GABA_B receptors in the centromedian/parafascicular thalamic nuclear complex: an ultrastructural analysis of GABA_BR₁ and GABA_BR₂ in the monkey thalamus. *J Comp Neurol*, 496, 269-87.
- VITELLARO-ZUCCARELLO, L., CALVARESI, N. & DE BIASI, S. 2003. Expression of GABA transporters, GAT-1 and GAT-3, in the cerebral cortex and thalamus of the rat during postnatal development. *Cell Tissue Res*, 313, 245-57.
- WALDMEIER, P. C., BAUMANN, P. A., WICKI, P., FELDTRAUER, J. J., STIERLIN, C. & SCHMUTZ, M. 1995. Similar potency of carbamazepine, oxcarbazepine, and lamotrigine in inhibiting the release of glutamate and other neurotransmitters. *Neurology*, 45, 1907-13.
- WALLACE, R., MARINI, C., PETROU, S., HARKIN, L., BOWSER, D., PANCHAL, R., WILLIAMS, D., SUTHERLAND, G., MULLEY, J., SCHEFFER, I. & BERKOVIC, S. 2002. Mutant GABA_A receptor γ 2 subunit in childhood absence epilepsy and febrile seizures. *Nature genetics*, 28, 49-52.
- WALZ, W., BOULTON, A. & BAKER, G. 2002. *Patch-Clamp Analysis: Advanced Techniques* Humana Press, Inc

- WANG, X., STEWART, L., CORTEZ, M. A., WU, Y., VELAZQUEZ, J. L., LIU, C. C., SHEN, L. & SNEAD, O. C., 3RD 2009. The circuitry of atypical absence seizures in GABA_BR_{1a} transgenic mice. *Pharmacol Biochem Behav*, 94, 124-30.
- WEI, W., ZHANG, N., PENG, Z., HOUSER, C. R. & MODY, I. 2003. Perisynaptic localization of delta subunit-containing GABA_A receptors and their activation by GABA spillover in the mouse dentate gyrus. *J Neurosci*, 23, 10650-61.
- WESTERINK, B. H. & DE VRIES, J. B. 2001. A method to evaluate the diffusion rate of drugs from a microdialysis probe through brain tissue. *J Neurosci Methods*, 109, 53-8.
- WHITE, H. S. 1997. Clinical significance of animal seizure models and mechanism of action studies of potential antiepileptic drugs. *Epilepsia*, 38 Suppl 1, S9-17.
- WHITE, J. H., WISE, A., MAIN, M. J., GREEN, A., FRASER, N. J., DISNEY, G. H., BARNES, A. A., EMSON, P., FOORD, S. M. & MARSHALL, F. H. 1998. Heterodimerization is required for the formation of a functional GABA_B receptor. *Nature*, 396, 679-82.
- WHITING, P. J. 1999. The GABA_A receptor gene family: new targets for therapeutic intervention. *Neurochem Int*, 34, 387-90.
- WILLIAMS, D. 1953. A study of thalamic and cortical rhythms in petit mal. *Brain*, 76, 50-69.
- WILLIAMS, S. R., TURNER, J. P. & CRUNELLI, V. 1995. γ -hydroxybutyrate promotes oscillatory activity of rat and cat thalamocortical neurons by a tonic GABA_B receptor-mediated hyperpolarization. *Neuroscience*, 66, 133-41.
- WILLIAMS, S. R., TURNER, J. P., HUGHES, S. W. & CRUNELLI, V. 1997. On the nature of anomalous rectification in thalamocortical neurones of the cat ventrobasal thalamus in vitro. *J Physiol*, 505 (Pt 3), 727-47.
- WISDEN, W., COPE, D., KLAUSBERGER, T., HAUER, B., SINKKONEN, S. T., TRETTER, V., LUJAN, R., JONES, A., KORPI, E. R., MODY, I., SIEGHART, W. & SOMOGYI, P. 2002. Ectopic expression of the GABA_A receptor $\alpha 6$ subunit in hippocampal pyramidal neurons produces extrasynaptic receptors and an increased tonic inhibition. *Neuropharmacology*, 43, 530-49.
- WISDEN, W., LAURIE, D. J., MONYER, H. & SEEBURG, P. H. 1992. The distribution of 13 GABA_A receptor subunit mRNAs in the rat brain. I. Telencephalon, diencephalon, mesencephalon. *J Neurosci*, 12, 1040-62.
- WISDEN, W. & SEEBURG, P. H. 1992. GABA_A receptor channels: from subunits to functional entities. *Curr Opin Neurobiol*, 2, 263-9.
- WU, L. G. & SAGGAU, P. 1997. Presynaptic inhibition of elicited neurotransmitter release. *Trends Neurosci*, 20, 204-12.
- WU, Y., ALI, S., AHMADIAN, G., LIU, C. C., WANG, Y. T., GIBSON, K. M., CALVER, A. R., FRANCIS, J., PANGALOS, M. N. & CARTER SNEAD, O., 3RD 2004. γ -hydroxybutyric acid (GHB) and gamma-aminobutyric acidB receptor (GABA_BR) binding sites are distinctive from one another: molecular evidence. *Neuropharmacology*, 47, 1146-56.
- WU, Y., CHAN, K. F., EUBANKS, J. H., GUIN TING WONG, C., CORTEZ, M. A., SHEN, L., CHE LIU, C., PEREZ VELAZQUEZ, J., TIAN WANG, Y., JIA, Z. & CARTER SNEAD, O., 3RD 2007. Transgenic mice over-expressing GABA_BR_{1a} receptors acquire an atypical absence epilepsy-like phenotype. *Neurobiol Dis*, 26, 439-51.
- XIONG, Z. Q. & STRINGER, J. L. 1999. Cesium induces spontaneous epileptiform activity without changing extracellular potassium regulation in rat hippocampus. *J Neurophysiol*, 82, 3339-46.

- XIONG, Z. Q. & STRINGER, J. L. 2001. Prolonged bursts occur in normal calcium in hippocampal slices after raising excitability and blocking synaptic transmission. *J Neurophysiol*, 86, 2625-8.
- YAMADA, J., FURUKAWA, T., UENO, S., YAMAMOTO, S. & FUKUDA, A. 2007. Molecular basis for the GABA_A receptor-mediated tonic inhibition in rat somatosensory cortex. *Cereb Cortex*, 17, 1782-7.
- YEUNG, J. Y., CANNING, K. J., ZHU, G., PENNEFATHER, P., MACDONALD, J. F. & ORSER, B. A. 2003. Tonically activated GABA_A receptors in hippocampal neurons are high-affinity, low-conductance sensors for extracellular GABA. *Mol Pharmacol*, 63, 2-8.
- ZHANG, N., WEI, W., MODY, I. & HOUSER, C. R. 2007. Altered localization of GABA_A receptor subunits on dentate granule cell dendrites influences tonic and phasic inhibition in a mouse model of epilepsy. *J Neurosci*, 27, 7520-31.
- ZHANG, Z. W. & DESCHENES, M. 1997. Intracortical axonal projections of lamina VI cells of the primary somatosensory cortex in the rat: a single-cell labeling study. *J Neurosci*, 17, 6365-79.
- ZONA, C. & AVOLI, M. 1990. Effects induced by the antiepileptic drug valproic acid upon the ionic currents recorded in rat neocortical neurons in cell culture. *Exp Brain Res*, 81, 313-7.

Publications

Articles

CHAHBOUNE, H., MISHRA, A. M., DESALVO, M. N., STAIB, L. H., PURCARO, M., SCHEINOST, D., PAPADEMETRIS, X., FYSON, S. J., LORINCZ, M. L., CRUNELLI, V., HYDER, F. & BLUMENFELD, H. (2009) DTI abnormalities in anterior corpus callosum of rats with spike-wave epilepsy. *Neuroimage*, 47, 459-66.

COPE, D. W., DI GIOVANNI, G., FYSON, S. J., ORBAN, G., ERRINGTON, A. C., LORINCZ, M. L., GOULD, T. M., CARTER, D. A. & CRUNELLI, V. (2009) Enhanced tonic GABA_A inhibition in typical absence epilepsy. *Nat Med*, 15, 1392-8.

Posters

DIGIOVANNI, G., ORBAN, G., FYSON, S.J., CRUNELLI, V. & COPE, D.W. (2009) Thalamic extrasynaptic GABA_A receptors are required for typical absence seizures *Themed meeting of Physiology Society "Cellular & Integrative Neuroscience", Poster session, Cardiff, U.K*

DIGIOVANNI, G., ORBAN, G., FYSON, S.J., CRUNELLI, V. & COPE, D.W. (2009) Thalamic extrasynaptic GABA_A receptor gain-of-function is necessary and sufficient for absence epilepsy *Society for Neuroscience, Poster session, Chicago U.S.A*

FYSON, S.J., COPE, D.W. & CRUNELLI, V. (2008) Postsynaptic GABA_B receptors control "tonic" GABA_A inhibition *Society for Neuroscience, Poster session, Washington D.C. U.S.A*

FYSON, S.J., COPE, D.W., ERRINGTON, A.C., DIGIOVANNI, G. & CRUNELLI, V. (2007) Extrasynaptic GABA_A receptor gain-of-function in absence epilepsy: GHB and THIP pharmacological models *Society for Neuroscience, Poster session, San Diego U.S.A*

... and they all lived happily ever after